NATIONAL AND KAPODISTRIAN UNIVERSITY OF ATHENS

SCHOOL OF SCIENCE

DEPARTMENT OF CHEMISTRY

DOCTORAL THESIS

Study Of Biogeochemical Processes In An Intermittently Anoxic Coastal System (Gulf Of Elefsis) Under Simulated Ocean Acidification Conditions

NATALIA KAPETANAKI
CHEMICAL ENGINEER - OCEANOGRAPHER

ATHENS
JUNE 2018

ΕΘΝΙΚΟ ΚΑΙ ΚΑΠΟΔΙΣΤΡΙΑΚΟ ΠΑΝΕΠΙΣΤΗΜΙΟ ΑΘΗΝΩΝ

ΣΧΟΛΗ ΘΕΤΙΚΩΝ ΕΠΙΣΤΗΜΩΝ

ΤΜΗΜΑ ΧΗΜΕΙΑΣ

ΔΙΔΑΚΤΟΡΙΚΗ ΔΙΑΤΡΙΒΗ

Διερεύνηση Των Μεταβολών Σημαντικών Βιογεωχημικών Διεργασιών Σε Παράκτιο Υποξικό Σύστημα (Κόλπος Ελευσίνας) υπό Συνθήκες Ανάλογες του Φαινομένου της Οξίνισης των Θαλασσών

ΝΑΤΑΛΙΑ ΚΑΠΕΤΑΝΑΚΗ
ΧΗΜΙΚΟΣ ΜΗΧΑΝΙΚΟΣ - ΩΚΕΑΝΟΓΡΑΦΟΣ

ΑΘΗΝΑ
ΙΟΥΝΙΟΣ 2018

DOCTORAL THESIS

Study Of Biogeochemical Processes In An Intermittently Anoxic Coastal System (Gulf Of Elefsis) Under Simulated Ocean Acidification Conditions

NATALIA KAPETANAKI

A.M.: 001222

SUPERVISOR:

Michael J. Scoullos, Professor Emeritus, Laboratory of Environmental Chemistry, Department of Chemistry, National and Kapodistrian Univeristy of Athens

THREE-MEMBER COMMITTEE:

Manos Dassenakis, Professor, Laboratory of Environmental Chemistry, Department of Chemistry, National and Kapodistrian Univeristy of Athens

Evangelia Krasakopoulou, Associate Professor, Department of Marine Sciences, University of the Aegean

Evangelos Bakeas, Associate Professor, Analytical Chemistry, Department of Chemistry, National and Kapodistrian Univeristy of Athens

SEVEN-MEMBER EXAMINATION COMMITTEE:

Manos Dassenakis, Professor, Laboratory of Environmental Chemistry, Department of Chemistry, National and Kapodistrian Univeristy of Athens

Evangelia Krasakopoulou, Associate Professor, Department of Marine Sciences, University of the Aegean

Evangelos Bakeas, Associate Professor, Analytical Chemistry, Department of Chemistry, National and Kapodistrian Univeristy of Athens

Maria Triantafylloy, Professor, Department of Geology, National and Kapodistrian Univeristy of Athens

Alexandra Pavlidou, Researcher, Institute of Oceanography, Hellenic Centre for Marine Research

Soultana Zervoudaki, Researcher, Institute of Oceanography, Hellenic Centre for Marine Research

Ekaterini Souvermezoglou, Researcher, Institute of Oceanography, Hellenic Centre for Marine Research

EXAMINATION DATE: 12/06/2018

ΔΙΔΑΚΤΟΡΙΚΗ ΔΙΑΤΡΙΒΗ

Διερεύνηση των Μεταβολών Σημαντικών Βιογεωχημικών Διεργασιών Σε Παράκτιο Υποξικό Σύστημα (Κόλπος Ελευσίνας) υπό Συνθήκες Ανάλογες του Φαινομένου της Οξίνισης των Θαλασσών

ΝΑΤΑΛΙΑ ΚΑΠΕΤΑΝΑΚΗ

Α.Μ.: 001222

ΕΠΙΒΛΕΠΩΝ ΚΑΘΗΓΗΤΗΣ:

Μιχαήλ Ι. Σκούλλος, Ομότιμος Καθηγητής ΕΚΠΑ

ΤΡΙΜΕΛΗΣ ΕΠΙΤΡΟΠΗ ΠΑΡΑΚΟΛΟΥΘΗΣΗΣ:

Εμμανουήλ Δασενάκης, Καθηγητής ΕΚΠΑ

Ευαγγελία Κρασακοπούλου, Αναπλ. Καθηγήτρια Πανεπιστήμιου Αιγαίου

Ευάγγελος Μπακέας, Αναπληρωτής Καθηγητής Τμήματος Χημείας, ΕΚΠΑ

ΕΠΤΑΜΕΛΗΣ ΕΞΕΤΑΣΤΙΚΗ ΕΠΙΤΡΟΠΗ:

Εμμανουήλ Δασενάκης, Καθηγητής Τμήματος Χημείας, ΕΚΠΑ

Ευαγγελία Κρασακοπούλου, Αναπλ. Καθηγήτρια Τμήματος Επιστημών της Θάλασσας, Πανεπιστήμιου Αιγαίου

Ευάγγελος Μπακέας, Αναπληρωτής Καθηγητής Τμήματος Χημείας, ΕΚΠΑ

Μαρία Τριανταφύλλου, Καθηγήτρια Τμήματος Γεωλογίας, ΕΚΠΑ

Αλεξάνδρα Παυλίδου, Ερευνήτρια Α’, Ινστιτούτο Ωκεανογραφίας, Ελληνικό Κέντρο Θαλασσίων Ερευνών

Σουλτάνα Ζερβουδάκη, Ερευνήτρια Β’, Ινστιτούτο Ωκεανογραφίας, Ελληνικό Κέντρο Θαλασσίων Ερευνών

Αικατερίνη Σουβερμέζογλου, Ερευνήτρια Α’, Ινστιτούτο Ωκεανογραφίας, Ελληνικό Κέντρο Θαλασσίων Ερευνών

ΗΜΕΡΟΜΗΝΙΑ ΕΞΕΤΑΣΗΣ 12/06/2018

ABSTRACT

There has been a focus recently, on the common co-occurrence of oxygen depletion and ocean acidification (OA) and their concurrent effects on ocean biogeochemistry. Normally atmospheric CO_2 is the major driver of OA; however, naturally occurring microbial decomposition of organic matter (OM) in coastal marine environments cause increased acidity in deeper layers similar or even exceeding the future predictions for global OA. Experimental studies in coastal areas with increased inputs of OM and nutrients, coping with intermittent hypoxic/anoxic conditions, provide better understanding of the mechanisms affecting nutrients and carbon biogeochemistry under the emerging effects of coastal pH decrease. Two laboratory CO_2-manipulated microcosm experiments were conducted using seawater and surface sediment from the deepest part of Elefsis Bay (Saronikos Gulf, Eastern Mediterranean) focusing to study the co-evolution of processes affected by the decline of dissolved oxygen and pH induced by (a) OM remineralization and (b) the future anthropogenic increase of atmospheric CO_2. Under hypoxic and more acidified conditions, a significant increase of total alkalinity was observed mainly attributed to the bicarbonate ions produced in favor of CO_3^{2-} to buffer the CO_2 increase and the reactive nitrogen species shift towards ammonium. Nitrate and nitrite decline, in parallel with ammonium increase, demonstrated a deceleration of ammonium oxidation processes along with decrease in nitrate production. Additionally, the decreased DIN:DIP ratio, the prevalence of organic nutrient species against the inorganic ones, the observations of constrained DON degradation and the higher DOC concentrations possibly reveal inhibition of OM decomposition under lower pH values. Similarly, dissolved As and V seemed to be restricted due to inhibition of OM; Ni, Cu, Co and Pb were found to incorporate in carbonate bonds and Fe/Mn oxyhydroxides, increasing their dissolved fraction under lower pH. During severe hypoxic and more acidified conditions, nutrients were found crucial in the calculation of carbonate system budget for Elefsis bottom, posing a considerable negative feedback for acidification while carbonate saturation states were already calculated around 1.5. Limited alkalinity increase, was observed and was correlated with the contribution of bicarbonates and organic matter constituents, namely DOC and organic phosphorus; ammonium oxidation was decelerated in this case and a nitrification mechanism was noticed. Phosphate was found significantly elevated for the first time in lower pH values, without reprecipitating after reoxygenation. As and V also appeared to related to OM remineralization; Fe(III) solubilization was favoured under

lower pH, alongside Fe(II) stability even in the increase of oxygen. Mn and Co were found to interrelate through combined redox processes; Cu was mainly incorporated in carbonate bonds while Ni was mainly adsorpted on Mn oxyhydroxies. Finally, our results highlight the need for detailed studies of the carbonate system in coastal areas dominated by hypoxic/anoxic conditions, accompanied by other biogeochemical parameters (e.g. nutrients, trace element species) and properly designed experiments to elucidate the processes sequence or alterations due to pH reduction.

SUBJECT AREA: Biogeochemical Processes

KEY WORDS: carbonate chemistry, carbon, nutrients, trace metals, hypoxia, coastal ecosystem, microcosm experiment, sediment, Ocean acidification

ΠΕΡΙΛΗΨΗ

Πρόσφατα το ενδιαφέρον έχει επικεντρωθεί στην παράλληλη συνύπαρξη έλλειψης οξυγόνου και οξίνισης των θαλασσών (ΟΘ) και των ταυτόχρονων επιπτώσεών τους στη βιογεωχημεία της θάλασσας. Συνήθως το ατμοσφαιρικό CO_2 είναι ο κύριος μοχλός της ΟΘ. Ωστόσο, η μικροβιακή αποσύνθεση της οργανικής ύλης (ΟΥ) στα παράκτια θαλάσσια περιβάλλοντα προκαλεί αυξημένη οξύτητα σε βαθύτερα στρώματα παρόμοια ή ακόμα και υπερβαίνουσα των μελλοντικών προβλέψεων για την παγκόσμια ΟΘ. Οι πειραματικές μελέτες σε παράκτιες περιοχές με αυξημένες εισροές ΟΥ και θρεπτικών συστατικών, παράλληλα με διαλείπουσες υποξικές/ανοξικές συνθήκες, παρέχουν καλύτερη κατανόηση των μηχανισμών που επηρεάζουν τα θρεπτικά και τη βιογεωχημεία του άνθρακα κάτω από τις αναδυόμενες επιδράσεις της μείωσης του παράκτιου pH. Δύο εργαστηριακά πειράματα μικρόκοσμων με ελεγχόμενη εισαγωγή CO_2 διεξήχθησαν με θαλασσινό νερό και επιφανειακό ίζημα από το βαθύτερο τμήμα του κόλπου Ελευσίνας (Σαρωνικός κόλπος, Ανατολική Μεσόγειος), με στόχο τη μελέτη της συν-εξέλιξης των διεργασιών που επηρεάζονται από τη μείσωση του διαλυμένου οξυγόνου και του pH λόγω α) της αποικοδόμησης της ΟΥ και (β) της μελλοντικής ανθρωπογενούς αύξησης του ατμοσφαιρικού CO_2. Στις υποξικές και περισσότερο οξυνισμένες συνθήκες, παρατηρήθηκε σημαντική αύξηση της αλκαλικότητας κυρίως λόγω των HCO_3^- που παράχθηκαν έναντι των CO_3^{2-} για να αντισταθμιστεί η αύξηση του CO_2, και στις μεταβολές των μορφών αζώτου προς παραγωγή NH_4^+. Η μείωση των NO_3^- και των NO_2^-, παράλληλα με την αύξηση των NH_4^+, κατέδειξε επιβράδυνση των διαδικασιών οξείδωσης αμμωνίου και μείωση της παραγωγής NO_3^-. Επιπλέον, ο μειωμένος λόγος DIN:DIP, η επικράτηση οργανικών μορφών θρεπτικών έναντι των ανόργανων, η περιορισμένη αποικοδόμηση DON και οι υψηλότερες συγκεντρώσεις DOC ενδεχομένως μαρτυρούν την αναστολή της αποσύνθεσης ΟΥ σε χαμηλότερα pH. Στις ίδιες συνθήκες, τα As, V παρουσιάστηκαν μειωμένα στη διαλυτή μορφή λόγω αναστολή της αποσύνθεσης ΟΥ. Τα Ni, Cu, Co και Pb βρέθηκαν να συνδέονται περισσότερο με τα ανθρακικά και με οξείδια Fe/Mn, επομένως αυξανόταν η διαλυτή τους μορφή σε χαμηλότερα pH. Κατά τη διάρκεια έντονων υποξικών και πιο οξινισμένων συνθηκών, τα θρεπτικά βρέθηκαν απαραίτητα για τον υπολογισμό του συστήματος των ανθρακικών στον πυθμένα της Ελευσίνας, παρουσιάζοντας σημαντική αρνητική ανάδραση στην οξίνιση, ενώ οι βαθμοί κορεσμού των ανθρακικών υπολογίστηκαν γύρω στο 1,5. Περιορισμένη αύξηση της αλκαλικότητας παρατηρήθηκε και συσχετίστηκε με τη συμβολή των HCO_3^- και οργανικών συστατικών όπως το DOC και το DOP. Η οξείδωση

NH_4^+ επιβραδύνθηκε στην περίπτωση αυτή και παρατηρήθηκαν διεργασίες νιτροποίησης. Τα PO_4^{3-} βρέθηκαν σημαντικά αυξημένα για πρώτη φορά σε χαμηλότερο pH, χωρίς ανακαταβύθιση κατά την επανοξυγόνωση. Τα As και V επίσης παρουσίασαν συνάφεια με τις διεργασίες αποικοδόμησης ΟΥ. Η διαλυτοποίηση του Fe(III) ευνοήθηκε καθ' όλη τη διάρκεια του μειωμένου pH παράλληλα με την αυξημένη σταθερότητα του Fe(II) ακόμα και ύστερα από την αύξηση του οξυγόνου. Τα Mn και Co βρέθηκαν να συνδέονται με ένα συνδιασμό διεργασιών οξειδοαναγωγής, ο Cu βρέθηκε κυρίως προσδεμένος σε δεσμούς με ανθρακικά ενώ το Ni με οξείδια Mn, που και τα δύο όμως οδηγούσαν σε αυξημένες συγκεντρώσεις στη διαλυτή τους μορφή. Τέλος, τα αποτελέσματά αυτά υπογραμμίζουν την ανάγκη για λεπτομερείς μελλοντικές μελέτες του συστήματος ανθρακικών στις παράκτιες περιοχές όπου κυριαρχούν οι υποξικές/ανοξικές συνθήκες, συνοδευόμενες από άλλες βιογεωχημικές παραμέτρους (πχ μορφές θρεπτικών, ιχνοστοιχείων) και κατάλληλα σχεδιασμένα πειράματα για την κατανόηση των διεργασιών ή των μεταβολώ λόγω μείωσης του pH.

ΘΕΜΑΤΙΚΗ ΠΕΡΙΟΧΗ: Βιογεωχημικές Διεργασίες

ΛΕΞΕΙΣ ΚΛΕΙΔΙΑ: σύστημα ανθρακικών, άνθρακας, θρεπτικά, ιχνημέταλλα, υποξία, παράκτιο οικοσύστημα, πειράματα μικροκόσμων, ιζημα, Οξίνιση των θαλασσών

I dedicate this work, from the bottom of my heart,

to my mother, to my father, to my sister,

always present and supportive during this laborious effort…

To everyone who has been there, keeping me going throughout this 5 years….

I thank you!

Αφιερώνω αυτήν την εργασία μέσα από την καρδιά μου,

στη μητέρα μου, στον πατέρα μου, στην αδερφή μου,

πάντα παρόντες και υποστηρικτές καθόλη τη διάρκεια αυτής της επίπονης προσπάθειας…

Σε όλους όσους ήταν εκεί κατά τη διάρκεια αυτών των 5 χρόνων, κρατώντας με να προχωρώ …

Σας ευχαριστώ!

RECOGNITIONS – AKNOWLEDGEMENTS

I would like to express my sincere thanks to my supervisor, Professor Michael Scoullos, for his significant contribution to the preparation of this work, his continuous guidance both in the experimental part and in the investigation and scientific documentation of the results. Apart from the scientific part, he has been a source of personal inspiration and a major factor in the outcome of this dissertation.

I also want to thank Professor Manos Dasenakis for his continuous support, guidance, corrections and important remarks that helped me to improve the scientific content of this work.

In addition, I would like to say a huge thank you to the deputy professor Eva Krasakopoulou, through which I had the opportunity to be acquainted with and to work on the major issue of Ocean Acidification. Through continuous discussions and explanations, despite the distance, I have greatly improved not only the outcome of the laboratory experiments and the overall investigation, but also the evolution of my scientific thinking and vision.

I want to thank Dr. Eleni Stathopoulou, member of the Environmental Chemistry Laboratory, for the continuous guidance and co-operation throughout these 5 years, both in the design of the work, during the implementation, during the laboratory analyses and the explanation of the results.

I would also like to warmly thank the researcher Dr. Tania Zervoudaki for the excellent collaboration, the opportunity to participate in the R/V AEGAEO and FILIA sampling procedures, her full support during the set-up and the experiment progress at the premises of the HCMR in Anavyssos.

I want to thank the researcher Dr. Aleka Pavlidou also for the excellent collaboration and the support in nutrient chemical. In addition, I would like to thank Eleni Rousselaki and Youla Zachioti for the discussions, their support and help during the analyses.

I would like to thank the members of the Environmental Chemistry Laboratory, Dr. Sotiris Karavoltsos, Dr. Viki Paraskevopoulou and Dr. Giorgos Katsiouras for their excellent collaboration and help in analyses using ICP-MS and AAS. Moreover, I thank Dr. Katerina Sakellari, Dr. Fotini Botsou also members of the Environmental Chemistry Laboratory and the Ph.D. candidate Elia Louropoulou for the excellent cooperation and support where this was deemed necessary.

I thank the postgraduate student Aspa Tziava for her help and valuable contribution in sediment treatment and analyses.

I wish to thank the GIS Lab of HCMR for preparing the Elefsis map. I would also like to thank the Athens Water Supply and Sewerage Company for supporting the field sampling. The support and assistance of the officers and crew of the R/V Aegaeo during sampling is highly appreciated.

In the end, I would also like to thank Dr. Yannis Karouzas for his contribution in the statistical analysis of the results and for the priceless moral support.

Finally, I would like to point out that besides the profound scientific background and the people who supported me in all aspects of this thesis, there were also people who ‘held’ me morally, mentally and physically, to the same or even to a greater extent. To all of them just a ‘thank you’ is not enough .... So until we come up with a new word...

ΕΥΧΑΡΙΣΤΙΕΣ

Θα ήθελα να ευχαριστήσω θερμά τον επιβλέπων καθηγητή μου Μιχαήλ Σκούλλο, για την τόσο σημαντική συμβολή του στην εκπόνηση αυτής της εργασίας, τη συνεχή καθοδήγηση, τόσο στο πειραματικό σκέλος όσο και στη διερεύνηση και επιστημονική τεκμηρίωση των αποτελεσμάτων. Πέρα από το επιστημονικό κομμάτι υπήρξε πηγή προσωπικής έμπνευσης και σημαντικότατος παράγοντας για την έκβαση αυτής της διατριβής.

Θέλω επίσης να ευχαριστήσω τον καθηγητή Μάνο Δασενάκη για τη συνεχή υποστήριξη, καθοδήγηση, τις διορθώσεις και τις σημαντικές επισημάνσεις που συνέβαλαν στη βελτίωση του επιστημονικού περιεχομένου αυτής της εργασίας.

Επιπλέον, θέλω να πω ένα τεράστιο ευχαριστώ στην αναπληρώτρια καθηγήτρια Εύα Κρασακοπούλου, μέσω της οποίας είχα την ευκαιρία να γνωρίσω και να εργαστώ πάνω στο τόσο επίκαιρο θέμα της Οξίνισης των Ωκεανών. Οι συνεχείς συζητήσεις μαζί της, παρά την απόσταση, και οι επεξηγήσεις της βελτίωσαν σημαντικά όχι μόνο την εξέλιξη των πειραμάτων και της συνολικής διερεύνησης αλλά και στην εξέλιξη της επιστημονικής μου σκέψης και οπτικής.

Θέλω να ευχαριστήσω θερμά τη Δρ. Ελένη Σταθοπούλου, μέλος του Εργαστηρίου Χημείας Περιβάλλοντος, για τη συνεχή καθοδήγηση και συνεργασία καθ’όλη τη διάρκεια των 5 αυτών χρόνων, τόσο κατά το σχεδιασμό της εργασίας, κατά την υλοποίηση, στη διάρκεια των εργαστηριακών αναλύσεων και στην επεξήγηση των αποτελεσμάτων.

Θα ήθελα επίσης να ευχαριστήσω θερμά την ερευνήτρια Δρ. Τάνια Ζερβουδάκη για την εξαιρετική συνεργασία, τη δυνατότητα να συμμετάσχω στους πλόες των Ω/Σ ΑΙΓΑΙΟ και ΦΙΛΙΑ για τις απαραίτητες δειγματοληψίες, την αμέριστη υποστήριξή της καθ’όλη τη διάρκεια στο στήσιμο και στην εξέλιξη των πειραμάτων στις εγκαταστάσεις του ΕΛΚΕΘΕ στην Ανάβυσσο.

Θέλω να ευχαριστήσω την ερευνήτρια Δρ. Αλέκα Παυλίδου επίσης για την εξαιρετική συνεργασία και την υποστήριξη σε χημικές αναλύσεις που αφορούσαν στα θρεπτικά συστατικά των πειραμάτων. Επιπλέον να ευχαριστήσω τις Ελένη Ρουσελάκη και Γιούλα Ζαχιώτη για τις συζητήσεις, την υποστήριξη και τη βοήθεια κάτα τη διάρκεια των αναλύσεων.

Θα ήθελα να ευχαριστήσω τα μέλη του εργαστηρίου Χημείας Περιβάλλοντος Δρ. Σωτήρη Καραβόλτσο, Δρ. Βίκη Παρασκευοπούλου και το Δρ. Γιώργο Κατσιούρα για την άριστη συνεργασία και τη βοήθειά τους στις αναλύσεις με χρήση ICP-MS και AAS.

Επιπλέον ευχαριστώ τη Δρ. Κατερίνα Σακελλάρη, Δρ. Φωτεινή Μπότσου μέλη επίσης του εργαστηρίου Χημείας Περιβάλλοντος, την υποψήφια διδάκτορα Έλια Λουροπούλου για την άριστη συνεργασία και υποστήριξη όπου αυτό κρίθηκε αναγκαίο.

Ευχαριστώ τη μεταπτυχιακή φοιτήτρια Άσπα Τζιάβα, για τη βοήθεια και πολύτιμη συνεισφορά της στην κατεργασία και ανάλυση των ιζημάτων.

Θα ήθελα να ευχαριστήσω το Εργαστήριο GIS του ΕΛΚΕΘΕ για την προετοιμασία του χειρόγραφου χάρτη της Ελευσίνας. Επίσης την Εταιρεία Ύδρευσης και Αποχέτευσης Πρωτευούσης (ΕΥΔΑΠ) για τη στήριξη της δειγματοληψίας πεδίου. Η υποστήριξη και η βοήθεια των αξιωματικών και του πληρώματος των Ω/Σ ΑΙΓΑΙΟ και ΦΙΛΙΑ κατά τη δειγματοληψία εκτιμάται ιδιαίτερα.

Θα ήθελα, στο τέλος, να ευχαριστήσω το Δρ. Γιάννη Καραούζα για τη συμβολή του στη στατιστική επεξεργασία των αποτελεσμάτων καθώς και την πολύτιμη ηθική υποστήριξη.

Τέλος, θέλω να επισημάνω πως εκτός από το βαθύ επιστημονικό υπόβαθρο και τους ανθρώπους που με στήριξαν από κάθε άποψη στην εκπόνηση αυτής της διατριβής, υπήρχαν και άνθρωποι που με ‘κράτησαν’ ηθικά, ψυχικά και σωματικά σε ίδιο και μεγαλύτερο βαθμό. Σε αυτούς όλους ένα ευχαριστώ δεν είναι αρκετό…. Μέχρι να ανακαλύψουμε μια καινούρια λέξη λοιπόν…

1511
1513
MEDITERRANEAN SEA
GREEK ARCHIPELAGO
KÓLPOS ELEVSÍNOS
KÓLPOS ELEVSÍNOS
ATTIKÍ
ATTIKÍ

CONTENTS

LIST OF FIGURES

LIST OF TABLES

PROLOGUE

Part of this research was funded by the EU Research Project "ARISTEIA-EXCELLENCE 640" (2012-2015) entitled *"Integrated Study of Trace Metals Biogeochemistry in the Coastal Marine Environment* (ISMETCOMAREN)*"*. Part of this project is implemented under the Operational Programme "Education and Lifelong Learning" and funded by European Social Fund and national resources.

ΠΡΟΛΟΓΟΣ

Μέρος αυτής της έρευνας χρηματοδοτήθηκε από το Ερευνητικό Έργο της ΕΕ "ΑΡΙΣΤΕΙΑ 640" (2012-2015) με τίτλο "Ολοκληρωμένη Μελέτη της Βιογεωμετρίας των ιχνοστοιχείων στο Παράκτιο Θαλάσσιο Περιβάλλον (ISMETCOMAREN)". Μέρος αυτού του προγράμματος υλοποιήθηκε στο πλαίσιο του Επιχειρησιακού Προγράμματος «Εκπαίδευση και Δια Βίου Μάθηση» και χρηματοδοτήθηκε από το Ευρωπαϊκό Κοινωνικό Ταμείο και εθνικούς πόρους.

CHAPTER : 1

PART I

OCEAN ACIDIFICATION

1.1 Introduction

Ocean acidification (OA) refers to the on-going decrease in ocean pH as a result of the uptake of anthropogenic carbon dioxide (CO_2) in the ocean [1]. The carbon dioxide (CO_2) concentration in the atmosphere has increased from 280 parts per million (ppm) in the preindustrial time period to a present-day value of 408 ppm [2, 3] and are expected to reach values of 700-1000 µatm in the end of the century [4]. World Oceans currently absorb about one fourth of the anthropogenic carbon dioxide (CO_2) emissions into the atmosphere [5]. It has been estimated that from 1800's until 1994 the ocean removed about 50% of the CO_2 emitted from the burning fossil fuels, or about 30% of total anthropogenic emissions [6]. Due to the rapid growth of global fossil fuel CO_2 emissions since 2000, the ocean storage of carbon has declined since the 1990's suggesting a weakening in ocean CO_2 sink due to climate variability and climate change [6].

The increasing CO_2 uptake by the oceans leads to an increase in partial pressure of CO_2 (pCO_2), a decline in pH along with elevated dissolved inorganic carbon (DIC) content in the surface seawater. Since the beginning of the Industrial Revolution the average pH of ocean surface waters has fallen by about 0.1 units and is expected to decrease by 0.2 to 0.4 units by the end of the century [7].

1.2 Ocean Acidification Process

CO_2 being a weak acid, once dissolved in seawater affects marine chemistry in several ways; bicarbonate ion concentrations and dissolved inorganic carbon (DIC) increase in parallel with carbonate ions and pH decrease [3]. The series of reactions due to CO_2 dissolution is as follows (the notations (g), (l), (aq) refer to the state of the species, i.e., a gas, a liquid or in aqueous solution respectively) [8]:

$$CO_2\ (g) \leftrightarrow CO_2\ (aq) \quad (1)$$

$$CO_2\ (aq) + H_2O(l) \leftrightarrow H_2CO_3\ (aq) \quad (2)$$

$$H_2CO_3\ (aq) \leftrightarrow H^+\ (aq) + HCO_3^-\ (aq) \quad (3)$$

$$HCO_3^-\ (aq) \leftrightarrow H+\ (aq) + CO_3^{2-}\ (aq) \quad (4)$$

The concentration of protons ($[H^+]$), which is proportional to the ratio $[HCO_3^-]/[CO_3^{2-}]$, increases and pH decreases, hence the increase in acidity. The expression 'ocean acidification' refers to the decrease in pH, but does not imply that the pH of surface-ocean waters will become acidic (below 7) any time soon [3].

1.3 Ocean Acidification Impacts

Whilst there is a high degree of certainty on future changes in the seawater chemistry based on CO_2 emissions to the atmosphere the impacts of these changes on the marine species physiology and development, foodwebs, biodiversity, biogeochemistry and ecosystems are less clear. Perturbation experiments performed in the laboratory and in field mesocosms and have been made in regions naturally acidified around the globe in order to estimate and possibly foresee future impacts of OA [10].

The changes associated with the uptake of the excess CO_2 by the ocean cause an additional abiotic stressor for marine ecosystems [8]. The oceans' response to acidification will not be uniform; different regions and different depths already exhibit different trends, and the activities of organisms may accelerate or modulate these trends [11].

In an acidifying ocean, microbial community responses to reduced seawater pH and elevated pCO_2 may act as positive or negative feedback to carbon and nitrogen critical biogeochemical processes. In coastal areas, even in the presence of oxygen, the flow of the organic load is high and the aerobic degradation of organic matter leads to a higher CO_2 production, causing dissolution of existing sedimentary carbonates [12, 8]. Furthermore, OA can interact with other natural and anthropogenic environmental processes in coastal areas, to accelerate local declines in pH and carbonate mineral saturation states [13].

Shallow-water sediments play an important role in the global carbonate cycle as they represent a large reservoir of $CaCO_3$ that can react to the decreasing saturation state of seawater, releasing alkalinity to the overlying water column [8]. This dissolution of sedimentary carbonates has certainly played a significant role in past variations of pCO_2 [14] buffering to a certain extent the excessive CO_2 content. As the rate of this reaction is both kinetically and physically limited and as the amount of $CaCO_3$ is not large enough, it cannot compensate for the actual very fast increase of atmospheric CO_2. As high-latitude sediments represent a much smaller $CaCO_3$ reservoir than tropical areas, it is very likely that they will not have the capacity for locally buffering anthropogenic increases in CO_2 [14].

1.4 Ocean Acidification in combination with other related processes (Warming, Eutrophication, Hypoxia/, Anoxia)

In the coming decades and centuries, the ocean's biogeochemical cycles and ecosystems will become increasingly stressed by at least three independent factors. Rising temperatures, OA and ocean deoxygenation will cause substantial changes in the physical, chemical and biological environment, which will then affect the ocean's biogeochemical cycles and ecosystems with distinct regional differences. The impacts of OA tend to be strongest in the high latitudes, whereas the low-oxygen regions of the low latitudes are most vulnerable to ocean deoxygenation. Of additional concern are synergistic effects, such as OA-induced changes in the type and magnitude of the organic matter exported to the ocean's interior, which then might cause substantial changes in the oxygen concentration there [15].

Warming

Ocean warming is the consequence of the ocean having taken up much of the extra heat accumulating in the Earth system as a result of the enhanced greenhouse effect. Between 1955 and 1998 alone, the ocean was responsible for more than 80 per cent of the total increase in the heat content of the Earth system. Most of this extra heat has accumulated in the near-surface ocean, causing a surface ocean warming of about 0.7 °C over the last 100 years. In contrast, the deep ocean changes are minuscule so far, so that the global

mean ocean temperature has increased by less than 0.04 °C between 1955 and 1998. This differential heating of the water column has increased the density gradient between the near-surface waters and the deep ocean, increasing the upper ocean stratification which may be further modified by the expected acceleration of the hydrological cycle in response to global warming. Stronger stratification tends to decrease upper ocean mixing and transport, thereby more strongly separating the upper ocean, which is in ready exchange with the atmosphere from the intermediate and deep ocean that contains the nutrients required for ocean productivity. Thus, two types of effects are expected with regard to ocean biogeochemistry and ocean ecosystems; first, there will be direct effects as a result of most rates of biogeochemical and biological processes being temperature dependent. Second, ocean warming-induced stratification and other changes in upper ocean mixing and transport will cause a range of indirect effects, such as a more favourable light regime for phytoplankton in the high latitudes, more nutrient stress for phytoplankton in the low latitudes and a generally reduced transport of gases (anthropogenic CO_2, chlorofluorocarbons (CFCs) and dissolved oxygen) from the near surface into the ocean's interior [15].

Hypoxia/Anoxia

Carbon and oxygen cycles are tightly linked through photosynthesis, respiration, and remineralization but decouple in air-sea gas exchange. Although CO_2 is a reactive gas, its hydration/dehydration kinetics are slow so its air-sea transfer rate is not chemically enhanced and it reaches equilibrium much more slowly than does O_2 [16, 17].

Regarding the terms of hypoxic/suboxic/anoxic conditions several thresholds have been proposed (mild/moderate/severe hypoxia [18, 19 and references therein]) regarding not only the O_2 concentration but also (a) the system it characterizes (e.g. open ocean, coastal, shelf), (b) the possible biological effects appearing under certain situations (e.g. effects on benthic animals, mortality of fauna or microbial communities), (c) the biogeochemical processes taking place (e.g. evidence of nitrate reduction and denitrification, high N_2O production).

Hypoxic or anoxic systems are more acidic than normal marine environments, as the biochemical oxygen consumption is inextricably linked to the production of soluble inorganic carbon, including CO_2 [20]. In hypoxic coastal systems, the gas exchange balance with the atmosphere is not achieved, meeting extremely high pCO_2 levels. The current magnitude of acidification that can be expected in hypoxic coastal areas (i.e., pCO_2>1,700–3,200 μatm [13, 21] is greater than what is predicted for the next few 100 years due to OA in the oxygenated surface ocean [8, 22]. Linear increases in DIC due to respiration lead to exponential increases in pCO_2; wind-driven upwelling can bring hypoxic and CO_2-enriched waters from below pycnoclines in contact with productive shallow water ecosystems [23].

From past research, it has become clear that OA, especially when combined with hypoxic phenomena [17], has direct impacts on carbon biogeochemistry, with dissolution of existing sedimentary carbonates [8] and alkalinity release in the supernatant water column [13], but also in nutrient cycles, with decline in nitrification rates, as a result of reduced oxidation rates of ammonia to nitrites [11, 13]. Moreover, concerning trace metals, OA tends to alter their forms and species, the complexes' stability in addition to the alterations in sediment mineral phases, causing changes in benthic fluxes in the sediment-water interface, making them more soluble thus bioavailable [24, 25, 26]. Therefore, combinational acidification-anoxia experiments for coastal environments are essential to fully understand and correlate the various observations [23].

Model calculations for the doubling CO_2 emission scenario [23] show that coastal hypoxic zones may easily encounter pCO_2 values of 3,400–4,500 μatm when most oxygen is consumed. Other habitats already enriched in DIC, for example oceanic oxygen-minimum zones, continental upwelling systems, estuaries and estuarine salt marsh system, will likely be impacted in a similar manner by future OA. It is important to stress that in oceanic oxygen-minimum zones, OA–enhanced pCO_2 will be encountered with a significant time delay, which is related to transit times of decades to a century, between last contact with the atmosphere and arrival in the OMZ [27]. In coastal waters with seasonal hypoxia, this time delay is on the order of months to 1 year. Hence,

such regions will feel the combined effect of OA and hypoxia almost instantaneously [23].

Eutrophication

The environmental consequences of nutrient enrichment of coastal ecosystems (e.g. increased phytoplankton production, increased turbidity with subsequent loss of submerged aquatic vegetation, oxygen deficiency, decreased in biodiversity, etc.) has been well documented but the role of the coastal zone as source or sink for atmospheric CO_2 is the subject of a long-lived controversy that mainly originates from the lack of sufficient field measurements, their probable inadequate spatial and/or seasonal coverage and the diversity and complexity of this marine realm from the point of view of carbon cycling [28, 29, 30].

Moreover, the modification of the capacity of coastal waters to absorb atmospheric CO_2 due to increased human pressure also remains poorly known. Model studies exploring the impact of increased nutrient and carbon loads on the heterotrophic or autotrophic status and the direction of the air–sea CO_2 exchanges in the global coastal area over the past 300 years conclude that the ecosystem trophic status and air–sea CO_2 exchanges have changed since the industrial revolution. In spite of some uncertainties, these studies show that worldwide coastal waters have probably acted as a net CO_2 source to the atmosphere for much of the past 300 years, but have recently switched, or will switch soon, to a net sink of CO_2, because of rising atmospheric CO_2 and eutrophication [31].

Synergistic Effects

While acidification in the open ocean is mainly driven by the atmospheric CO_2, in coastal zones this process may be minor particularly where excessive nutrient loading and organic matter production have been associated with hypoxic events [32, 33, 34]. The combination of low oxygen conditions, elevated pCO_2, global warming and eutrophication, may pose coastal marine ecosystems at high environmental risk possibly acting synergistically to reduce oxygen content [35].

Perhaps best studied so far is the impact of OA on future marine oxygen levels. One possible mechanism is that OA increases the carbon to nitrogen ratio of OM [52], which then requires more oxygen per unit nitrogen to be remineralized when it sinks through the water column. This enhanced oxygen demand would occur throughout the water column, but its impact would be greatest at the depths where oxygen is minimum leading in up to 50 per cent increase in the volume of suboxic waters by the end of this century [36]. In addition to creating dead zones, this would increase marine denitrification substantially and hence affect the marine nitrogen inventory.

Another mechanism to affect marine oxygen levels is the possible OA-induced reduction of marine calcification, which would result in the production of a smaller amount of mineral $CaCO_3$ that tends to counterweight' OM on its way down through the water column. As a result, OM would tend to sink less rapidly, leading to a shallower remineralization and an upward shift and compression of the oxygen demand profile. This results in a substantial reduction of oxygen in the shallower parts of the thermocline, where oxygen is already low, while the deeper parts of the ocean gain oxygen.

A third potential mechanism is linked to the possibility that OA increases marine nitrogen fixation [37]. This would tend to cause an increase in OM export and ocean interior oxygen demand, with consequences similar to those associated with the OA-induced high carbon to nitrogen ratio of marine export production.

An entirely different set of synergistic effects might occur at the physiological level. Elevated levels of dissolved CO_2 might reduce the amount of energy gained from the oxidation of OM. This will increase the respiratory stress of higher order organisms at low oxygen concentrations, effectively resulting in a higher oxygen concentration when the hypoxic threshold is reached. This results in the paradoxical situation in which the volume of hypoxic waters that are lethal to higher order organisms increases, while the actual oxygen concentration remains unchanged.

As OA progresses, and the available CO_2^{-3} ions are titrated away, the dissolved CO_2 concentration will increase overproportionally, leading to a

faster development of respiratory stress. Furthermore, rising temperatures would similarly increase the oxygen demand for higher organisms, yet tend to reduce the supply of oxygen. Finally, elevated CO_2 and lower O_2 levels might reduce the thermal tolerance of certain organisms, increasing the impact of ocean warming. Even in the absence of a substantial warming, the reduction in the thermal tolerance by OA and deoxygenation could cause substantial shifts in species diversity and ecosystem composition through the reduction of the habitat range [15].

1.5 General Aspects of OA effects on Mediterranean Sea and Mediterranean coastal environments

The Mediterranean Sea is a land-locked relatively small marine ecosystem connected to the Atlantic Ocean, that represents approximately 0.8% of the world's ocean surface area, and a particular system with respect to its physical and biogeochemical processes [38, 39]. It receives surface Atlantic waters flowing Eastwards and exports intermediate waters to the Atlantic contributing thus to the global overturning circulation exporting warm and salty intermediate water into the Atlantic Ocean through the shallow and narrow Strait of Gibraltar affecting the global thermohaline circulation [38, 39]. Due to its semi-enclosed nature and the short residence time of water masses, the Mediterranean Sea is sensitive to external forcing, making it a ‘hotspot’ for climate change effects, having the potential to provide an early warning for global ocean changes [40, 41].

The Mediterranean Sea is also unique in terms of CO_2 dynamics, global carbon cycle and anthropogenic CO_2 drawdown and storage [38]. Its waters are characterized by high alkalinity (~ 2600 $\mu molkg^{-1}$ [2, 41]) compared to other oceans and are slightly more basic (~0.25 less compared to the Atlantic waters at corresponding depths [38]), thus attracting more easily CO_2 from the atmosphere.

The higher uptake ability of atmospheric CO_2 of Mediterranean waters seems to be related to its active overturning circulation, along with the high total alkalinity (A_T) and temperature prevailing throughout the water column combined with the relatively low Revelle factor (the ratio of instantaneous

change in carbon dioxide (CO_2) to the change in total dissolved inorganic carbon (DIC), and is a measure of the resistance to atmospheric CO_2 being absorbed by the ocean surface layer) of its surface waters [2; 38]. In shallow nearshore Mediterranean areas, although seawater pH is influenced by various natural and anthropogenic processes other than CO_2 uptake [43, 44, 32], long term data-based estimations at coastal monitoring sites also indicate a shift towards more acidic conditions [e.g. 40, 45].

Recent studies in the Mediterranean Sea report that anthropogenic carbon has penetrated throughout the water column with concentrations much higher than those recorded in other oceanic areas [2, 38, 46]. Indeed, from the pre-industrial period until 2013 the pH in Mediterranean Sea has decreased by 0.055 - 0.156 pH units, posing this semi-enclosed sea as one of the most affected regions by acidification globally [41, 47]. Model simulations predict a further decrease in the pH of Mediterranean surface waters of 0.3-0.4 units by the year 2100 [48, 40]. The waters of the Western basin of the Mediterranean have been generally found more acidic (average pH=8.061±0.033) than those of the Eastern basin (average pH=8.087±0.024). This is related to the difference of the renewal time in each Mediterranean basin, i.e. the renewal time of the Western deep waters is shorter than the Eastern one (20–40 years in the Western basin and about 100 years in the Eastern basin). This fact also explains the higher accumulation of C_{ANT} in the Western basin which is more invaded by C_{ANT} than the Eastern basin [41].

All Mediterranean waters are strongly saturated with respect to both calcite and aragonite ($\Omega>1$) with the saturation state of both minerals exhibiting a clear longitudinal gradient with increasing values eastward at all depths [41].

Ω levels, however, have decreased in the Mediterranean waters within a range from 0.37 to 2 for Ω_{cal} and from 0.24 to 1.3 for Ω_{ar}, reflecting the aggravated effect of the excessive anthropogenic CO_2 penetration, and thus of the ocean acidification on the calcium carbonate states [41]. During the period 1967−2003, the estimated Ω_{ar} in a coastal site in the western Mediterranean (Ligurian Sea) displayed a decreasing trend and fluctuated between the highest value of 4.3 observed in 1968 and a minimum of 3.1 in 2003 [40].

It has been pointed out that the inorganic carbon system annual cycle in Mediterranean coastal systems, such as in the Adriatic Sea (e.g. Gulf of Trieste), with specific hydrographic characteristics (e.g. increased summer temperatures, seasonal hypoxia) is primarily controlled by changes of the circulation patterns, the seawater chemical composition, namely local freshwater inputs, biological processes, and air–sea CO_2 exchange [50, 34, 49]. Normally, during low seawater temperatures anthropogenic CO_2 adsorption is fauvoured [51]; during summer, intense remineralisation of organic carbon in the deeper waters releases CO_2, reinforcing the temperature-driven pCO_2 increase and leading to bottom values up to 1043 matm during hypoxic periods [50]. Water column mixing concominantly drives the penetration of these increased amounts of CO_2 to the surface waters, resulting in their supersaturation, and eventually emitting CO_2 to the atmosphere [51]. However, a low effect on the pH of the system is observed due to the riverine inputs of total alkalinity which set a low Revelle factor and a great capacity to store atmospheric CO_2 buffering these inputs [51, 50].

PART II

ELEMENT BIOGEOCHEMISTRY

1.6 Measurable Carbonate System Parameters

The components of the carbonate system in natural waters can be characterized by measuring at least two of the measurable parameters, pH, total alkalinity (A_T), total dissolved inorganic carbon (DIC) and the partial pressure of CO_2.

Partial Pressure of CO_2 (pCO_2)

The partial pressure of carbon dioxide (pCO_2) assigned to a seawater sample refers to the partial pressure of CO_2 in the gas phase that is in equilibrium with that seawater sample (at a specified temperature). The pCO_2 of a particular seawater sample is a strong function of temperature, changing about 4.2% per Kelvin. The pCO_2 of a seawater sample is usually determined by equilibrating a large volume of seawater with a small volume of gas. Then the mole fraction of CO_2 in the gas phase is determined from which the partial pressure is calculated [52]. The partial pressure of a gas in a mixture is given by the expression:

$$pCO_2 = x(CO_2)p,$$

where $x(CO_2)$ is the mole fraction of the CO_2 in the gas phase, and p is the total pressure [55].

The quantity that drives the physical process of CO_2 exchange between ocean and atmosphere, is the partial pressure and not the mole fraction. The net exchange of CO_2 across the air – sea interface varies latitudinally, largely as a function of pCO_2 in surface waters, which, in turn, is affected by temperature, upwelling or downwelling, and biological production. Cold, high-latitude waters take up carbon, while warm, lower-latitude waters tend to release carbon (outgassing of CO_2 from tropical gyres) [56].

Total dissolved inorganic carbon (DIC)

The total dissolved inorganic carbon in a sea water sample is defined by:

$$C_T = [CO_2] + [HCO_3^-] + [CO_3^{2-}]$$

Less than 1% of the carbon exists as dissolved CO_2. More than 99% of the DIC exists as bicarbonate and carbonate anions [57].

Total Alkalinity

The total alkalinity of a sample of sea water is a form of mass-conservation relationship for hydrogen ion. It is rigorously defined [175] as ". . . the number of moles of hydrogen ion equivalent to the excess of proton acceptors (bases formed from weak acids with a dissociation constant K ≤ 10–4.5 at 25°C and zero ionic strength) over proton donors (acids with K > 10–4.5) in 1 kilogram of sample." Thus:

$$A_T = [HCO_3^-]+2[CO_3^{2-}]+[B(OH)_4^-]+[OH^-]+[HPO_4^{2-}]+$$

$$+2[PO_4^{3-}]+[H_3SiO_4^-]+[NH_3]+[HS^-]+\ldots.$$

$$-[H^+]-[HSO_4^-]-[H_3PO_4]-\ldots.$$

In the majority of ocean areas, the three first factors of the equation are the main contributors to alkalinity budget. Under anoxic conditions, however, the HS^- and NH_3 factors contribute significantly in total alkalinity [58].

In the open ocean, in general, the A_T does not change appreciably with photosynthesis and respiration processes. For example, A_T increases with the depletion of NO_3^- and NO_2^- and diminishes with the depletion of NH_4^+ [55].

Total hydrogen ion concentration - pH_T

pH is important because of the information it can provide on other equilibrium processes within a solution.The pH can control nutrient and metal concentrations or biological availability in natural waters and can also be used to predict the solubilities of certain minerals in solution, or to influence intracellular functions [56].

In open ocean pH is always between 7.8-8.2; seawater is considered a buffer solution mainly due to its carbonic acid content and to a lesser extent due to boric acid. Under a general scope, pH vertical profile suggests a significant fluctuation in the first 100m with maximum pH values of 8.2-8.3. pH then decreases between 200-1200m to 7.5-7.7 with a poossible intermediate maximum value of ~7.9 at around 400m. In deeper waters, pH stabilizes according to various prevailing conditions. In shallow well-aerated areas with

intense sunlight, pH can increase beyond 8.9 whereas in areas of restricted circulation and water mixing, the development of anoxic conditions and the subsequent hydrogen sulfide release decreases pH beyond 7.5-7.0 despite the parallel generation of ammonia [58].

In pure or dilute solutions, pH is a measure of the activity of the hydrogen ion. However, the convention used to define chemical activity does not accurately estimate activity coefficients for solutions with an ionic strength greater than approximately 0.1 mol kg^{-1}. Therefore, this scale should not be used in natural waters with nominal salinities greater than ~5. The IUPAC NBS pH scale is based on low ionic strength buffer standards from the US National Bureau of Standards (NBS) and is universally used in laboratories. The difference between the ionic strengths of the NBS pH buffers and seawater samples results in significant changes between calibration and sample measurements, and particularly affects the liquid-junction potential when using potentiometric pH systems [60]. In seawater, hence, pH should instead be measured on a concentration scale. This confusion often stems from the multitude of different scales that can be applied to define pH on a concentration scale [56].

Currently, pH can be presented on three different pH concentration scales – the free, total, or seawater pH scale. Within the ocean pH range, the concentration scales are defined as:

- $pH_F = -log\{[H^+]\}$ (free proton concentration)
- $pH_T \approx -log\{[H^+] + [HSO^{-4}]\}$ (total proton concentration)
- $pH_S \approx -log\{[H^+] + [HSO^{-4}] + [HF]\}$. (seawater proton concentration))

The free pH scale (pH_F) only takes into account free hydrogen ions, whereas the total pH scale (pH_T) also considers sulfate, and the seawater-pH scale (pH_S) includes sulfate and fluoride complexes [66, 67].

It is possible to convert a pH value from the total scale to the free scale and vice versa [67] in seawater of a known salinity, and software tools are available to achieve this [68]. Despite that none of these scales are universally promoted as a standard definition of pH in seawater, in oceanic carbonate-chemistry research, the total scale is most commonly used and is the recommended pH scale [69]. The use of the total pH scale avoids

problems associated with uncertainties in the stability constants for fluoride complexes, which are required for the seawater-pH scale [65, 66, 67, 68, 69]. In seawater, potentiometric pH measurements are made using hydrogen sensitive glass/reference electrodes calibrated using a seawater buffer. The precision of potentiometric systems can be as good as ±0.001−0.003 units of pH. The sample pH (pH_X) is defined to be relative to the standard pH of the buffer, pH_S, calibrated with the standard hydrogen electrode by:

$pH_X = pH_S - (E_X - E_S)k$

where E_S is the electrical potential of the standard buffer solution measured with the glass electrode, E_X is the electrical potential of the unknown sample, and k is the Nernst slope ($k = \{RT \ln(10)\}/F$) [67].

Temporal variation in carbonate system parameters can also be large, over scales as short as diel cycles over seasons. As the balance between photosynthesis and respiration varies over diurnal, seasonal, or other periods, there is a corresponding variation in DIC, pH, and other ocean carbonate system parameters. DIC removal into phytoplankton blooms leads to an elevation of pH, $[CO_3^{2-}]$, Ω_{cal} and Ω_{ar} during late spring and summer [71].

1.7 Saturation States of Calcium Carbonate Minerals in Seawater

There are three primary biogenic carbonate-containing mineral phases that occur in seawater: aragonite, calcite, and magnesian calcite. Aragonite and calcite are naturally occurring polymorphs of calcium carbonate with differing crystal lattice structures and hence solubilities, aragonite being about 1.5 times more soluble than calcite at 25°C.

The dissolution equilibria for calcite and aragonite can be written as:

$CaCO_3(s) \Leftrightarrow Ca^{2+}(aq) + CO_3^{2-}(aq)$

where (s), (aq) indicate the solid phase. The corresponding equilibrium constant is the solubility product $K_{sp}(X) = [Ca^{2+}]\,[CO_3^{2-}]$ where the effect of the different crystal structure of the particular solid phase is now implicit in the solubility product itself (X stands for aragonite or calcite). Strictly, aragonite and calcite have different standard Gibbs free energies, thus even when ionic

medium standard states are used, the solubility products for the two minerals will have different values.

The most common use of such solubility products – particularly in ocean acidification research – is to calculate the saturation state of seawater with respect to a particular calcium carbonate mineral X. The saturation state, Ω_X, is defined by the expression: $\Omega_X = [Ca^{2+}]\ [CO_3^{2-}]/\ K_{sp}(X)$. If $\Omega_X = 1$, the solution is in equilibrium with that mineral phase, if $\Omega_X > 1$the solution is supersaturated with respect to that particular mineral phase, and if $\Omega_X < 1$it is undersaturated [55].

1.8 Nutrients

1.8.1 Nitrogen

Nitrification

Nitrification is a biological process that uses oxygen as an electron acceptor and CO_2 as a carbon source to oxidize NH_4^+ to nitrite/nitrate (NO_2^-/NO_3^-) under aerobic conditions. Under anaerobic conditions, the NO_2^- and NO_3^- produced by nitrification are used as electron acceptors in denitrification, anammox, and DNRA; therefore nitrification is an intermediate process that connects aerobic and anaerobic inorganic N cycles. Nitrification proceeds in two steps: oxidation of NH_4^+ to NO_2^- by an ammonia oxidizer; and oxidation of NO_2^- to NO_3^- by a nitrite oxidizer. The rate of nitrification is limited by low O_2; nitrifiers cease to work at O_2 concentrations of 1 to 6 µM. In coastal ecosystems increased rates of growth of phytoplankton can deplete O_2 concentrations and thereby decrease nitrification rates through O_2 deficiency [72,73, 74].

Anaerobic Ammonium Oxidation (Anammox)

Anammox bacteria consume NH_4^+ as an electron donor, NO_2^- as an electron acceptor, and CO_2 as a C source, and oxidize NH_4^+ anaerobically to N_2 under anoxic conditions. Nitrifiers oxidize NH_4^+ to NO_2^- or NO_3^-, which diffuses to anaerobic zones where anammox occurs. However, denitrifiers also consume NO_2^-, so competition for NO_2^- uptake with denitrifiers is a potent regulating factor for anammox activity. With respect to NH_4^+ supply, the mineralization of

organic matter and subsequent release of NH_4^+ are tightly related to high anammox rates; high anammox rates were observed in the upper oxygen minimum zones because high ammonification near the surface supplies NH_4^+ to anammox bacteria. However, the presence of organic matter can indirectly inhibit anammox rates because it accelerates denitrification, which in turn hinders anammox activity by competing for NO_2^- [72].

Denitrification

Denitrification is the conversion of NO_2^-/ NO_3^- to N_2 gas and is one of the processes by which fixed N moves from ocean to the atmosphere. Denitrifiers are heterotrophs and use NO_2^-/ NO_3^- as an electron acceptor and organic matter as an electron donor and C source. Most denitrifiers are facultative anaerobes that use O_2 as an electron acceptor when it is available, but use NO_2^-/ NO_3^- as an electron acceptor and reduce it to N_2 gas when O_2 is low.

The anaerobic conditions required for denitrification occur in coastal and shelf sediments and in ocean water columns in which ODZs are created by high O_2 consumption rates driven by organic matter decomposition coupled with low ventilation rates (e.g., Arabian sea, Black sea). Because most denitrifiers are heterotrophs that use organic C as an energy source, denitrification rates can be limited by organic C contents. Incubation experiments have showed that an input of organic C increased the denitrification rates in the ODZs of the Eastern Tropical North and South Pacific oceans and central Baltic Sea. However, under C-rich conditions such as benthic sediments and shelf regions, denitrification rates were limited by O_2 and NO_3^-, and C quality rather than C quantity [72].

pH likely plays an indirect role in controlling ammonia oxidation rates because it changes the chemical speciation of NH_3/NH_4^+ and covaries with other factors with depth and across ocean basins. At pH 8.0 in the ocean, NH_3 constitutes just 5% of total NH_3/$NH4^+$, and by 2100, ocean acidification could reduce available NH_3 by 50%. According to recent estimates, nitrification within the euphotic zone supplies NO_3^- that supports ~32% of global oceanic primary production, with another ~26% of oceanic primary production

supported by upwelled, previously nitrified NO_3^- by phytoplankton. This NO_3^- eventually remineralized to NH_4^+ will be substantially reduced by ocean acidification along with the proportion converted back to NO_3^- by nitrification, ultimately depleting upper water column NO_3^- over time [11].

All published data indicate that ammonia oxidation slows as pH decreases (11 and references within): across multiple experiments conducted in high and low productivity regions of two oceans, ammonia oxidation rates declined by 8–38%. If these findings are applied broadly, ammonia oxidation rates would decline by 3–44% in response to the 0.1 decrease in ocean pH expected over the next 20–30 y [11].

The ammonium-rich water when upwelled and mixed with overlying seawater will rise the pH. In the absence of light, nitrification will resume and nitrate will be formed; in the presence of light, phytoplankton will readily assimilate ammonium as a source of nitrogen for growth. Generallly, diatoms show a preference for growth on nitrate; this substantial shift in the chemical form of nitrogen supplied to phytoplankton communities would favor smaller organisms (e.g. dinoflagellates) that are more competitive for NH_4^+posing large diatoms at a disadvantage. This could potentially lead in the development of harmful algal blooms (HAB's) and in important implications for oceanic food webs, fisheries, and carbon export to the deep sea [11, 75].

Since nitrite and nitrate both serve as substrates for denitrifying bacteria, it is possible that the inhibition of nitrification and the subsequent reduction of nitrite and nitrate concentrations could result in a decrease of denitrification rates [75]. Especially in oxygen-depleted zones, if the upwelling water is low in nitrite and nitrate concentrations, denitrification processes could be substantially reduced resulting in the buildup of nitrogen and concomitant eutrophication phenomena with unpredictable potential ecological impacts [75].

In previous mesocosm experiments [76], it was suggested that decreasing seawater pH could affect sediment nitrogen cycling by impacting the process of nitrification. In the open ocean the impact of acidification on nitrification [75] demonstrated that rates of ammonium oxidation to nitrite or nitrate

(nitrification) were reduced by ~50% at pH 7, by >90% at pH 6.5 and were completely inhibited at pH 6 [77].

Changes in seawater pH have not been found to impact on the carbon or nitrogen content of sediments [77]. Experiments regarding benthic fluxes suggest that in coarse grain sediments pH decline led to increased ammonium release and decreased nitrate and nitrite release; in muddy sediments only ammonium efflux was found in pH<6 [77].

1.8.2 Phosphorus

Phosphorus in the ocean exists in both dissolved and particulate forms throughout the water column. Particulate P includes living and dead plankton, precipitates of phosphorus minerals, phosphorus adsorbed to particulates, and amorphous phosphorus phases. The organic and inorganic particulate and dissolved forms of phosphorus undergo continuous transformations. The dissolved inorganic phosphorus (usually as orthophosphate) is assimilated by phytoplankton and altered to organic phosphorus compounds. A large fraction of the organic phosphorus taken up by zooplankton is excreted as dissolved inorganic and organic P [78].

Dissolved inorganic and organic P is also adsorbed onto and desorbed from particulate matter sinking in the water column moving between the dissolved and the particulate fractions. Much of this cycling and these transformations occur in the upper water column, although all of these processes, with the exception of phytoplankton assimilation, also occur at depth, throughout the water column [78].

DIP depth profiles in the oceans exhibit a “nutrient trend” such that surface waters are depleted due to intense biological uptake in the euphotic zone and concentrations increase with depth as a result of conversion of organic P forms to DIP (also called regeneration). Within deep waters, an increase in DIP concentrations is also observed with increasing deep water age due to continuous accumulation of sinking particulate matter and its regeneration [78, 78]. The DOP depth distribution in the ocean, in contrast, is characterized by high concentration in the surface ocean, where most of the marine life which synthesizes these organic compounds. Much of this DOP is hydrolyzed by

bacteria to DIP (which is rapidly taken up and utilized by organisms) within the surface layer, and only a small fraction is transferred to the deep ocean; thus, the concentration of DOP is typically lower at depth. Interestingly, the DOP concentrations at depth in all oceanic basins are quite similar, suggesting a relatively long residence time for the majority of components of the DOP pool in the deep ocean [78].

Sediments are the main repository in the oceanic phosphorus cycle. P is delivered to marine sediments primarily as sinking particulate matter but P has been also associated with metal oxides and hydroxides. The relative contribution of specific sinks to P burial in the sediments depends on sedimentary redox conditions (abundance of oxidizing and reducing substances). Oxygen bearing (oxic) surface sediments are often rich in ferric iron and manganese phases which take up large amounts of phosphate by adsorption and mineral formation, while anoxic (oxygen-free) sediments are depleted in these phases so that phosphate is predominantly bound to calcium minerals [80]. Phosphorus in sediments can be remobilized during degradation of organic matter and reduction of iron oxides; when sediment is resuspended in coastal areas, significant amounts of DIP may be released into the water column. In areas of low oxygen bottom water concentrations, some of the pore water P may diffuse from the sediment into seawater [78].

Compared to nitrogen, relatively little research effort has been directed toward understanding the effects of high CO_2 on the marine phosphorus cycle. The dominant form of inorganic phosphorus in seawater at pH 8 is HPO_4^{2-} (~ 87%), but the fraction of $H_2PO_4^-$ will increase marginally with future acidification [36]. From limited previous experiments, no statistical significant effects of pCO_2 on P biogeochemistry have been reported [36].

1.8.3 Nutrient Ratios and Limiting factors

Redfield et al. 1963 noted that the ratio of C:N:P within particulate organic matter is ubiquitous at 106:16:1. Hence, they hypothesized that phytoplankton required these elements in the above ratios for balanced growth. Global oceanic surveys of dissolved inorganic nutrients discovered that over short time scales, N was the most important nutrient in limiting phytoplankton

growth in the open ocean [80]. In recent years, the debate of N versus P limitation has also come to include the role of trace elements, such as iron, and other nutrients, such as silica. With many studies showing the potential growth limiting effects of these other elements in various environments limiting the rate of N -fixation and the growth of N -fixing organisms [80, 72].

The effects of changing pCO_2 on phytoplankton stoichiometry (C:N:P) have been examined in many experiments. Despite this fairly large body of results, there is still no consensus on whether phytoplankton elemental ratios are likely to be altered in a systematic, predictable manner in a future acidified ocean [36].

1.8.4 Silica

DSi plays an important role in the production of phytoplankton and the burial of carbon in the coastal zone and in deep-sea sediments. Silicon is an essential nutrient for the growth of diatoms. Diatoms take up DSi and use it to build their siliceous cell wall or “frustule”. Consequently, transport of continental DSi to the oceans is an important component in oceanic primary production, a large part of which consists of diatoms [81].

Changes in Si inputs to marine ecosystems, especially in the coastal ocean, can significantly influence the species composition of oceanic primary producers, especially the balance of production between diatoms and non-siliceous phytoplankton [81].

Biogenic silica is produced by siliceous organisms in the photic layer. Marine organisms (e.g. diatoms, silicoflagellates, radiolarians) build up their skeletons by taking up silicic acid from seawater; after these organisms die the biogenic accumulated silica dissolves. Part of this flux is directly recycled in the surface ocean and part is exported to the deep ocean. The exported biogenic silica continues to dissolve as it sinks through the deep ocean, regenerating silicic acid [82]. Within sediments silica is a labile component: Some of the silicic acid produced from seabed dissolution diffuses up into the overlying water and another portion is mobilized and involved in the formation of aluminosilicate mineral phases [83].

The effects of CO_2 on silicon is similar to that of phosphorus. The dominant form of dissolved silicon in the ocean is silicic acid (H_4SiO_4), which, like phosphorus, comprises a buffer system in seawater. The relatively basic pKa values for the dissociation of H_4SiO_4 (pKa1 = 9.84, pKa2 = 13.2) mean that it is nearly all present in the fully protonated form at pH 8.Further decreases in seawater pH are unlikely to substantially shift the chemical speciation of dissolved silicon. Only a handful of studies have examined acidification effects on diatom silicification, and these few suggest that direct pCO_2 impacts are generally small. The biggest effect of pCO_2 that Milligan et al. observed [84] was not on live diatom cells but on dissolution rates of empty silica frustules; dissolution rates were much higher at 750 ppm CO_2 than at 370 ppm. They were uncertain about the reasons for these low-pH-enhanced silica dissolution rates, but their results do suggest the possibility that increasing pCO_2 could enhance Si remineralization rates from sinking particles, and thus potentially cause shoaling of silicate vertical profiles and increased Si availability in surface waters. At present, the P and Si cycles seem less likely to be directly affected by rising ocean pCO2, but they undoubtedly will react indirectly to the expected changes in the C and N cycles [36].

1.9 Trace Metals

The influence of changing ocean acidity and temperature on trace metal biogeochemistry is more complex than a direct pH/temperature relationship with solubility. Metal solubility is controlled by the interrelationship of inorganic solubility, organic complexation, redox chemistry, and the phytoplankton−trace metal feedback mechanisms [85]. In this section, typical trace metal biogeochemistry in seawater and sediment is stated for the analysed elements (Al, As, Cd, Cr, Co, Cu, Pb, Ni, V, Fe and Mn), thereinafter the OA impact on these elements' according to equilibrium sequences and simulation experiments that have been conducted globally.

1.9.1 Aluminium (Al)

The factors that control the concentration and distribution of dissolved Al in seawater are poorly known. It has been proposed that Al is regulated by thermodynamic equilibria between seawater and various aluminosilicate

minerals found in marine sediments**.** The geochemical cycles of Si and Al in seawater are coupled. Al, however, is not incorporated into the siliceous cells of living diatoms and subsequently released by dissolution after the death of the organisms as would be expected [86].

The nutrient-like distribution of dissolved Al in the Mediterranean was first attributed to be biologically controleld due to the observed correlation with dissolved Si [87]. The general pattern affecting the biogeochemical cycle of dissolved Al in the Mediterranean Sea is that dissolved Al concentrations are probably produced by Al dissolution of eolian dust and advective mixing of Al-rich deep waters into the surface layer, balanced by biologically associated removal processes. The Al removed from the surface layer redissolves during settling in the deep water to raise Al concentrations at high levels [87].

1.9.2 Arsenic (As)

The dissolved arsenic species are limited to arsenate [As(V)], arsenite [As (III)], and the organoarsenic compounds, monomethylarsonic acid (MMA) and dimethylarsinic acid (DMA) with the latter three species being derived from biological activity. As(III) is a thermo- dynamically unstable oxidation state which is maintained in oceanic surface waters by continual biological reduction of As(V). The concentration of total dissolved arsenic in seawater is normally between 1.0 and 2.0 µg/l (13-27 nmol l^{-1}). Aside from one report of appreciable particulate arsenic in a coastal region, arsenic in this phase is negligible in seawater [88].

Phosphorus and arsenic have similar chemical properties and display similar geochemical behaviors; whereas phosphorus is an essential nutrient, arsenic is toxic to most living organisms. Nevertheless, phytoplankton readily uptakes As dependently on the availability of dissolved phosphate and is subject to some discrimination [89].

The sediments are the largest geochemical reservoir of arsenic, containing in excess of 99.9% of the element [88]. Arsenic concentrations in near-shore unpolluted marine sediments are normally between 0.1 and 50 µg/g. In sediments subject to anthropogenic inputs, especially from mines and smelters, the arsenic content can exceed 1000 µg g^{-1}; the capacity of marine

sediments to bind up large quantities of arsenic derived from human activities is noteworthy, however [88].

The mobility of arsenic is closely linked to iron biogeochemistry. Fe (hydr)oxide minerals strongly adsorb dissolved inorganic arsenic via complexation. Reductive dissolution of these (hydr)oxides can release dissolved arsenic into the porewater and result in fluxes of arsenic to the overlying water column [64]. Sediment fractionation studies reveal that, arsenic is also associated with organic and carbonate. These two phases bind a very minor portion of sedimentary arsenic. Arsenic levels in anoxic sediments are similar to those in oxic sediments but it is associated with quite different mineral phases in these two environments. As release from the decomposition of organic matter in sediments has not been demonstrated, even in anoxic sediments where ammonia and phosphate concentrations increase markedly with depth [88].

1.9.3 Cadmium (Cd)

Cadmium presents an ocean distribution closely related to the phosphate/nitrate distributions [90]. In seawater cadmium is thought to exist almost entirely as $CdCl_2$ and $CdCl^+$ complexes. There is no evidence for the organic chelation of cadmium in seawater. In anoxic conditions, cadmium may be present as the soluble bisulphide complex [91].

The adsorption of cadmium on to particulate material increases with increasing pH, but decreases with increasing ionic strength. In seawater, cadmium uptake by particulates is negligible. The only inorganic components to show appreciable adsorption of cadmium particularly in seawater, are hydrous manganese oxides, but their importance is concentration dependent [91]. The observed desorption of cadmium from sediments by resuspension in seawater is greater than for any other heavy metal. The controlling factor in remobilization is redox potential, which regulates the solubility of manganese, which in turn regulates cadmium availability. Manganese, and hence cadmium, can be mobilized under anoxic conditions and coprecipitated under oxic conditions [91].

The background concentration of cadmium in all waters is between 0.01 and 0.1 µg l^{-1} and 0.1-1.0 µg g^{-1} Cd dry weight in sediment. Generally, increased surface concentrations are encountered in land-locked and shallow seas, as are found in the Mediterranean, Baltic and North Sea, where circulation and turnover of the water masses are limited and/or estuarine/atmospheric inputs are large. The mean surface water values in the seas cited above are 2-4 times greater than those of the open oceans. In deep ocean waters, the dissolved cadmium concentration increases from 0.01 µg/l at the surface to about 0.1 µg/l at a depth of 1000-2000 m and bears a direct relationship to the dissolved phosphate concentration [91].

The depletion of cadmium (and phosphate) in surface waters relative to deep water may be explained by its uptake by plankton and subsequent loss from the faecal pellets produced by grazing zooplankton. Some cadmium will not be regenerated and return to surface through upwelling, it will accumulate in the sediment and therefore elevated levels of cadmium may be expected in sediments underlying areas of high productivity [91].

1.9.4 Chromium (Cr)

Chromium can exist in the oxidation states of Cr(III) or Cr(VI)which then controls its aqueous concentrations, the toxicity of chromium but also its mobility in different geologic environments. Chromium chemistry is quite complex. Cr(III) can be oxidized to Cr(VI) by dissolved oxygen when available and but the main oxidants are the higher valent manganese oxides; there are many reductants (e.g., Fe(II), organic matter, S^{2-}) that can reduce Cr(VI) to Cr(III). Aqueous concentrations of Cr(III) are primarily controlled by precipitation/dissolution reactions of Cr(III) compounds whereas aqueous concentrations of Cr(VI) are controlled either by precipitation/dissolution or by adsorption/desorption reactions in near-neutral to acidic conditions [92].

1.9.5 Cobalt (Co)

Cobalt is an essential micronutrient for phytoplankton growth in the oceans as the central metal cofactor in vitamin B_{12}, but the processes which control its geochemistry in seawater are poorly understood. Depth profiles of Co in the oceanic water column do not display nutrient-like features seen for other

micronutrient trace elements but rather a scavenged-type distribution displaying decreasing concentrations with depth [93, 94]. This has been attributed to redox processes, analogous or related to the geochemistry of Mn leading to enhanced scavenging in mid and deep waters in oceanic water columns.

Cobalt can exist as Co(II) or Co(III) within the pH and Eh range of natural waters. Co(II) exists as a divalent cation which can form strong but labile organic complexes. Co(III) forms inert complexes or oxides. Co(III) is the thermodynamically favored state in oxygenated seawater and Co scavenging in the water column may be due to the oxidation of soluble Co(II) to particle reactive or inert Co(III) on surfaces. The oxidation of Co(II) to Co(III) can be accomplished by coprecipitation with Mn oxides by Mn-oxidizing bacteria and is thought to be an important mechanism for cobalt removal in coastal waters [93]. Since Mn is also removed by oxidation of soluble Mn(II) to insoluble Mn (III,IV) oxides, this could account for the similarities in their geochemistries [94].

1.9.6 Copper (Cu)

Copper is a transition element, with oxidation numbers +1 and +2, and is a vital trace element for most organisms.The surface oxidation of its minerals leads to the release of the Cu^{2+} ion, which may be bonded with carbonate and oxides. Thus, these natural sources feed the marine environment with copper through the leaching of soil, rivers and atmospheric deposition [95]. Many industrial processes contribute significantly to the pollution of the seas by copper, such as plating, jewelery and electric cables, galvanization, electronic circuits, etc. with the most significant anthropogenic addition coming from copper extraction and metallurgy [96, 97].

Copper is normally depleted in the surface layers, as are the nutrients nitrate, phosphate and silicate with scavenging mechanisms prevailing in deep and intermediate waters [97]. Generally, in enclosed bays and coastal areas, Cu largly precipitates in particulate form relatively close to its entrypoint. Research has shown that the largest proportion of Cu in recent sediments directly affected by anthropogenic activities is incorporated outside the

mineral matrix, associated with organic substituents and authigenic sulphides. However, despite the significantly increased concentrations of Cu in many coastal areas of the world, the concentration of the open seas has not been measurably affected [96].

Like zinc, copper in aerobic conditions can be released from particulate matter, due to oxidation of organic matter, desorption and formation of ionic pairs and complexes. The desorption of copper by the suspended solids depends on the dilution ratios and the pH of the seawater [96].

1.9.7 Lead (Pb)

Pb follows all known input mechanisms in the marine environment, but is transported mainly through the atmosphere. For this reason, the vertical distribution of Pb has a maximum in surface water. The rivers feed the sea with Pb in particulate forms, colloid-soluble complexes with organic ligands and soluble ionic pairs and complexes with inorganic substituents. The vast majority of these forms are precipitated by particulate phases in coastal waters and only a small fraction of soluble Pb reaches the open sea. Thus, Pb is removed from the water column very quickly, mainly attached to disintegration products of biological origin. In sea sediments, a large proportion of Pb is associated with organic substitutes and sulphides, with a significant portion of it being bound to iron and manganese hydroxides, as well as to carbonate minerals [96].

1.9.8 Nickel (Ni)

Nickel in the water column presents a nutrient-like distribution, resembling to those of phosphate and silicate. Although Ni has no reported biochemical function, it is clear from vertical profiles that the element is involved in the cycle of surface uptake and deep regeneration characteristic of all chemical species incorporated in organisms [90]. The nickel contents of near-shore surface waters range between 0.5 and 5.2 μg l^{-1} with an average of 1.8 μg l^{-1}; those of the open-ocean waters vary between 0.3 and 3.4 μg l^{-1} with an average of 1.2 μg l^{-1} [99].

1.9.9 Vanadium (V)

The concentration of vanadium in natural waters is very low and usually in the range 0.5–2.5 μg l^{-1}. The redox chemistry of vanadium leads to a decrease in the solubility of this element on going from an oxidizing to reducing environment [101]. $VO_3(OH)_2$ is the dominant form of V above pH 7.4 [100].

Upon extraction of the crude oil and accidental deposition on surface sediments, bacterial decomposition, dissolution and oxidation of most of the organic components, V can be incorporated in the sediment load, increasing the background levels of metal content of the local sediment [101].

Release of dissolved V from the sediment, through remobilization processes, is supposed to be negligible: (i) vanadium seems to be present as a refractory element in deep suspended matter,being hardly mobilized through alteration processes. Up to 70% of the anthropogenic V content of dust is solubilized when entering seawater but not mobilized through biological uptake. Much of this anthropogenic flux seems to be redeposited close to its sources; it is estimated that only 10% reaches ‘remote areas'.[102]

V is distinguishable from other trace metals like Cd, Cu, Ni or Pb which show noticeable enrichments in the Mediterranean Sea as compared to their mean oceanic concentrations. In addition, no strong variation is observed and in particular no surface or deep enrichments such as those observed for the above-mentioned trace elements. This indicates that biological uptake in the Mediterranean is not efficient enough to remove V from surface waters. On the contrary, the Mediterranean water seems to be slightly depleted (10%) which may be explained by an efficient scavenging onto suspended matter [102].

1.9.10 Iron (Fe)

Iron is one of the most reactive elements in aquatic environments, and its cycling is coupled to that of the major biogeochemical elements (C, O, S and P) and heavy metals. Apart from nutrients’ availability, Fe also has been speculated to have a limiting control on primary productivity. In the hydrosphere it is present under two oxidation states, II and III, which are thermodynamically stable under anoxic and oxic conditions, respectively.

Fe(III) forms complexes with organic acids and oxyhydroxide colloids [103]. Iron solubility in surface seawater is low, ranging in the picomolar and low nanomolar levels depending on temperature, and the speciation is largely controlled by organic complexation and photochemical redox processes [104; 105].

Iron inorganic speciation and organic complexes in seawater is very complex and not yet fully understood. In general, iron in oxic seawater around pH 8 is present predominantly in the particulate iron oxyhydroxide, which has an extremely low solubility, and thermodynamically stable 3+ oxidation state [104]. Recent studies suggest that the Fe(III) solubility is controlled by organic complexation [103, 104] which, subsequently, regulates dissolved iron concentrations in seawater.

Fe(III) oxyhydroxides undergo reductive dissolution in most aquatic sediments. The reductive dissolution can be coupled directly to the oxidation of organic matter by specialized bacteria, or it may proceed via abiotic reactions with inorganic or organic reductants [103].

1.9.11 Manganese (Mn)

In nature Mn occurs in three different oxidation states, +II, +III, and +IV. In general, Mn(II) is thermodynamically favoured in the absence of oxygen and at low pH, whereas Mn(III) and Mn(IV) are favoured in the presence of oxygen and at high pH [106]. The redox properties of manganese (Mn), make it central to a variety of biological processes and result in significant and often rapid biogeochemical cycling that is mediated by abiotic and biotic oxidation and reduction, biological uptake, and mineral formation [107].

Manganese occurs in seawater mainly as Mn^{2+} or $MnCl^{+}$ [107] but may also occur as insoluble phosphates and carbonates or as a minor constituent of other minerals. Mn (II) can exist up to millimolar concentrations in natural waters, even in the presence of oxygen. Due to the high activation energy, the oxidation of Mn(II) to Mn(III) and Mn(IV) is largely catalyzed by microorganisms and requires oxygen in most cases although Mn(II)→Mn(IV) oxidation coupled to denitrification is thermodynamically favorable [106]. At the conditions prevalent in seawater (EH +0.4 V, pH 8), the stable form of Mn

is seen to be the aqueous species, Mn^{2+}, and not any of the solid phases of Mn. The fact that Mn oxides are abundant on the seafloor can be explained on the basis that the Mn oxyhydroxides initially formed in seawater are not pure mineral phases but have significant concentrations of transition elements and are fine grained, both of which help to stabilize them [107].

The dissolved Mn concentration in the open ocean is in range 0.2-3 nmol kg^{-1} which is above the equilibrium concentration with respect to MnO_2 or MnOOH. This situation reflects the slow rate of oxidation of Mn^{2+} in solution. Photoreduction of particulate MnO_2 to Mn(II) takes place in the surface waters resulting in 99% of the Mn in the surface waters (0-100 m) being in the dissolved form. By contrast, only 80% of the Mn in the deep water (500-4,000 m) is in the dissolved form, Mn therefore behaves in seawater as a scavenged-type metal. Mn is also influenced by redox processes in the water columnwith both dissolved and particulate Mn display maxima at the oxygen minimum zone [107].

1.9.12 Fe and Mn Oxy-hydroxides biogeochemistry

Fe-Mn oxy-hydroxides shuttle (diffusion of reduced and dissolved Mn and Fe oxyhydroxides from suboxic/anoxic zone of sediment into oxic sediment-water interface and subsequent precipitation Fe and Mn as oxyhyroxides) is an important mechanism for i) removal of many toxic elements and trace metals from water into sediment and, ii) microbial stratification in sediment and sediment-water interface [12, 24, 108].

Iron and manganese hydr-oxides are characterized by competitive adsorption capacities similar to those of clay; this supports the reliance that Cd and Cu distribution is ultimately determined by the solubilization/precipitation of Fe and Mn oxy-hydroxides [109].

A wide range of organic and inorganic compounds are able to chemically reduce manganese and iron oxides. These possible reductants include: sulfide, nitrite, Fe^{2+} (for manganese oxides), organic acids and certain aromatic compounds [110]. For diverse dissimilatory metal-reducing bacteria, Mn oxides serve as excellent electron acceptors in the oxidation of organic matter or H_2 in the absence of O_2. Mn oxides also abiotically oxidize a variety

of reduced inorganic and organic compounds; they can oxidize natural organic matter producing low-molecular-weight organic compounds, hydrogen sulfide, Fe(II) and reduced forms of other metals such as Se, As and Cr influencing toxic metal availability by oxidative precipitation or solubilization. Mn oxides possessing high sorptive capacities, adsorb a wide range of anions controling the distributions and bioavailability of many toxic/essential elements [106]. As biotic and abiotic processes both play important roles in the oxidation and reduction of Mn biologically Mn(II) oxidation is generally fast relative to abiotic Mn(II) oxidation processes suggesting the former is the dominant process in the environment [106].

1.9.13 Benthic Fluxes at the Sediment / Water Interface (SWI)

For most elements present in seawater, a variety of reactions taking place in the seawater-sediment system can involve both release and uptake of dissolved components to or from the solid phase of sedimentAt the sediment/water boundary, substances in the dissolved phase can be exchanged with the interstitial water and move along the sediment, in an ascending or descending direction, through diffusion (migration through interstitial water from higher to lower concentration regions) and advection (flow of pore water through the sediment because of pressure gradient). Bioturbation and bioirrigation are organism-mediated processes that result in a transport of interstitial water along the sediment column influencing also the diagenetic reactions.

Benthic fluxes affect the element’s concentration in both interstitial water and overlying seawater. When a positive benthic flux prevails, the sediment acts as a source of dissolved elements for the overlying water, releasing thus elements that had been previously deposited on the sea bottom. The question posed is whether this mechanism is significant on a local or global perspective and whether it may represent a measurable threat in areas with contaminated sediments. Loss of metals from sediments to the overlying seawater, may occur not only in fine-grained organic-rich contaminated sediments, but also in sandy sediments that suffer occasional hypoxia due to an occasional increase of organic matter deposition on the seafloor [111].

It seems that in polluted near-shore sediments the confinement of anthropogenic trace elements in subsurface layers of anoxic sediments may present an important secondary pollution source for the overlying seawater. Because the Mediterranean Sea coastline is densely populated, hosting a multitude of urban and industrial activities, contaminated near-shore sediments are present along great parts of the coast and the magnitude of their impact on trace element enrichment of the marine coastal environment has to be evaluated. In the deep Mediterranean Sea, there are already indications that sediments may also have enhanced metal concentrations, which could be attributed to contaminated settling particles linked to a diffusion flux from the metal-enriched interstitial water. Trace elements transported to the seafloor with biogenic or non-biogenic SPM, after burial in the sediment they can be released into the interstitial water through diagenetic reactions and migrate towards the sediment surface together with dissolved Mn formed in the reducing sub-surface layers. On the oxic sediment surface trace elements can either co-precipitate with solid Mn-oxides enhancing thus the metal concentrations of the surface of deep-sea sediments, or be released in a dissolved form into the overlying water [111].

1.10 Ocean Acidification and Trace Metal Biogeochemistry

1.10.1 General Aspects

Both OH^- and CO_3^{2-} form strong complexes in ocean water with metals that are divalent and trivalent [112]. These anions are expected to decrease in surface waters by 82% and 77%, respectively due to CO_2 increase. Metals that form strong complexes with OH^- and CO_3^{2-} will have a higher fraction in their free forms at lower pH. These changes in speciation will also increase the thermodynamic and kinetic activity of these metals. Metals that form strong complexes with chloride will see little if any change in speciation because decreasing the pH will not change the chloride concentration [112].

The lower pH will also affect the adsorption of metals to organic material. Acidification in the ocean also leads to an increased concentration of H^+. As a result, competition for binding sites increases between H^+ and metals. Surface

sites become less available to adsorb metals in the presence of increasing H^+, potentially making acidification and metal toxicity antagonistic [113].

Furthermore, most organic particles in seawater are negatively charged. As pH decreases, the surface sites will become less available to adsorb metals. Finally, most metals are more soluble in acidic waters so their concentrations are expected to change as well [112].

The effect of pH on the speciation of metal organic complexes in the marine environment is not as well characterized as the inorganic ligands due to the nonhomogenous composition and unknown structures of the organic ligands. It is highly likely that the marine dissolved organic material that can complex metals will be a function of pH. This relationship is due to the presence of phenolic and carboxylic functional groups present on organic material that may be responsible for the chelation of metals. These substances exhibit a charge dependence that is a function of pH, and each bind metals with varying degrees of strength [112].

Additionally, any changes in the processes taking place in the upper section of marine sediments have an intense effect on global cycles of many trace elements; CO_2 leakage and acidification can significantly alter these biogeochemical processes with profound impacts on bacterial processes and other biological activities. Especially coastal sediments subjected to elevated anthropogenic inputs of certain toxic metals [12], after CO_2 leakage and acidification they are expected to be source for some toxic metals [108]. The mobilization of metals due to CO_2 seepage in the sediment and from the suspended matter in the water column depends on: i) dissolution of particles and release of adsorbed metals on the surface of the solids, and ii) changes of decomposition rates of biogenic particulate material due to decreased pH and pE. The effect of CO_2 on the mobilization of metals depends on whether the sediment and the suspended matter originate from biogenic materials or consist mainly of inorganic particles such as iron and manganese oxyhydroxides. Additionally, sediment characteristics such as organic matter content, geochemical and physical conditions (porosity and size distribution) of the sediment may play important roles on the metal solubility under CO_2

seepage. Control of the trace metal mobilization by the microbial community also cannot be ruled out [24].

Metals such as Cu^{2+} form strong complexes with carbonate. Such metals will be more affected by acidification and their free ionic concentration (which is generally more toxic than complex forms) will increase by as much as 115% in coastal waters in the next 100 years due to reduced pH [113, 114].

Other metals such as Cd^{2+} form strong complexes with chloride; since Cl^- is pH insensitive, speciation of Cd will be minimally affected by OA [113, 25].

Specifically for Fe, at the current pH of seawater, Fe(III) is at its minimum solubility. As pH decreases, solubility increases. A decrease in pH from 8.1 to 7.4 will increase the solubility of Fe(III) by about 40% [105, 112]. Through experimental studies [105], increased dissolved Fe concentrations were found during higher CO_2 treatments which were partly attributed to biological activity. In addition, higher CO_2 treatments showed higher Fe(II) values compared to lower CO_2 treatments. The solubility of Fe(II) is significantly greater than for Fe(III) and at lower pH levels the oxidation rates of Fe(II) are much lower; Also, reoxidation of Fe(II) to Fe(III) is expected to enhance the formation of Fe colloids and induce severe changes in organic iron complexation and Fe(II) oxidation rates. The relatively slow Fe(II) oxidation rates at low pH may increase the bioavailability of iron via allowing for a larger standing stock of Fe(II) in higher CO_2 systems. Apart from that, mobility and dissolution of iron can influence the mobility of other metals that are associated with the solid phase of iron in the sediment (such as oxides or sulphides). For example, it is known that adsorption on Fe (III)-precipitates is the main mechanism responsible for As migration in an oxidising environment. Under acidic conditions, arsenate is less soluble than arsenite and can therefore be adsorbed more easily onto Fe (III)- precipitates.

Additionally, the influence of changing ocean acidity and increasing temperature on trace metal biogeochemistry is more complex than a direct pH/temperature relationship with solubility. Me solubility is controlled by the interrelationship of inorganic solubility, organic complexation, redox chemistry, and the phytoplankton trace metal feedback mechanisms. The majority of the

total concentration of bio-active metals such as Fe, Co, Cd, Cu, Ni and Pb are not in their inorganic form, but bound to organic complexes. The ligand-bound fraction of metals can be up to 100% for Co [94], >99% for Fe and Cu and >70% for Cd [85]. Possible effects of rising oceanic CO_2 concentrations on organic Me ligands will therefore play a major role in overall trace metal bioavailability in the future ocean [85]. Apart from temperature rise and pH decline, model predictions suggest a future increase in precipitation, water vapor and evaporation, while regional variations are pronounced. Altered patterns in wind and precipitation, as well as riverine transport, will ultimately modify the supply of trace metals to the open ocean; climate change is, therefore, likely to influence global trace metal biogeochemistry by affecting both metal sources and cycling in the future ocean [85].

1.10.2 Experimental Studies on Ocean Acidification effects on trace elements

Several experimental studies have been published regarding various marine ecosystems investigating trace element fate under decreasing pH [e.g. 105, 24, 108, 76, 77, 113, 25, 26, 115, 116, 117, 118].

Through experimental studies [108] in Trondheim Fjord, Norway, it has been shown that CO_2 seepage dissolved metals in the sediment and suspended particles in the seawater and mobilized metals such as Fe, Mn and Co. However, as the experiment proceeded this mobilization was observed in a lesser extent; it was suggested that an initially enhanced release of Fe, Mn, and Co from sediment was found with a subsequent decline in dissolved metal concentration enrichment due to effective extraction of the easily leachable metal fractions from the sediment and suspended particles. The same study also indicated that Fe-Mn shuttle in surface sediment and sediment-water interface was disturbed by CO_2 leakage and acidification possibly causing enhanced concentrations of toxic heavy metals and trace elements in the seawater.

De Orte et al. [115], through an experimental setup in Huelva estuary (South Spain), have shown that a linear decrease of total As is observed as the pH of pore water decreases in areas with large amounts of Fe. Therefore, total As is

less available in the sediments when the pH decreases; however, an increase of the toxicity occurs due to the increased proportion of the most harmful species of arsenic, As (III). Additionally, in the same experiment, porewater Co, Pb increased as pH decreased while Cr remained unaffected.

Ardelan et al., [24] have also suggested similar trends for other trace metals as well in previous experiments regarding a Trondheim Fjord (Norway). Al and Cr were found elevated in dissolved forms under higher pCO_2 experimental conditions. This was attributed to either the effective removal of dissolved Al and Cr as a result of the presence of excess suspended particle, or an increase in the solubility of Al and Cr due to enhanced CO_2 acidification with time. Dissolved fractions of Ni, Cu, Cd and Pb all increased in higher CO_2 concentrations relative to control. Increase in the dissolved fractions of Ni, Cu and Cd (DNi, DCu and DCd) with CO_2 seepage was substantial in the early stage of the experiment. These data suggest that in addition to a direct extraction from the sediment, dissolution of all metals from the suspended material become more effective especially for Ni, Cd and Cu in the early phase of the CO_2 leakage.

Atkinson et al., [26], conducting an experimental study in New South Wales, Australia, has shown that under various pH values (high=8.1, mid=7.2, low=6.0), Cd, Mn and Pb were only released from sediment in the low treatment, while Fe was released in both mid and low pH treatments. Atkinson et al. also suggested that metal release from metal-contaminated sediments was influenced by Fe/Mn redox chemistry namely by pH impact on (i) the rate of oxidation of Fe(II), and (ii) the binding of metals to organic-, Fe- and Mn-based metal-binding phases.

Similarly, Rodriguez-Romero et al. [116] also examining three pH treatments in Southwest Iberian Peninsula (pH: 7.1, 6.6 and 6.1) found an increase of Fe, Mn, Cu and As in seawater in the lower pH values, with the Cu and As increase being greater in contaminated sediments.

In conclusion, trace element biogeochemistry is strongly affected by OA but through various studies it becomes obvious that there is not a unique pattern

determining their distribution. Trace metal fate is strongly affected by a complex grid of processes (e.g. site specific physicochemical characteristics: T, salinity, pH range) and reactions (e.g. dissolution, precipitation, OM remineralization). Additionally, the final main concern regarding these elements is their possible toxicity on living organisms; the main factor controlling trace metals biological effects is their chemical speciation, rather than their total concentration. Even if OA does not affect directly dissolved or particulate Me concentrations, it has been well documented to alter several Me speciation or complex ability, ultimately determining their availability and fate in a particular system.

Many changes have been marked theoretically for heavy metals due to pH reduction, mainly on the basis of the various bonds with which they are found in seawater. However, physicochemical parameters that determine coastal systems to a greater extent than open ocean are a further variable to be investigated in order to fully comprehend OA's impact practically. Experiments that have been carried out (and have been reported in 1.9.2) focus on specific metals or groups of metals without considering other elements (such as organic carbon or nutrients), the sequence of their biogeochemistry and how these interelations could be influenced by possible pH reduction. Finally these sequences, coupled with the distinctive physicochemical conditions governing coastal systems, are thought to be significant and possibly more sensitive to alterations that would not act individually but in synergy,with unpredictable outcomes for the final form of the data.

CHAPTER : 2

STUDY AREA – SAMPLING PROCEDURES – GENERAL EXPERIMENTAL SETTINGS

2.1 Study Area Characteristics

Elefsis Bay is a small and shallow (68 km^2 with a mean and maximum depth of 20 m and 35 m, respectively), almost enclosed embayment in the Aegean Sea (Longitude: between 23° 25’ 48’’E, 23° 36’ 36’’E; Latitude: between 27° 59’ 24’’ N and 38° 03’ N; Eastern Mediterranean Sea). It is located northern of Saronicos Gulf and is connected to Saronikos by narrow and shallow channels on both the eastern and western side (8 m minimum depth at the western and 12 m minimum depth at the eastern; **Figure 1**).

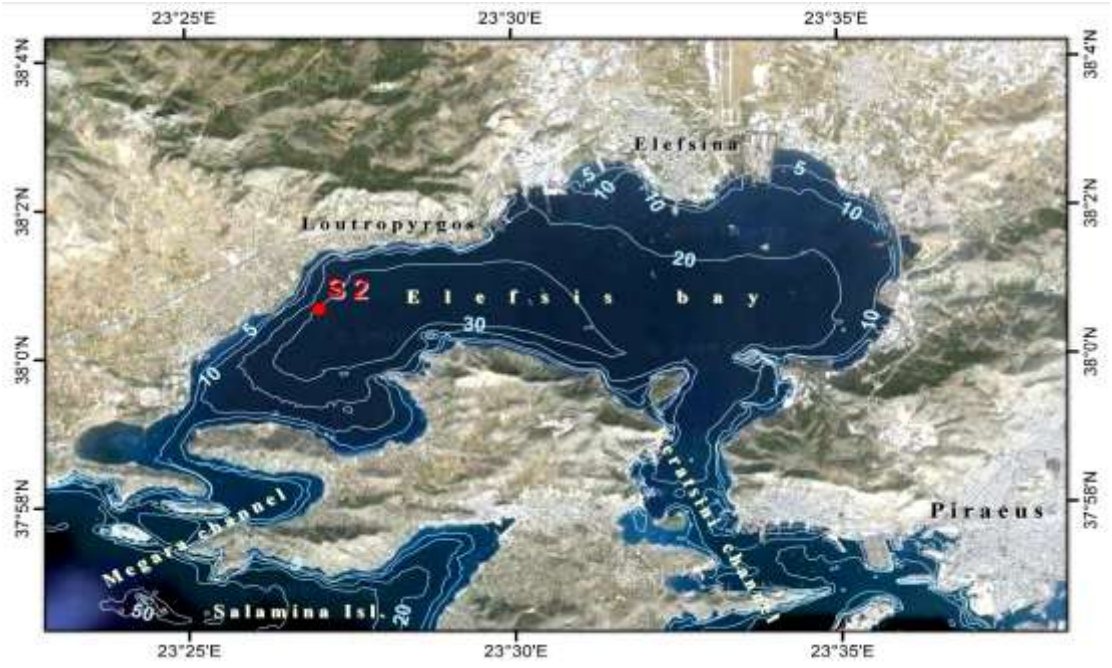

Figure 1. Bathymetric map of Elefsis Bay, Attica, Greece

Elefsis Bay bathymetry is differentiated in two parts; the eastern part with smaller depth (10–25 m) and the western part, tectonically subsided, which shows depth of more than 30 m and which acts as a sediment trap [119].

The sea water of the Elefsis Bay, being an almost isolated shallow water body, is strongly coupled with the atmosphere and exhibits a broad seasonal

cycle in its temperature and salinity throughout the year [119]. Water circulation in the gulf of Elefsis is both thermohaline and wind driven. Surface waters enter the bay via both channels, mix with less saline waters and exit again via both channels [120]. Water circulation in the summer is influenced by a temperature difference between the water in the bay and the Saronic Gulf. A net flux from east to west of 450 m^3/s has been reported by various studies. In the winter, a much lower, reversed water flux of 240 m^3/s is observed, caused by differences in salinity [122].

Due to its specific morphology and water circulation, the bay experiences hypoxic or intermittently anoxic conditions in its deeper part, during the stratification period [119]. During autumn and winter months however, episodic rainfalls provide freshwater into the bay through four ephemeral streams, the small Koumoundourou Lake (via a narrow channel) as well as via submarine groundwater discharges, resulting in lower salinity values in both surface and bottom waters [121].

The Elefsis Bay differs from the Saronikos Gulf not only regarding its morphology, but also in the extent of pollution suffered during the last decades [119, 122]. The industrial zone of Athens is situated at the Elefsis area with numerous polluting activities including shipyards, oil refineries, food industries, iron steelworks, cement factories, cable manufacturing, waste recycling plants, landfills, military installations including a naval military base and an airport [124]. For several decades, the industrial activity in the wider Thriasion-Elefsis basin along with the shipping activity has contributed in sizeable volumes of wastes to Elefsis Bay waters and sediments [122]. Additionally, apart from direct inputs to the bay's waters/sediments some activities contaminate the soils or the groundwater affecting the marine environment via runoff and/or submarine groundwater discharges [124].

Elefsis Bay also constitutes the natural marine gateway of the city of Athens and the Piraeus harbor which receives the treated wastes of ~4 million people through a bottom source at a depth of 65 m in the northeast just south of the Psittalia island. Until 1994, Keratsini channel was receiving the untreated domestic and industrial sewage of the Athens Metropolitan area which was discharged into the surface water layer of the channel and enriched the bay

with metals, nutrients and organic matter. After1994, the sewageofthe Athens Metropolitanarea was primarily treated in the Psitallia Sewage Treatment Plant and discharged into the inner Saronikos Gulf. Additionally, by the end of 2004, the secondary stage of the Psittalia Sewage Plant has become operational [119]. In conclusion, extended water pollution caused by both organic matter and metal enrichment from hot spots has been well reported in Elefsis.

More recently, Elefsis Bay was recognized as an area of major environmental concern in a report on priorities for the Mediterranean environment, jointly issued by the European Environment Agency (EEA) and the United Nations Environment Programme/Mediterranean Action Plan [122, 125].

2.2 System Biogeochemistry

Water Column

During the warm period (May–late October) a strong temperature-driven pycnocline is developed in the deepest western part (>25 m depth) of the Bay resulting to insufficient oxygen supply from either atmospheric or photosynthetic sources and subsequently to the isolation of the deeper waters. Documented anoxic conditions in the area date back since 1973 [119]. The anoxic layer in Elefsis Bay is an intermittent feature that is developed every year but its intensity varies; as a consequence, the near-bottom layers remain periodically hypoxic and anoxic (0.00 mM) with parallel accumulation of silicate, phosphate and ammonium near the sediment-water interface (SWI [119, 126]).

Depth profiles at Elefsis Bay have shown that in winter DO, ammonium, nitrite, phosphate and silicate concentrations remain almost stable with depth. During the stratified period (August–October), nutrients and oxygen remain constant between 0 and 10 m; below 10 m, there is a rapid decrease of oxygen reaching near extinction at 20 m and anoxia near the bottom. The thickness of the hypoxic/anoxic zone varies between the sampling periods from 1-3 m to 8–10 m above the bottom. The ammonium concentrations increase significantly with depth against nitrite and nitrate in parallel with silicate and phosphate, suggesting the occurrence of organic matter

remineralization processes [119]. Regarding phosphate, the fraction of sediment-released phosphorus increases rapidly when oxygen concentration declines significantly. Sorbed phosphate is released from sediments to pore waters from host Fe-oxyhydroxides. Once released to pore waters, phosphate can escape from sediments via diffusional transport, resuspension, or irrigation by benthos [119]. Increased silicate is produced by the biochemical degradation of biodetritus, either in the water column or at the sediment interface [127].

The chemical characteristics of the anoxic layer indicate that denitrification occurs, even though this has not been confirmed by direct measurements of denitrification or measurements of sulfide concentrations. Denitrification and nitrate reduction are apparent from the decrease and disappearance of nitrites and low values of oxygen with increasing depth [128]. In the absence of oxygen, facultative heterotrophs switch over to alternate respiratory oxidants (electron acceptors) and the most abundant in seawater is NO_3^-. Denitrification removes most of the NO_3^-, and as sulfate reduction sets in, NH_4^+ accumulates in the anoxic waters. The ammonium, phosphate and silicate accumulation results from the oxidation of organic matter accompanying the reduction of first nitrate and then, sulfate [131]. MnO_2 reduction follows, with Mn^{4+} being the electron acceptor, followed by SO_4^{2-} as an electron acceptor, and sulfate reduction occurs with H_2S accumulation in anoxic waters [119]. However, there is no available time series of dissolved and particulate manganese in the Elefsis Bay; data concerning the period 1992–1995, showed that in many cases (i.e. September 1994), elevated dissolved (112 mg/L) and particulate Mn (171 mg/L) concentrations were recorded in the near-bottom waters when anoxic conditions occur but the role of Mn in the area has not been established yet [119].

During the September period, however, nitrate and nitrite peaks are normally observed at 20 m; in some cases, waters with adequate oxygen contain relatively high amounts of nitrite. This relatively high nitrite content could be explained either by the reduction of nitrate or by the oxidation of ammonium. Previously, anoxic peaks of NO_3^-, ingrowth of N_2, and reduced NH_4^+ concentrations have confirmed anoxic nitrification [132]. Similar findings have

been pointed out through time series for Elefsis [119] possibly indicating suboxic/anoxic nitrification process. Despite that no data of manganese exist to support this hypothesis, probably, manganese reduction occurs via suboxic nitrification [132, 133]. According to Scoullos [122, 134], in Elefsis bay, at a depth where oxic /anoxic conditions occur, Mn^{4+}, present mainly as MnO_2 in the sediments, is reduced to dissolved Mn^{2+} which eludes from the sediment and moves slowly upwards. As oxygen becomes available, Mn liberated from the sediments quickly re-precipitates as MnO_2 at the interface of the oxic/anoxic layer which is very close to the bottom. According to this theory, it is obvious that the Mn oxide dissolution and precipitation can play an important role in the water chemistry and act as a chemical process analogous to the physical resuspension of bottom sediments.

DIN:DIP ratio also decreases below the pycnocline, from 13.1 in the surface layer to 4.2 in the near-bottom waters, showing a N-deficit in the near-bottom waters during summer. It is likely that, besides the remineralization of organic matter and the possible phosphate release from the sediment, an additional process takes place and contributes to such low values of the ratio. Denitrification occurs within the water column and the upper few millimeters of the sediments under low oxygen conditions, converting nitrate to nitrogen gases released from the system and represents a sink of nitrate. It is evident that denitrification cannot be the controlling factor of the DIN:DIP values in the near-bottom waters of Elefsis Bay [119].

Significant pH decrease has been reported since 1970’s in Elefsis bay but it has never been correlated with nutrients or biological parameters and moreover, the impacts on the biogeochemical processes have not been estimated. Since 1975, reports within the warm period report pH fluctuations of 8.4 to 7.9 from surface to bottom [131]. Scoullos [126] had reported already decreased pH since 1977 (

Table 1) with the bottom values ranging between 7.9-7.5.

Table 1. Reported pH values for the entire water column of the selected station, indicating acidification since 1977 [126].

depth (m)	Feb 1977	Mar 1977	Apr 1977	May 1977	Jul 1977	Aug 1977	Sep 1977	Nov 1977	Jan 1978	Feb 1978
0	7.95	7.85	8.05	8.30	8.15	8.12	8.05	7.92	7.92	8.25
10	7.93	7.93	7.95	-	8.50	8.12	7.80	7.92	7.90	8.15
20	7.92	7.93	7.92	-	-	7.83	7.90	7.88	7.67	8.00
30	7.83	7.92	7.87	7.75	7.92	7.52	7.52	7.82	7.82	7.85

Sediment Characteristics

Hypoxic and anoxic conditions in the water column above the SWI are also leading to an enrichment of organic matter in the sediments. The dark to black color of the surface sediments is an index of the high content of organic matter. Careful observations during the winter period (hypoxic conditions in the water column above the sediment–water interface) have shown a very thin grey-brown layer, like a thin film (less than 1 mm) of oxidized surface sediments. During the summer period, anoxic conditions in the water column above the sediment–water interface lead to totally anoxic conditions in the bottom sediments (black color) with an intense odour revealing the presence of H_2S [119, 135].

In the 1980's organic carbon content was reported to vary from 0.9% at the eastern end of the Bay to 1.86% at the western part [135]; Pavlidou et al. [119] recently reported similar values with OM fluctuation between 0.8-1.3%.

It has been of great interest whether the hypoxic/anoxic conditions in the bay are a phenomenon of the last decade or a historical natural phenomenon of the system. Through sediment core analyses (with an estimated sedimentation rate of 0.29 cm per year using ^{210}Pb [119]), several hypoxic and anoxic events have left their imprint the last 5,000 years based on organic matter content of up to 3.0% even in deeper layers. It seems that both oceanographic–climate and anthropogenic pressures have played a role as drivers for hypoxia through time. The occurrence of hypoxia in Elefsis Bay on the "geological" timescale seems to be related to climate fluctuations with warmer periods contributing to the stratification of the water column and to relatively higher productivity.

To conclude, Elefsis Bay seems to be very complicated and variable. Its variability is probably related to the differences in anoxia intensity and the amount of the organic material accumulated. In general, low nitrite content and ammonium-rich waters are observations in the anoxic layers. Nitrite is the first intermediate of denitrification and provides a diagnostic tool for its occurrence. Probably, denitrification at very low rates occurs without much accumulation of nitrite. However, mineralization processes (i.e. ammonification) are favored and supported by the high concentrations of organic matter. On the other hand, benthic nutrient recycling could be another source for the supply of the water column with ammonium [119].

2.3 Previous Findings for the Area

Saronikos and Elefsis are the only water bodies in Greece which have been systematically monitored from 1985 onwards in the framework of two projects: the 'National Monitoring Program for the Assessment and Control of Marine Pollution in the Mediterranean' MAP/UNEP MED-POL and the 'Monitoring of the Saronikos Gulf ecosystem under the influence of the Psittalia sewage outflow' supported by the Athens Water Supply and Sewerage Company [124].

The application of the eutrophication index (EI) based on the annual nutrient and chlorophyll-a concentrations [136], has showed a significant improvement of the ecosystem quality in the western part of Elefsis after 1997, despite the intermittent hypoxic/anoxic conditions. The mean annual phosphate and ammonium concentrations showed a decreasing trend after 1998, whereas, the mean annual nitrate concentrations decreased after 2007. In general, station S2 (see Chapter 3.3) has been upgraded from the BAD trophic status before the operation of the Wastewater Treatment Plant in Psittalia, to POOR trophic status [137].

Similarly, metals (Cd, Cu, Ni, Pb, Zn, Fe and Mn) exhibit a decreasing trend during the last 40 years. This trend can be attributed to improvements in production processes in the industries, reduction of emissions and discharges due to legislation provisions and their implementation through the installation of filters and depolluting devices, shut-down of some industries and decrease

in production levels of others, as well as changes to the fuels used (replacement of heavy oil by gas) and the use of unleaded gasoline for vehicles [124]. The general trend during the decade 1994–2004 of the operation of the Psittalia wastewater treatment plant is that the high values recorded until 1994 have demonstrated a gradual decrease. Cd for example has decreased dramatically from 152 and 76 ng/L in the Elefsis Gulf in 1987 and 1994 respectively, to 27 ng/L in 2004 [138]; particulate Cd has also decreased (21 ng/L in 1987, 27 ng/L in 1994 and 0.68 ng/L in 2004, in the Elefsis Gulf).

The change in the site of the effluent disposal and the installation of treatment plants in some of the industries in the coastal area, contribute to the observed decrease in trace metals in the Gulf of Elefsis. However, this area still receives considerable loads of trace metals and poses the most polluted part of the Saronikos Gulf. However, the generally observed decreasing trend is partially interrupted in the cases of dissolved Mn, dissolved and particulate Ni and particulate Pb between 2000 and 2004, with their concentrations having slightly increased [124, 138]. It has not been clarified though whether this disturbance of the general picture is attributed to circumstantial polluting incidents which could not be isolated in such a complex natural system or represents a new increasing trend. This would be difficult to assess, since no adequate data are available and the monitoring program was discontinued between 2000 and 2004 [138].

Regarding sediments of Elefsis bay, studies have shown nutrients [134] and several heavy metal concentrations (Hg, As, Cr, Zn, Sb, Co, Pb) being in excess of natural levels and adjacent territories as a result of industrial and domestic waste water discharges [128, 129, 122, 126]. An improvement of the contamination situation in the Elefsis Bay has been observed the last few years [124, 119, 138], with decreasing N, P, Cu and Mn inputs, Ni being stabilized throughout Elefsis seidments, and Fe still increasing until 2004 [67].

The last years, ex-situ incubation experiments [139, 140, 141, 142] have been conducted in Elefsis Bay regarding benthic fluxes between sediment and water. These studies were trying to estimate the exchange rates of nutrients

and trace metals to better elucidate whether sediments act as a trap or as a source towards the water column for these substances.

Nutrient dynamics have demonstrated seasonal variability. Sediment effluxes of N-species were found to prevail during July, with nitrite and ammonia distributions suggesting that ammonification is the main process controlling the fluxes [141]. At DO levels <30 μmol l^{-1}, nitrate concentration normally decrease while phosphate and ammonium increase, indicating that denitrification is the controlling mechanism, suggesting that sediment could act as a source of nutrients to the overlying water column. During oxygenated periods (114 μmol l^{-1}) oxygen and nitrate concentration follow a common distribution pattern; as DO increases, nitrate also increases, probably through nitrification process [139].

Incubation experiments [142] showed that in the presence of oxygen, the bottom sediments of Elefsis Bay (in the specific station, S2) can act as a sink for Fe and Mn and as a source for Ni; Cu, Cd and Pb have been also found to be released from the sediment to the water column. Different patterns, however, have been found in the eastern part of Elefsis bay suggesting the complex dynamics that control the fate of these three metals in the area.

2.4 Objectives and Experimental Approaches followed in this Thesis

Sediments are expected to release metals to bottom water, depending upon the chemical state of the element and the pH and Eh of every system [143]. Considering Elefsis as a system characterized by high concentrations of heavy metals and nutrients plus its particular physiographic characteristic of seasonal oxygen deficiency, emerges the additional interest of how the decrease in pH (due to globally occuring OA) would further affect Elefsis biogeochemistry. Would OA 1. possibly make heavy metals/nutrients more bioavailable for the various organisms or 2. pose sediments as a trap for binding various substances and thus functioning as a buffer mechanism to normal existing pollution?

Thus, the main scope of this research was to simulate how pH decline (emerging from OA) would influence major biogeochemical cycles (e.g. C,N,P) and trace element distribution in addition to the intermittent parameter

of oxygen depletion in the specific coastal system (Elefsis Bay). These two physicochemical variations pose several modifications individually in a particular system; the following experiments aim to assess possible alterations of major and minor biogeochemical cycles and shifts to different mechanisms in combination (e.g. coupling, decoupling), ultimately affecting elements' fate in the water column. Additionally, in the framework of the EU Research Project "ARISTEIA- EXCELLENCE 640" entitled *"Integrated Study of Trace Metals Biogeochemistry in the Coastal Marine Environment* (ISMETCOMAREN)*"* under which part of this project was implemented, the application of an analytical method aiming in final trace element determinations with ICP-MS was designated for the first time. For this reason, a standard method protocol from EPA was chosen, in order to be set up, implemented and evaluated for this study and for future analytical works carried out in the Laboratory of Environmental Chemistry.

2.5 Sampling Procedures

Field sampling was performed at one site (S2 Station; Longitude: 23° 25' 48''E; Latitude: 38° 03' N; Depth: 33m; Figure 1) located at the western part of Elefsis bay, in June 2014 and September 2014, onboard the R/V AEGAEO (Hellenic Centre for Marine Research, HCMR). Hydrographic properties (salinity, temperature, depth) were recorded through a Sea Bird Electronics CTD instrument (SBE-9) associated with a General Oceanic rosette sampler, equipped with twelve 10 L Niskin bottles. Subsamples of seawater from the deepest part of Elefsis were collected and measured immediately for pH and Redox potential with laboratory pHmeter and Redox potential probe (Jenway 3310). Field samples were also collected for the immediate determination of D.O. and total alkalinity. Seawater (unfiltered) was collected in Nalgene Polycarbonate bottles from the maximum depth of the sampling site; surface sediment (0-10 cm, untreated) was collected using a 0.1 m^2 box corer. Seawater and sediment were transferred to the laboratory, placed into four 25 L Nalgene Polycarbonate bottles (at a proportion 80% and 20%, respectively). The sediment was placed first at the bottom of the experimental tanks evenly followed by the seawater transport gradually into the tanks using silicone

tubes in order to avoid any further disturbance and oxygenation in the system (Figure 2).

Measurements and determinations from the two sampling procedures indicated substantially different physicochemical parameters (temperature, pH, Redox and Dissolved oxygen) in the bottom of Elefsis Bay and are presented in Table 2. For this reason, two different experiments were designed and set up (I and II are described in chapters 5 and 6 respectively), with different temperature and D.O. concentrations (based on the ones measured *in situ)* and different pH value regarding the control condition (C) of the experiment, in order to simulate as close as possible the natural system.

Table 2. Physicochemical Parameters measured in situ during sampling procedures (for the maximum depth, 33 m)

Sampling Procedure	T (°C)	pH	Redox (mV)	Redox (RmV)	DO (ml/l)	DO (%)
June 2014	16.0	7.85	194.3	398.5	2.26	46.5
September 2014	17.5	7.75	-50.7	143.0	0.00	0.0

2.6 General Experimental Settings

In both experiments, the controlled CO_2 supply was achieved, using a continuous flow system (IKS Aquastar, IKS Computer Systeme GmbH), which automatically adjusted CO_2 gas addition to the microcosms in order to maintain pH stability. Each tank was monitored constantly (every 5 minutes) throughout the experiment by the IKS System using probes recording temperature, pH, Redox and D.O. IKS probes were calibrated daily, using certified buffers, to avoid drifting. Potentiometric probes (pH, Redox, D.O) were also used in order to correct possible drifts of the IKS probes. The measured pH values by the IKS system were corrected with the parallel use of a laboratory pH meter (Jenway 3310) calibrated in NBS scale; the pH values were then converted to the total scale ($pH_{T,}$ [1]).

The pH values selected for the two treatments (experiment conditions) were: (i) for the control tanks (C), the pH value measured during sampling (7.85 and 7.75, NBS scale for experiment I and II respectively) and (ii) for the ocean acidification tanks (OA) the pH value selected was the one predicted for the year 2300 (6.80 NBS), regarding the highest CO_2 emission scenarios (20,000

Pg C), for latitudes corresponding to the Mediterranean Sea [8]. Each one of the two treatments was applied in 2 replicate tanks. All results regarding seawater samples for OA and C conditions refer to the mean value of two replicates (standard deviation is included in diagrams for every parameter). Samples of the overlying seawater were taken from the microcosms approximately every 3 days. Any change occurring in the C condition tanks was considered to be a change naturally observed, theoretically, in order to investigate and fully comprehend the effects of acidification on the selected parameters. In every case, the experimental design and setup was accomplished according to, Barry et al., Widdicombe et al. and Havenhand et al. [118, 144, 145]. The overall experimental setting appears in Figure 3, Figure 4, Figure 5.

Figure 2. Seawater transport in the experimental tanks which followed the sediment transport. The use of silicone tubes was necessary to avoid any further disturbance and oxygenation in the experimental set-up.

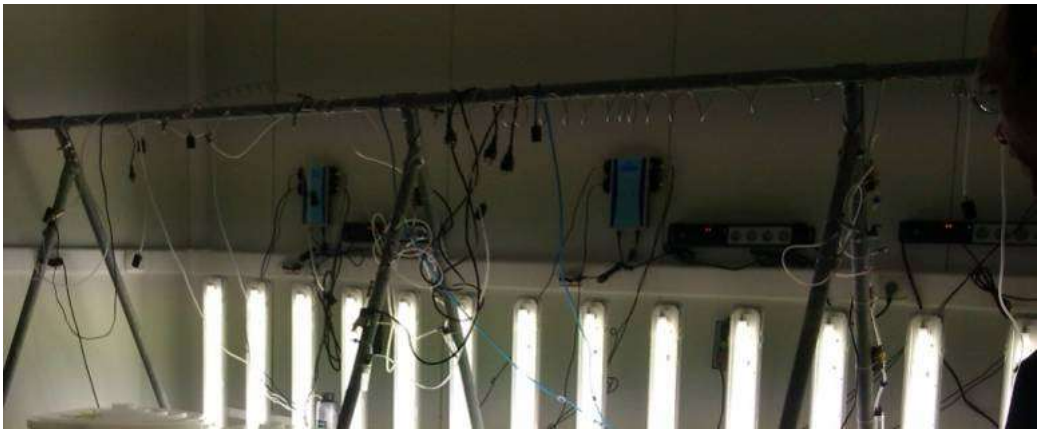

Figure 3. Experimental Setup of IKS System in the thermostated room

Figure 4. Experimental tanks in the thermostated room before the experiment begins

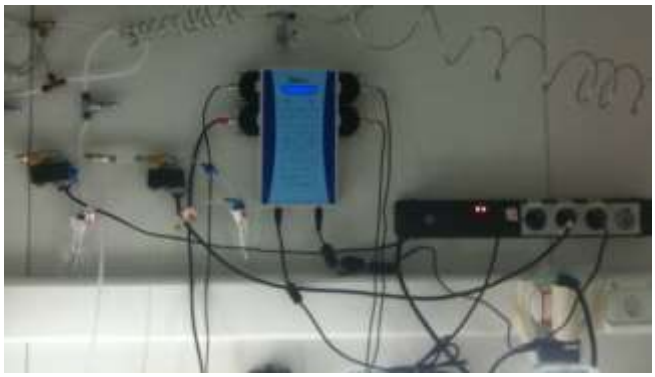

Figure 5. IKS system with CO2 gas and air supply

It should be noted that despite the automatic and adjusted CO_2 addition through the IKS systems, pH monitoring in the tanks was not easily stabilized and the parallel use of a laboratory pHmeter to check any unexpected fluctuations was necessary. Additionally, sediments were found to be crucial regarding the buffering mechanism of the system during any alteration

attempted in pH and DO. The steep CO_2 addition to lower the pH according to the value selected was not immediately detectable due to the high buffer capacity of the sediment, so in several occasions the pH could drop significantly below the selected value. For this reason, the CO_2 addition was eventually attained above the water surface so a slower equilibration could be achieved between the air and the underlying seawater and the pH decrease would be smoother.

Regarding the addition of Ar gas during Experiment II, the DO decrease was also buffered to a large extent. DO never reached 0 values as in field possibly due to DO eluding from the sediment pore water.

Sampling from microcosms

Samples of the overlying seawater were taken from the microcosms approximately every 3 days. Surface sediment samples were collected from all tanks, at the end of the experiment I (on the 20th day). For the experiment II, surface sediment was collected on the 18th day and on the 33th day (after the reoxygenation). In any case, the system volume, both water and sediment was not reduced to more than 15% of the initial one, in order to be considered undisturbed [71].

During sediment sampling, attempt was made to cause the minimum disturbance possible in the system; however, sediment perturbation and resuspension was eventually inevitable.

CHAPTER 3:

ANALYTICAL METHODS – DATA ANALYSIS

Previously in the Laboratory of Environmental Chemistry (LEC), the multiple determination of trace elements in seawater was performed either by preconcentration techniques such as chelating resins (Chelex-100 or DGT films) [109, 126, 146, 147]. Direct techniques such as ASV have also been used [109, 148].

The implementation of a new technique was decided as a result of the restricted selectivity factor of the resin Chelex-100 regarding certain elements (e.g. As, V, Co).

The specific standard method was selected in order to use Inductively Coupled Plasma Mass Spectrometry (ICP-MS) as the final determination procedure and aimed basically in the analyses of very low-concentration elements such as (As, Co, V etc).

3.1 Determination of Trace Elements in Water by Preconcentration and Inductively Coupled Plasma Mass Spectrometry (ICP-MS)

Scope and Application

This method was designed for the preconcentration and determination of dissolved elements in seawater samples combined with ICP-MS analysis; it may also be used for the determination of total recoverable element concentration. This method was developed following the EPA 1640 standard procedure which has been evaluated by EPA and considered applicable for As, Cd, Cu, Pb, Ni, Zn [149].

Preconcentration procedure using reductive precipitation by sodium tetrahydroborate

In this procedure, trace elements are preconcentrated based on their reductive precipitation by sodium tetrahydroborate. Iron and palladium are added to samples to aid coprecipitation of metal borides and to enhance the precipitation of metals coming out in the elemental form. The solution is vacuum-filtered through a 0.4 μm filter. The precipitate is dissolved in nitric

acid and analytes are determined by ICP-MS [149]. The analytical procedure is presented in ANNEX I.

ICP-MS Operation Parameters

The digested samples were analysed through ICP-MS by a Thermo Scientific ICAP Qc (Waltham, MA USA). Measurements were carried out in a single collision cell mode, with Kinetic Energy Discrimination (KED) using pure He gas (Operation Parameters are shown in Table 3).

Table 3. Operation Parameters of ICP-MS ICAP QC (LEC)

Gas Flow (Ar)	Cool flow	14 L/min
	Auxiliary flow	0.8 L/min
	Nebuliser flow	1.06 L/min
RF Generator	Supply Voltage	37.9 V
	current	41.4 A
Plasma Power		1550 W
Detector Voltage		1175 V

The proprietary iCAP Q interface consists of a pair of solid Ni cones. The iCAP Q sample-introduction system consists of an efficient, low-flow concentric nebulizer, paired with a compact, peltier-cooled cyclonic spray chamber, providing optimum short and longterm signal stability.

RAPID Lens Technology — 90° Ion Optics Done Right Ions extracted from the iCAP Q interface are accelerated via an initial ion lens stack into the RAPID (Right Angle Positive Ion Deflection) lens that efficiently deflects analyte ions by 90° before entry into the QCell. The RAPID lens ensures neutrals from the plasma are unaffected and do not impact on the QCell, leading to stable cell performance and eliminating routine maintenance.

The use of flatapoles in the QCell allows for a reduced cell volume, leading to shorter gas fill and flush times and corresponding increases in sample throughput. When pressurized with an inert gas such as He, the flatapoles provide powerful interference reduction for a simpler ICP-MS spectrum in all sample types.

In He QCell KED mode, the iCAP Q ICP-MS has sufficient sensitivity to provide single figure ppt detection limits for low mass elements such as Li, Be and B. The iCAP Q therefore allows full mass range analysis of routine samples in environmental, clinical and food applications.

From now on, whenever an ICP-MS analysis is mentioned in this study, the aforementioned parameters have been utilized.

3.2 Determination of Trace Elements in Sediments using ICP-MS

In order to digest sediment samples for final determination with ICP-MS, the implementation of EPA 3050b standard method was chosen [150]. For the digestion of samples, a representative 1-2 gram (wet weight) or 1 gram (dry weight) sample is digested with repeated additions of nitric acid (HNO_3) and hydrogen peroxide (H_2O_2). The resultant digestate is reduced in volume while heating and then diluted to a final volume of 100 mL for ICP-MS analysis. The analytical procedure is presented in ANNEX I.

3.3 Determination of Fe Species in Seawater and Sediments

3.3.1 Fe species in seawater

The method employed for the iron speciation in aqueous samples was that of Nicolas S. Bloom [151], based on Stookey [152], by ferrozine complexation colorimetric detection at 562 nm. This method is for the colorimetric determination of divalent iron (Fe(II)) and total iron (Fe) in aqueous solutions. Trivalent iron (Fe(III)) is determined operationally by the difference between total Fe and Fe(II). Fe(II) forms a stable red-violet complex with the dye ferrozine [3-(2-pyridyl)-5,6-bis(4-phenylsulfonic acid)-1,2,4-triazine] in buffered solutions. The complex can be measured photometrically at the maximum absorbance of 562 nm. To determine total iron, Fe(III) is reduced by ascorbic acid prior to analysis. The detection limit was determined to be 2 μg l^{-1} (0.036 μmol l^{-1}) when using a 2.0 cm photometer cuvette (40 ml vial). The analytical procedure is presented in ANNEX I.

3.3.2 Fe species in sediments

The colorimetric determination in sediments is based on the same principles as for seawater determination based on a method proposed by GEOMAR [153]. The analytical procedure is presented in ANNEX I.

3.4 Evaluation of Methods

3.4.1 ICP-MS Analyses

3.4.1.1 Limits of Detection (LOD) and Quantification (LOQ) for EPA1640

All measurements resulting for ICP-MS are expressed in μmol/l (or μM). To calculate the limits of detection and qualification for the implementation of EPA 1640 standard method, 10 blanks were analyzed in different days of ICP-MS measurements and the standard deviation was calculated. The LOD of each trace element was calculated as 2.998 times the standard deviation of blanks; the LOQ was calculated as 2.998 the LOD. The results are given inTable 4.

Table 4. Standard Deviations of blanks analysed and the calculation of LOD and LOQ (in ppb and μM; μmol l^{-1}) for trace elements regarding the EPA 1640 standard method

	As	Cd	V	Ni	Cu	Pb	Co	Mn	Cr	Al
St. Dev.	0,016	0,039	0,103	0,161	0,179	0,212	0,005	0,096	0,955	5,28
LOD (ppb)	0,047	0,116	0,309	0,481	0,537	0,635	0,015	0,289	2,864	15,82
LOQ (ppb)	0,140	0,347	0,927	1,443	1,611	1,903	0,046	0,867	8,587	47,43
LOD (μM)	0,001	0,001	0,006	0,008	0,008	0,003	0,0003	0,005	0,055	0,586
LOQ μM	0,003	0,003	0,018	0,023	0,023	0,009	0,0009	0,015	0,165	1,758

Other Trace Elements

The use of ICP-MS offered the opportunity to determine in parallel other trace elements such as Rb, Te, Tl, Ba, Sr which had never been measured before in the LEC. However, this is considered as a collateral analysis since it was not plotted appropriately from the beginning of the study. This means, that neither the preconcentration method was initially evaluated for these elements, nor the CRMs used were certified for these elements' concentrations. Nevertheless, the limits of detection and quantification are presented in Table 5.

Table 5. Standard Deviations of blanks analysed and the caculation of LOD and LOQ (in ppb and μM; μmol l^{-1}) for the elements Rb, Te, Tl, Ba and Sr for EPA1640 (for seawater samples)

	Rb (ppb)	**Te (ppb)**	**Tl (ppb)**	**Ba (ppb)**	**Sr (ppb)**
St. deviation	0,012	0,019	0,003	0,738	0,136
LOD (ppb)	0,037	0,056	0,008	2,213	0,408

	Rb (ppb)	Te (ppb)	Tl (ppb)	Ba (ppb)	Sr (ppb)
LOQ (ppb)	0,112	0,168	0,025	6,635	1,224
LOD (μM)	0,0004	0,0004	0,00004	0,016	0,005
LOQ (μM)	0,0013	0,0013	0,00012	0,048	0,014

3.4.1.2 Certified Reference Material Analyses

Seawater Analyses

For the evaluation of both the ICP-MS analysis and the preconcentration method, two different CRMs were used, CASS-5 and NASS-6 (properties are shown in ANNEX - Table 13). The CRM recoveries are shown in Table 6.

Table 6. Recoveries (%) for seawater CRM's (CAAS-5, NAAS-6) for As, Cu, Ni, Mn, Co, V (for n=9 analyses; mean, minimum and maximum values along wiith standard deviation)

% Recovery	As	V	Cu	Ni	Mn	Cd	Co	Cr	Pb	Al
Mean value	61.0	71.0	105.0	114.2	96.7	101.6	100.7	100.4	93.5	101.0
Minimum value	50,0	57.1	76.5	93.1	72.6	85.5	71.7	73.6	67.2	70.9
Maximum value	72,2	82.0	131.3	128.4	132.0	128.2	128.1	126.1	131.3	127.4
St. dev*	10,3	13.8	28.3	14.6	27.7	16.1	27.8	22.2	31.5	27.4

*Different Days of sample treatment and analysis

For trace metals such as Cd, Co, Cr, Pb, both CRM's used were below the LOD of the preconcentration method. For this reason in order to evaluate the determinations, the median value of all CRM samples analysed was calculated for CASS-5 and NASS-6 and were used as reference values. The same applied for Al as well, since the CRM's were not certified for its concentration.

Sediment Analyses

For the evaluation of ICP-MS analysis and the digestion method, one CRM was used, (QTM 089MS; properties are shown in Annex - Table 14). The CRM recoveries are shown in

Table 7.

Table 7. Recoveries (%) for sediment CRM (QTM 089MS) for As, Cu, Ni, Mn, Pb and Cr (for n=6 analyses; mean, minimum and maximum values along wiith standard deviation)

% Recovery	**As**	**Ni**	**Cu**	**Pb**	**Cr**	**Mn**
Mean value	**84.8**	**77.8**	**86.1**	**98.1**	**87.5**	**71.0**
Minimum value	73.2	63.6	71.7	78.1	79.0	62.2
Maximum value	96.8	86.5	96.8	111.7	99.7	85.2
Standard Deviation*	11.8	12.3	12.9	17.7	10.8	12.4

*Different Days of sample treatment and analysis

For Cd, Fe and Al which were analysed with GFAAS and FAAS respectively the CRM recoveries are shown in Table 8.

Table 8. Recoveries (%) for sediment CRM (QTM 089MS) for Cd, Fe and Al (for n=6 analyses; mean, minimum and maximum values along wiith standard deviation)

% Recovery	**Cd**	**Fe**	**Al**
Mean value	**52.5**	**76.9**	**35.8**
Minimum value	40.2	64.6	28.7
Maximum value	64.8	89,2	45.7
Standard Deviation*	17.4	17,4	7.4

3.4.1.3 Comparison of ICP-MS with AAS

The use of AAS (both FAAS and GFAAS) in the LEC has been established, frequently evaluated and certified for several trace elements. For this reason, in order to fully evaluate the results coming from the first use of ICP-MS in the LEC, some samples (both seawater and sediments) were also analyzed in either GFAAS or FAAS, whenever this was possible. Mn, Al (and Fe for sediments) were analysed in FAAS while Cd was analysed in GFAAS. The comparison of ICP-MS with the AAS techniques is presented in Table 9.

Table 9. Comparison of the results for the different analytical techniques (GFAAS-FAAS and ICP-MS) used for their final determination

	Cd	Mn	Al	Fe
Preconcentration method	% ICP-MS/GFAAS	% ICP-MS/FAAS	% ICP-MS/FAAS	% ICP-MS/FAAS
EPA1640				**Ferrozine Method (sediments)**
Mean		65	114	119
Median		69	109	132
Min		36	29	60

	Cd	Mn	Al	Fe
Preconcentration method	% ICP-MS/GFAAS	% ICP-MS/FAAS	% ICP-MS/FAAS	% ICP-MS/FAAS
EPA1640				**Ferrozine Method (sediments)**
Max		88	310	139
St.dev.		15	63	25
EPA 3050b				
Mean	80		82	91
Median	79		83	92
Min	44		37	67
Max	138		95	105
St.dev.	17		11	10

3.4.2 Fe Speciation Analyses

The method for Fe speciation presented in this research was applied for the first time in the Laboratory of Environmental Chemistry of National and Kapodistrian University of Athens. Since there were no CRM's available to examine the method's recovery, only numerical and statistical data are presented here (

Table 10); all measurements are expressed in μmol l^{-1}.)

Table 10.Data for Method Validation of Fe speciation in seawater for the various days of analysis. Considering a linear equation that associates absorbance (x) with concentration(y), y=ax+b, the analyses' parameters (Slope: a, Intersection: b, linear Regression: R) are presented.

Fetotal			**Fe (II)**		
a	b	R	a	b	R
0,0010	0,0112	0,9967	0,0017	0,0414	0,9981
0,0020	-0,0016	0,9989	0,0020	0,0023	0,9980
0,0020	0,0002	1	0,0021	0,0019	0,9980
0,0021	-0,0013	0,9992	0,0020	0,0018	0,9974
0,0018	0,0022	0,9992	0,0019	0,0002	0,9998
0,0020	-0,0013	0,9996	0,0020	0,0011	0,9989
0,0019	0,0033	0,9996	0,0019	-0,0014	0,9992
0,0021	0,0000	1	0,0023	0,0024	0,9984

Regarding the limit of detection for this method, 8 blanks were analyzed as samples and the standard deviation was calculated; the limit of detection was calculated as 2.998 times the standard deviation of blanks. The results are given in

Table 11.

Table 11.Standard Deviations of blanks analysed and the caculation of LOD and LOQ for Fetotal and Fe(II)

	Fetotal	**Fe(II)**
blank's conc. (μmol l^{-1})	0,06	0,03
	0,06	0,05
	0,06	0,02
	0,05	0,02
	0,01	0,03
	0,03	0,00
	0,04	0,01
	0,02	0,01
Standard deviation	0,02	0,02
LOD (μM)	**0,06**	**0,05**

3.5 Determination of Physicochemical Parameters, Dissolved Organic Carbon, Nutrients and Carbonate System Parameters in seawater and sediment samples

The DO determination was accomplished according to Winkler Method, modified by Carpenter [154]; the total alkalinity determination was attained following Perez et al. [155, 156] potentiometric determination. The presicion of A_T analysis was determined by titrating bottled seawater samples having the same temperature and salinity and was 8.1 μmol kg^{-1}, calculated as 3 times the standard deviation of 10 measurements. The accuracy was assessed by titration of sodium carbonate standard with known alkalinity fortified to the ionic strength of seawater and was 8.4 μmol kg^{-1}, calculated as 3 times the standard deviation of 12 measurements. The DOC analysis was performed with the High Temperature Catalytic Oxidation method, using a Shimadzu 5000 total organic carbon analyzer in the LEC following the instrument's standard procedures (LOQ: 39.5±4.9 μmol l^{-1}).

Nutrients were determined spectrophotometrically with a Varian Cary 1E UV-visible spectrophotometer in the LEC, using a 1 cm cell for nitrate, ammonium and silicate while for nitrite and phosphate a 5 cm cell was used. The analytical procedures followed were the ones described in [157]; for ammonium (4500-NH3 –F [and 158], LOQ: 0.8±0.2 μmol l^{-1}), nitrite (4500-

NO2– B, LOQ: 0.14±0.02 μmol l^{-1}), nitrate (4500-NO3 -E, LOQ: 0.21±0.07 μmol l^{-1}), phosphate (4500-P -E., LOQ: 0.11±0.03 μmol l^{-1}), silicate (4500-SiO2 -E., LOQ: 0.6±0.2 μmol l^{-1}). Total dissolved nitrogen (TDN, LOQ: 0.13±0.04 μmol l^{-1}) and total dissolved phosphorus (TDP, LOQ: 0.21±0.07 μmol l^{-1}) was determined as described in [159]. Dissolved organic nitrogen (DON) and phosphorus (DOP) were calculated by subtraction of dissolved inorganic nitrogen forms from TDN and of phosphates from TDP.

Based on pH_T and A_T values, the rest of the carbonate system parameters, specifically pCO_2, CO_2 concentration, dissolved inorganic carbon (DIC), bicarbonate (HCO_3^-) and carbonate (CO_3^{2-}) ions, aragonite's and calcite's saturation states ($\Omega_{ar.}$ and $\Omega_{calc.}$ respectively) were calculated through the 'Seacarb' software package [160] including also the respective phosphate and silicate concentrations. The Seacarb calculations were performed using the apparent dissociation constants of carbonic acid (K_1 and K_2) from [161], the equilibrium constant of hydrogen fluoride from [162], the stability constant of hydrogen sulfate ion from [163] and the boron to chlorinity ratio from [164].

The organic carbon (OC) and total nitrogen content of the sediment was determined with a Thermo Scientific FLASH 2000 CHNS elemental analyzer in HCMR (Institute of Oceanography). Organic carbon was determined after removal of inorganic carbon by acidification of samples with 20μL of 6 N HCl at 60°C (this treatment was conducted five times in 12-h intervals). After the inorganic carbon removal, the samples were dried at 60°C overnight. After drying, the containers were pinched closed, compacted, and formed into a ball. The balls then were placed in the autosampler of CHN analyzer for the determination of C and N concentrations. Inorganic carbon was calculated by subtracting organic carbon from the total carbon, and subsequently carbonate content was calculated. The precision of the method was between 5% for both carbon and nitrogen [67].

Total phosphorus and sulfur content was determined through X-ray fluorescence (XRF) analysis. Furthermore, an X-ray powder diffraction (XRD) analyses was conducted to evaluate the main minerals prevailing in the sediment phases.

3.6 Data Analysis

Following the evaluation of all results, a statistical data analysis was performed in order to distinguish statistical difference between C and OA conditions and the better comprehension of parameters' (co-)variation.

A one-way ANOVA was performed to test the statistical significance of variation ($p<0.05$) between the two experimental conditions for both water and sediment samples [145]. Data were first checked to ensure they conformed to the assumptions of ANOVA (normality: Kolmogorov-Smirnov test and homogeneity of variance test). Results of ANOVA for seawater parameters are presented in ANNEX I (Table 3 for Experiment I, Table 4 for Experiment II) Principal component analysis (PCA) was performed to evaluate the effects of the selected experimental treatments (pH) on nutrient species and carbon-carbonate parameters of the water-sediment laboratory systems. For the latter, a Promax with Kaiser Normalization was used for rotation method, converged in 3 iterations. Both ANOVA and PCA analyses were performed using the SPSS software package. Additionally, a correlation analysis is presented in order to evaluate strong statistical dependence (≥0.75 or ≤-0.75) between the parameters analyzed, for each condition independently.

All parameters found below the detection limit for the respective method used, were excluded from data analysis.

3.7 Discussion on Analytical Methods

Use of EPA 1640 for seawater preconcentration

The selection of this method was based on the need of determining low-concentration elements, (e.g. As) in addition to trace metal routine analyses (e.g. Cd, Cu, Ni). Although this method has been certified only for As, Cd, Cu, Pb, Ni and Zn, in this study it was checked for other elements as well (e.g. Mn, Cr, Al, V and Co).

From CRM parallel measurements, As recoveries through EPA 1640 was found between 50-70% (with a standard deviation of 10%), suggesting an underestimation in As concentrations in seawater samples. The same applied for V as well, with recoveries between 57-82% (with a standard deviation of

14%). Following this, all sample results regarding these two metals were corrected appropriately according to CRM recoveries. Although this method was selected for such low concentration elements, its performance cannot be considered satisfactory. For future As and V analyses, another method should be selected and applied for more accurate results. Considering the other elements (Cu, Ni, Mn, Cd, Co, Cr, Pb, Al), all CRM recoveries varied between 70-114%, values that are considered quite satisfactory without requiring any correction for the respective sample concentrations.

Use of EPA 3050 for sediment digestion

Due to the multielement analysis of ICP-MS, some trace elements, such as Cd and Al, could not be measured simultaneously with the other elements due to their concentration range. The appropriate dilution for most of the metals was extremely low for Cd determinations, and very high for Al concentrations. For this reason, these elements were only analyzed using GFAAS and FAAS respectively.

The technique used for total element contents of sediments is ISO-14869-1:2000, according which sediment samples are subjected to complete dissolution with an acid mixture of HNO_3-$HClO_4$-HF and subsequently are analyzed in GFAAS or FAAS. Due to the ICP-MS final analysis, the use of HF for sediment treatment was unacceptable. In such case, the use of HNO_3-H_2O_2 mixture (under heating) was selected but could not extract the total trace element quantity especially of the content embedded in mineral grids. Such elements with considerable amount present mainly within the grid are Fe and Al. However this trace element content cannot be released under normal circumstances so it is considered unavailable for biogeochemical processes.

Comparison of ICP-MS with AAS

Comparing the different procedure followed during this study both in avoiding the use of Cheelex-100 as a preconcentration method and in the use of a new analytical technique (ICP-MS instead of GFAAS/FAAS) normally used for routine trace element detrminations in the LEC, the limits of detection and quantification are presented in Table 14 (ANNEX). All trace metal LOD's (and LOQ's) Cd, Cu, Ni, Mn, Pb and Al were all lower measured with ICP-MS in

relation to AAS. For As and V with few previous efforts of their determination, despite the underestimation of the preconcentration method, the simultaneous use of CRM's could also assist in their analysis with EPA1640 and ICP-MS.

ICP-MS provides the benefit of simultaneous determination of a variety of elements (major or trace elements; found in a wide range of concentrations), also requiring smaller sample volume than AAS. In conclusion, the analysis as a whole is recommended in occasions were sample volumes are limited and multielement analyses are required.

Other Elements (Rb, Te, Tl, Ba and Sr)

The determination of other elements (Rb, Te, Tl, Ba and Sr) in seawater samples with ICP-MS was evaluated by calculating the detection limits of the preconcentration method EPA 1640 combined with ICP-MS analysis. Also, an evaluation through CRM analyses was attempted in order to comprehend if the preconcentration method could be considered appropriate for those elements as well and whether it could be used in the future for such measurements. Considering the average seawater concentrations reported for these elements (where possible; ANNEX Table 16), the results showed that the LOD of Rb is quite low but the preconcentration method should be considered inappropriate since the CRM measurements varied extremely between the different days of the procedure; the same applies for Sr and Ba as well. Regarding Te and Tl the LOD is approximately in the range of its natural occurence (and the CRM measurements) so the entire method is considered inappropriate.

The evaluation of these elements' determinations, using the digestion method EPA3050 in sediments, was also performed through a CRM analysis. It should be noted that the specific CRM was not certified either for these values. The results showed that although CRM's measurements were all higher than LOD, the concentrations varied significantly so in this case too, this method should not be considered appropriate for such elements.

Fe Speciation

The spectrophotometric determination of Fe was performed for the first time in the LEC. Since the preconcentration method of dissolved trace metals used

for ICP-MS final analysis, included the addition of Fe stock solution, dissolved Fe in samples should be determined alternatively. Regarding the limit of detection for Fetotal and the range concentration found for the specific coastal area, the method was found adequate. For Fe(II), in hypoxic conditions it was mainly below LOD so future use of this method might only be applied during severe hypoxic or anoxic conditions. For other uses, a flow injection analysis would be preferable to obtain lower LOD's.

Caution should be given in sampling, especially when near bottom or from a microcosm tank because sediment could be also collected and measured as dissolved Fe, leading in contamination and Fe overestimation. Additionally, samples should be taken with the minimum interaction with the overlying air in order to avoid Fe(II) oxidation to Fe(III).

3.8 Concluding remarks for Analytical Methods

Regarding the use of EPA 1640 for seawater preconcentration trace metal such as As and V were found to be underestimated suggesting that a fraction of these two elements could not be fully bound and be further determined through ICP-MS analysis; with the parallel use of a CRM these values can be obtained and corrected. Trace metals such as Cd, Co, Cu, Mn, Ni, Pb and Al although they are normally found in a quite wide range of concentrations, were all simultaneously preconcentrated and analysed with quite satisfactory recoveries, despite that the specific method had not been verified for Mn, Al and Co. Cr has been found below LOD at all times in all samples so this method cannot be applied for Cr determination.

For sediment analyses, the use of EPA 3050b (despite that there cannot be full sediment solubilization since HF is not used) was found very accurate regarding elements such as As, Ni, Cu, Pb, Cr and Mn. Fe and Al, normally found complexed within the mineral grid (along with Cd) could not be fully estimated so if this method is selected for future analyses the use of a CRM is requisite for these metals.

Colorimetric Fe speciation in seawater was found satisfactory regarding the elevated dissolved Fe content found in both samplings and during the experiment.

CHAPTER 4:

EXPERIMENT I (HYPOXIA)

4.1 Experimental Setup

During the experiment I (June 2014), the tanks containing seawater and sediment were placed in a thermostated room at 15.0 °C, in the dark (Figure 6). The seawater-sediment systems were left to equilibrate, untreated, for a week with controlled air supply through a pump, in order to maintain sufficient dissolved oxygen (D.O.) concentration. Subsequently, the 20 days-experimental period of controlled CO_2 aeration followed.

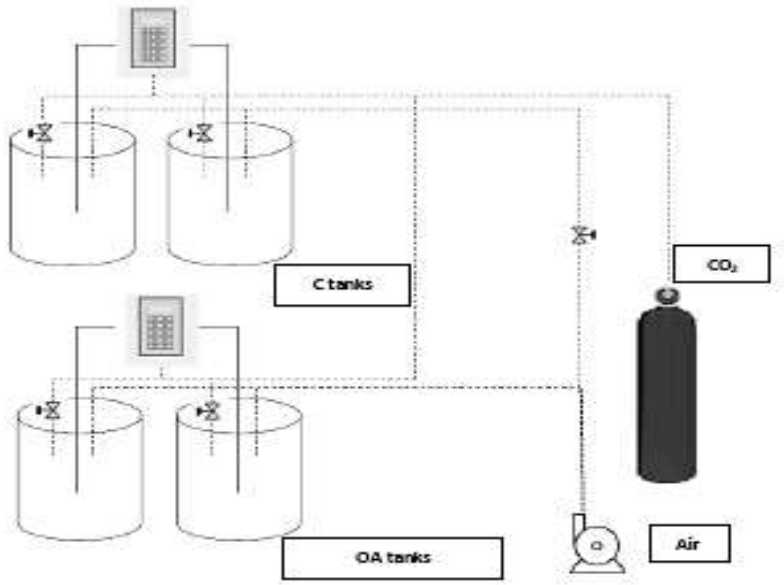

Figure 6. Design of the experimental set-up. two tanks for each pH treatment (OA and C), the IKS system monitoring the CO2 gas supply and the air pump providing air to the systems

4.2 Results

4.2.1 Physicochemical Parameters

During sampling, the vertical distribution of temperature, salinity and dissolved oxygen are presented in Figure 3. pH and Redox potential in Elefsis bottom seawater were 7.85 and 194.3 mV, respectively, dissolved oxygen was found relatively low (70.65 μmol kg^{-1} suggesting hypoxic conditions [19]) while A_T

attained rather high concentration (2769.3 μmol/kg). Relatively elevated nitrate concentrations (4.401 μmol l^{-1}) were measured followed by nitrite (1.322 μmol l^{-1}) and phosphate (0.077 μmol l^{-1}) along with high silicate (13.99 μmol l^{-1}) values (Figure 4). The pCO_2 calculated in the bottom seawater of Elefsis bay was 797 μatm, almost double the current atmospheric pCO_2 value [165]; however both Ω_{ar} and Ω_{calc} were calculated well above 1, indicating saturated conditions (see ANNEX – Table 17).

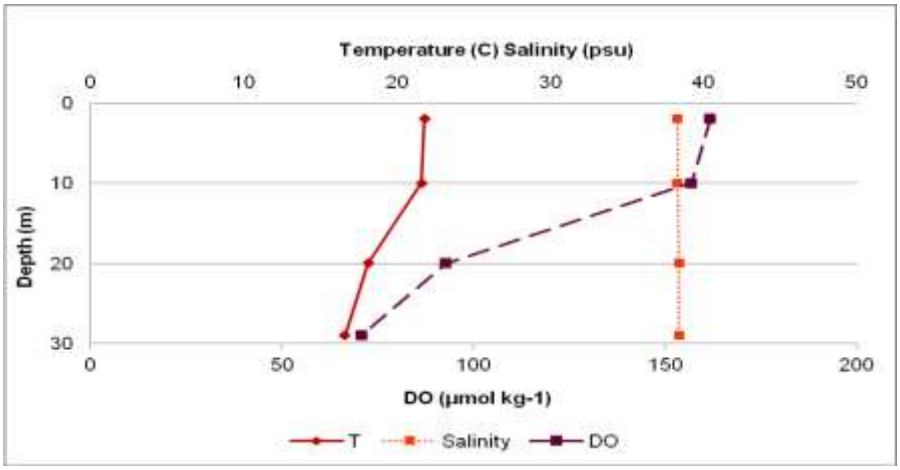

Figure 7. Vertical distribution of physicochemical characteristics T(°C), Salinity (psu) and DO (in μmol kg^{-1}) in Elefsis Bay during September 2014

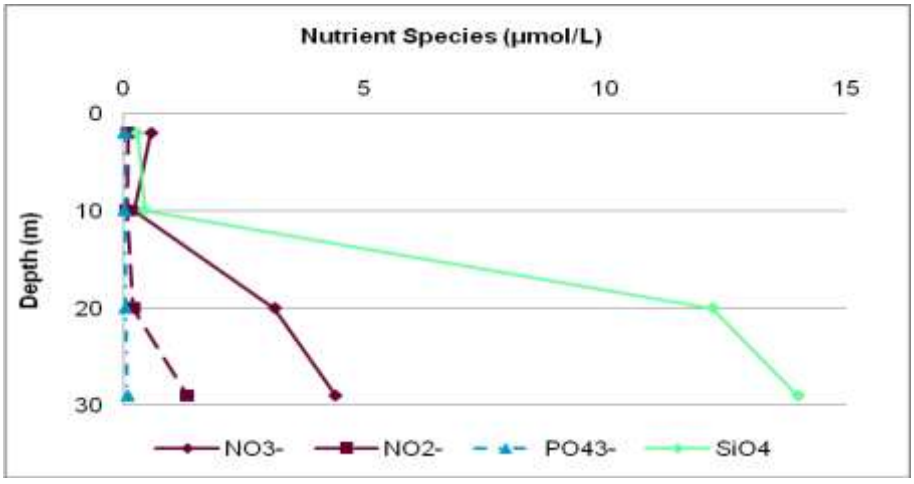

Figure 8. Vertical distribution of nutrinets NO_3^-, NO_2^-, PO_4^{3-} and SiO_4 (in μmol l^{-1}) in Elefsis Bay during September 2014

During the experiment, temperature was kept stable at 15.1±0.31°C inside the incubator room. DO varied between 130±6 μmol kg^{-1} and 138±12 μmol kg^{-1} for OA and C conditions respectively (Figure 9a) showing no statistical difference (F=0.504, p=0.494). Salinity was constant throughout the

experiment at 38.7. pH_T fluctuated slightly in both treatments (6.63±0.18 units for OA and 7.82±0.15 units for C treatment, Figure 9b).

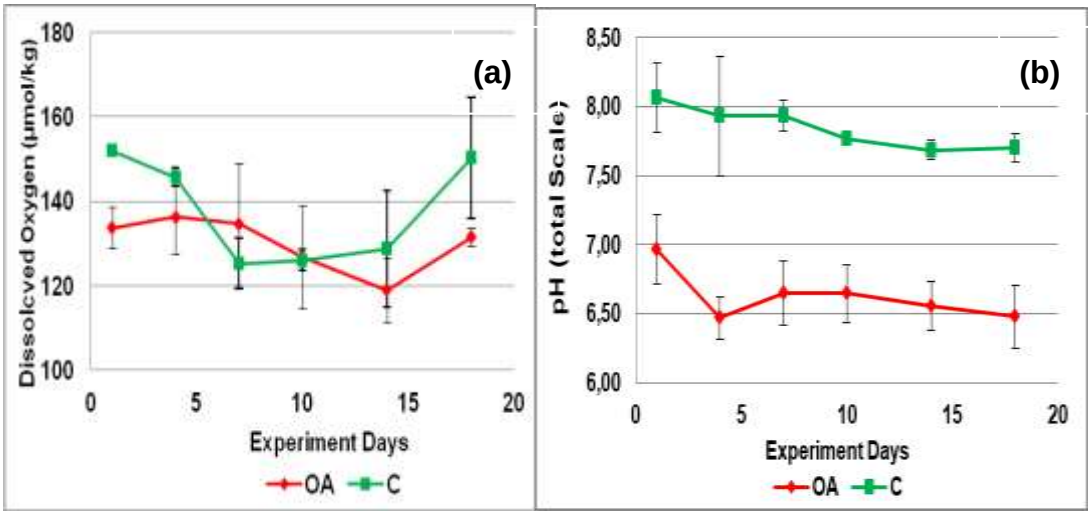

Figure 9. Dissolved Oxygen concentrations (in µmol kg-1) and pH (total scale) for the duration of the experiment (mean values and standard deviations for the two replicates of each treatment).

4.2.2 Carbonate System Parameters

The contribution of phosphate and silicate concentrations in the computation of the carbonate parameters via the Seacarb was checked. The results showed that their inclusion in the calculations did not alter significantly the computed carbonate system parameters being <0.04% lower than the values calculated without considering nutrients.

Total alkalinity (A_T, Figure 10a) in OA condition increased dramatically, with the significant increase occurring between the 4th and the 10th day of the experiment, while in C condition little variations were observed (F=7.688, p=0.020). Total dissolved inorganic carbon (DIC, Figure 10b) also increased in both conditions, with elevated values for OA especially during the last days of the experiment (F=20.758, p=0.001). During the course of the experiment, bicarbonate ions (Figure 10c) were found to increase in both C and OA conditions reaching considerably higher levels in OA (F=11.797, p=0.006). Carbonate ions (Figure 10d) decreased substantially in OA (F=54.706, p=0.000), in favor of HCO_3^- and DIC, probably reflecting the shift of carbonate system equilibria to compensate the CO_2 increase; CO_3^{2-} for C followed the pH slight variations. In C conditions, saturation states for the two carbonate

minerals ($\Omega_{ar.}$, $\Omega_{calc.;}$ ANNEX – Table 17) were calculated above 1, whereas in OA conditions, both Ω_{ar} and Ω_{calc} were calculated below 1.

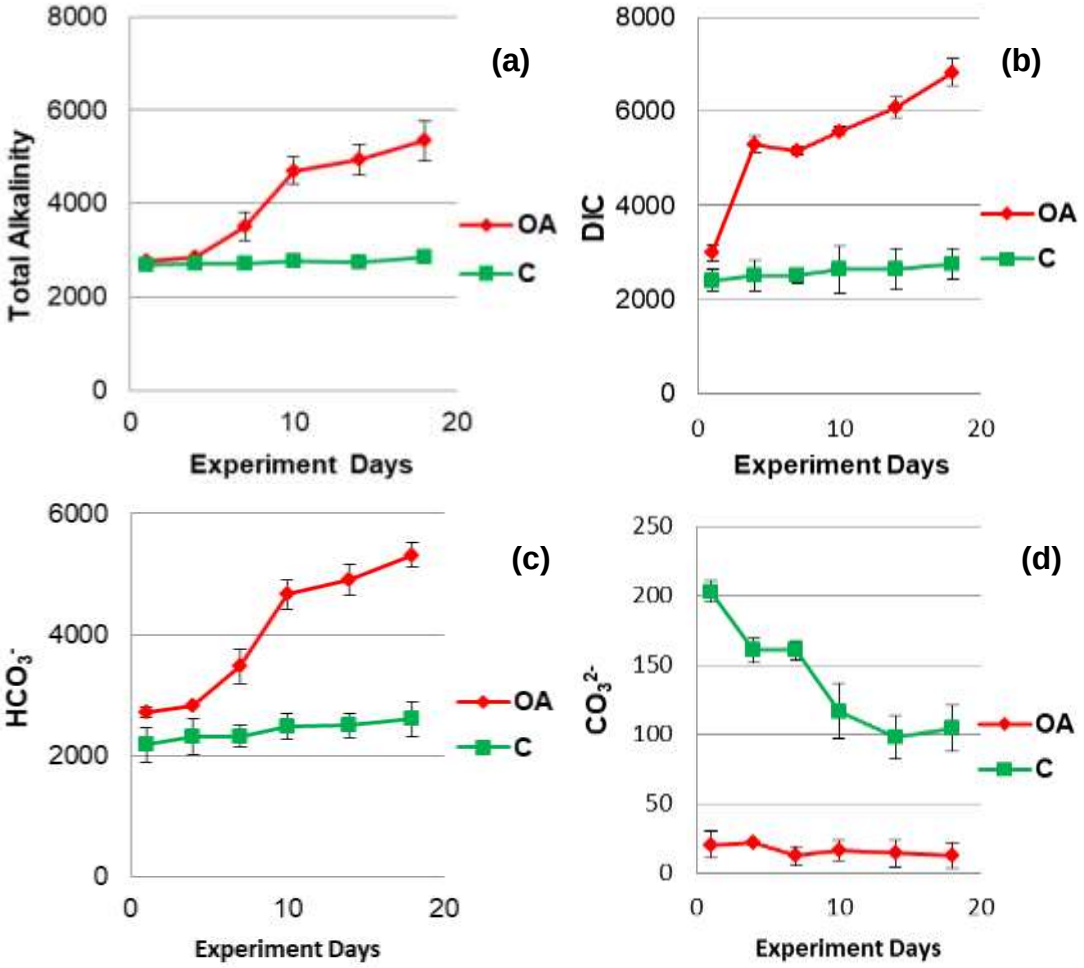

Figure 10. Alkalinity, DIC, Bicarbonates ($HCO_{3.}$) and Carbonates (CO_3^{2-}) concentrations (in μmol kg–1) for the duration of the experiment (mean values and standard deviations for the two replicates of each treatment).

4.2.3 Nutrient Species and Carbon Analysis

During the experiment, nitrate in C condition presented a sharp increase (from 2.7 μmol l^{-1} to 21.5 μmol l^{-1}) until the 7th day, followed by a declining trend to 15.3 μmol l^{-1} (Figure 11a). In OA condition, nitrate showed similar pattern until the 7th day (from 2.5 to 12.6 μmol l^{-1}), with final values remarkably lower than the ones determined in C condition (F=9.982, p=0.010). Nitrite (Figure 11b) in C condition similarly showed a significant increase (from 0.2 μmol l^{-1} to 1.6 μmol l^{-1}), followed by a decreasing trend to values corresponding to the initial

ones (0.3 μmol l^{-1}). In OA condition, nitrite slightly increased from 0.2 to 0.5 μmol l^{-1}, followed by a declining trend to values below the LOQ of the method (F=3.698, p=0.083). Ammonium (Figure 11c) in C condition showed a decreasing trend from 1.9 to values below LOQ. On the contrary, in OA condition after the decrease observed until the 4th day (from 1.4 μmol l^{-1} to 0.8 μmol l^{-1}) an increase was found until the end of the experiment (2.2 μmol l^{-1}; F=6.474, p=0.029).

DON folowed the same decreasing pattern with ammonium in C conditions till the end of the experiment (Figure 11d); in OA conditions DON varied between 22.2 μmol l^{-1} and 38.0 μmol l^{-1} reaching a final value of 27.6 μmol l^{-1} (F=9.982, p=0.010). DIN:DIP ratio (Figure 11e) in C conditions increased from 8.0 to 79.4 until the 7th day followed by a decrease to 32.1. In OA conditions, this increase was less significant (from 8.0 to 31.5 on the 10th day) and then the ratio remained constant at 21 (F=5.620, p=0.039).

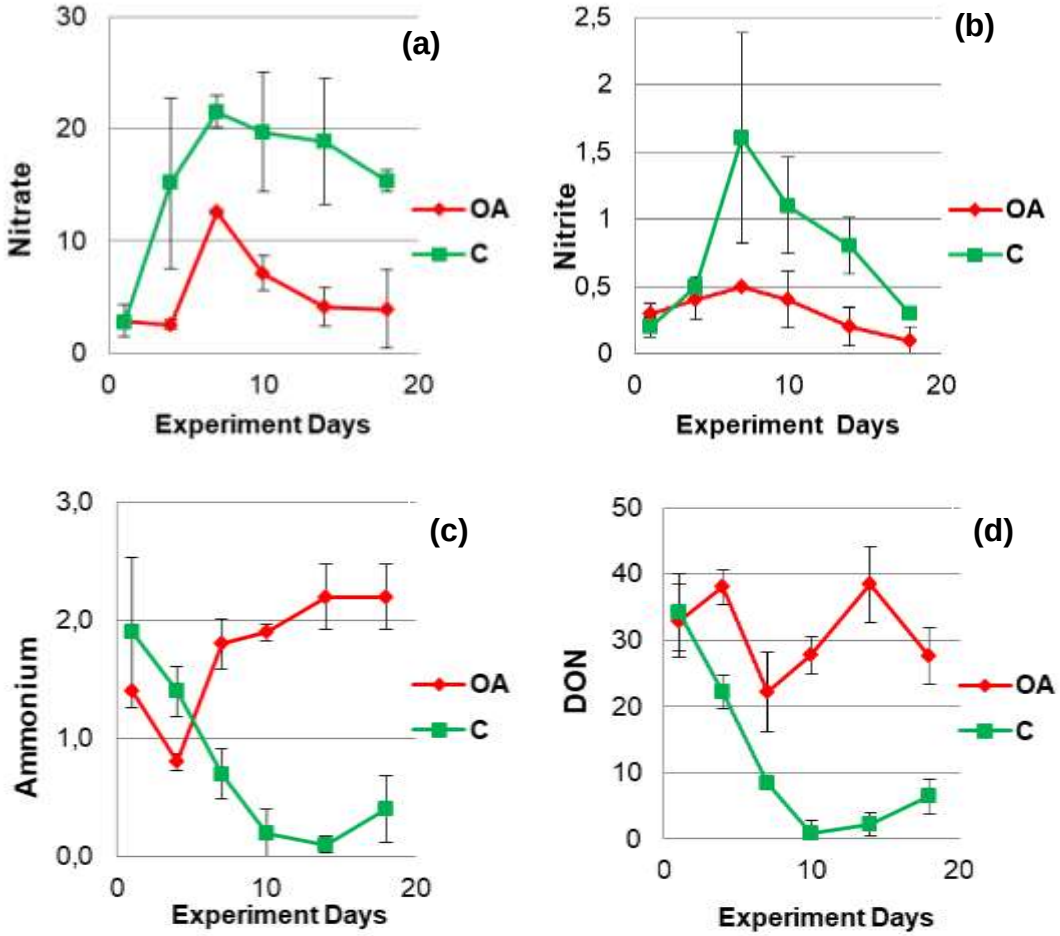

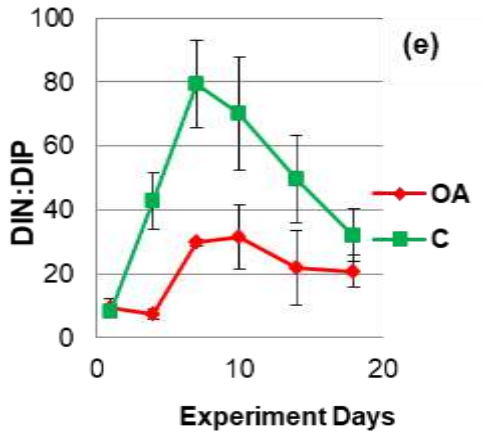

Figure 11. Nitrate, Nitrite, Ammonium, DON concentrations (in µmol/l) and DIN:DIP ratio for the duration of the experiment (mean values and standard deviations for the two replicates of each treatment)

Phosphate (Figure 12a) showed a decreasing trend in C condition until the 10th day (from 0.6 µmol l^{-1} to 0.3 µmol l^{-1}) followed by a slight increase (0.6 µmol l^{-1}) until the end of the experiment; in OA condition, phosphate appeared constant until the 10th day (0.5 µmol l^{-1}) and then followed the same trend with C condition to final values of 0.5 µmol l^{-1} (F=0.065, p=0.804). DOP (Figure 12b) showed similar increasing trend for both conditions until the 14th day of the experiment, and a decrease at the end of the experiment (F=0.191, p=0.672).

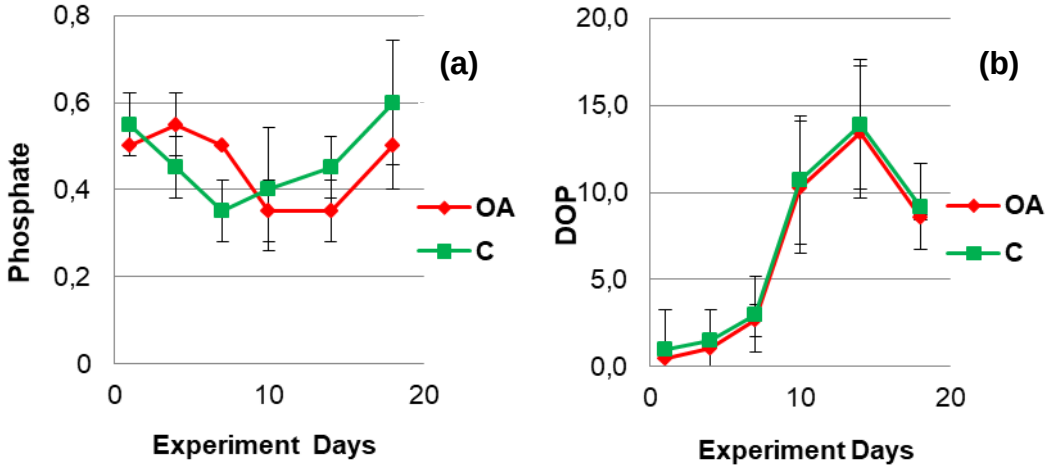

Figure 12. Phosphate and DOP concentrations (in µmol/l) for the duration of the experiment (mean values and standard deviations for the two replicates of each treatment)

Silicate concentrations (Figure 13a) presented negligible variations between the two conditions (F=1.193, p=0.188). Dissolved organic carbon (DOC) concentrations (Figure 13b) showed the same trend in both conditions until the 10th day, while increased values were recorded for OA conditions towards the end of the experiment.

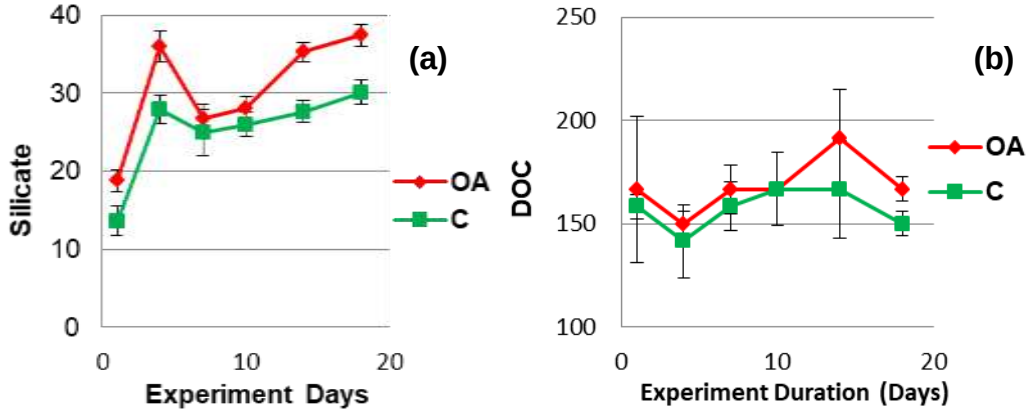

Figure 13. Silicate and DOC (in µmol/l) concentrations for the duration of the experiment (mean values and standard deviations for the two replicates of each treatment)

4.2.4 Trace Metal Determinations

For all trace metal determinations LOD is also included in the diagrams (points represent mean values along with standard deviations deviations for the two replicates of each condition). Al, Cr and Fe(II) were all found below LOD for OA and C conditions, during the experiment and are presented only in figures in ANNEX (Figure 45).

As presented similar trends in both conditions; in C conditions an increase was observed at the end of the experiment (from 3.5 ppb to 5.0 ppb). In OA conditions As was found decreased in relation to C conditions with negligible variations during the experiment (Figure 14a). V also presented the same trend with As in both conditions with an increase at the end of the experiment for both conditions (from values of 4.0 to 6.0 ppb and 2.9 to 4.1 ppb for C and OA respectively; Figure 14b). Cd presented the same trend in both conditions, similar with As and V reaching final values of 0.46 ppb and 0.44 ppb in C and OA conditions respectively (Figure 14c). Pb also presented similar trends in both conditions with As, V and Cd with Pb (Figure 14d) concentrations in OA

being higher than C conditions at all times; Pb values were found below LOD in the middle of the experiment and only in OA conditions increased at the end of the experiment (0.8 ppb). Co in C conditions was relatively stable (3.66-2.94 μmol l^{-1} at the beginning and at the end of the experiment respectively); in OA conditions, Co constantly decreased from initial values of 6.50 μmol l^{-1} to final values of 2.48 μmol l^{-1} (Figure 14e). Mn decreased constantly in C condtion with final values of 0.71ppb. In OA condition Mn significantly increased to final values of 11.1 ppb (Figure 14f).

Ni in C condition increased throughout the experiment but the concentrations remained lower than in OA condition at all times (Figure 15a); Cu increased until the 15th day and then decreased at the end of the experiment (Figure 15b). Both Ni and Cu presented the same trend in more acidified conditions with an initial increase between the 1st and the 5th day and an increase at the end of the experiment between the 15th and 19th day.

Fetotal (Figure 16a) and Fe(III) (Figure 16b) presented the same trends (since Fe(II) was found below LOD). Fe was found increased in more acidified conditions compared to C condition.

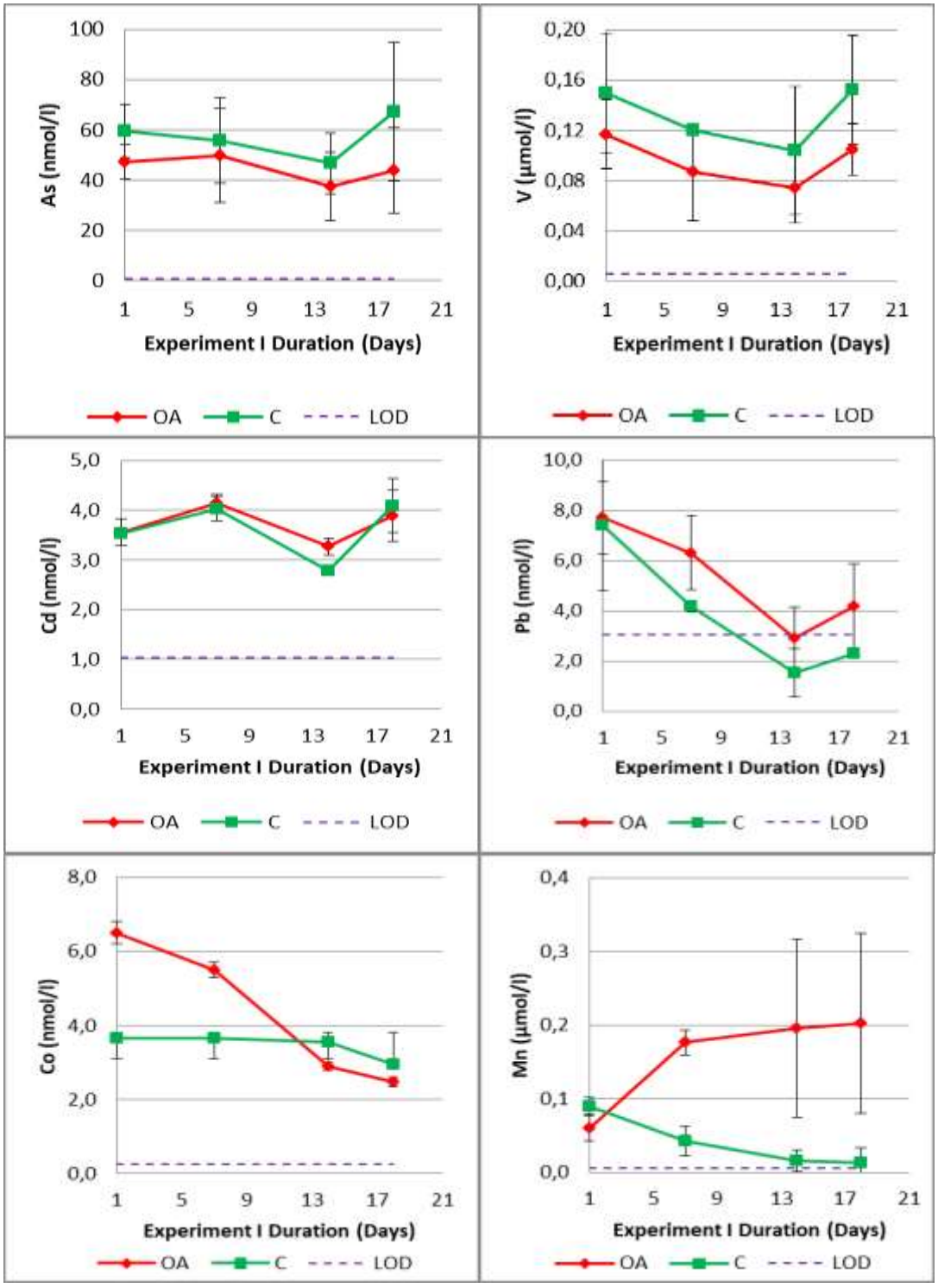

Figure 14. As, Cd, Pb, Co concentrations (in nmol l-1) and V, Mn (in µmol l-1) for the duration of the experiment (mean values and standard deviations for the two replicates of each treatment).

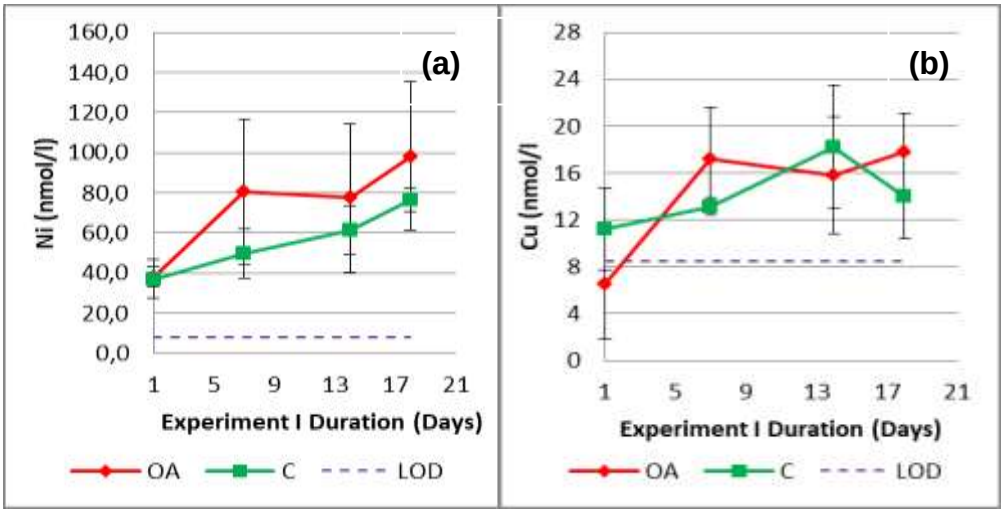

Figure 15. Ni and Cu concentrations (in nmol l^{-1}) for the duration of the experiment (mean values and standard deviations for the two replicates of each treatment).

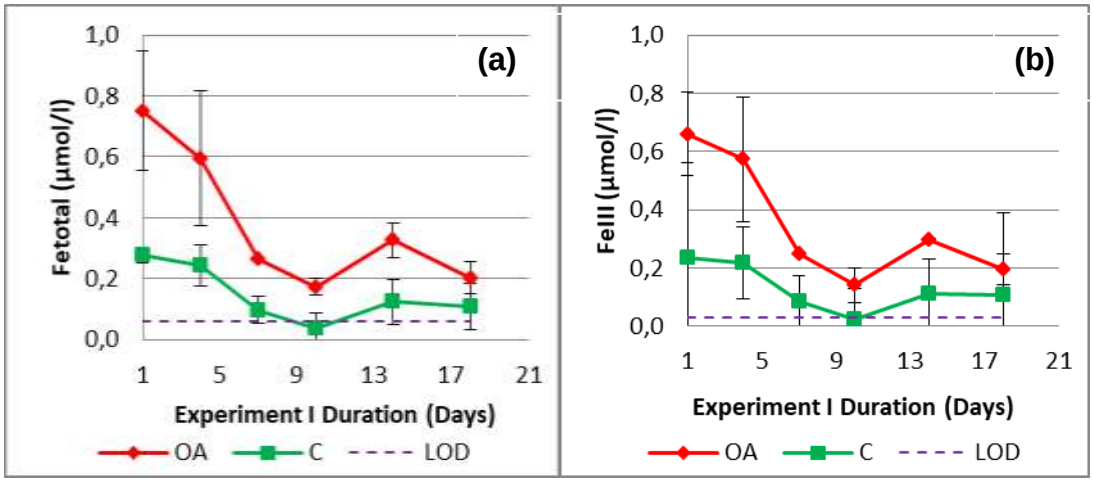

Figure 16. Fetotal and Fe(III) concentrations (in µmol l^{-1}) for the duration of the experiment (mean values and standard deviations for the two replicates of each treatment).

4.2.5 Sediment Composition

Sediment granulometry showed that Elefsis Bay is characterized by fine surface sediments of <63µm in a percentage between 95-100%. Sediment moisture was ~61%, suggesting high sediment water content. The main sediment minerals were calcite ($CaCO_3$) and quartz (SiO_2), followed by aragonite ($CaCO_3$) and cinochlore ($Mg_5Al)(AlSi_3)O_{10}(OH)_8$. This indicates sediment phases rich in carbonates and silica along with aluminium and magnesium. The carbonate content of the Elefsis Bay sediment was 46.8±0.95%; the respective values for OA and C were 47.6±2.6% and

47.0±1.3% respectively. The OC analyses in sediment revealed high organic content (2.35%) and showed a decrease throughout the experiment for both conditions (1.77±0.14%, 1.67±0.25 for OA and C respectively). The sulfur content was found 0.80±0.01 % with no variations during the experiment. The sediment nitrogen content (TN) for field samples was found 0.27±0.02%; for OA treatment TN varied between 0.20±0.01% and for C treatment 0.19±0.02.The phosphorus sediment content (TP) for field samples was found 0.07±0.02% with negligible variations for both treatments (all results in Figure 17).

Regarding trace metals, As was determined 15.9 mg kg^{-1} in field with negligible variations for OA and C conditions (15.3±1.2 mg kg^{-1} and 15.4±1.6 mg kg^{-1} respectively; Figure 19); Mn also presented similar trend (330.0 mg kg^{-1} in field, 327.0±11.1 mg kg^{-1} and 325.0±32.5 mg kg^{-1} for OA and C respectively; Figure 20) as well as Al (3.5%in field, 3.2±0.1% and 3.2±0.1% for OA and C respectively; Figure 20).

Cr increased during the experiment in both conditions in relation with field (101.8 mg kg^{-1} in fiend, 130.7±6.9 mg kg^{-1} and 120.5±12.2 mg kg^{-1} for OA and C respectively; Figure 18). Co also increased in both conditions during the experiment (5.26 mg kg^{-1} in fiend, 6.25±0.91 mg kg^{-1} and 6.34±1.20 mg kg^{-1} for OA and C respectively; Figure 19).

Cu on the contrary declined dramatically in both conditions in relation to field values (63.2 mg kg^{-1} in fiend, 25.4±1.5 mg kg^{-1} and 29.1±1.1 mg kg^{-1} for OA and C respectively; Figure 18). Similar trend was found for Ni with field values of 130.1 mg kg^{-1} and 118.9±0.7 mg kg^{-1} for OA and 114.5±2.7 mg/kg for C condition (Figure 18). Pb also decreased in both conditions (80.8±2.4 mg kg^{-1} and 77.6±33.4 mg kg^{-1} for OA and C respectively) in relation to field values (108.4 mg kg^{-1}; Figure 18). Cd decreased in both conditions (0.342±0.063 mg kg^{-1} and 0.353±0.137 mg kg^{-1} for OA and C respectively; Figure 19) in relation to field values (0.431 mg kg^{-1}).

V slightly increased in OA condition while in C there was negligible variation (66.2 mg kg^{-1} in field, 63.5±1.5 mg kg^{-1} and 65.6±0.8 mg kg^{-1} for OA and C respectively; Figure 18).

Fe decreased in both conditions throughout the experiment (2.08 % in field, 1.85±0.03% and 1.84±0.00% for OA and C respectively; Figure 20). Colorimetric Fe speciation in sediments (Figure 21) showed that the ratio of Fe(II)/Fetotal is present in a percentage of ~95% both in field and in OA condition with a drop at ~89% in C condition (the relevant percentages of Fe(III) were 5% for field and OA conditions and 11% for C conditions).

The one-way ANOVA results, showed no statistically significant difference of the sediment characteristics between the two treatments (ANNEX I – Table 27).

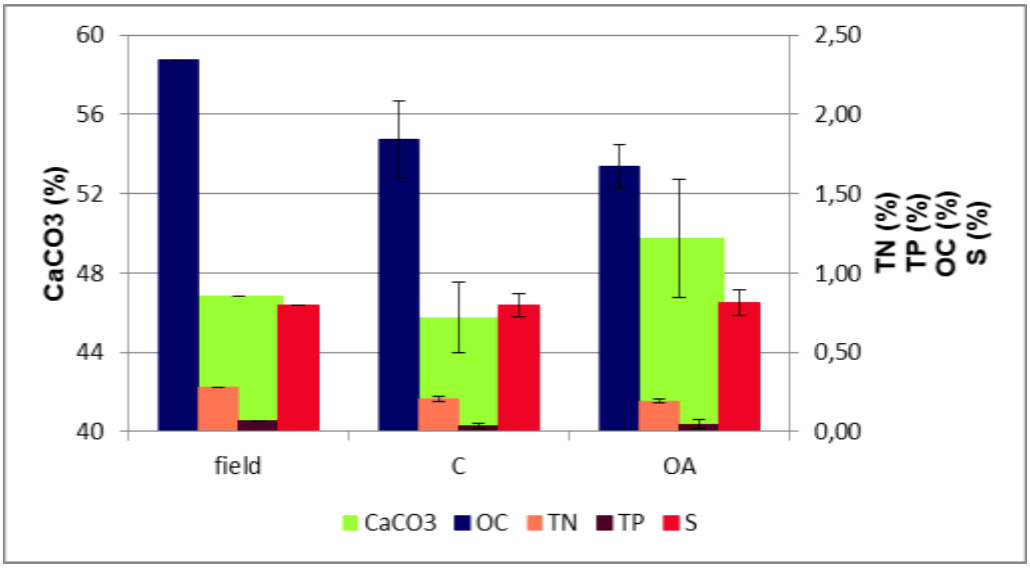

Figure 17. Sedimentary $CaCO_3$, OC, TN, TP and S concentrations (in %) for the C and OA conditions of the experiment (mean values and standard deviations for the two replicates of each treatment).

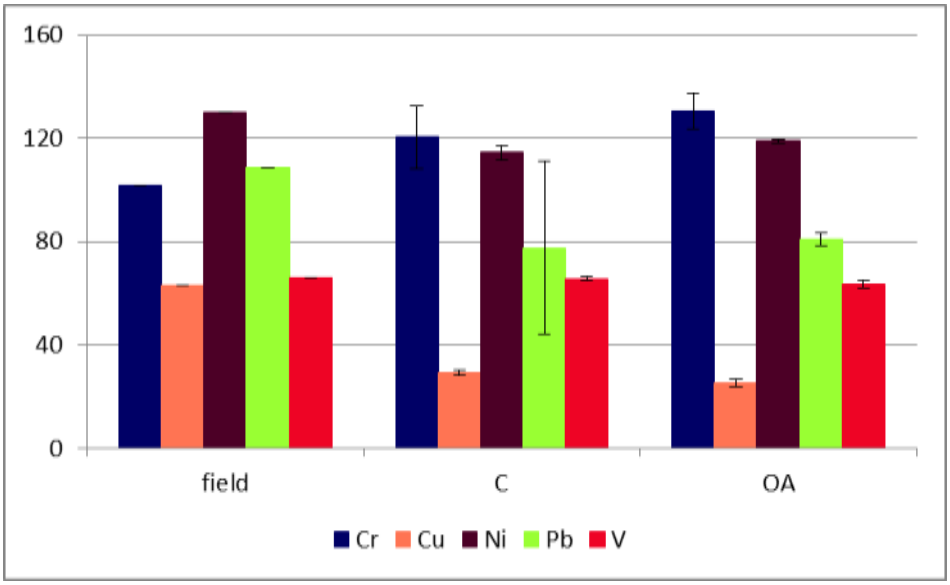

Figure 18. Sedimentary Cr, Cu, Ni, Pb and V concentrations (in mg kg^{-1}) for the C and OA conditions of the experiment (mean values and standard deviations for the two replicates of each treatment).

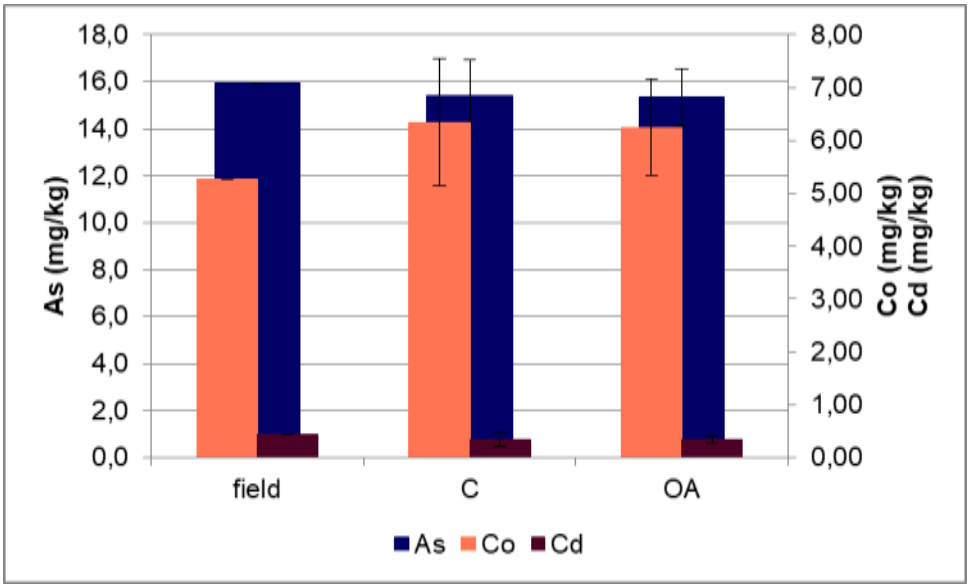

Figure 19. Sedimentary As, Co and Cd concentrations (in mg kg^{-1}) for the C and OA conditions of the experiment (mean values and standard deviations for the two replicates of each treatment).

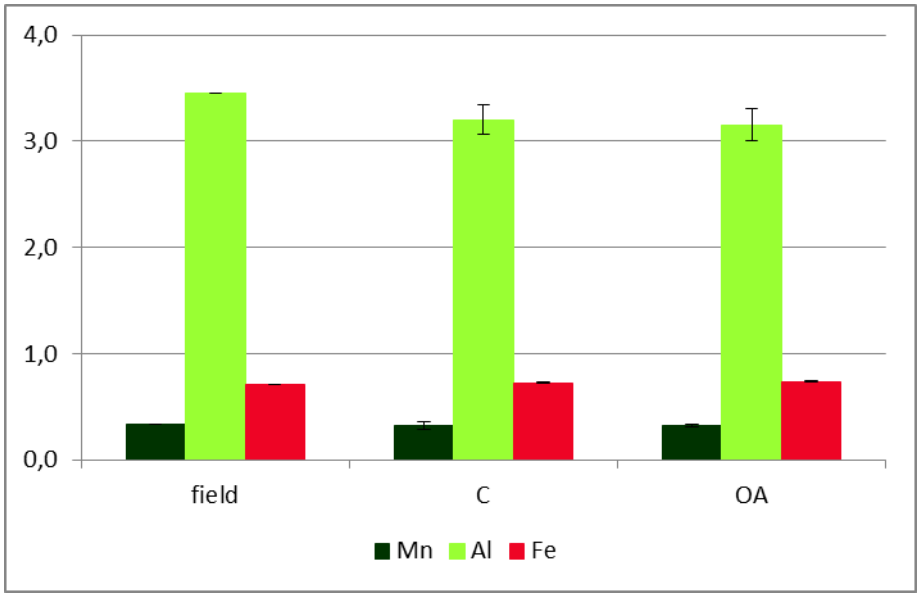

Figure 20. Sedimentary Mn, Al and Fe concentrations (in %) for the C and OA conditions of the experiment (mean values and standard deviations for the two replicates of each treatment).

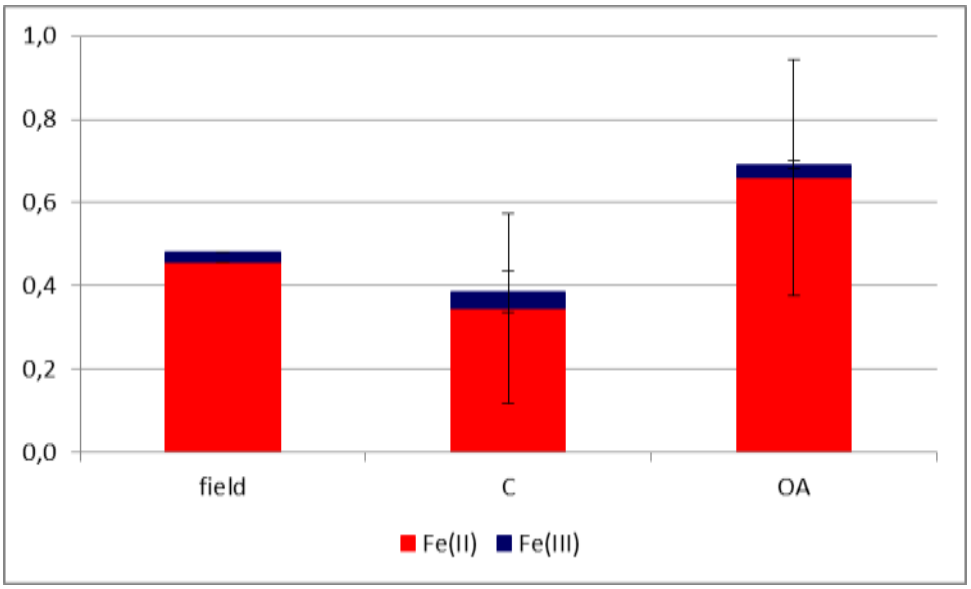

Figure 21. Sedimentary Fe species (Fe(III) and Fe(II)) concentrations (in %) for the C and OA conditions of the experiment (mean values and standard deviations for the two replicates of each treatment).

4.2.6 Principal Components Analysis (PCA)

PCA for the C treatment explained 86.0% of variation in the first two principal components (Figure 22a). The first axis (PC1) explained 60.8% of total variance and was positively related to pH (0.98), CO_3^{2-} (0.98), NH_4^+ (0.89), TDN (0.88), DON (0.85), Mn (0.97), Co (0.83) and Pb (0.94) and was negatively related to A_T (-0.93), DOP (0.89), pCO_2 (-0.99), HCO_3^- (-1.00) and DIC (-1.00), SiO_4 (-0.96), TDP (-0.84), DOP (-0.84) and Ni (-1.00). The first axis was associated with a sequence of processes; on one hand, there is evidence of pH decline impact on carbonate system and on the other hand Ni and Pb dissolution. Additionally, DON, DOP, NH_4^+, SiO_4 appear to contribute to A_T, while Co, Pb are found to associate with reduction processes (e.g. Fe, Mn dissolution) producing HCO_3^-, thus, being also related to A_T increase. The second principal component (PC2) explained 25.2% of total variation and was positively correlated with PO_4^{3-} (0.84), As (0.85) and V (0.92) and was negatively correlated with DO (-1.00), NO_2^- (-0.89) DIN:DIP (-0.81) and DOC (-0.75). The second component was associqated with nitrogen and phosphorus species transformations due to OM degradation (in parallel with DO decrease) also pointing out As and V coherence with OM and PO_4^{3-}.

PCA analysis for OA treatment explained 87.7% of variation in the first two principal components (Figure 22b). The first component (PC1) explained 59.9% of total variance and was positively related with A_T (0.94), pCO_2 (0.94), HCO_3^- (0.95), DOP (0.88), NH_4^+ (0.99), DIC (0.95), SiO4 (0.98), TDP (0.87), DOP (0.88), Cu (0.90), Mn (0.97) and Ni (0.91) and was negatively related to pH (-0.98), CO_3^- (-0.85), PO_4^{3-} (-0.85), Fetotal (-0.90), Fe(III) (-0.91), Co (-0.94) and Pb (-0.93). This first component was associated similarly with C condition with pH decline affecting carbonate system and Ni and Pb dissolution due to acidification. Furthermore, PO_4^{3-} was found to contribute to A_T along with Cu dissolution due to pH decrease.

The second component (PC2) explained 27.9% of total variance and waspositively correlated with NO_3^- (-0.92), DIN (0.91) and Cd (0.94) and was negatively correlated with DON (-0.95). The second component was associated with restrained degradation of DON, subsequently affecting

affecting NO_3^- distribution. An association was also indicated between Cd with NO_3^- .

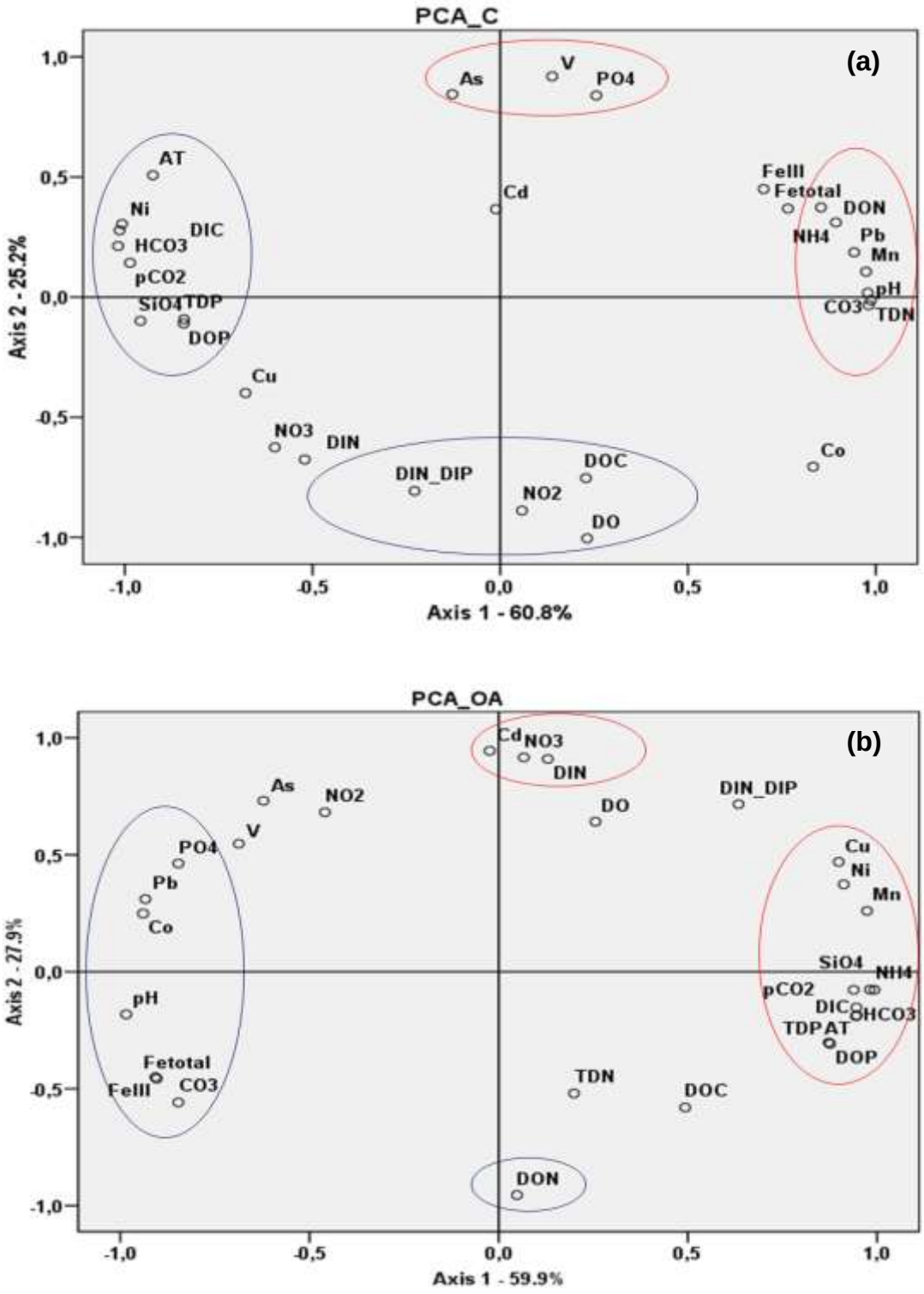

Figure 22. Principal Component Analyses (PCA) Graphs for C (a) and OA (b) treatments. Red circles indicate positive significant correlations while blue circles indicate negative significant correlations

4.3 Discussion

This study, which was based on a microcosm lab simulation, was a first overall assessment of basic biogeochemical interactions/alterations of nutrients and carbon that are taking place in a restricted marine system under the emerging effects of coastal pH decrease. Previous studies were focused either in predicting the effects of future pH reduction or investigating the biogeochemical outcomes of coastal pH decline on certain organisms' response/survival or merely on the processes ultimately determining CO_2 fate and impact in aquatic systems [e.g. 8, 77, 166, 167]. Marine systems however, constitute of specific features, more complex than simple chemical or thermodynamic equilibria which are necessary, nonetheless, for any calculation or prediction model. So this experimental study tries to fill this gap by examining the co-evolution of basic geochemical processes.

4.3.1 Carbonate system processes – Evidence of alkalinity generation

Following the *in situ* DO measurements (99.45 μmol kg^{-1}), the experiment DO values increased for both C and OA treatments but was still conducted under l conditions characterized as hypoxic for shallow habitats (values between 55-193 μmolO_2 kg^{-1}; [19]). This increase in DO during the transfer from field into the experimental setting was due to seawater oxygenation. DO fluctuations during the Experiment I were between ~130-140 μmol kg^{-1} for both C and OA conditions suggesting hypoxia as well [19]. It should noted here, the strong buffering mechanism of the sediment possibly realeasing oxygen as well through the pore waters.

pH variations observed during both conditions are related to large container volumes and to the strong pH-buffering capacity of the sediments, especially in the lower pH values. Similar findings were also observed in previous experiments [13, 26, 166, 167, 168, 169], even due to technical problems or with smaller container volumes, and were not found to affect the experiment progress and the final results.

In C condition, carbonate ions decrease throughout the experiment with a 50% decline in final values; carbonate mineral saturation states also present the same trend. This carbonate decrease is probably attributed to precipitation

on the surface sediment, which is not depicted however on the sediment carbonate content, neither is supported by the declining trend of carbonate mineral saturation states. Total alkalinity, DIC and bicarbonate ions slightly increase in this case due to CO_2 produced by OM degradation. Although CO_2 was periodically injected in C condition tanks in order to maintain a stable pH value, CO_2 concentration and pCO_2 exhibit considerable increase from the beginning till the end of the experiment. The naturally occurring respiration and organic matter degradation as well as the modification of the equilibria between the different forms of dissolved inorganic carbon with an increase of the proportion of both CO_2 and bicarbonate ions at the expense of carbonate ions are the most likely processes to explain the observed trends. .

In OA condition, an immediate decrease in carbonate ions in relation to C condition is found at the beginning with stable concentrations till the end of the experiment. These variations lead to Ω_{ar} and Ω_{cal} values below 1, while in sediments no differentiations were observed. The system response to CO_2 addition was immediate for DIC (since CO_2 contributes in its concentration) probably also augmented by the decaying phytoplankton cells and zooplankton carcasses present in the experimental tanks. Total alkalinity and bicarbonate ions amplification followed as expected (Figure 10).

A significant increase of 90% was observed for A_T with a corresponding DIC increase of 120%, making clear that other mechanisms besides the carbonate system equilibria affect alkalinity. The enhanced A_T in more acidified conditions is generally attributed to carbonate minerals dissolution from sediment [8, 170].

However, no noticeable decrease of sedimentary carbonates was found here. This is not surprising if the high $CaCO_3$ content of the sediment, as well as the relatively short duration of the experiment, are considered. Assuming that the observed A_T increase (ΔA_T = ~2500 μmol kg^{-1}) in the overlying water was generated by the dissolution of sedimentary $CaCO_3$, then the corresponding change in inorganic carbon percentage of the sediment would be about 0.002% w/w that is much lower than the methodological error of the particulate inorganic carbon determination and thus cannot be safely detected. However it seems very likely that the pH decline in the overlying

water has lead to an analogous shift of pH in sediment porewater that induced the development of under-saturated conditions for calcium carbonate minerals in pore waters leading to dissolution of $CaCO_3$ and DIC and A_T generation. Unfortunately, as no pH, A_T and/or DIC data were aquired for the sediment porewater during this study, it is impossible to assess the response of the sediment to pH changes in porewater and valuate the contribution of this process to the observed ΔA_T. A previous study in Saronikos Gulf has shown that under dark conditions DIC efflux from the sediment towards the water column takes place that is negatively related with DO suggesting mineralization processes [171].

It has to be noted that variations in the overlying water A_T are not only due to carbonate dissolution; several other biogeochemical processes could contribute to the A_T increase that was recorded in the current study. Important alkalinity generation (benthic alkalinity) in shallow sediments due to anaerobic degradation of disposed organic matter has been well reported [34, 170, 172]. Remineralization of particulate organic matter and subsequent nutrient release directly affect A_T, depending on the reactive nitrogen species produced (e.g. 1 mole of ammonium or nitrate release leads to an increase or decrease, respectively, of A_T by 1 mole [55]). During more acidified conditions, in this study, the steady increase of ammonium over time along with the respective decrease in nitrate and nitrite concentrations could contribute positively to A_T levels. Moreover, recent estimates of alkalinity fluxes from coastal marine sediments underline the significant contribution of net sulfate reduction to alkalinity generation (up to 70-82% [170]), especially in sediments in highly productive and/or oxygen-depleted coastal waters (e.g. in the Black Sea [173]). It is definite that organic matter degradation and nutrient related processes could not be solely responsible for the significant A_T increase reported here. During organic matter oxidation, when the available oxygen diminishes, respiration processes retreat while sulfate and Fe reduction take over; sulfate reduction producing hydrogen sulfide followed by Mn and Fe reduction result in bicarbonate generation which in turn increase total alkalinity [133, 170, 174].

PCA performed on the C treatment results revealed the effect of pH change on carbonate system parameters primarily, and on ammonium and DOP secondarily (PC1) as well as organic matter degradation and denitrification resulting in nitrogen and phosphorus species transformations , as a result of oxygen availability (PC2).

The same analysis performed on OA treatment results showed the strong impact of OM degradation, ammonium, silicate, organic phosphorus and bicarbonates on A_T (PC1). The fact that under more acidified and low oxygen conditions, only OM degradation and bicarbonate ions are correlated in the first component could also be an indication of sulfate reduction processes releasing considerable amounts of bicarbonates. Through net denitrification and net sulfate reduction, nitrate and sulfate transfer their negative charge to HCO_3^- by oxidizing organic carbon producing the anion which contributes to DIC and alkalinity [133, 170, 174]. High values of hydrogen sulfide measured *in situ* at the near bottom water layer support the sulfate reduction scenario (Pavlidou & Hatzianestis unpublished data). Bicarbonate, sulfide, ammonium and phosphate concentrations utterly contribute in the final A_T concentration [175]. As it appears here, these chemical species affect A_T to a larger extent under lower pH values; from the PCA analysis for OA treatment, ammonium, DOP, HCO_3^-, and DIC were found to contribute strongly to A_T, while phosphate seem to have a negative feedback on it. Normally, phosphate contribute positively to A_T by definition, which indicates that in more acidified conditions with lower available oxygen, a strong complex of phosphate is formed with other substances (e.g. metals or carbonates) which in turn seem to be a reducing factor in the final A_T budget [176]. Furthermore, it has been shown that in areas with restricted mixing, and/or characterized by appreciable autotrophic DOM production and/or significant inputs of DOM from land, organic bases contribute significantly in A_T [55, 176]. Accumulation of DOM in the near-bottom layer of Elefsis Bay, which is enriched in phosphorus relatively to carbon and nitrogen, has been reported during conditions of stratification [119] which could be a further contribution to the system alkalinity.

4.3.2 Processes affecting organic carbon and nutrients

Considering that the basic biogeochemical processes were investigated, the normal mechanisms of the specific study area could be summarized as those pointed out for C condition. In C condition the DON appeared to degrade converting to ammonium which in turn was consumed and rapidly oxidized to NO_2^- and further to NO_3^-. This process reached a plateau in the middle of the experiment after which NO_2^-/NO_3^- were no longer produced . Nitrite and nitrate, were favoured against ammonium in this case throughout the experiment, indicating nitrification to be the main prevailing process. In addition, sedimentary TN decreased indicating dissolution into soluble forms; ammonium and nitrite efflux from the sediment to the water column have been reported for the specific area [139].

In OA condition, after the 5th day of the experiment, DON degradation was constrained, in relation to C condition. In parallel, the originally existing ammonium was no longer oxidized and as the experiment proceeded, ammonium accumulated while nitrate production declined, implying reduction in nitrification process. It has been reported that in Elefsis Bay sediment acts as a source of ammonium to the overlying water, under specific conditions (e.g. hypoxia [139]). Additionally, OA was previously found to cause ammonium efflux from fine-grained sediment towards water [118]; OA can also reduce nitrification rates, reducing oxidized nitrogen supply in the upper water layers [11]. The increased N-content, under lower pH with higher dissolved organic N forms pointed out here, indicates inhibited organic N mineralization processes and a possible N-buildup. The suppression in ammonium oxidation mechanism followed by decrease of nitrate production and subsequently ammonium accumulation, is in consistency with already published studies showing a deceleration of the ammonium oxidation mechanism as pH decreases [11 and references therein]. Efflux of nitrate and nitrite has been previously reported under lower pH values [118] depending on sediment granulometry. The signal of TN release from the sediment is not depicted in the concentrations of nitrite and nitrate, possibly indicating a nitrification mechanism. The phosphate trend presents similar trend with C condition, with negligible variation up to the 10th day. No significant

acidification impact was observed in phosphate and silicate, as has been reported in previous studies [118, 177].

The concentration of the sedimentary organic carbon drops by 20% in C condition and by 30% in OA condition at the end of the experiment, as a result of the first step of its degradation, fueling the DOC pool of the overlying water that exhibits a 20% increase in DOC concentration in both cases. DOC was found relatively high throughout the experiment in both treatments. The final higher DOC concentrations observed for OA condition, although not statistically different from those in C condition, could implicate inhibition of dissolved organic matter decomposition during lower pH values. A possible explanation of the limitation of DOC decay could be relevant to the reactivity of the compounds produced in the first step of organic matter degradation during which particulate organic carbon is converted to dissolved forms. The produced compounds may be resistant to further degradation, due to their inherent stability or as a result of abiotic reactions that protect the molecule from enzymatic attack [178]. Despite any indications revealed here, no similar published results were found; earlier experiments, conducted under CO_2-perturbed conditions that also included the sediment phase, have not examined the features and fate of DOC released by the sedimentary organic carbon degradation. Experiments with pelagic CO_2-manipulated mesocosms have shown a general lack of consensus among the obtained results concerning the effects of ocean acidification on DOM production and fate [179 and references therein, 180 and references therein, 181 and references therein]. However, recent results from mesocosm experiments in the Mediterranean that examined the effect of increased pCO_2 and/or nutrient concentrations on dissolved organic matter dynamics indicated that eutrophication modified the structure of the organic matter into more complex material, while a weak aromatization of the DOM was observed under higher pCO_2 conditions [180] influencing the organic matter lability. Furthermore, experimental observations demonstrated that at lower pH, dissolved organic molecules are becoming more condensed being thus less susceptible or even refractory to biodegradation [182].

The DIN:DIP ratio was found decreased in more acidified conditions; since no prominent variation was observed in phosphate concentrations, the DIN reduction is considered to be the main factor affecting the DIN:DIP ratio. The decreased DIN:DIP ratio, the prevalence of organic nutrient species against the inorganic ones, the observations of constrained DON degradation and nitrate production decline and the higher DOC concentrations under lower pH values can also support inhibition of organic matter decomposition.

4.3.3 Processes affecting trace element biogeochemistry

Regarding coastal OA and trace metal biogeochemistry previous references were primarily focused on the interactive impacts of metal toxicity and acidification in living organisms and bioaccumulation effects [e.g. 76, 113, 25, 26, 115, 116,118, 183). Lately, investigations have been also focused on certain elements' biogeochemistry (e.g .As, Ni, Mn, Cu, Fe, Co) and possible process/species alteration due to decreased pH values and in some cases in combination with additional abiotic stresses (e.g. warming, hypoxia/anoxia [100, 24, 108, 77, 112, 85, 117, 185, 186]).

Arsenic in C condition was only positively correlated with Cd (0.82) and V (0.93) and negatively correlated with DOC (-0.98). The prime mechanism for As release is the dissolution of hydrous oxide phases to which it is adsorbed. As dissolution normally occurs by Fe (III) and Mn (IV) reduction to their soluble lower oxidation states, Fe (II) and Mn (II) [64, 187]; As release from the decomposition of organic matter in sediments has not been demonstrated, even in anoxic sediments [88]. In this case, As seems to be decoupled of Fe and Mn, appearing to be complexed with OM; PCA analysis also supports As dependency only on OM remineralization processes which ends up presenting similar trends with nutrients, e.g. nitrite and phosphate. In OA condition, As was negatively correlated with DOC, TDP, DOP, DON and positively correlated with PO_4^{3-}, Pb and V. Under hypoxic and more acidified conditions, As biogeochemistry has also negligible interactions with Fe or Mn and is clearly coupled with OM; in addition, while Mn and Fe seem to dominate in more solubilized forms, As dissolution appears restricted under lower pH. The negative correlation between As and OM (carbon, nitrogen and

phosphorus) suggests that As complexation to OM is the key factor of As mobility in the dissolved phase; the restricted dissolved As found in OA conditions could also suggest inhibited OM degradation. Finally, the strong As coherence with phosphate could also indicate similar geochemical behaviors and possibly a competitive trend regarding biological uptake.

Vanadium in C condition, is negatively correlated with DO, DOC and positively correlated with As; this suggests a similar trend with As and coupling of dissolved V with OM decomposition and oxygen availability. In more acidified conditions V is correlated positively with As and Pb and correlated negatively with DOC, TDP, DOP indicating only association with OM degradation and a similar distribution with As and Pb. The also decreased dissolved V concentrations suggest the strong coherence with As and OM, reinforcing the inhibition of OM degradation.

Through PCA, Pb in C condition was associated with pH, pCO_2, HCO_3^-, A_T, DIC, CO_3^{-2} , NH_4^+, SiO_4, TDN, TDP, DON, DOP, Ni, Fetotal, Mn and Co. Pb is known to be bound to carbonate minerals, organic substances but also in particulate phases like iron and manganese hydroxides [96]; it seems here that Pb is bound in carbonate phases but also adsorpted on Fe/Mn oxides. In OA condition, Pb is correlated with PO_4^{3-}, A_T, pCO_2, HCO_3^-, CO_3^{-2}, DIC,NH_4^+, SiO_4, TDP, DOP, Fetotal, Fe(III), Mn, Ni, Cu and Co. It seems that Pb behavior is unaffected under lower pH conditions with carbonate-bearing phases and Fe/Mn oxides being dissolved under lower pH values releasing dissolved Pb in the water column.

Cobalt in both C and OA conditions presented similar associations with Pb (through PCA) suggesting Co incorporation in carbonate bonds and possibly bonds within Fe/Mn oxides which dissolve due to increasing CO_2, increasing Co dissolved content under lower pH. Co is an essential micronutrient for phytoplankton growth but its geochemistry does not display nutrient-like features; this has been attributed to redox processes, analogous or related to the geochemistry of Mn [94]. Co(II) exists as a divalent cation which can form strong but labile organic complexes [93, 112]. Co(III) forms inert complexes or oxides. The oxidation of Co(II) to Co(III) can be accomplished by coprecipitation with Mn oxides by Mn-oxidizing bacteria and is thought to be

an important mechanism for cobalt removal in coastal waters [93]. It was suggested here that in lower pH values Co, similarly with Pb, is more available in dissolved forms due to bonds related with Fe/Mn oxides and carbonate phases due to decreasing pH.

Nickel concentrations increased under more acidifying conditions, despite not being statistically significant. Ni, through PCA, presents association with different nutrients as expected (e.g. silicate and phosphate; [99]); additionally correlation with ammonium was found in both conditions.Ni presented similar correlations with Pb in both conditions, suggesting inclusion in carbonate bonds and incorporation in Fe/Mn oxides; Ni precipitation and dissolution is now associated closely with Fe (hydr-)oxide reduction eluding dissolved Ni under increasing CO_2 conditions.

Copper in more acidifying conditions was found to correlate similarly with Pb, Ni and Co suggesting bonding with carbonate ions and Fe/Mn oxides. Cu normally presents nutrient-type distributions while as Cu^{2+} it can be bonded in carbonates and oxides. Cu in the seawater of Elefsis is to a large extent bound to organic ligands [24, 188]; it seems here that Cu is bonded with carbonates and with Mn oxides but coherence is also suggested between Cu and organic forms of nutrients.

From previous experiments [24], Ni and Cu have been shown to efflux from sediment to the overlying water and dissolve more effectively from suspended material under higher CO_2 concentrations. Both sedimentary Ni and Cu were found to decrease substantially from field during both C and OA conditions possibly indicating dissolution to pore water and fluxes towards dissolved forms due to resuspension initially and then due to induced lower pH values.

Cd presented similar trend in both conditions with negligible variations due to decreasing pH; since Cd is mainly complexed with chloride in seawater, negligible changes were expected since chloride concentrations remain unaffected [91, 112]. In OA condition, however, Cd is correlated with DON, DIN and NO_3^- suggesting an association with nitrate and organic N degradation to nitrate eventually. Cd remobilization is usually controlled by redox potential, which regulates the solubility of manganese, which in turn

regulates cadmium availability [91]. In this case, no association between Cd and Mn was pointed out. Cadmium normally presents an ocean distribution closely related to the phosphate/nitrate distributions, as was observed during this experiment [90] but most similarities are usually found with phosphate [91].

Mn in C condition was associated with pH, pCO_2, HCO_3^-, A_T, DIC, CO_3^{-2} , NH_4^+, SiO_4, TDN, TDP, DON, DOP, Ni, Fetotal, Pb and Co. Manganese occurs in seawater as insoluble phosphates and carbonates [106]; also, Mn(II)→Mn(IV) oxidation coupled to denitrification is thermodynamically favorable. In this case in C conditions, association of Mn with phosphate is not suggested and only carbonate bearing Mn phases seem to dominate and restrict Mn dissolution to the water. Apart from this, Mn oxides also abiotically oxidize a variety of reduced inorganic and organic compounds as also appeared here by the direct effect on Co, Pb and Ni concentrations. Mn oxides can also oxidize natural organic matter [106] an association also apparent here considering the strong coherence between Mn and N/P organic phases. Finally, a complex sequence of processes appears to take place between Mn and nutrients in hypoxic conditions, with parallel nitrification (NH_4^+ oxidation to NO_2^- and further oxidation to NO_3^-) and Mn reduction mechanisms. In OA condition, Mn was correlated with PO_4^{3-}, A_T, pCO_2, HCO_3^- , CO_3^{-2}, DIC,NH_4^+, SiO_4, TDP, DOP, Fetotal, Fe(III), Pb, Ni, Cu and Co. Lower pH seemed to induce elevated dissolved Mn(II) through sedimentary carbonate dissolution and reduction of Mn(IV) sediment phase which released dissolved Pb, Co, Ni,Cu and Fe(III). Mn involvement in nitrification mechanism, despite hypoxic conditions, is implied in this case [122, 133].

Fetotal in C condition was associated similarly with Mn. Fe correlation with nutrients reinforces its role in N-related processes along with oxyhydroxide phases (e.g. Mn). In OA condition, Fetotal and Fe(III) were also correlated similarly with Mn, also suggesting their strong coherence through Fe/Mn oxyhydroxides under hypoxic and more acidified conditions.

Under higher CO_2 concentrations, Fe and Mn have been previously found to be mobilised and transported from the sediment to the overlying water [108]. However, re-suspended Mn particles seemed to be dissolved very quickly

under lower pH indicating that the effect of CO_2 on the dissolution of Mn oxyhydroxides was much greater than on the dissolution of Fe oxyhydroxide. These variations were not depicted in sedimentary Fe and Mn content (since the respective concentrations vary between ~0.7 and 0.3 % respectively and such fluctuations in dissolved forms would be quite lower than the standard deviation of the determination).

It could be concluded that As, V are interrelated with OM which also seem to restrict their dissolved concentrations under lower pH values due to inhibition of OM degradation.

Cd is found to associate with nitrate and organic forms of N reacting and producing nitrate finally.

Fe, Mn present seem interrelated in both conditions, associated with Fe/Mn oxyhydroxide which, influenced by pH decline, dissolve other trace metals such as Ni, Cu, Pb and Co.

Ni, Cu, Co and Pb are presented to incorporate in carbonate bonds and possibly bond within Fe/Mn oxides which dissolve due to increasing CO_2, increasing Co dissolved content under lower pH.

4.3.4 Implications for enclosed embayment in future CO_2 conditions

The results of this study showed that the near bottom waters of Elefsis Bay during June were characterized by mild hypoxic conditions [19] and presented increased acidity (7.85 in NBS scale) in relation to typical surface values (pH=~8.1). In some of the oldest studies regarding Elefsis Bay (June 1975; May-June, 1977), surface pH values of 8.4-8.5 have been reported along with seasonal near bottom pH decrease reaching values of 7.9-7.8 (all in NBS scale [126, 131]); this pH difference between surface and near bottom waters has been solely pointed out through individual studies and unfortunately systematic high-frequency pH measurements were never performed. The bottom pH nowadays (7.85, June 2014) was found to be at the same level with values reported about 40 years ago for corresponding time periods, implying that the area has been well affected by the seasonal pH decline manifoldly and in quite unpredicted pathways. Elefsis Bay is a restricted coastal system with intensive urban and industrial activities, receiving

increased N and C inputs, which enhance biological primary productivity and promote subsequent organic matter decomposition. The dramatic DO decrease during stratification along with enhanced CO_2 production and more elevated pCO_2 values caused by OM degradation, induce non-equilibrium between bottom and surface layers.

Total alkalinity in Elefsis bottom water (2769 μmol kg^{-1}) was found markedly higher to the values reported recently for open Eastern Mediterranean Sea waters (2600 μmol kg^{-1} [38]). This value is similar to those reported for the deep layer of the Gulf of Trieste in the northern Adriatic Sea that is a coastal system with shallow depths and seasonal stratification [e.g. 34, 50]. This enhanced alkalinity first of all reflects the alkalinity input in Mediterranean coastal areas by the weathering of the land limestones; additionally, this study revealed the significant contribution of nutrient species and possibly of sulfate reduction in total alkalinity (Chapter 4.2.2). The penetration of anthropogenic CO_2 into the Mediterranean has led to lower saturation degree of calcium carbonate in relation to the preindustrial era [38]. During the period 1967−2003, the estimated Ω_{ar} in a coastal site in the western Mediterranean displayed a decreasing trend and fluctuated between the highest value of 4.3 observed in 1968 and a minimum of 3.1 in 2003 [40]; the calculated $\Omega_{ar.}$, in the bottom waters of Elefsis Bay was found 2.19. Similar low Ω_{ar} values have been recorded in the deep layer of the Gulf of Trieste, under the occurrence of strong remineralization processes during summer [50]. Considering that the anoxic layer in Elefsis Bay is an intermittent feature that is developed annually from depths >15 m [119, 120, 122, 134] and that the same processes promoting hypoxia also acidify the water column [33] during stratification periods, it would be expected to detect more increased DIC and CO_2 concentrations, higher pCO_2 (probably above 1000 μatm) and eventually even lower pH values. Concomitantly, the water column would be more corrosive in respect to aragonite and calcite, an effect relevant to what is expected in the future due to OA, but with undefined impacts on the ecosystem. Relevant findings were reported for the Gulf of Trieste [50] where the intense remineralization of organic carbon in its deeper waters releases CO_2, leading to pCO_2 values up to 1043 μatm during hypoxic periods. After mixing and

respiration, this increased pCO_2 penetrates the surface waters, resulting in their supersaturation with respect to CO_2, and eventually emitting CO_2 gas to the atmosphere [51].

When hypoxic conditions characterize the marine ecosystem, both nitrification and denitrification processes can occur [21] and since nitrite and nitrate both serve as substrates for denitrifying bacteria, it is possible that an inhibition of nitrification could result in a decrease of denitrification process as well [75]. Denitrification and nitrate reduction to nitrite are typical processes taking place during June in Elefsis bottom waters that are becoming evident from the decrease and disappearance of nitrate and the low values of oxygen [119, 128]. Moreover, the OA would decrease ammonium conversion to nitrate through nitrification processes and eventually would deplete nitrate supply in surface waters. In this way, smaller phytoplankton organisms, such as dinoflagellates will be favored, against diatoms which show a preference for growth on nitrate [189], possibly triggering the development of HABs (Harmful Algal Blooms [11, 75]). In Elefsis Bay, the occurrence of HABs is sporadic in time and recurrence of the causative species [190]. Eventually, more acidified conditions could impact the processes determining the final N-species available for biological consumption, a shift which is controlled by a series of biological and physical interactions including global climatic changes [191].

Previous studies have also pointed out the effect of increased CO_2 concentrations on trace metal distribution and fluxes as well with their possible toxicity on certain organisms. Elefsis Bay has been well affected by heavy metal pollution due to its industrilization [e.g. 121, 124, 146]. Acidification would impact on trace metal biogeochemistry in various ways: i) by stabilising or making dissolved forms more available, ii) through OM remineralization processes, iii) through dissolution of carbonate-phase and iv) through reduction of adsorpted Me on Fe/Mn oxyhydroxide phases. All these processes have unpredicatble final pathways for the ecosystem by either releasing more dissolvable forms or by trapping and settling down Me in sedimentary phases.

4.4 Concluding Remarks for Experiment I

This experimental study was an integrated simulation that examined the response, alterations and interactions of nutrients and carbon biogeochemistry under the emerging effects of coastal pH decrease. It has been clearly shown that in coastal areas such as the Elefsis Bay, characterized by temperature-induced stratification and increased inputs of OM and nutrients through anthropogenic activities, more acidified conditions have already been pointed out. It is a fact that the 'hot, sour, and breathless' conditions predicted for the future open ocean [15] can already be found in today's coastal zones during summer, and especially within the close-to-the-bottom layer where pH and DO levels are generally lower than the upper water column [33]. The pH decline in coastal ocean and nearshore waters is already of high scale, exceeding OA resulting from atmospheric CO_2 inputs. The main differentiation between the evolvement of acidification in coastal zone and in open ocean is that the initiative in the former has a bottom to surface orientation. Despite this significant discordance, both mechanisms are expected to present similar final outcomes in coastal systems' biogeochemistry.

It has been demonstrated that under more acidified conditions, significant alkalinity release occurred, whereas the water became undersaturated in both carbonate minerals, namely aragonite and calcite. This alkalinity increase was associated not with sedimentary carbonate dissolution but with the bicarbonate ions that are produced in favor of CO_3^{2-} in order to buffer the CO_2 increase and the reactive nitrogen species shift. In addition there is strong evidence that organic compounds containing basic functional groups originating from the DOM pool and sulfate reduction processes would contribute to the alkalinity production during the experiment.

The ammonium production by the organic matter degradation and the subsequent ammonium oxidation normally occurring under hypoxic conditions, are intercepted in more acidified conditions. The decline of nitrate and nitrite in parallel with ammonium increase, indicate a deceleration of the ammonium oxidation processes along with decrease in nitrate production. These could lead in a decline of nitrification mechanisms that could eventually

affect the phytoplanktonic community composition and the relative species abundances. Phosphate and silicate were not affected by the further pH decline. Organic forms of N and P along with DIN:DIP ratio during more acidified conditions imply possible N-limitation and inhibition of organic matter decomposition.

Regarding trace elements, it was found here that As, V, are directly associated with OM degradation processes which is responsible for the deliverance of their dissolved forms in the water column. Additionally, As was completely decoupled of Fe and Mn particulate phases and only present in complexes with OM. It could also be concluded that Pb, Co, Ni, Cu, Fe, Mn present the same trend in more acidified conditions, mostly found within carbonate bonds and Fe/Mn oxyhydroxide phases influenced by pH decline triggering eventually their elevated dissolved content.

Although Elefsis Bay is one of the most studied areas in Greece, there is a sparseness of recent pH measurements. The pH decline has been documented since the 1970's; the weak water mass renewal, in combination with organic load and high biological production, result in the entrapment and recycling of a large amount of organic matter [119]. The microbial decomposition of this organic matter has caused a local bottom increase in CO_2 concentrations causing carbonate system alterations similar to the future predictions for global OA. This CO_2 release by respiratory processes, along with the development of hypoxia and anoxia has altered decidedly the biogeochemical cycling of carbon and nutrients in the subpycnocline waters of Elefsis Bay; upward spreading of these waters would have potentially important consequences in the biogeochemistry of the upper pycnocline layer.

Currently, OA is not the main factor affecting the Elefsis Bay but long-term trends in pH, resulting from increased prevalence of bottom-water hypoxia is known to be substantial compared to the pH trend resulting from anthropogenic CO_2 acidification, in coastal waters [32]. It has also been suggested that the eutrophication-induced hypoxia could amplify the susceptibility of coastal waters to OA [21], thus making the coastal realm most vulnerable to ecological and biogeochemical perturbations.

CHAPTER 5:

EXPERIMENT II (SEVERE HYPOXIA)

5.1 Experimental Setup

During the experiment II, the pH recorded was 7.75, a value which is already close to future scenarios for open ocean for 2100¸while total absence of oxygen was also recorded. In this case, the tanks containing seawater and sediment were placed in a thermostated room at 17.5 °C, in the dark. The seawater-sediment systems were left to equilibrate, untreated, for a week, while Ar gas was supplied in order to maintain zero D.O. conditions. Subsequently, the 33 days-experimental period of CO_2 aeration followed. During the 25th and the 33th day, the Ar supply was stopped and the tanks were left to reoxygenate.

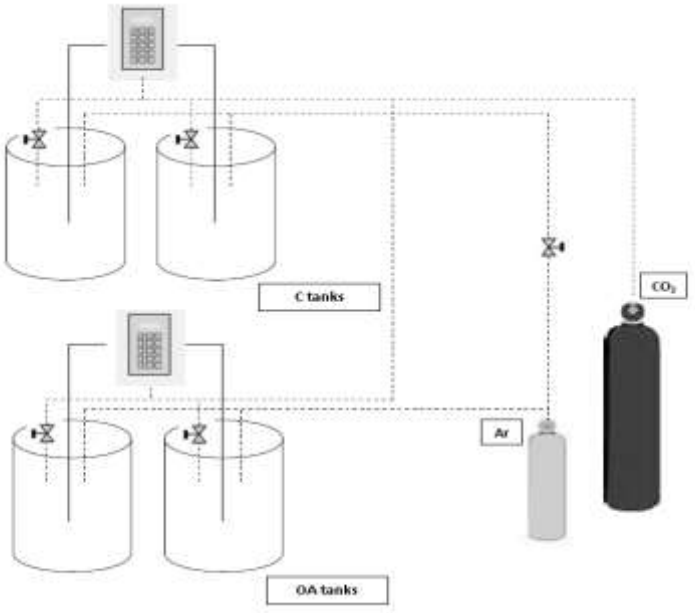

Figure 23. Design of the experimental set-up. two tanks for each pH treatment (OA and C), the IKS system monitoring the CO_2 gas supply and the Ar gas supply in order to maintain the anoxic conditions

In both experiments, the controlled CO_2 supply was achieved, using a continuous flow system (IKS Aquastar, IKS Computer Systeme GmbH), which automatically adjusted CO_2 gas addition to the microcosms in order to

maintain pH stability. Each tank was monitored constantly (every 5 minutes) throughout the experiment by the IKS System using probes recording temperature, pH, Redox and D.O. IKS probes were calibrated daily, using certified buffers, to avoid drifting. Potentiometric probes (pH, Redox, D.O) were also used in order to correct possible drifts of the IKS probes. The measured pH values by the IKS system were corrected with the parallel use of a laboratory pH meter (Jenway 3310) calibrated in NBS scale; the pH values were then converted to the total scale (pH_T) [175].

5.2 Results

5.2.1 *In situ* Parameters

5.2.1.1 Physicochemical and Carbonate System Parameters

Measurements recorded through CTD (Figure 24) indicated a temperature decline of 26.7°C in the surface to 17.5°C in the bottom; salinity decreased from 38.67 to 38.39 psu in 33m. DO determinations showed a well oxygenated upper part until the first 10m (~140 μmol kg^{-1}); in 20m depth, DO was found 33 μmol kg^{-1} suggesting severe hypoxic conditions [19]. In the deepest part, complete oxygen depletion was found, indicating full anoxic conditions.

During May and September surface temperatures of up to 25°C with a difference of 10°C in relation to the bottom is a common phenomenon, being the main driver of a strong stratification persisting for about 5 months [119]. Depth profiles at Elefsis Bay have showed that during the warm/stratified period (August–October), nutrients and oxygen remain constant between 0 and 10 m, whereas, below 10 m, there is a rapid decrease of oxygen reaching near extinction at 20 m and anoxia near the bottom; this was also suggested in this study, with the pycnocline located between 10 and 20m depth.

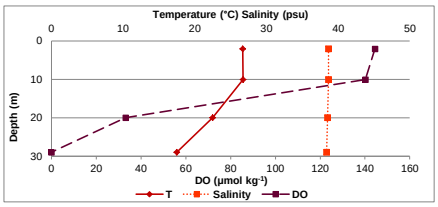

Figure 24. Vertical distribution of physicochemical characteristics T(°C), Salinity (psu) and DO (in μmol kg^{-1}) in Elefsis Bay during September 2014

The pCO_2 calculated in the surface water was 522.6 μatm with significant increase in the deeper parts, reaching eventually 1538.4 μatm in the bottom of Elefsis Bay (Table 21). Total Alkalinity (A_T; Figure 25), in the field, was not significantly affected by the pycnocline, with its value being relatively steady (~2975-2990 μmol kg^{-1}) at all depths. Bicarbonates and DIC (Figure 25) presented similar vertical distributions, increasing below 10m depth (pycnocline formation); carbonates (Figure 25) and carbonate saturation states (Table 21) decreased significantly with depth; surface CO_3^{2-} from ~307 μmol kg^{-1} reached values of 100 μmol kg^{-1} near the bottom while Ω_{ar} was found 4.80 in surface reaching 1.51 in the bottom waters.

Elefsis vertical distribution of bicarbonates and DIC appear similar, increasing below the pycnocline. Bicarbonates trend reinforces the hypothesis that apart from sedimentary carbonate dissolution, anaerobic processes (e.g. sulfate reduction, ammonium prevalence due to OM remineralization etc) produce significant amounts of HCO_3^-. What was found here is that DIC and A_T seem to associate with different processes; apart from bicarbonate production which augment both parameters, sedimentary carbonate dissolution contributes more notably to A_T than to DIC (by definition of A_T; [175]) and possibly organic substances and nutrient species also significantly contribute (positively or negatively) in A_T content.

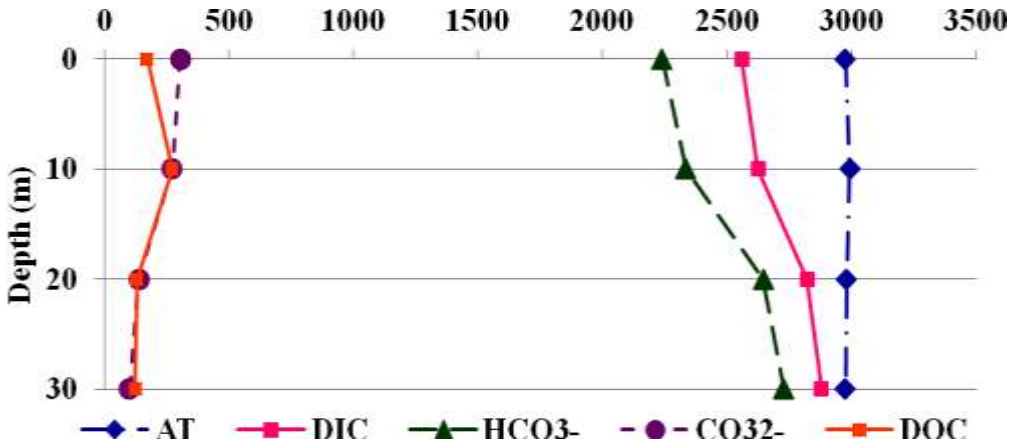

Figure 25. Vertical distribution of carbonate system parameters (A_T, DIC, HCO_3^-, CO_3^{2-}) and DOC (in μmol kg^{-1}) in Elefsis Bay during field sampling.

5.2.1.2 Nutrient and Carbon Analyses

Nitrate and nitrite in Elefsis Bay were found maximum in 20m depth (Figure 26a). Reaching 20m, ammonium, phosphate and silicate begin to increase while in the bottom, they were all found significantly higher than in shallower waters along with elevated DON, TDN, DOP and TDP concentrations. Nitrate and nitrite on the contrary, were found minimum in the deepest part. During September, NO_3^- and NO_2^- peaks are normally observed at 20 m; in some cases, waters with adequate oxygen contain relatively high amounts of nitrite. This relatively high nitrite content could be explained either by the reduction of NO_3^- or by the oxidation of NH_4^+. Previously, anoxic peaks of NO_3^-, ingrowth of N_2, and reduced NH_4^+ concentrations have confirmed anoxic nitrification (see chapter 3.1.2).

The indication of the pycnocline prevailing form depths between 10-20m and deeper, is also reinforced by increasing ammonium, phosphate and silicate well below the 10m depth. During stratified period, the relative contribution of N species in total dissolved inorganic N is distinguished relatively to winter period; NO_3^- accounts for 24% of dissolved inorganic nitrogen (DIN), NO_2^- represents only the 9% of DIN and NH_4^+ 67% above pycnocline. In the near-bottom layer, (1–2 m thick) ammonium is the dominant nitrogen species, representing the 93% of DIN [119]. The same was found for September 2014, with NO_3^- and NH_4^+ varying between ~42-44% above the pycnocline and NO_2^- accounting of ~13% of DIN; in 20m depth, NH4+ increases to 48% of DIN

while NO_3^- and NO_2^- reach 36% and 16% respectively. Below 20m and near the bottom, NH_4^+ is the prevailing species (98% of DIN) with negligible contributions of NO_3^- and NO_2^- (During winter, the relative contribution of NO_3^-, NO_2^- and NH_4^+ in DIN content is 78%, 8% and 13% respectively [119]).

The normal pattern in Elefsis Bay is an increased DIN content (of ~8 μmol l^{-1}) during warm period (mean integrated for the whole water column) with a subsequent decrease to ~2 μmol l^{-1} followed by a DON increase; this suggests that during summer, organic nitrogen oxidation prevails.

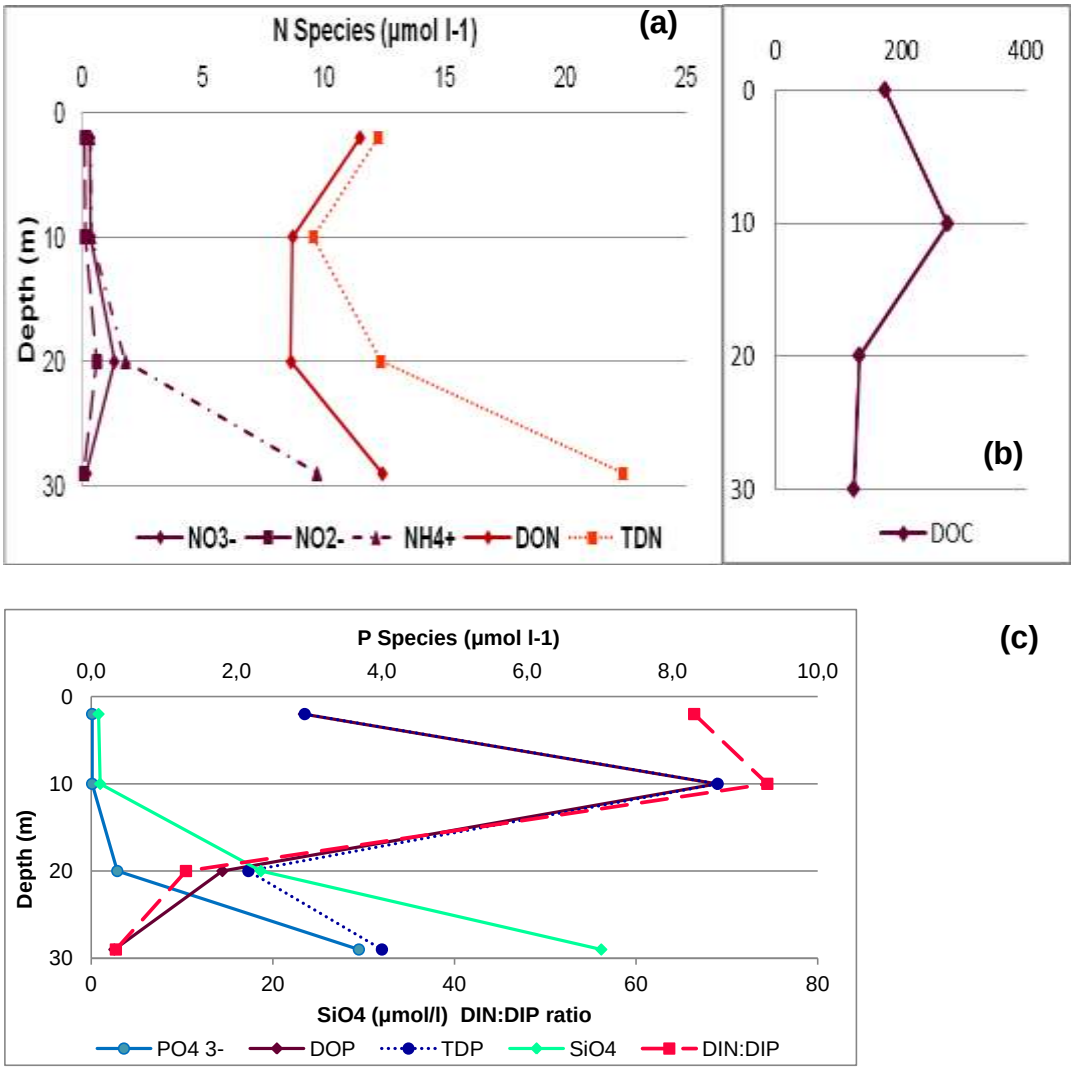

Figure 26. Vertical distribution of nutrients DIN:DIP ratio and DOC (in μmol l^{-1}) in Elefsis Bay during September 2014

Phosphate and silicate (Figure 26) remain stable through the first 10m; below this depth their concentration increases to 0.358 μmol l^{-1} and 18.7 μmol l^{-1} respectively in 20m reaching 3.7 μmol l^{-1} and 56 μmol l^{-1} in 33m. Sediment-released phosphorus increases rapidly when oxygen concentration falls significantly. Sorbed phosphate is released from sediments to pore waters from host Fe-oxyhydroxides. Once released to pore waters, phosphate can escape from sediments via diffusional transport, resuspension, or irrigation by benthos [119].

DIN:DIP ratio through time series also decreases below the pycnocline, from 13.1 in the surface layer to 4.2 in 33m, clearly showing a N-deficit in the near-bottom waters in summer [119]. In this case, surface DIN:DIP ratios of ~70 have been found with a decrease to ~10 in 20m and values of ~3 in the deepest part (Figure 26). The elevated surface ratios indicates P-limitation and could suggest a P-depleted water mass probably due to increased phytoplankton activity.

DOC varied between 125-275 μmol l^{-1} throughout the water column (Figure 26b). Maximum concentration was located in 10m while minimum was found in the bottom layer. DOC values of 77-140 μmol l^{-1} are quite common due to specific anthropogenic activities taking place in the area [119]. The lowest DOC value in 33m suggests increased OM remineralization processes, typical for the specific period of the year.

5.2.1.3 Trace Metal Analyses

Trace element determinations for the water column of Elefsis Bay showed significantly higher values in the deepest part for As, Cd, Co, Cr, Mn, Fetotal and Fe(III); Fe(II) was also elevated in relation to surface and smaller depths (Figure 27, Figure 28a, b).

As presents low concentrations in the first 10m in relation to typical oceanic values (13-27 nmol l^{-1}; [88]) without exceeding values of 22 nmol l^{-1} even in the bottom of Elefsis. As also appears similar to phosphate as expected [88] with maximum bottom concentrations, suggesting similar geochemical behaviours in Elefsis water column. The only available published data on dissolved As in Elefsis bay, are from the 1990's for near-coast areas with

surface values between 2.9-3.6 μg l^{-1} (38.7-48.1nmol l^{-1}) [193]; the present study indicates that nowadays, the inner Elefsis bay, presents lower As concentrations despite the significant industrial activities still dominating the surrounding area.Al, Pb and Ni presented maximum concentrations in 10m depth (Figure 27, Figure 28a); Cu and V showed maximum content in surface with minimum values in 33m depth (Figure 27). No previous studies were found regarding V for the specific area. A normal range for V in natural waters ranges between 0.5–2.5 μg l^{-1} (9.8-49.1 nmol l^{-1}) the values determined *in situ* were found lower; since V is a known by-product of crude oil processing, these limited concentrations suggests that despite the operation of oil refineries in the adjacent area for decades, no V pollution is detected nowadays. Biological uptake is not expected to affect solubilized forms of V [102], something that is also supported in this study. It seems that V entering surface seawater is solubilized (hence its maximum concentrations near-surface) but then probably follows a scavenging mechanism on particulate matter becoming inert in dissolved forms. Al, which normally presents a nutrient-like distribution [87] similar to silicate seems to follow a different pattern in this case.

The expected theoretical trend for dissolved trace metals such as Cu is a decrease due to co-precipitation of their sulphides with FeS as depth increases; dissolved Mn and Ni however, are expected to increase due to reduction and dissolution of iron-manganese oxides [138]. Cu along with V vertical distributions in September 2014, follow this theory; Ni however does not present maximum values in the deepest part but in the 10m depth along with A_T, DOC, Al and Pb, suggesting that probably in the specific coastal area Ni, Al and Pb are not adsorpted in Fe/Mn oxy-hydroxides but are rather associated with biological activity; these elements seem to be incorporated in living organisms which are subsequently released due to disintegration products of biological origin.

At the deepest part of Elefsis Bay, during stratification periods, both dissolved Mn and Fe usually occur at significantly higher concentrations in the deepest part presumably as a result of their dissolution from surface sediments. Dissolution of sinking Fe-particles and formation of soluble Fe-species (e.g.

$Fe_3(PO_4)_2$, Fe organic complexes etc) has been also suggested [122, 193]. The same pattern was found as well during this study with bottom Fe and Mn values even a scale higher than in shallower depths.

The elevated bottom Mn values due to reduction of sedimentary MnO_2 to dissolved Mn^{2+}, in combination with the NO_3^- and NO_2^- peaks found in 20m (see chapter 6.2.1.1), could support an anoxic or suboxic nitrification hypothesis (see chapter 3.1.2) and Mn important role in Elefsis Bay water and sediment chemistry.

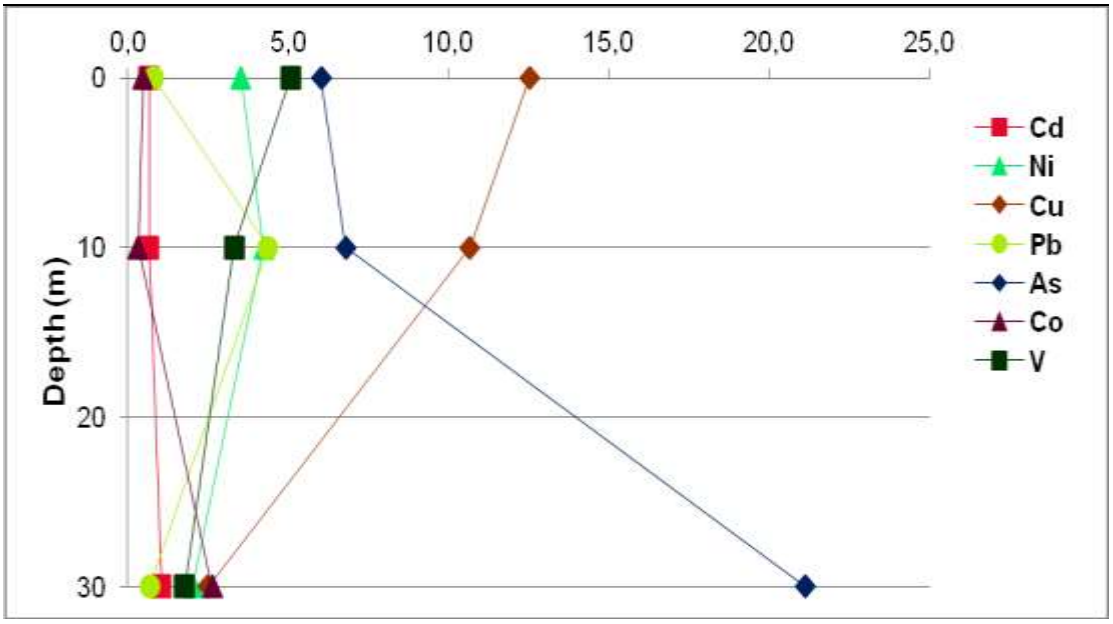

Figure 27. Vertical Distribution of Cd, Ni, Cu, Pb, As, Co and V (in nmol l-1) in Elefsis Bay during September 2014

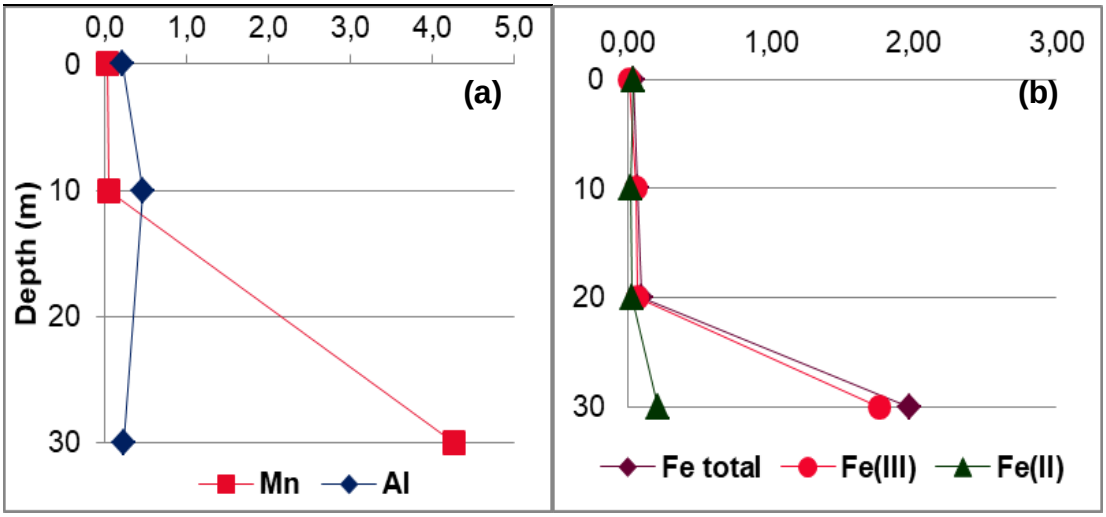

Figure 28. Vertical Distribution of Al, Mn, Fe total and Fe species (in µmol l^{-1}) in Elefsis Bay during September 2014

5.2.2 Experiment Parameters

5.2.2.1 Physicochemical Parameters

Temperature was kept stable at 17.8±1.3°C inside the incubator room. Salinity was constant throughout the experiment at 38.4.

pH (total scale) fluctuated slightly in both conditions; after reoxygenation pH increased from 7.57 to 7.71 in C condition and from 6.58 to 6.73 in OA condition despite the automatic CO_2 supply (Figure 29a).

Dissolved oxygen, at the beginning of the experiment was at ~11 µmol l^{-1} for both conditions, but during the experiment a constant increase was observed reaching values of ~35 µmol l^{-1} just before the reoxygentaion ($F= 0.012$, $p=0.913$; Figure 29b); after the systems were left without Ar supply, DO concentrations were found ~70 µmol l^{-1}.

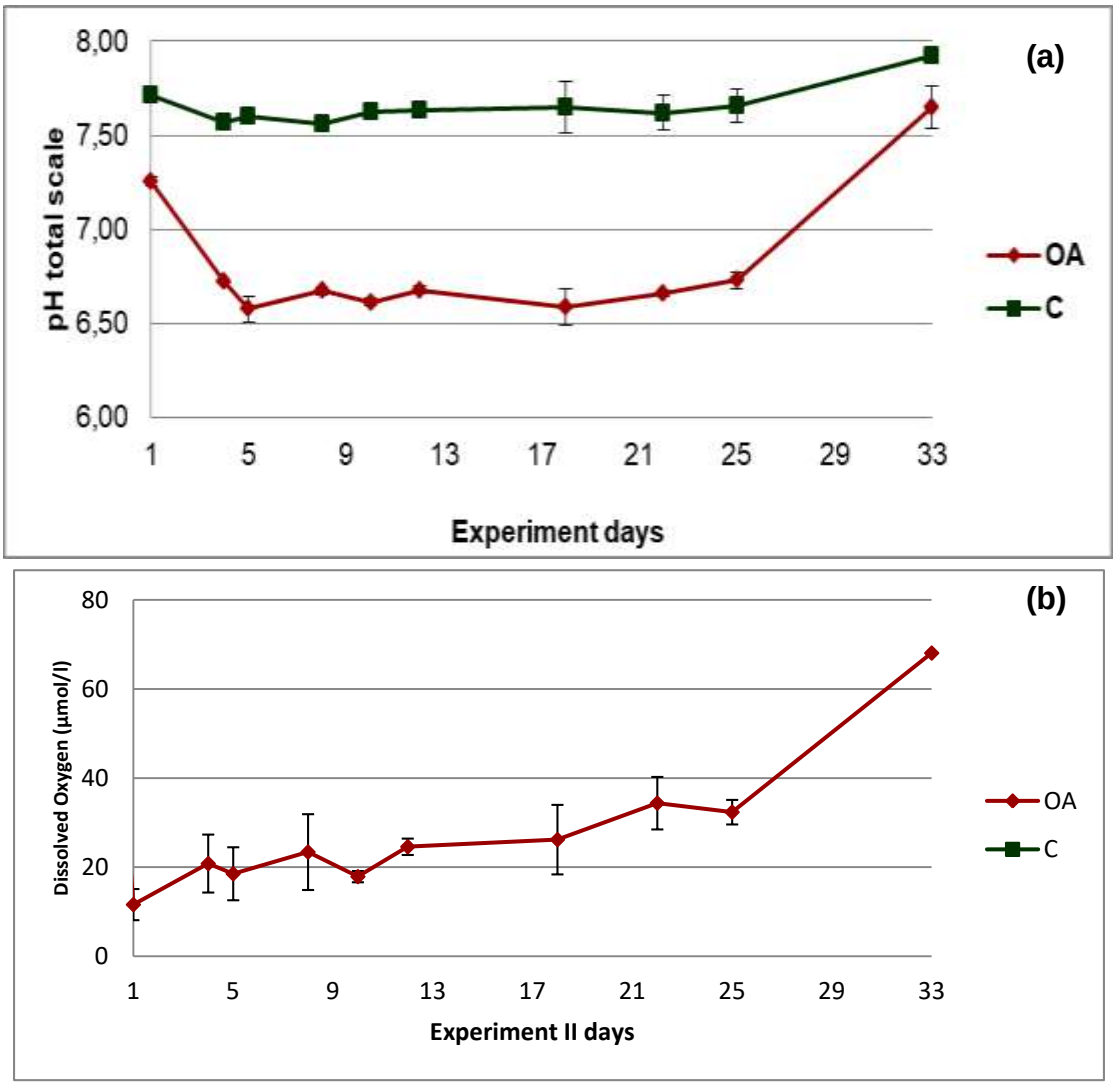

Figure 29. Dissolved Oxygen concentrations (in µmol l^{-1}) and pH (total scale) for the duration of the experiment (mean values and standard deviations for the two replicates of each treatment).

5.2.2.2 Nutrient, Carbon and Carbonate species

The contribution of phosphate and silicate concentrations in the computation of the carbonate parameters via the Seacarb was checked. The results showed that their inclusion in the calculations did not alter significantly the computed carbonate system parameters for OA conditions, being between ±0.01-0.09% compared to the values calculated without considering nutrients (as was previously found in Experiment I, See Chapter 4.3.1). However, this did not coincide with the results found for C conditions; the CO_2 concentrations and pCO_2 values calculated without considering phosphates

and silicates, were found between 40- 500% and 37-88% respectively, higher than when nutrients were taken into account. In addition, carbonates and carbonate saturation states were underestimated up to 80% when nutrients were not included in the calculations, while bicarbonates and DIC were overrated to a lesser extent (between 4-22%).

A_T, during OA conditions, increased after the 5th day and remained constantly elevated compared to C conditions showing no statistical difference (Figure 30; F=3.462, p=0.079). Bicarbonates and DIC (Figure 30) were found significantly higher during OA conditions, throughout the experiment, while during the reoxygenation phase a decrease was observed (F=10.787, p=0.004 and F=15.725, p=0.001 respectively). Regarding carbonates, in OA conditions, an initial decrease from 46.4 μmol kg^{-1} to 14.8 μmol kg^{-1} was observed and remained steady until the 25th day (Figure 30); after the reoxygenation, carbonates increased dramatically to 165.9 μmol kg^{-1} (F=9.934, p=0.006). In C conditions, carbonates remained steady throughout the experiment until the 21st day; on the 21st day an increase was found that could be attributed to sediment sampling and turbation which was amplified by the reoxygenation to final values of 231.2 μmol kg^{-1}. Aragonite and calcite saturation states also followed the same trend with carbonates in both conditions.

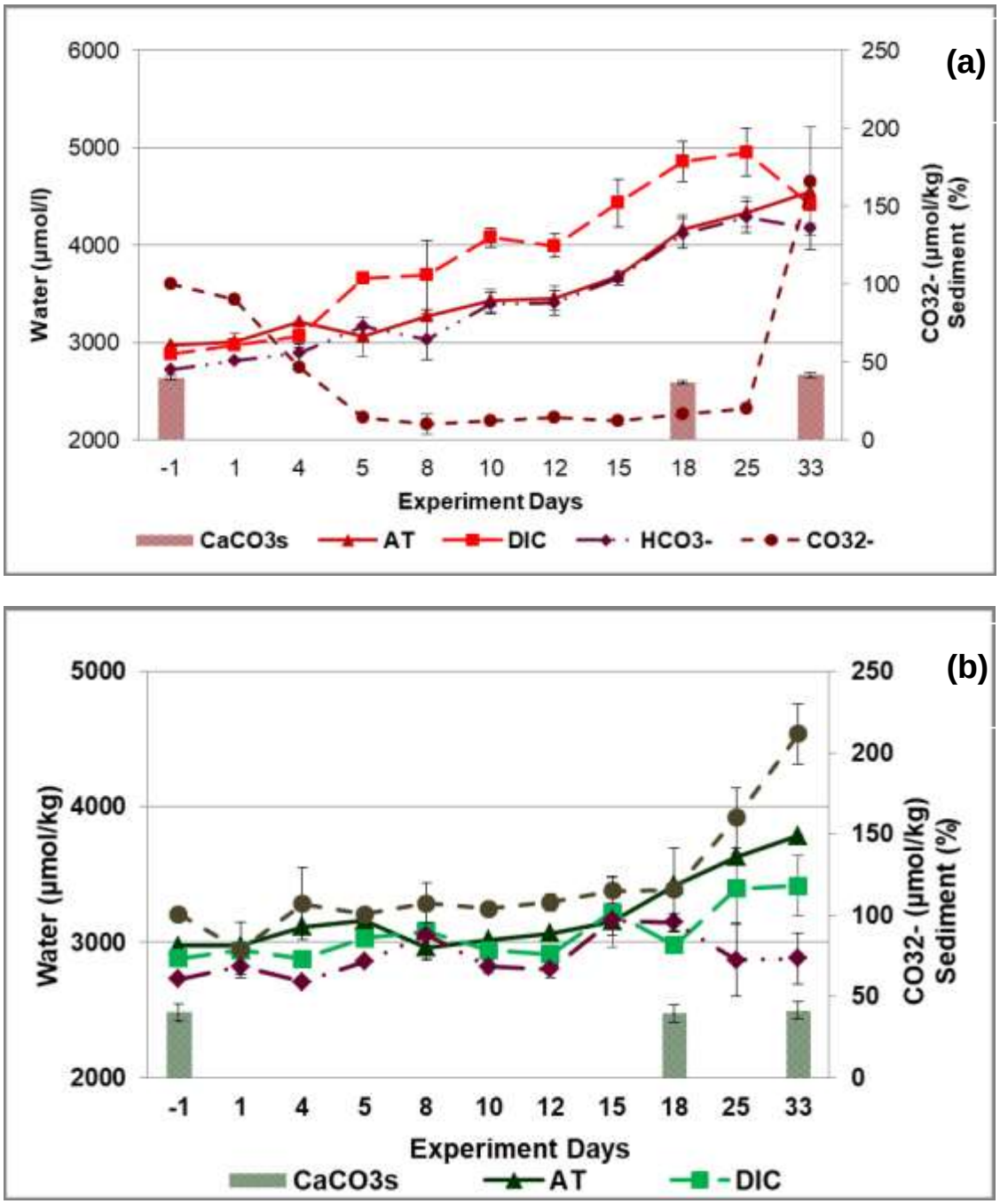

Figure 30. Carbonate system parameters in seawater (AT, DIC, HCO32-, CO32- in µmol kg-1; lines) and sedimentary CaCO3 (%; columns) for OA (a) and C conditions (b) during the experiment (mean values and standard deviations for the two replicates of each treatment)

Nitrate (Figure 31), during the experiment, showed similar trends in both treatments until the 21st day; subsequently, while in C condition they remained stable they were found to increase significantly in OA condition until the 33rd day ($F=0.148$, $p=0.705$). Nitrite (Figure 31) on the contrary, were

found to increase during C condition until the 15th day and then they decreased to minimal values until the end of the experiment; in OA condition, nitrites showed a steady increase throughout the experiment, especially after the reoxygenation (F=3.662, p=0.072). Ammonium, in C treatment, declined throughout the experiment to minimum values (Figure 31); in OA treatment, were found steady during the first 15 days while their concentrations declined in the end of the experiment (F=1.882, p=0.187). DON presented a significant increase until the 12th day and remained higher than C condition throughout the experiment (Figure 31; F=0.164, p=0.691). Phosphate (Figure 32) showed the same trend in both conditions, with constantly elevated concentrations in OA condition. DOP and DOC also presented respective trends in both conditions, with slightly elevated final values for OA condition (Figure 32, Figure 34; F=0.002, p=0.967 and F=0.470, p=0.502 respectively). Silicate (Figure 33b) presented the same trend as well (F=0.005, p=0.943). DIN:DIP ratio decreased gradually in C condition while in OA condition it remained constant throughout the experiment (Figure 33a; F=1.369, p=0.257).

The reoxygenation phase during C conditions, slightly affected nitrates and ammonium concentrations, while nitrites, DON and DIN:DIP ratio decreased. Phosphate, DOP and DOC, on the contrary, increased through this process. In more acidified conditions, nitrates and nitrites both increase as well with DOP and DOC; ammonia and DON declined while DIN:DIP ratio remained constant.

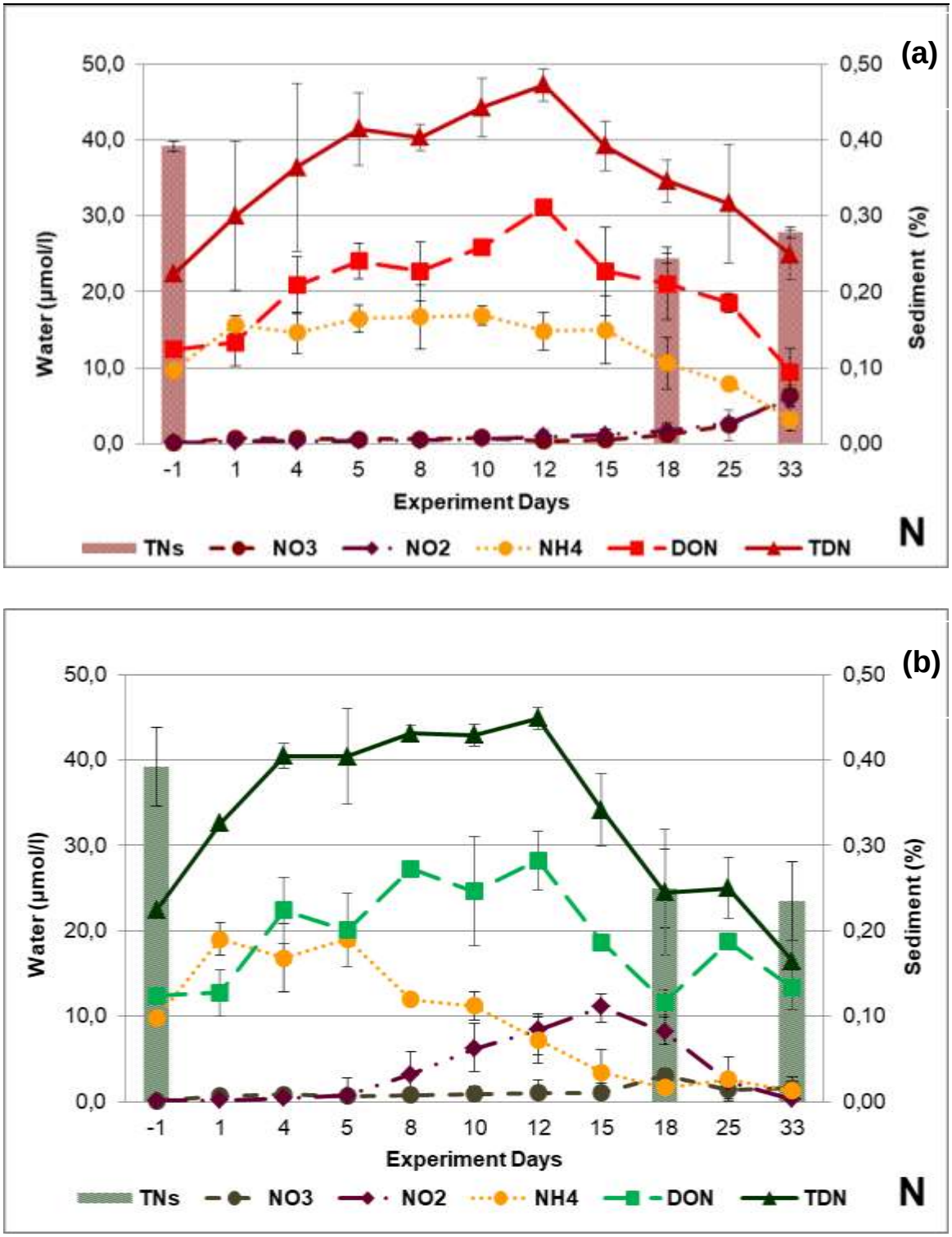

Figure 31. Nitrogen dissolved species (NO_3^-, NO_2^-, NH_4^-, DON, TDN in µmol l^{-1}; lines) and sedimentary TN (%; columns) for OA (a) and C conditions (b) during the experiment (mean values and standard deviations for the two replicates of each treatment).

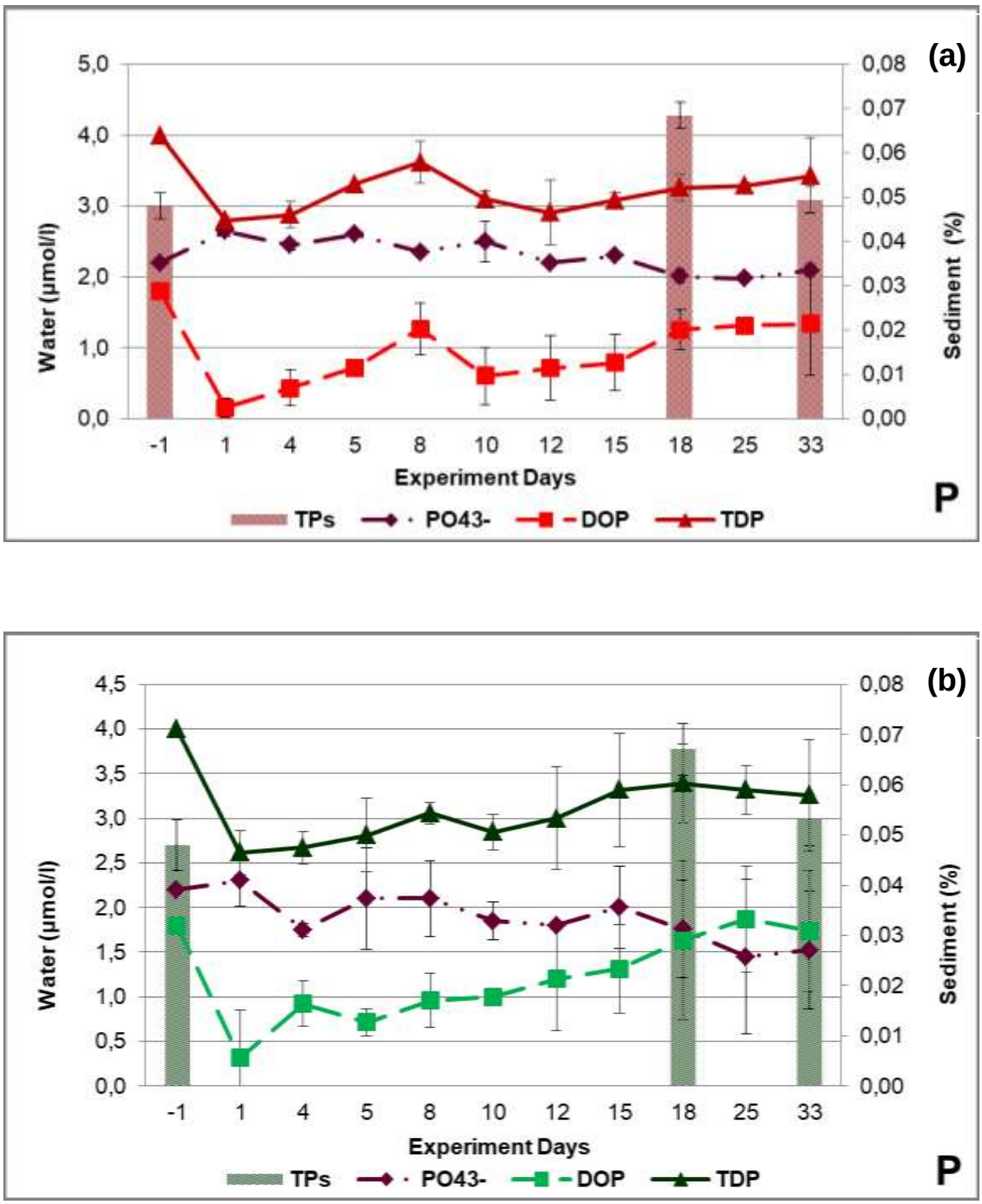

Figure 32. Phosphorus dissolved species (PO_4^{3-}, DOP, TDP in µmol l^{-1}; lines) and sedimentary TP (%; columns) for OA (a) and C conditions (b) during the experiment (mean values and standard deviations for the two replicates of each treatment).

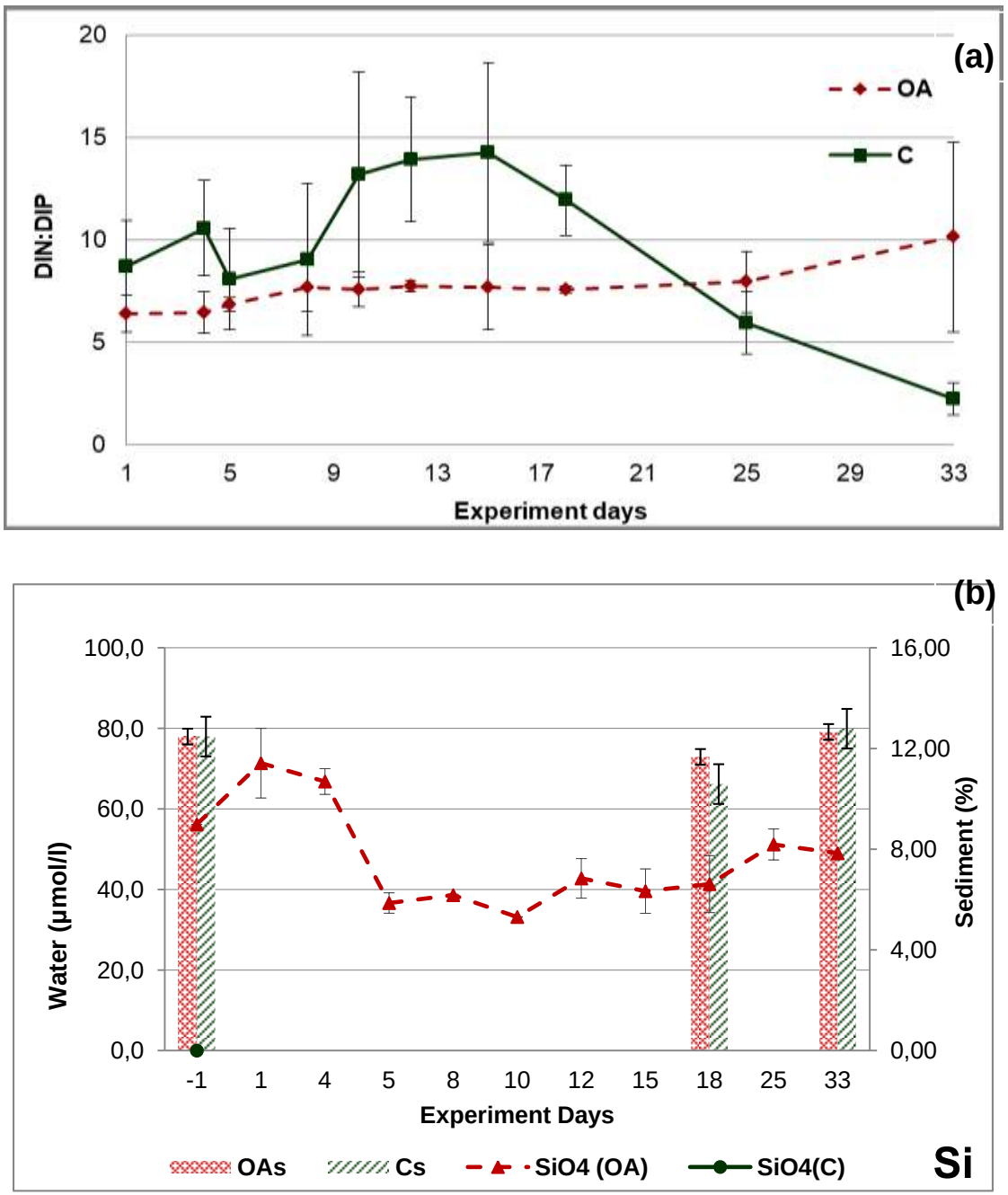

Figure 33. DIN:DIP ratio (a), Silicate (µmol l^{-1}; lines) and sedimentary Si (%; columns) for OA (dashed line/red) and C conditions (continuous line/green) (b) during the experiment (mean values and standard deviations for the two replicates of each treatment).

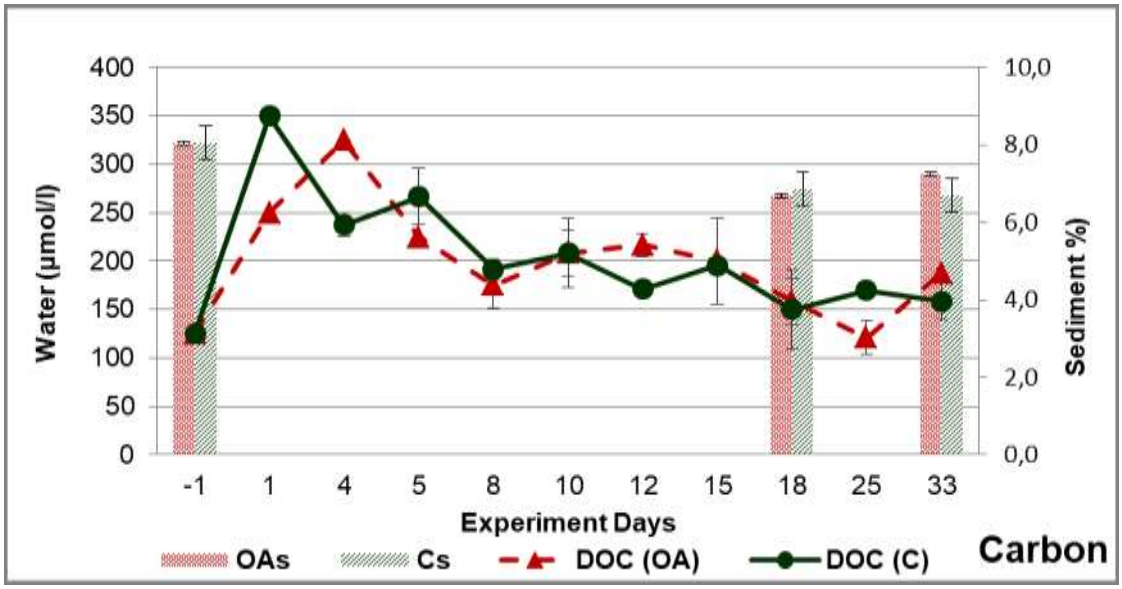

Figure 34. DOC (µmol kg^{-1}; lines) and sedimentary OC (%; columns) for OA (dashed line/red) and C conditions (continuous line/green) during the experiment (mean values and standard deviations for the two replicates of each treatment).

5.2.2.3 Trace Metal Analyses

For all trace metal determinations points represent mean values along with standard deviations for the two replicates of each condition. Pb, Cr and Al were all found below LOD for OA and C conditions, during the experiment and are presented only in ANNEX - Figure 46.

During the experiment, As showed the same trend both in OA and C conditions (Figure 35), with elevated initial values in relation to field values (42.65-44.86 nmol l^{-1} and 21.53 nmol l^{-1} respectively), followed by small variations until the end of the experiment; in OA condition the concentrations appear significantly lower than in C condition, with no effect of the re-oxygenation phase ($F=7.816$, $p=0.012$).

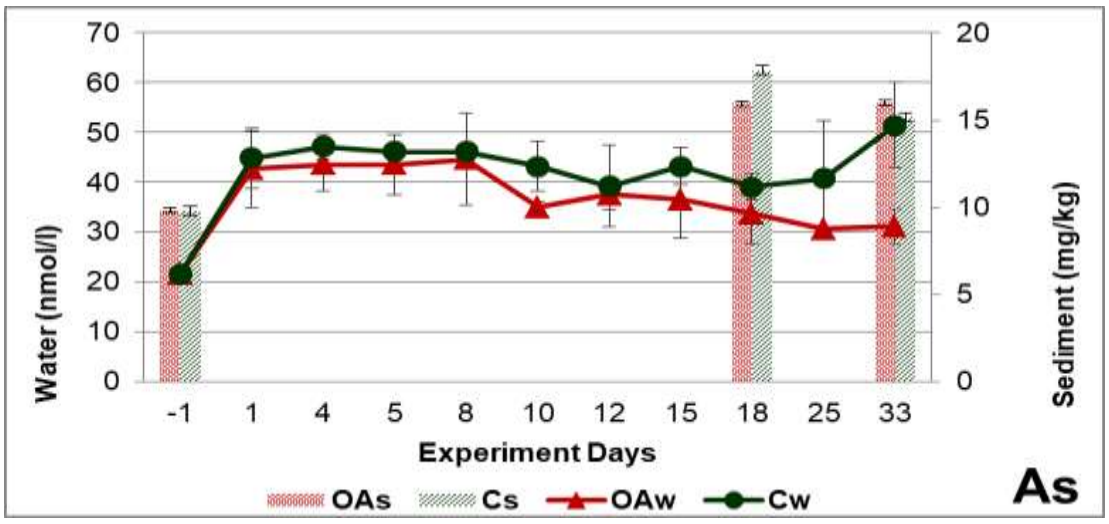

Figure 35. Dissolved As (nmol l-1; lines) and sedimentary As concentrations (mg kg^{-1}; columns) for the duration of the experiment (mean values and standard deviations for the two replicates of each treatment).

Mn concentrations showed similar trends in both OA and C conditions, with significantly decreased values in relation to field values (0.11-0.19 μmol l^{-1} and 4.27 μmol l^{-1}, respectively; F=10.070, p=0.005). In OA conditions the total dissolvable Mn concentrations appeared constantly higher than in C conditions with similar final concentrations after the re-oxygenation (~0.03 μmol l^{-1}).

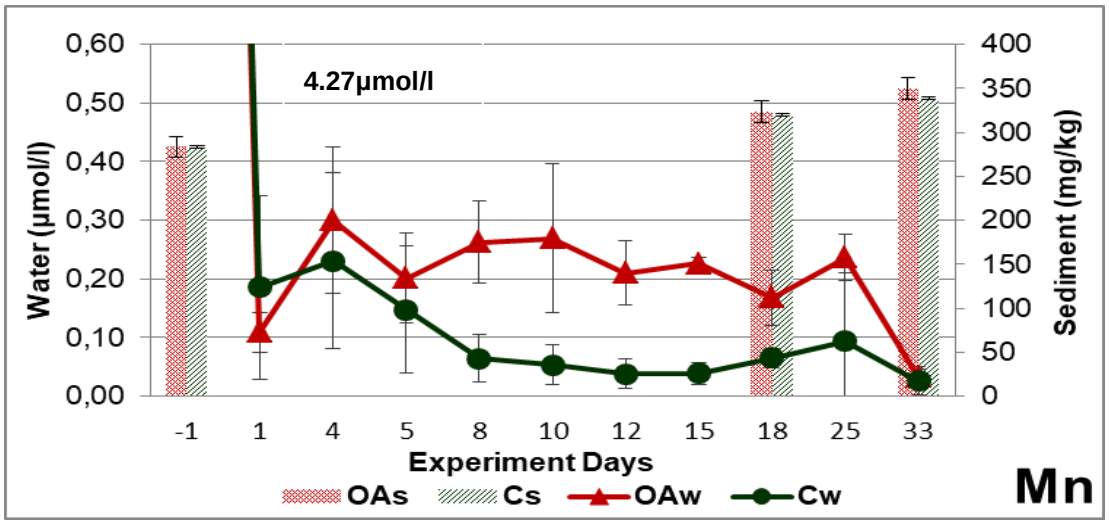

Figure 36. Dissolved Mn (μmol l^{-1}; lines) and sedimentary Mn concentrations (mg kg^{-1}; columns) for the duration of the experiment (mean values and standard deviations for the two replicates of each treatment).

Co also presents the same trend with Mn in both C and OA conditions. In C condition, Co concentrations decreased gradually until the 15th day (from

1.41 nmol l^{-1} to 0.38 nmol l^{-1}) and then increased again until the 25th day (0.97 nmol l^{-1}). Co concentrations were higher during OA condition until the 17th day (values from 0.88 nmol l^{-1} to 0.51 nmol l^{-1}) and then increased until the 25th day (1.07 nmol l^{-1}). After the reoxygenation Co decreased in both conditions, with this decrease being more intense in more acidifying conditions. (F=0.052, p=0.823)

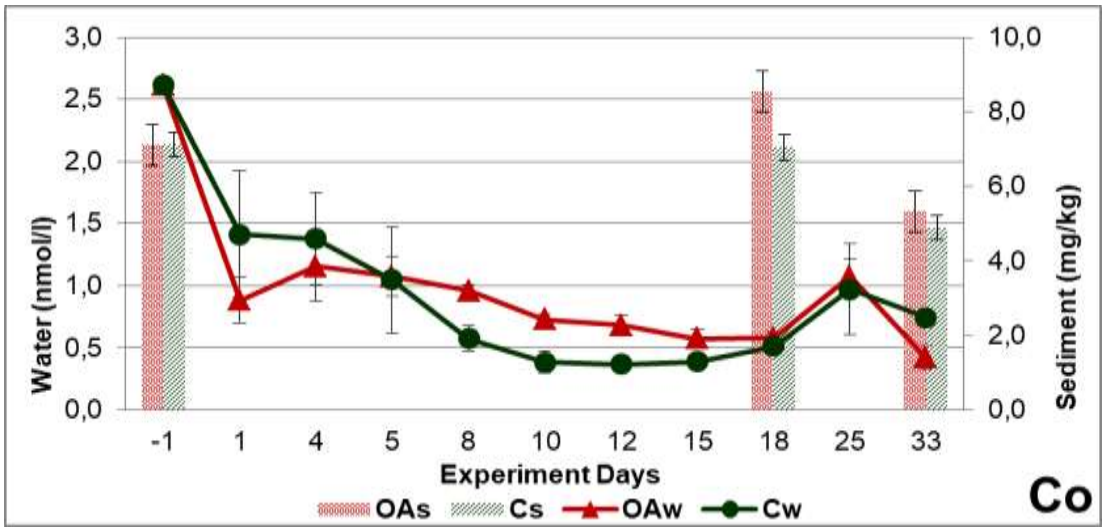

Figure 37. Dissolved Co (nmol l^{-1}; lines) and sedimentary Co concentrations (mg kg^{-1}; columns) for the duration of the experiment (mean values and standard deviations for the two replicates of each treatment).

At the beginning of the experiment, total Fe showed decreased values for both OA and C conditions in relation to the field values (0.54-0.62 μmol l^{-1} and 1.97, respectively; Figure 38), having the same trend until the 25th day. From day 5th, in OA conditions, total dissolvable Fe increased significantly in relation to C conditions (F=7.391, p=0.014) until the 25th day when re-oxygenation took place leading to approximate final concentrations of 0.63 μmol l^{-1} and 1.22 μmol l^{-1} respectively.

Fe (III) showed an increasing trend until the 5th day in both conditions (Figure 38c); for C conditions Fe (III) decreased gradually until the re-oxygenation phase when it increased. In OA, Fe(III) increased more on the 11th day and decreased gradually till the end of the experiment (F=6.957, p=0.017). Fe (II) appeared to decrease from field values in relation to experiment initial values for both OA and C conditions (0.21 μmol l^{-1} and 0.04-0.02 ppb, respectively); during the experiment Fe(II) was above LOD at all times (Figure 38c) with

significantly higher concentrations for OA conditions (F=11.458, p=0.003). The reoxygenation phase, decreased Fe(II) in C condition below LOD while in more acidified conditions Fe(II) was maintained stable.

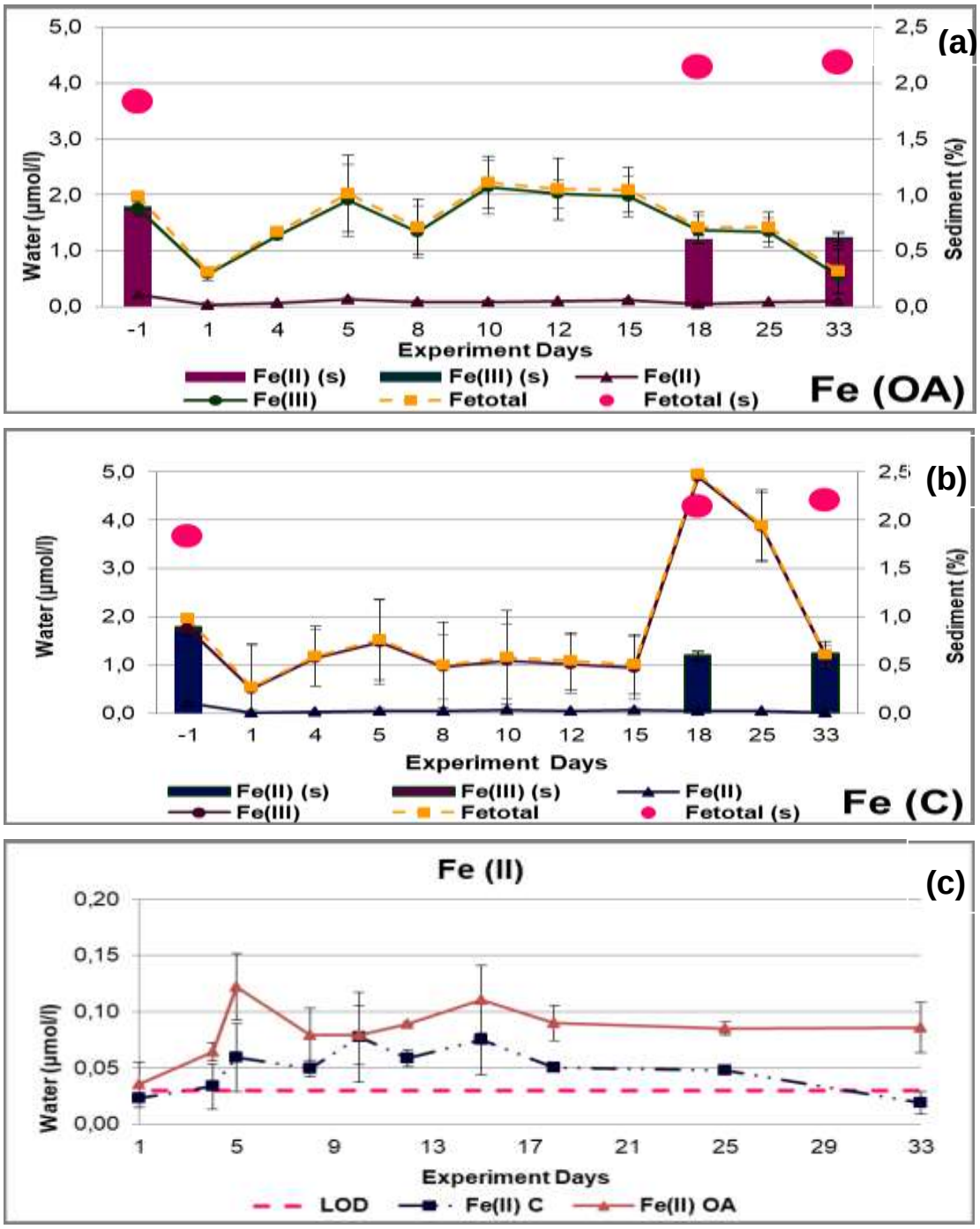

Figure 38. Fe dissolved species (Fe(II), Fe(III), Fetotal in µmol l^{-1}; lines) and sedimentary Fe (%; columns) for OA (a) and C conditions (b) during the experiment. Fe(II) in µmol l^{-1} (c) for the duration of the experiment (mean values and standard deviations for the two replicates of each treatment). Pink circles represent sedimentary total Fe after digestion with EPA3050b and FAAS analysis.

In C condition, V decreased gradually until the 15th day of the experiment (from 66 nmol l^{-1} to 39 nmol l^{-1}). Then, V increased until the end of the experiment to final values of 113 nmol l^{-1}. V in OA condition showed an initial increase (from 41 nmol l^{-1} to 94 nmol l^{-1}) on the 5th day and then continuously decreased until the 25th day to values of 47 nmol l^{-1}; during the reoxygenation however, V increased again (75 nmol l^{-1}).These V variations however showed no statistical difference between the two conditions (F=0.894, p=0.357).

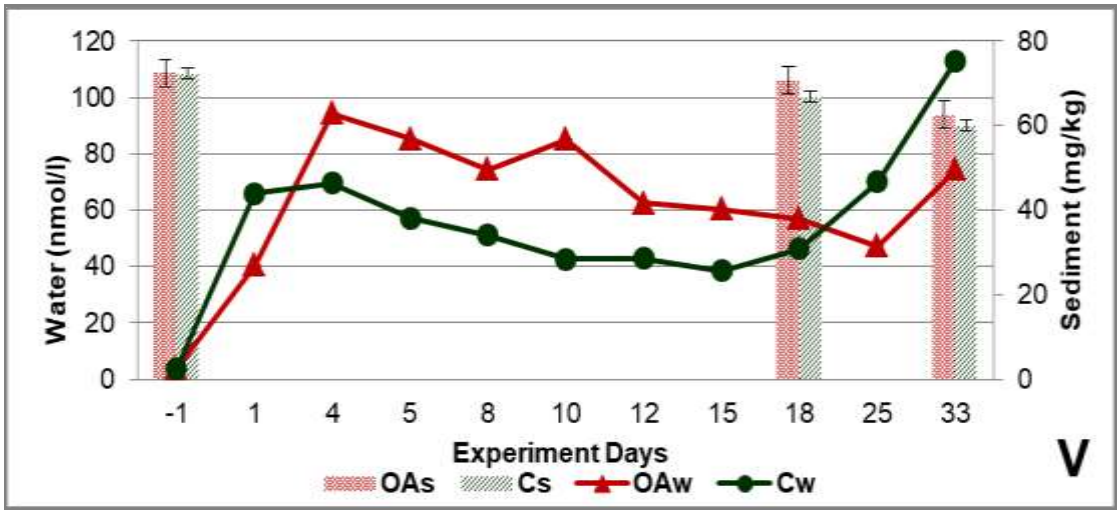

Figure 39. Dissolved V (nmol l^{-1}; lines) and sedimentary V concentrations (mg kg^{-1}; columns) for the duration of the experiment (mean values and standard deviations for the two replicates of each treatment).

Cu showed similar trends in both conditions until the 15th day (F=0.015, p=0.904); in C condition, Cu increased on the 18th day (from 17.09 to 18.95 nmol l^{-1}) and then decreased again with negligible variations after reoxygenation.

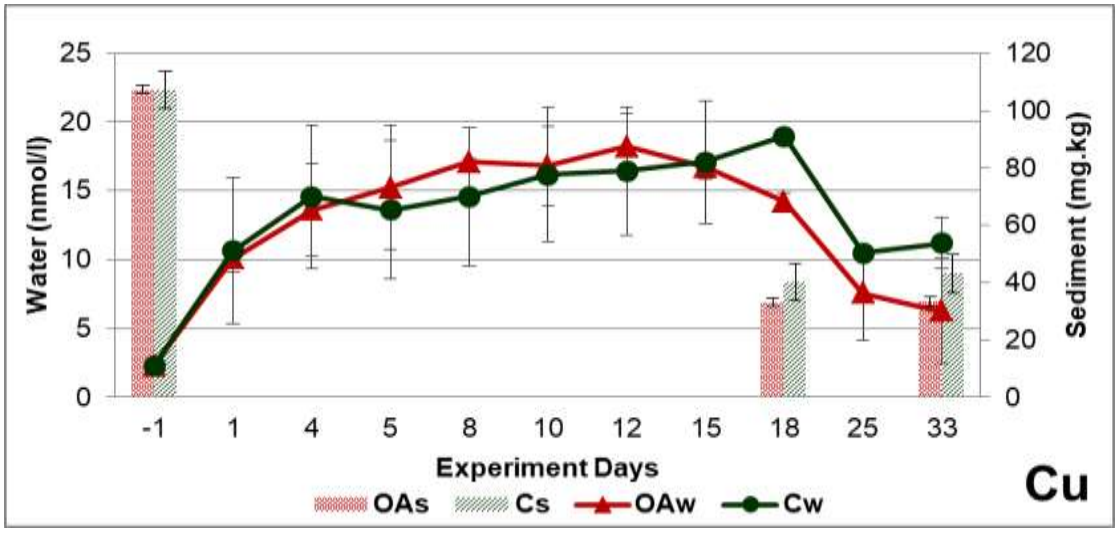

Figure 40. Dissolved Cu (nmol l^{-1}; lines) and sedimentary Cu concentrations (mg kg^{-1}; columns) for the duration of the experiment (mean values and standard deviations for the two replicates of each treatment).

Ni showed similar trends in both conditions with significantly higher values in OA condition throughout the experiment (F=141.033, p=0.000); Ni initially increased in OA and remained higher with negligible variations, even after the reoxygenation. In C condition, small variations were observed with an increase occurring on the 25th day (possibly due to sediment sampling) which was then maintained after the reoxygenation.

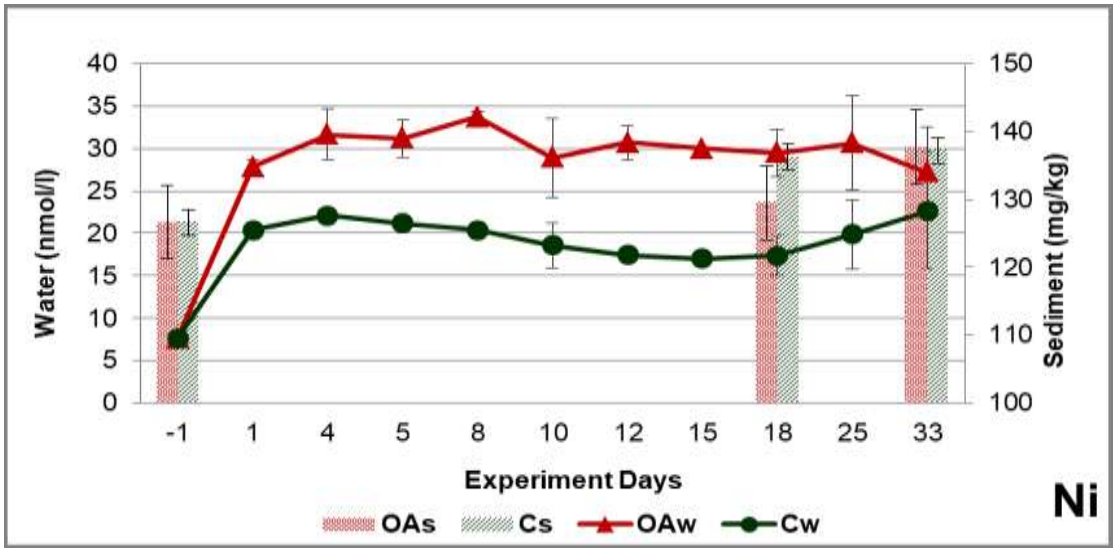

Figure 41. Dissolved Ni (nmol l^{-1}; lines) and sedimentary Ni concentrations (mg kg^{-1}; columns) for the duration of the experiment (mean values and standard deviations for the two replicates of each treatment).

Cd showed the same trend in both conditions with slightly lower concentrations in OA condition (F=0.984, p=0.334). At the end of the experiment, Cd was below LOD for both conditions.

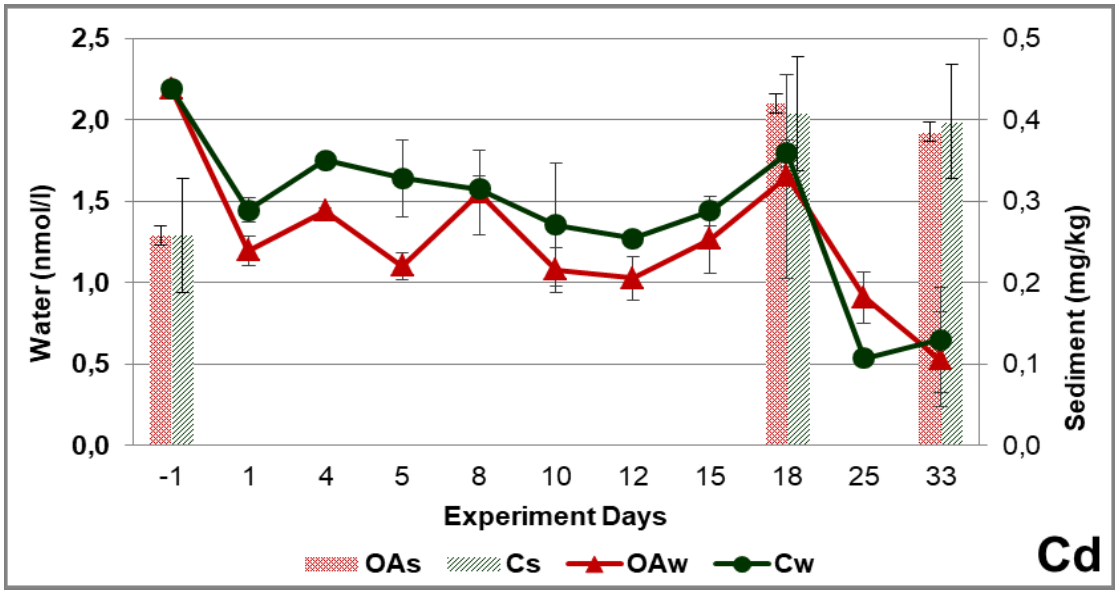

Figure 42. Dissolved Cd (nmol l^{-1}; lines) and sedimentary Cd concentrations (mg kg^{-1}; columns) for the duration of the experiment (mean values and standard deviations for the two replicates of each treatment).

5.2.3 Sediment Composition

The field OC content was 3.64±0.15%; during both OA and C conditions, it was found similar (3.46±0.28% and 3.47±0.08% respectively) while after the systems reoxygenation, OC decerased to 2.84±0.28% and 2.62±0.08% respectively for the two conditions (all results are presented in ANNEX I, Table 6). TN in the field was 0.59±0.10%. In OA conditions TN content was 0.49±0.16% and 0.71±0.16% before and after the oxygenation respectively; in C conditions TN was 0.60±0.31% and 0.77±0.31% respectively. TP in the field was 0.05±0.01%; in OA conditions, TP was found 0.08±0.02% initially while after the reoxygenation it decreased to 0.05±0.02%. In C conditions, TP was constant in 0.06±0.01%. Regarding sulfur content, in the field it was found 0.97±0.01%; in OA conditions it was 0.86±0.02% and after the reoxygenation it was 0.94±0.02%. In C conditions, S was 0.81% and after the reoxygenation it increased to 0.88%.

Regarding trace metals, As (Figure 35) was determined 9.81 mg kg^{-1} in field with a significant increase for both OA and C conditions (15.87±0.14 mg kg^{-1} and 16.6±0.08 mg kg^{-1}) respectively which was maintained even after the reoxygenation; Al (Figure 43) also increased in the same manner (3.26%in field, 3.48±0.14% and 3.57±0.05% for OA and C respectively).

Mn (Figure 36) also presented similar trend (283.7 mg kg^{-1} in field, 323.6±10.1 mg kg^{-1} and 319.5±11.2 mg kg^{-1} for OA and C respectively) with the increase continuing after the reoxygenation phase (349.8±26.9 mg kg^{-1} and 338.5±9.0 mg kg^{-1} for OA and C respectively).

Cr (Figure 43) slightly declined during the experiment in both conditions in relation with field (116.8 mg kg^{-1} in field, 107.8±1.0 mg kg^{-1} and 103.3±4.8 mg kg^{-1} for OA and C respectively) but after the reoxygenation increased again (128.5±14.6 mg kg^{-1} for OA and 122.1±3.6 mg kg^{-1} for C).

Co (Figure 37) also increased in both conditions during the experiment (7.12 mg kg^{-1} in field, 8.53±0.30 mg kg^{-1} and 7.04±0.73 mg kg^{-1} for OA and C respectively) but the reoxygenation decreased its concentrations (5.32±1.07 mg kg^{-1} for OA and 4.89±1.22 mg kg^{-1} for C).

Cu (Figure 40)on the contrary declined dramatically in both conditions in relation to field values (76.0 mg kg^{-1} in fiend, 47.3±2.3 mg kg^{-1} and 50.6±5.3 mg kg^{-1} for OA and C respectively) with the decrease continuing even after the reoxygenation (42.0±4.2 mg kg^{-1} for OA and 45.4±23.5 mg kg^{-1} for C).

Ni (Figure 41) had slight variations throughout the experiment in relation to field values (126.7 mg kg^{-1} in field, 129.5±2.7 mg kg^{-1} for OA and 136.2±6.1 mg kg^{-1} for C condition respectively) and continued increasing after the reoxygenation (137.7±10.4 mg kg^{-1} for OA and 137.3±3.5 mg kg^{-1} for C).

Pb (Figure 43) increased slightly in both conditions (106.1±7.3 mg kg^{-1} and 111.0±4.8 mg kg^{-1} for OA and C respectively) in relation to field values (101.6 mg/kg) and remained similar after the reoxygenation (110.5±16.0 mg kg^{-1} and 107.1±3.5 mg kg^{-1} for OA and C respectively).

Cd (Figure 42) increased in both conditions (0.489±0.013 mg kg^{-1} and 0.475±0.037 mg kg^{-1} for OA and C respectively) in relation to field values (0.301 mg kg^{-1}) and slightly decreased after the reoxygenation in OA condition

(0.448±0.033 mg kg^{-1}) while for C remained almost stable (0.463±0.204 mg kg^{-1}).

V (Figure 39) decreased throughout the experiment in both conditions (72.3 mg kg^{-1} in field, 70.8±0.4 mg kg^{-1} and 66.8±3.5 mg kg^{-1} for OA and C respectively) and continued its decrease even after the reoxygenation (62.6±5.1 mg kg^{-1} for OA and 60.0±1.6 mg kg^{-1} for C).

Fe increased in both conditions similarly (1.83 % in field, 2.14±0.08 % and 2.18±0.14 % for OA and C respectively; Figure 38) and remained stable after the reoxygenation (2.14±0.13 %g for OA and 2.20±0.22 % for C).

Fe speciation in sediments showed that Fe(II) is present in a percentage of ~20% in field and in both conditions; after the reoxygenation, there was a drop only in OA condition where Fe(II) constituted the ~17% of Fetotal while in C condition this ercentage remained stable ~20%.

The one-way ANOVA results, showed no statistically significant difference of the sediment characteristics between the two treatments (ANNEX I – Table 28).

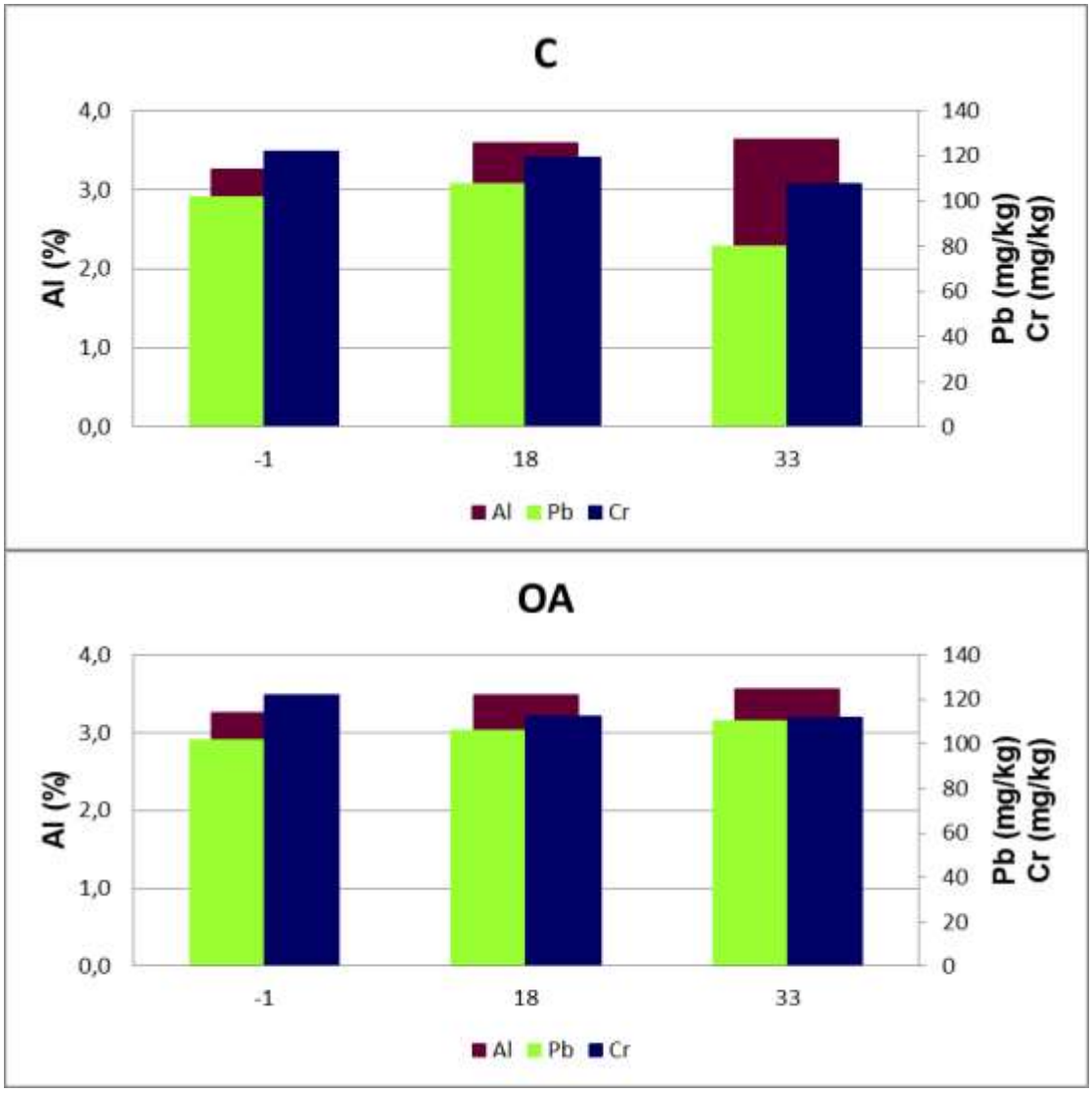

Figure 43. Sedimentary Pb, Cd (in mg kg^{-1}) and Al (in %) concentrations for the C (a) and OA (b) conditions of the experiment (mean values and standard deviations for the two replicates of each treatment).

5.2.4 Principal Components Analysis (PCA)

PCA for the C treatment explained 65.9% of variation in the first two principal components, (Figure 44a). The first axis (PC1) explained 37.4% of total variance and was positively related to DIN (0.95), DIN:DIP (0.97), TDN (0.82), NH_4^+ (0.79), PO_4^{3-} (0.93), Cd (0.77) and As (0.77), and was negatively related to DO (-0.90) and A_T (-0.92). This first axis was associated with DO decline and OM degradation impact on A_T. What was pointed out through this analysis was the decoupling of DIC and A_T, suggesting that different processes ultimately determine their distribution during the experiment.

PC2 explained 28.5% of total variation and was positively correlated with Ni (0.83), Co (0.81) and V (0.77) and was negatively correlated with NO_2^- (-0.92) and Fe(II) (-0.86). PC2 was associated with coupled redox processes including N species transformations and reduction processes leading to increased Fe(II) and Co and Ni dissolution.

PCA analysis for OA condition explained 71.5% of variation in the first two principal components (Figure 44b). The first axis (PC1) explained 44.4% of total variance and was positively related with pCO_2 (0.92), TDN (0.92), DON (0.94), Fetotal (0.92), Fe(III) (0.92) and Cu (0.90) and was negatively related to pH (-0.87), CO_3^{2-} (-0.85) and SiO_4 (-0.85). The first axis was associated with dissolution of sedimentary $CaCO_3$ due to CO_2 increase and DON, Fe(III) solubilization .

The second axis (PC2) explained 27.0% of total variance and was positively associated with DO (0.92), A_T (0.96), DIC (0.93), HCO_3^- (0.98), NO_2^- (0.84) and DOP (0.89) and was negatively correlated with NH_4^+ (-0.82) and PO_4^{3-} (-0.88). This axis was associated with OM degradation products and decreased DO concentrations, producing HCO_3^- affecting both A_T and DIC.

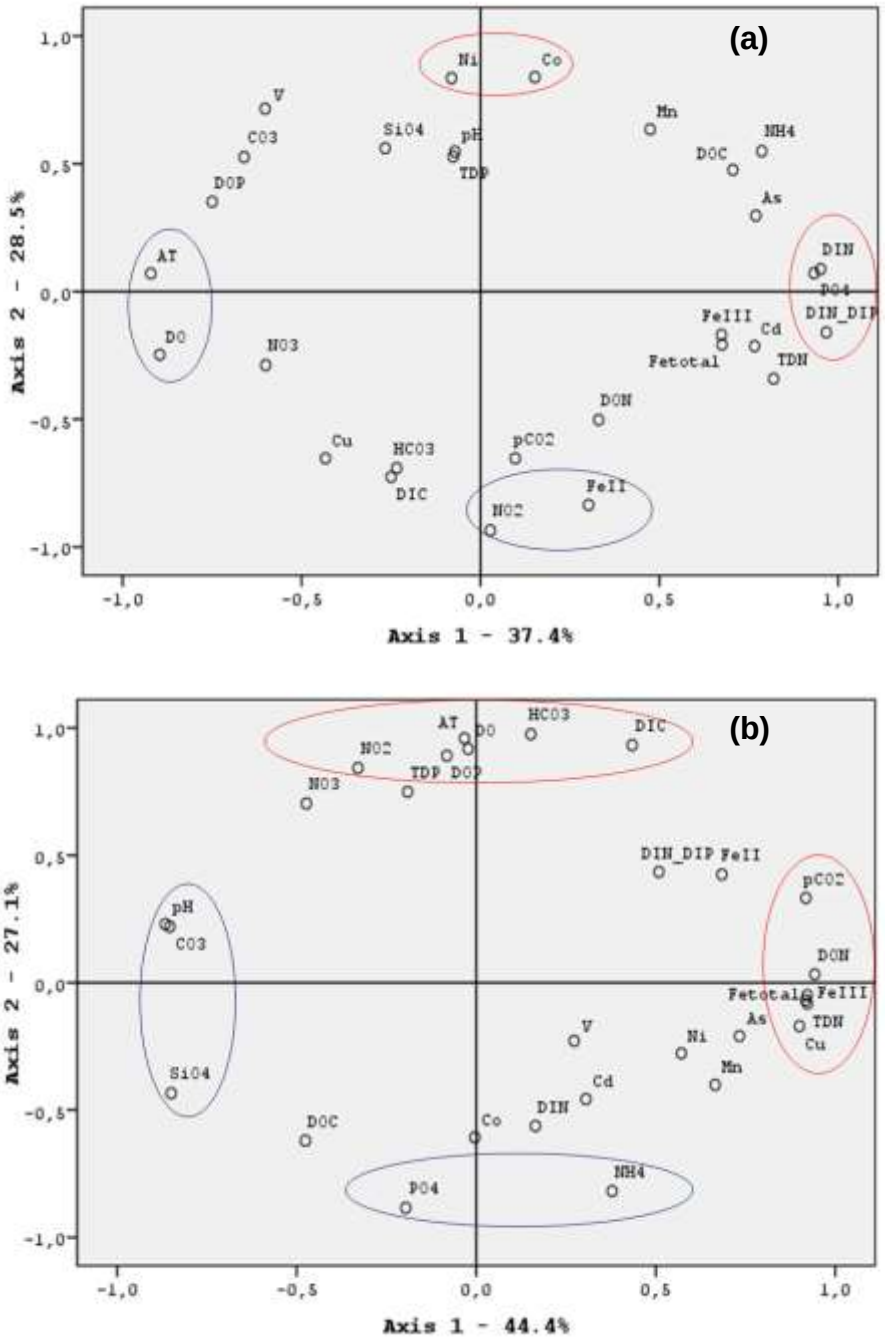

Figure 44. Principal Component Analyses (PCA) Graphs for C (a) and OA (b) treatments. Red circles indicate positive significant correlations while blue circles indicate negative significant correlations

5.3 Discussion

This work follows and contributes additionally to Experiment I in order to study the emerging effects of coastal pH decrease in the specific restricted marine system characterized by enhanced OM degradation and intermittent anoxia. This parameter in addition to bottom to surface acidification could implicate basic biogeochemical processes of carbonate, nutrients and carbon and establish a seasonal coupled interchange of these major cycles. This experimental simulation could highlight some of these processes which might have been neglected until now for the better understanding and foresight of the system's future evaluations.

During this study, the basic biogeochemical processes were investigated and it is considered that the normal mechanisms of the specific study area could be summarized as those pointed out for C condition.

5.3.1 Carbonate system and related processes

During sampling, complete depletion of oxygen (anoxia) was found. However, during the experiment despite the controlled Ar supply for maintaining this condition, DO levels suggested severe hypoxic to hypoxic conditions for both treatments [18, 19] which could be attributed to the strong buffering capacity of the sediment. After the systems were left to reoxygenate naturally, DO did not reach normal oxidizing conditions but fluctuated between values characterizing still hypoxic conditions.

pH fluctuated slightly during this experiment, due to the buffering capacity of the sediment. After reoxygenation, pH increased significantly also proving the strong interrelation of hypoxic/anoxic conditions with acidification.

Following the seacarb calculations for carbonate system parameters in C condition, phosphate and silicate contribute significantly in the carbonate system budget and seem to act as a considerable negative feedback for acidification mechanisms. This acts as a naturally occurring buffer to a certain extent for the increased CO_2 concentrations in the water column due to OM degradation.

In C condition, carbonates were only affected by sediment irrigation during sampling which was then augmented by system reoxygenation; this could suggest carbonate dissolution from sediments which was not depicted however in decreased sedimentary carbonates.Bicarbonates and A_T present similar distributions suggesting that this is the main constituent determining A_T. Bicarbonates showed negligible variations after the reoxygenation but then carbonate dissolution further contributed to A_T increasing its final concentration. Carbonate saturation states (Ω_{ar} and Ω_{cal}) followed the carbonate trend. However, even for C condition in the absence of oxygen Ω_{ar} varies between 1.48 and 1.62 which is in close proximity to system undersaturation for the specific mineral. When reoxygenation occurred, Ω_{ar} increased again suggesting that acidification was buffered. It was noticed here, through PCA, that A_T and DIC were uncoupled meaning that different processes seem to define their concentration. Indications of benthic alkalinity production due to OM degradation and reduction processes (e.g. sulfate reduction, Fe/Mn oxide reduction) are also apparent here.

In OA condition, total alkalinity increased to higher values comparing with C condition showing no statistical difference, however. It was also noticed that in relation with Experiment I (final values ~5300 μmol kg^{-1}), alkalinity increased to a lesser extent in more acidified conditions (final values ~4550 μmol kg^{-1}); since A_T can act as a negative feedback to elevated pCO_2 [170, 172, 174,195, 196], severe hypoxia seems to intercept this buffering mechanism. Bicarbonates also increase coinciding with alkalinity trend, suggesting that this is the decisive carbonate species contributing to alkalinity budget.DIC was found incresead in relation to A_T due to the steep addition of CO_2, following similar patterns however ; here it seems that in more acidified conditions these two parameters are coupled again, unlike in C conditions. Considering that the reoxygenation phase preserved a stable bicarbonate content in both treatments, it is suggested that anaerobic processes could trigger HCO_3^- production which are maintained even when oxygen increases. Carbonates were significantly lower than in C condition but only oxygen penetration in sediment seemed to increase their concentrations, suggesting sediment carbonate dissolution which was not depicted in sediment carbonate

reduction. Carbonate mineral saturation states followed carbonate trend as well, but both Ω_{ar} and Ω_{cal} were calculated below 1 suggesting system undersaturation; in this case too, reoxygenation increased dramatically Ω_{ar} and Ω_{cal} well above 1 suggesting that despite the high CO_2 concentration, oxygen availability buffers acidification mechanisms to some point.

As was mentioned previously (Chapter 4.2.2) enhanced A_T in more acidified conditions is generally attributed to sedimentary carbonate dissolution [8, 170]; nor in this case however, any notable sedimentary carbonate decrease was observed. Regarding the high $CaCO_3$ content of the sediment, as well as the relatively short duration of the experiment it can be assumed that the observed A_T increase (ΔA_T = ~1500 μmol kg^{-1}) in the overlying water was generated by the dissolution of sedimentary $CaCO_3$. Then the corresponding change in inorganic carbon percentage of the sediment would be about <0.001% w/w which is much lower than the methodological error. However it seems very likely that the pH decline has lead to a pH decrease in sediment porewater that induced the development of under-saturated conditions for calcium carbonate minerals leading to dissolution of $CaCO_3$ and DIC and A_T generation.

Additionally to carbonate dissolution, when anaerobic degradation occurs, bicarbonates are released through several processes such as denitrification, manganese, iron and sulfate reduction producing both A_T and DIC, regardless of carbonate dissolution [23, 133, 172, 195]. In this case, OM degradation products are released in both treatments, augmenting alkalinity, but in more acidified conditions these products are either solubilized more rapidly or become more stable.

PCA performed on the C treatment results revealed the oxygen depletion along with organic matter degradation impact on A_T (PC1). As OM is consumed, inorganic N forms and phosphate are produced and accumulated near the sediment-water interface with significantly higher concentrations than usual, affecting manifoldly system's A_T. Additionally, coupled redox processes with nitrogen species transformations to NO_2^- (either NO_3^- reduction or NH_4^+ oxidation) and Fe(II) oxidation or precipitation in other forms were revealed on one side and reduction mechanisms producing dissolved amounts of Co and

Ni on the other side (PC2). What was remarked here is the decoupling of A_T and DIC which seem to be designated by different processes.

PCA performed on the OA treatment results revealed the strong impact of increased CO_2 on dissolution of carbonates along with silicates and on organic N possibly eluding from the sediment surface (PC1); reduction of Fe oxyhydroxides is also suggested dissolving Fe (as Fe(III)) and Cu to the watercolumn. Additionally, the strong consistency of A_T, HCO_3^- and DIC with DO availability and OM remineralization products (e.g. NH_4^+, PO_4^{3-}) was revealed, suggesting anaerobic processes producing bicarbonates, affecting both A_T and DIC quite significantly (PC2). Processes such as denitrification, manganese, iron and sulfate reduction on the continental shelves all generate alkalinity despite the dissolution of $CaCO_3$ [195].

5.3.2 Processes affecting carbon and nutrient species

In C condition, organic N initially increased and began to decompose on the 12th day in parallel with ammonium oxidation from the 5th day; after sediment sampling, DON increased while ammonium was maintained minimum. Sediment irrigation seemed to trigger organic N release in the overlying water suspending decomposition processes. Nitrite increased and was the main product up to the 15th day, with parallel nitrate increase while ammonium constantly reducedindicating nitrification processes . After the 15th day both ammonium and nitrite are consumed, with nitrate being the main DIN form, finally. DON increased again after sediment sampling also suggesting sediment N release in soluble forms. The reoxygenation phase, slightly affected nitrate and ammonium concentrations, while nitrite, DON and DIN:DIP ratio decreased.

DON in OA condition again increased after sediment sampling up to the 12th day; this organic input, after degradation preserved an elevated ammonium budget. As the experiment continued, DON degraded to inorganic forms with significant ammonium decrease after the 15th day, and subsequent nitrate and nitrite release, with nitrate being the main final DIN product; despite the considerable decrease, DON exceeded all DIN forms at the end of the experiment. It was previously shown that under lower pH values ammonium

oxidation decreases significantly, up to 50-90% for pH values 7-6.5 respectively [11, 75, 77]. This was found in consistency with Experiment I, under hypoxic and more acidified conditions, with ammonium accumulation instead of ammonium conversion to nitrite and nitrate. In severe hypoxic conditions here, however, it seems that more of a deceleration rather than a suppression mechanism of ammonia oxidation is observed, which utterly converts ammonium to nitrite and nitrate in turn, leading in nitrate being the final dominant inorganic N-species. In more acidified conditions, as well, a belated nitrification mechanism is observed despite the low oxygen availability. High organic N content degrades leading in ammonium accumulation which is then oxidized in nitrite and furthermore to nitrate; Hulth et al. [133] have shown that in anoxic regions, the introduction of Mn-oxides from oxidized surface sediments result in anoxic nitrification, and net production of nitrate and nitrite. Within organic and Mn-rich regions of continental margin sediments where O_2 is absent, NO_3^- can be produced during Mn-oxide reduction with the rate of anoxic nitrification being directly proportional to the quantity of Mn-oxide available. In Elefsis Bay, in the absence of O_2, Mn (IV) mainly present as MnO_2 in sediment is reduced to dissolved Mn(II) eluding from sediment to the overlying water [122]. Data from the specific study (see Section 6.4.3) show that in more acidified conditions, Mn appears elevated in soluble forms which in addition to the accumulation of NO_3^- and NO_2^- could be an indication for anoxic nitrification settlement [132, 133]. During reoxygenation, nitrate and nitrite both increase as well as DOP and DOC; ammonium and DON declined while DIN:DIP ratio remained constant.

Phosphates presented the same trend in both C and OA conditions but were found significantly higher in OA being the dominant phase against organic P throughout the experiment. In addition, under lower pH values, system reoxygenation slightly affected PO_4^{3-} concentrations, indicating restricted particular phase re-precipitation as is normally expected. In previous studies [77, 36 and references within,177, 56] and during Experiment I, no impact of CO_2 enrichment on phosphates was found. Here, it is suggested that in lower pH values in combination with less available oxygen than Experiment I,

phosphate solubility is favored at all times against reprecipitation even when DO increases in the water column. DOP also presented similar trends in both conditions, with higher (but not statistically different) concentrations in OA condition.

DIN:DIP fluctuated between 10 and 2 in C treatment, with minimum values at the end of the experiment after the reoxygenation while in OA treatment, the ratio was between 6-7 with negligible variations; in both cases N-limitation is maintained.

For silicate, no significant acidification impact was observed as has been reported in previous studies [77, 177] and during Experiment I.

Sedimentary OC dropped by 28% in C condition after the reoxygenation phase leading in a 58% DOC increase; this could implicate release of sedimentary organic compounds in the overlying water which being in excess were accumulated and could not be decomposed. The respective sedimentary OC decrease in OA condition was 22% with a subsequent 49% increase in DOC suggesting that acidification had minor impacts on the fate of OC and only oxygen availability affected organic matter degradation/accumulation; reoxygenation also increased DOC in OA condition.

Sediment TN decreases in both conditions in relation to field values and continues decreasing in C condition after reoxygenation; in OA condition a slight increase is observed from the 18th to the 33rd day; these variations could be associated with NO^{3-} and NO^{2-} increase.

5.3.3 Trace Metal Biogeochemistry

Iron

Fe(II) decline during the experiment (compared to initial field values) could be attributed to oxygenation of seawater during the transfer to the laboratory and experiment set-up. Additionally, the severe hypoxic conditions (and not anoxia as was found *in situ*) could be responsible for the Fe(II) decrease suggesting oxidation to Fe(III) but still Fe(II) was present at all times during the experiment in both treatments. From PCA analysis, in C condition, Fe(II) was

related negatively in the second axis which represented coupled redox processes of N, Fe oxidation/reduction and other trace elements (e.g. Co, Ni and V). It was found here that Fe(II) in more acidified conditions was significantly higher throughout the experiment (in relation to C condition) whereas Fe(II) remained stable even after oxygen increased to 70 μmol l^{-1} (hypoxic conditions [19]). Fe(III) and Fetotal increased significantly during OA conditions in relation to C condition. At the current surface pH of seawater, Fe (III) is at its minimum solubility; a decrease in pH from 8.1 to 7.4 would increase the solubility of Fe (III) by about 40% [112]. This is evident in this experiment as well, with sedimentary Fe dissolution and increased soluble Fe(III) in lower pH values. Additionally, under acidified conditions, Fe (II) is expected to show increased stability [105] that is evident during Experiment II, from the 18th day until the end (OA condition), with no oxidation to Fe (III) despite the system re-oxygenation.

Manganese

Sediment irrigation/oxygenation during the transfer to the laboratory, affected Mn concentration by precipitation on sediment surface; this was also recently observed in benthic fluxes incubations for the specific area [142]. Apart from the decreased initial values, Mn presented similar trends in both conditions but with significantly elevated concentrations in OA treatment.

In C condition, Mn was only positively correlated with NH_4^+ and Co; this suggests that severe hypoxic conditions favor simultaneously those processes which end up in the oxidation of ammonium to other N-species (NO_2^- and NO_3^-) and the precipitation of Mn oxy-hydroxides with related elements incorporated in this phase.

In OA condition, Mn was found to strongly correlate with As and Ni and strongly negatively correlate with pH and CO_3^{2-}. Apart from Fe/Mn oxyhydroxides, Mn appears to be mainly bonded with carbonate minerals; after CO_3^{2-} dissolution due to pH decline, Mn prevails in more soluble forms and only after re-oxygenation, a precipitation mechanism is observed.

The low solubility plus rapid oxidation rate of Fe could be responsible for its precipitation, and thus removing other metals by adsorption. Additionally, a disturbance in the Fe–Mn shuttle in the sediment could lead to increased concentrations of toxic metals [24]. From previous experiments [108], Fe and Mn precipitation as hydroxides can be disturbed by more acidic conditions leading to inhibited removal of dissolved Fe, Mn forms in sediment which could result in increased concentrations in the seawater. This process could be attributed to the extraction of the easily leachable metal fractions from the sediment and suspended particles during the early phase of CO_2 insertion. The elevated dissolved values for these two trace metals during OA conditions in Experiment II could also indicate an inhibited precipitation mechanism from water to sediment, preserving an elevated Fe/Mn content in the water column.

Arsenic

For As, it appears that sediment oxygenation and irrigation leads to sediment release towards the water column with elevated initial values for the experiment in relation to field values

Arsenic, in more acidified conditions appears slightly decreased in relation to C conditions with steady concentrations from day 18^{th} till the end of the experiment and no re-oxygenation effects . It appears that OA, in addition to severe hypoxic conditions, acts as a restrictive factor for As dissolution. The total dissolved As concentration decrease due to acidification has been previously reported in experiments conducted with CO_2 [183]. From PCA, in C condition As behavior is relevant to nutrient species produced through OM degradation (ammonium and phosphate) and is strongly affected by oxygen availability and related to processes which increase A_T. In OA conditions, correlation analysis As is related as well with nutrient species produced through OM degradation (ammonium and phosphate) and is strongly affected by oxygen availability; additionally, a negative correlation between As and A_T was found in lower pH values, suggesting that processes originating from OM degradation affect their distribution simultaneously. This indicates that in this case too, in the absence of oxygen a decoupling of As biogeochemistry with both Fe and Mn is achieved and As is only affected by OM remineralization.

Cobalt

Through PCA analysis, Co in C condition was related positively in the second axis, appearing to take part in a combined series of redox processes. Although no such correlations were found, in both conditions Co followed similar pattern with Mn, presenting elevated field values which then decreased at the beginning of the experiment; Co continued following Mn distribution throughout the experiment. In previous acidification experiments [108], Co has been found to be released from the sediment under higher CO_2 concentrations; in this case no significant Co release was observed under more acidified conditions. Cobalt can exist as Co(II) or Co(III) within the pH and Eh range of natural waters; the oxidation of Co(II) to Co(III) can be accomplished by coprecipitation with Mn oxides and is thought to be an important mechanism for cobalt removal in coastal waters [93]. Since Mn is also removed by oxidation of soluble Mn(II) to insoluble Mn (III,IV) oxides, this could account for the similarities in their geochemistries [94]. In Experiment II, it appears that Co is inextricably linked with Mn biogeochemistry either by Co(II) present in dissolved forms or being reduced to Co(III) through Mn-oxide coprecipitation. Since this mechanism could not be supported by the findings of Experiment I, it is probable that the lack of oxygen (severe hypoxic conditions) pose a process alteration concerning Co fate in the specific system.

Cadmium

Cd seems to precipitate due to sediment sampling and irrigation. From PCA analysis, Cd in C condition was found to be positively related in the first axis which was interpreted as oxygen depletion along with organic matter degradation impact on A_T; in more acidified conditions, no alterations in processes were observed. Cd ocean distribution is closely related to the phosphate/nitrate distributions and it is not known to be complexed in organic substances in seawater [90, 91]. Cd adsorbs significantly on hydrous Mn oxides (dependently on concentration) while Cd desorption by sediment resuspension is greater than for any other trace metal; the controlling factor in Cd remobilization is redox potential, which regulates Mn solubility which in turn regulates Cd availability. In this case however, this strong coherence

between Cd and Mn and Cd desorption due to sediment irrigation did not apply. Cd and Mn distributions were different throughout the experiment. Neither in field sampling nor in sediment sampling in the middle of the experiment, did Cd solubilize to the water column. On the contrary, after sediment sampling on the 18th day a Cd precipitation mechanism was found. Surface depletion of cadmium (and phosphate) in relation to deeper waters have been mentioned and may be explained by its uptake by plankton and subsequent loss from the faecal pellets produced by grazing zooplankton [91]. It seems here that Cd behavior is closely related with phosphate, which also presented the same trend, implying that Cd could be uptaken by plankton which after dying are accumulated on sediment surface.

Copper

From PCA analysis, in OA condition Cu was found to correlate positively in the first axis which represented the impact of increased CO_2 on dissolution of carbonates along with all substances related to this phase; it is suggested here that when oxygen is depleted, Cu is mostly incorporated in carbonates which as pH declines Cu-dissolved forms elude into the overlying water. Cu^{2+} forms strong complexes with carbonates and is expected to increase by as much as 115% in coastal waters due to reduced pH [113, 114]. In previous experiments [24], increased Cu concentrations have also been observed under elevated CO_2 conditions. However, during this experiment Cu trend in both conditions was similar (with slightly elevated concentrations in OA treatment between 4th and 15th day), with negligible alterations due to reoxygenation.

Nickel

From PCA analysis, in C condition Ni was found to be related in the second axis which represented coupled redox processes with (a) nitrogen species transformations to NO_2^- (either NO_3^- reduction or NH_4^+ oxidation) and (b) reduction mechanisms producing dissolved Co, Ni and V escaping in the overlying water. In OA condition, Ni was only positively correlated with Mn suggesting that Ni is mainly adsorbed on Mn oxyhydroxides. Increased

dissolved fractions of Ni have been previously reported due to elevated CO_2 [24].

Vanadium

In C condition V was strongly associated with DOP and Ni, presenting a distribution similar to that of carbonates during the experiment. It seems that V takes place in coupled redox processes including carbonate dissolution and those processes affecting ultimately A_T. In OA condition, V was found increased until the 18th day suggesting dissolution due to decreasing pH. It is implied here that V is probably involved in carbonate bonds as well as Fe/Mn oxides which dissolve under increased CO_2, releasing V in the water column.Implications for enclosed embayment in future CO_2 conditions

5.3.4 Implications for enclosed embayment in future CO_2 conditions

Elefsis surface pCO_2 was calculated at 522 μatm and approximately stable throughout the first 10 m; in 20m depth, however, pCO_2 doubled, reaching values of 1538 μatm in the deepest part. This value is already higher than the OA surface water predictions for the end of the century. Elefsis Bay surface (down to 10m) presented pH values similar to the values reported regarding midsummer for the North Adriatic [50]; Elefsis bottom, however, was found already acidified (7.75) in relation to surface values (8.16). As was mentioned previously, Elefsis Bay has been subjected to pH decline since the late 70's, with bottom values of 7.9-7.8 (see Chapter 3.1.2) even under hypoxic conditions. In Elefsis Bay, the pycnocline is an intermittent feature (Chapter 3.1.2) which after collapse could permit the CO_2 enriched bottom waters to penetrate in smaller depths (a bottom to surface acidification mechanism). Elefsis Bay is part of the Thriasio basin, restricted to a certain extent, and has been a heavy industrialized, urban area for several decades [65]. In consequence, Elefsis may present higher CO_2 emissions than neighboring areas; estimating that the surface water and the atmosphere above are equilibrated regarding CO_2, local surface pCO_2 is expected to be higher than adjacent areas or other Mediterranean systems with similar hydrometeorological characteristics. Indeed, De Carlo et al. [60] published a time-series for NW Mediterranean presenting atmospheric pCO_2 values ~380-

400 μatm and corresponding seawater values of ~340-450 μatm. This suggests that apart from the bottom to surface acidification due to OM degradation, increased atmospheric CO_2 in areas similar to Elefsis Bay could already be increasing surface water pCO_2 to a lesser extent than anthropogenic CO_2 but acting cumulative to unpredicted pathways.

A_T in Elefsis Bay was found higher (2974-2990 μmol kg^{-1}) than the values reported for open Mediterranean Sea waters (2600 μmol kg^{-1} [39,41]) even higher than those reported for the north Adriatic (up to 2700 μmol kg^{-1} [50, 61]). These findings reveal the significant local alkalinity input by the land limestones weathering along with the possible contribution of organic substances to alkalinity budget. It has been pointed out for similar areas with restricted mixing and/or characterized by significant inputs of DOM from land that organic bases contribute significantly in A_T [183]. As a result, Elefsis Bay is prone to absorb higher atmospheric CO_2 quantities in relation to adjacent areas of Mediterranean, being even more sensitive regarding carbonate system variables. The fully formed pycnocline and the remarkably increased nutrients in the bottom of Elefsis Bay, did not seem to react on A_T; the maximum A_T value was identified in 10m depth coinciding with the also maximum values of DOC and DOP.

Time series regarding a coastal site in the western Mediterranean [40, 61] show that during 1967−2003, the estimated Ω_{ar} was 4.3 with a minimum value of 3.1 in 2003; in Elefsis Bay, Ω_{ar} was calculated 4.80 in the surface while in the bottom it decreased dramatically to 1.51. Even if carbonate saturation states are mostly well above 1 throughout the year, a seasonal significant decrease related with dissolved oxygen availability could already impact calcareous organisms, which require Ω values much higher than 1 [50], with unpredictable alterations for the specific ecosystem.

It is also emphasized that in this study, the carbonate system calculations based on pH values and A_T without considering nutrients were found misleading. Despite the fact that this check was performed previously regarding Elefsis Bay (during Experiment I) with negligible differences, it seems that during severe hypoxic conditions nutrients contribute significantly in the carbonate balance. In the absence of oxygen, significant amounts of

ammonium, phosphate and silicate accumulate near the bottom which pose a negative feedback to the increasing CO_2 due to oxidation of organic matter and act as a drawback to the undersaturation of carbonate minerals. For this purpose, nutrients could not be neglected in future system assessments regarding OA and carbonate parameters especially where seasonal hypoxic/anoxic phenomena have been spotted and should be correlated with any future biological indices for system evaluation. From published time-series of the NW Mediterranean [60] the trends in nutrient concentrations and pCO_2 provide evidence of a link between these and associated biological processes.

Under low oxygen conditions, in Elefsis Bay, denitrification normally occurs within the water column and the upper surface sediments [119]. Through denitrification most of the nitrate is removed, ammonium, phosphate and silicate accumulate due to the oxidation of organic matter. MnO_2 reduction occurs next, followed by sulfate reduction with Mn_4^+ being the electron acceptor at first, followed by SO_4^{2-} as an electron acceptor. Data from the specific study (Chapter 6.4.3) show that total dissolvable Mn (dissolved and particulate Mn) varies between 0.04 and 0.05 μmol l^{-1} in the first 10m and increases to 4.26 μmol l^{-1} near the bottom. Such findings are not uncommon, with previous reports (between 1992-1995) of elevated dissolved (2,04 μmol l^{-1}) and particulate Mn (3.11 μmol l^{-1}) during anoxic periods [119]. In combination with previous findings [133], suggesting Mn induced anoxic nitrification, the available Mn in dissolved forms could be responsible for triggering nitrification phenomena under anoxic/suboxic conditions. Considering also that the exact role of Mn has not been verified yet in the area, it is likely that a complex biogeochemical coupling of all nitrogen, sulfur, carbon, oxygen and manganese is established rather than a simple redox reaction succession in surface sediments.

In addition, when oxygen concentration diminishes in Elefsis Bay phosphate dissolution occurs from sediments to pore waters from host Fe-oxyhydroxides; then, dissolved phosphate escapes via diffusional transport, resuspension, or irrigation by benthos [119]. In this study, in more acidified conditions, the sediment irrigation and re-oxygenation did not cause phosphate

reprecipitation, maintaining a high P content in the system. As a consequence, an invariable DIN:DIP ratio around 7 is observed. From timescales, DIN:DIP varies between 13 (surface) and 4 (bottom) during stratified periods [119], leading in near-bottom N-deficit. Under lower pH values, it seems that N is not depleted as usual but a constant N-budget is obtained.

Regarding trace metals, the processes found to affect their distributions were various and need further investigation in the future to fully comprehend their fate in the system. For Fe(II) it seems that, more acidified conditions increase its dissolved content and make Fe(II) more stable even after oxygen penetration; Fe(III) solubilization is also favoured under lower pH values. Mn and Co were found to interrelate through combined redox processes. Mn seems to be bonded in carbonate phases which under dissolution elude dissolved Mn in the water; after reoxygenation Mn reprecipitates on surface sediments. Co is probably present as dissolved Co(II) or is reduced to Co(III) through Mn-oxide coprecipitation. Cu is probably incorporated in carbonate bonds which as CO_2 increases, they dissolve and release Cu in the water column. Ni is mainly adsorbed on Mn oxyhydroxides and is released in more acidified conditions. Dissolved As seems to be restricted under lower pH values, decoupled of Fe/Mn oxyhydroxides and only related to OM remineralization processes. V also found to be related with OM degradation but also elevated under lower pH values.

5.4 Concluding Remarks for Experiment II

This study is closely associated with a previous work concerning the area of Elefsis Bay (Experiment I). Following those primary findings, the interest here was focused on the alterations that severe hypoxia could implicate in the already high CO_2 Elefsis bottom. In coastal areas such as the Elefsis Bay, characterized by certain hydrometeorological conditions and anthropogenic activities, more acidified conditions have already been pointed out. These acidification phenomena originating from the aforementioned specific characteristics are already of high scale, exceeding OA resulting from atmospheric inputs. The last decades, OA has become an environmental

challenge of great significance especially for coastal oceans; for this reason, Elefsis Bay could present a great natural example and first indication of expected future alterations due to OA.

Organic matter elevated input with its subsequent degradation in combination with the seasonal formed pycnocline, increases the CO_2 concentration near bottom and results in pCO_2 values predicted for the surface oceans for the end of the century. The pycnocline in the area is an intermittent phenomenon well investigated for the past 40 years; when the pycnocline gradually breaks, the bottom enriched CO_2 waters would normally reach smaller depths (acidification of a bottom to surface orientation) affecting in undefined ways Elefsis Bay biogeochemistry. Additionally, Elefsis surface pCO_2 was already found elevated in relation to other systems of the Mediterranean; this in combination with higher bottom CO_2 waters and restricted circulation could obstruct CO_2 reinstatement to normal values for the entire water column. Since these findings have never been correlated with nutrient or biological indicators time series before, a significant factor has been excluded until now for Elefsis system evaluation.

Total alkalinity in Elefsis Bay is believed to be affected by organic matter constituents such as DOC and organic phosphorus; Total alkalinity increase under lower pH was found limited in relation to Experiment I (hypoxic conditions). In this case too, alkalinity was mainly affected by bicarbonates and only after the reoxygenation carbonates significantly contributed to its final concentration; this suggests that apart from sediment carbonate dissolution, OM degradation and related process (e.g. sulfate reduction) were the main factors affecting A_T. Due to lack of former relevant studies, it was pointed out here the significance of dissolved nutrients (e.g. phosphate and silicate) in the calculation of carbonate budget and the final evaluation of the system regarding carbonate saturation state and its possible impact on biology. Former assumptions that nutrients negligibly contribute in carbonate budget in similar coastal areas could have leaded in misleading results and conclusions. Despite that none of the carbonate satutation states were calculated below 1 in Elefsis Bay, the significant decline calculated from

surface to bottom and this intermittent variation in Ω-values could be of great importance regarding the calcifying organisms.

In more acidified conditions, ammonium oxidation is not prevented (as was found in Experiment I) but was achieved with deceleration. It was also indicated that a nitrification mechanism prevailed despite oxygen deficiency; this in correlation with high dissolved Mn concentrations found in the anoxic bottom water could suggest an anoxic/suboxic nitrification mechanism also present in Elefsis bottom even under severe hypoxic conditions.

For the first time, it was suggested that in Elefsis Bay simulated acidification lead to a significant increase in phosphate concentrations with negligible reprecipitation after system reoxygenation. Although this could not be compared or correlated with previous findings in coastal areas, due to complex redox chemical reactions possible dissolution of Fe-oxyhydrooxides is intensified under lower pH solubilizing phosphate and preventing its reprecipitation even when oxygen becomes available again.

Ultimately, the role of trace metals in such impacted coastal systems has been well mentioned. The further contribution of OA in Elefsis Bay that could alter those processes controlling trace metal distributions, either restraining or releasing them in the water column, is of major interest and remains to be further investigated in the future. Studies that would permit (a) metal species determination in common conditions (in both stratified or unstratified periods) (b) model predictions for species alterations (c) trace elements interrelations in these varying conditions would make clear whether certain elements become bioavailable or inactive due to reduction of pH.

CHAPTER 6:

GENERAL CONCLUSIONS – FUTURE PERSPECTIVES

Conclusions for Analytical Methods Used

The use of EPA 1640 for seawater preconcentration and ICP-MS analysis for trace metals such as Cd, Co, Cu, Mn, Ni, Pb and Al, despite in a wide range of concentrations, was found quite satisfactory. As and V were underestimated with the application of this procedure but with the parallel use of a CRM they could be also determined. This method cannot be applied for Cr determination.

For sediment analyses, the use of EPA 3050b was found very accurate regarding elements such as As, Ni, Cu, Pb, Cr and Mn. Fe and Al could not be adequately determined so a CRM is requisite for these metals' analysis.

Colorimetric Fe speciation in seawater was found satisfactory regarding the elevated dissolved Fe content found in both samplings and during the experiment.

Experiment Conclusions

The two experiments were initially designed to simulate hypoxia (Experiment I) and complete anoxia (Experiment II) based on the *in-situ* oxygen observations. Due to the seawater oxygenation during transport and experimental set-up and the strong sediment buffer capacity, the different conditions that were finally attained for the two experiments were hypoxia in shallow habitats (Experiment I) and severe hypoxia (Experiment II). The difference in experiment duration (Exp.I: 20 days, Exp.II: 33 days) is attributed to the sediment sampling on the 18^{th} day during the Experiment II due to the disturbance to the system which required several days to regain stability, and the additional process of physical aeration required in this case. Apart from the detailed description of the experimental findings that follows, the similarittes and differences between the two experiments are presented briefly in Table 12.

During Experiment I, more acidified conditions led to significant alkalinity release associated with sedimentary carbonate dissolution along with the bicarbonate ions that are produced in favor of CO_3^{2-} in order to buffer the CO_2 increase; there is also evidence that organic and sulfate reduction processes would contribute to the alkalinity production during the experiment. Carbonate system calculations suggest an immediate decrease in carbonate ions during lower pH values with stable concentrations till the end of the experiment leading to Ω_{ar} and Ω_{cal} values below 1. In sediments no differentiations in carbonates were detected since the change in dissolved forms would account a negligible percent of the total carbonate sediment content. Additionally, a deceleration of ammonium oxidation in parallel with decrease in nitrate production was observed; organic forms of N and P along with DIN:DIP ratio during more acidified conditions imply possible N-limitation and inhibition of organic matter decomposition. Phosphate and silicate were not affected by the further pH decline. Trace metal analysis showed that As, V, Cd, Co and Pb follow the same pattern under lower pH values being directly associated with OM degradation processes which lead in the deliverance of their dissolved forms in the water column. Ni, Cu, Mn present the same trend in more acidified conditions along with Fetotal and Fe(III), which are influenced by pH decline and are mostly found within carbonate bonds and Fe/Mn oxyhydroxide phases.

During Experiment II, the carbonate system calculations based on pH values and A_T without considering nutrients were found misleading. Despite the fact that this check was performed during Experiment I with negligible differences, it seems that during severe hypoxic conditions nutrients (OM degradation products) contribute significantly in the carbonate balance posing a negative feedback to the increasing CO_2 leading to the undersaturation of carbonate minerals. For this purpose, nutrients could not be neglected in future system assessments regarding OA and carbonate parameters especially where seasonal hypoxic/anoxic phenomena have been spotted.

Throughout Experiment II total alkalinity also increased to a lesser extent comparing with Experiment I. bicarbonates are as well the main carbonate species contributing to A_T.

Despite that no similar findings were found previously, simulated acidification conditions lead to a significant increase in dissolved phosphate in Elefsis Bay which is maintained even after reoxygenation, possibly preventing its reprecipitation.

Regarding trace elements different patterns were observed under more acidified and severe hypoxic conditions; As dissolution was restrained maintaining lower dissolved concentrations. Ni, Co and Mn present similar distributions suggesting that they are strongly linked through coprecipitation with Mn oxides. Cd was possibly related to phosphate distribution while Cu was found mainly bonded with carbonates dissolving due to lower pH values, eluding Cu in the seawater. V was also found elevated during OA conditions, but through correlation analysis it was found to be mainly affected by OM degradation.

Table 12. Overall Information regrading the two expperimental setup, different conditions described, different results, findings

	EXPERIMENT I	**EXPERIMENT II**
Physicochemical Conditions Described	Hypoxia in shallow habitats	Severe Hypoxia
Carbonate System Parameters	significant A_T release (sedimentary $CaCO_3$ dissolution-mainly HCO_3^- production)	A_T release (limited in relation to Experiment I-HCO_3^- production-after reoxygenation $CaCO_3^-$ contribution – sediment carbonate dissolution/OM degradation&related processes)
Nutrient and DOM Processes	Interception of NH_4^+ oxidation – $NH_4^+\uparrow$ NO_2^- /$NO_3^-\downarrow$ - possible ↓nitrification	NH_4^+ oxidation not intercepted-achieved with deceleration Nitrification processes despite severe hypoxia – complex Mn-N biogeochemistry (also present in Elefsis bottom)
	Possible inhibition of OM (DOC,organic N) degradation	Dissolved PO_4^{3-} and SiO_4 significantly contributed in carbonate system paramaters Significant PO_4^{3-} increase in more acidified conditions
Trace Element Biogeochemistry	As, V ↔ OM degradation processes Ni, Cu, Mn and Fe(III),Fetotal, Co and Pb mostly found within carbonate bonds and Fe/Mn oxyhydroxide	As ↔ OM degradation processes Cd, Cu similar trends in both conditions V, Co, Ni, Mn and Fe(III),Fetotal influenced by pH decline - mostly found within carbonate bonds and Fe/Mn oxyhydroxide phases

	EXPERIMENT I	EXPERIMENT II
	phases influenced by pH decline	

Future Perspectives

Elefsis Bay poses a coastal system of great significance which has been well investigated the last 40 years, through several National or European Research projects from various organizations. There are long time series regarding parameters such as nutrients and trace elements; however, pH is one of the parameters not included in monitoring projects so there are huge gaps between individual research investigations. It would be of great importance, to include accurate pH measurements in monitoring programs, in order to create data bases which would depict the actual pH variation throughout the different depths along with the seasonal variations due to stratification. This parameter should also be included in system evaluation and biology indexes since it may pose an additional stressor for the different organisms.

The key findings of this study may contribute to future research efforts regarding the carbon and nutrient cycling in relation with increasing atmospheric CO_2 in intermittently hypoxic/anoxic coastal systems of the Mediterranean Sea. However, in such highly variable coastal environments high-frequency monitoring of the marine carbonate system is essential in order to document and interpret the long-term trends in inorganic carbon dynamics and regional OA. In parallel, detailed studies of other biogeochemical parameters accompanied by properly designed experiments are needed to improve our understanding of the factors that regulate the carbonate system and elucidate the possible impact of the increasing CO_2 on the complex biogeochemical processes taking place in coastal areas.

The results of this study also highlight the need for detailed research of the carbonate system not only in Elefsis Bay but also in coastal areas similarly dominated by hypoxic/anoxic conditions. Oxygen depletion accompanied by additional specific hydrographic and biogeochemical parameters should be properly investigated through experimental setups to elucidate the processes sequence or even alterations due to pH reduction.

ABBREVIATIONS - ACRONYMS

CRM	Certified Reference Material
As	Arsenic
AT	Total Alkalinity
Cd	Cadmium
Co	Cobalt
CO_3^{2-}	Carbonate ions
Cu	Copper
DIC	Dissolved Inorganic Carbon
DIN	Dissolved Inorganic Nitrogen (Stands for NO_3^-+NO_2^-+NH_4^+)
DIP	Dissolved Inorganic Phosphorus (Stands for PO_4^{3-})
DOC	Dissolved Organic Carbon
DON	Dissolved Organic Nitrogen
DOP	Dissolved organic Phosphorus
EI	Eutrophication Index
Fe	Iron
Fe(II)	Divalent Iron
Fe(III)	Trivalent Iron
HAB	Harmful Algal Bloom
HCO_3^-	Bicarbonate ions
Mn	Manganese
NH_4^+	Ammonium
Ni	Nickel
NO_2^-	Nitrite
NO_3^-	Nitrate
OA	Ocean Acidification
OM	Organic Matter
Pb	Lead
PO_4^{3-}	Phosphate
SiO_4	Silicate
SWI	Sediment-Water interface
TDN	Total Dissolved Nitrogen
TDP	Total Dissolved Phosphorus
V	Vanadium

ANNEX I ANALYTICAL METHOD DESCRIPTION

EPA 1640 Method Application [149]

Preconcentration procedure using reductive precipitation by sodium tetrahydroborate

Reagents

- Aqueous Ammonia—28% aqueous (ultrapure grade).
- Iron—99.999% pure metal (Aldrich or equivalent).
- Palladium—99.999% pure metal (Aldrich or equivalent).
- 1-Pyrrolidinecarbodithioic acid ammonium salt, 98%— (Kodak or equivalent)
- Ammonium hydroxide, 20%—ultrapure grade.
- Hydrogen peroxide, 30%—ultrapure grade.
- Sodium tetraborohydride—99% pure (Aldrich or equivalent).Borohydride solution, 5% (w/v)—Dissolve 2.5 g of sodium tetraborohydride in 50 mL of reagent water.

Ammonium pyrrolidinedithiocarbamate (APDC) solution, 2% (w/v) — Dissolve 2 g 1-Pyrrolidinecarbodithioic acid ammonium salt in approximately 50 mL of reagent water and dilute to 100 mL with reagent water.. Store at 4°C when not in use.

Nitric acid, 70%—Dilute 700 mL concentrated nitric acid to 1 L with reagent water.

Sample Preservation, and Storage

Samples and field blanks should be preserved immediatelyat the laboratory; for all metals, preservation involves the addition of 10% HNO_3 to bring the sample to pH <2. For samples received at neutral pH, approx 5 mL of 10% HNO_3 per liter will be required.

Store the preserved sample for a minimum of 48 h at 0–4°C to allow the acid to completely dissolve the metal(s) adsorbed on the container walls. The sample pH should be verified as <2 immediately before an aliquot is withdrawn for processing or direct analysis. If, for some reason such as high

alkalinity, the sample pH is verified to be >2, more acid must be added and the sample held for 16 h until verified to be pH <2.

Procedures for Sample Preparation and Analysis

Transfer a 100-mL aliquot of sample to a polyethylene bottle . Add 500 µL of iron solution and 500 µL of palladium solution.

Adjust the pH of the sample to between 7 and 10 with ammonium hydroxide. As iron hydroxides precipitate, the solution will develop an orange tint.

Add 1 mL of borohydride solution and gently swirl the bottle. Within a few minutes, the solution will darken as palladium and analytes precipitate.

Add 0.25 mL of APDC solution, swirl the bottle and allow the solution to sit for 15-20 hours.

Filter the sample by vacuum through a 0.45-µm filter; rinse the reaction bottle with reagent water to remove precipitate residue and filter the rinsate along with the sample.

Handling the filters with forceps, fold the filters into eighths and place each filter in a clean, dry 15-mL centrifuge tube.

To each filter add 0.25 mL of concentrated nitric acid and cap the tube; the filter must be completely submersed in the nitric acid. Heat the tubes at 65$^{\circ}C$ for 30 minutes in a laboratory oven. The solution should be bright orange.

If some precipitate remains undissolved, add 0.5 mL of 30% hydrogen peroxide. Heat the tubes again at 65$^{\circ}C$ for 30 minutes in a laboratory oven. For analysis with ICP-MS, a final concentration of 2% (v/v) HNO_3 is suggested so a further dilution step is required.

The same procedure was also followed for the parallel analysis of a CRM and a blank for the final evaluation of the method.

EPA 3050b Application [150]

Step 1

1 g of dry sediment sample is placed in Teflon containers; 10 ml of conc. HNO_3 is added while stirring. Then, the containers are placed on a hot plate covered with a watch glass and are heated in 95°C for 10-15 minutes

(cautiously in order to avoid boiling). The samples are left to cool; then another 5 ml of conc. HNO_3 is added, the samples are covered again and are heated for 30 minutes. If brown fumes are generated, indicating oxidation of the sample by HNO_3 repeat this step (addition of 5 mL of conc. HNO_3) over and over until no brown fumes are given off by the sample indicating the complete reaction with HNO_3. The solution is then allowed to evaporate to approximately 5 mL without boiling or heat at 95°C±5°C without boiling for two hours. A covering of solution over the bottom of the vessel should be maintained at all times.

Step 2

When step 1 is completed, the samples are left to cool and 2 ml of water and 3 ml of H_2O_2 (30%) are added. The containers are covered with a watch glass and are heated on a hot plate in order to start the peroxide reaction. The heating continues until effervescence subsides and samples are left to cool. The addition of 1-ml H_2O_2 (30%) continues while heating until the effervescence is minimal or until the general sample appearance is unchanged.

NOTE: A total of 10 mL H_2O_2 (30%) should be the maximum volume added.

The samples are covered and the the acid-peroxide digestate heating continues until the volume has been reduced to approximately 5 mL or heat at 95°C±5°C without boiling for two hours. A covering of solution over the bottom of the vessel should be maintained at all times.

After cooling the digestate is diluted to 100 ml with water. Particulates in the digestate should then be removed by centrifugation and when particulates remain the samples should be filtered through 0.45µm polycarbonated membranes. The diluted digestate solution contains approximately 5% (v/v) HNO_3. For analysis with ICP-MS, a final concentration of 2% (v/v) HNO_3 is suggested so a further dilution step is required.

Fe Species in Seawater Application [151, 152]

Apparatus and Materials

UV-Visible Spectrophotometer. Milton Roy Spectronic-20. Spectrometer Cuvettes 5.0 cm. 40-mL clear glass vials VOA vials. The EPA Level-2 pre-cleaned for trace metals borosilicate glass vials for lowest blanks was used.

Reagents

- *Reagent Water* - ultra-pure deionized water.
- *Concentrated Hydrochloric Acid (HCl)* - Trace metals grade HCl, found to contain undetectable levels of Fe. The HCl should be purged for 1 hour with N_2 at 500 mL min-1 (in the hood!) to eliminate any entrained Cl_2 which could oxidize Fe(II) to Fe(III).
- *0.2 M HCl Solution* - Dilute 2.0 mL of concentrated HCl to 100 mL with reagent water, and store in an acid cleaned plastic bottle.
- *Fe(II) Standard* - A stock solution of 1000 mg l^{-1} Fe(II) is made by dissolving 7.84 g ammonium iron(II) sulfate hexahydrate and 1.00 grams of $NH_2OH.HCl$ in 1.00 liter of 2% HCl. Working Fe (II) standards (5.0 to 1,000 mg l^{-1}) are prepared daily by serial dilution of the stock standard in a mixture of 2% HCl plus 0.1% $NH_2OH.HCl$.
- *Fe(III) Standard* - A stock solution of 1,000 mg l^{-1} Fe(III) can be purchased from a commercial source as an AAS standard ($FeCl_3$) in dilute HCl. Working Fe(III) standards (5.0 to 1,000 mg l^{-1}) are prepared by serial dilution of the stock standard in a mixture of 2% HCl.
- *Ferrozine solution (0.02M)* - Dissolve 1.028 g of ferrozine (3-(2-pyridyl)-5,6-bis(4- phenylsulfonic acid)-1,2,4-triazine) in 100 ml of reagent water, and store in an acid cleaned polyethylene bottle.
- *Ammonium Acetate Buffer* - Dissolve 35.0 ml concentrated NH_4OH and 40 g of CH_3COONH_4 (both trace metal grade) in about 25 ml water, and then dilute to 100 ml. Store in an acid-cleaned plastic bottle.
- *1% Ascorbic Acid Solution* - Dissolve 1.00 g of ascorbic acid ($C_6H_8O_6$) in about 50 ml of water, and dilute to exactly 100 ml. Store in an acid-cleaned plastic bottle during use, but prepare this reagent freshly for each analytical day.

Sample Collection, Preservation, and Handling

Any exposure of the samples to air must be avoided, as Fe(II) is easily oxidized by air. Therefore the samples should be collected by submerging the bottle under water and capping it while still submerged, or by pumping with a peristaltic pump into a glass bottle held within an N_2 purged box. If dissolved Fe(II) is needed, samples must be filtered by in-line filtration and pumping with a peristaltic pump into a glass bottle held within a N_2 purged box. Alternately, samples can be vacuum filtered immediately after collection in a N_2 purged glove box. Samples should be held in completely full glass bottles with Teflon lined caps, and they should be field preserved immediately with 1% (v/v) of N_2 purged HCl. In the lab, the samples should be acidified (if not field preserved) and analyzed within 24 hours for Fe(II). If the samples are not filtered the Fe species determined are referred as total dissolvable Fe(III) and Fe(II).

Analytical Procedures

Total Iron Analysis

1. Place 20.0 ml of sample or standard solution (or an aliquot containing less iron than the highest calibration standard) in a 40 ml glass vial.

2. If the sample was not field preserved to 1% v/v with HCl, add 0.200 ml of concentrated HCl to acidify the sample.

3. Add 1.0 ml of 1% ascorbic acid to reduce Fe(III) to Fe(II).

4. Add 0.200 ml of ferrozine solution, cap, and shake to homogenize.

5. Add 0.400 ml of ammonium acetate buffer, shake, and wait 3 minutes for full color development.

6. Wipe the outside of the glass vial to remove fingerprints and dust, then place the vial into the photometer and measure the absorbance at 562 nm. The complex is stable for at least 3 hours.

Iron(II) Analysis

1. Place 20.0 ml of sample or standard solution (or an aliquot containing less iron than the highest calibration standard) in a 40 ml glass vial.

2. If the sample was not field preserved to 1% v/v with HCl, add 0.200 ml of concentrated HCl to acidify the sample.

3. Add 1 ml of reagent water.

4. Add 0.200 ml of ferrozine solution, cap, and shake to homogenize.

5. Add 0.400 ml of ammonium acetate buffer, shake, and wait 3 minutes for full color development.

6. Wipe the outside of the glass vial to remove fingerprints and dust, then place the vial into the photometer and measure the absorbance at 562 nm. The complex is stable for at least 3 hours.

Determination of Iron(III)

The concentration of Fe(III) is determined as [Total Fe] – [Fe(II)]

Calibration

A calibration curve between 0–100 µg l^{-1} is determined daily from the analysis of 5 different dilutions of the Fe(III) standard. The respective calibration for Fe(II) was chosen to be between 0-50 µg l^{-1}. The standards must be analyzed in exactly the same manner and configuration as the samples. The blank is used to zero the instrument, therefore the calibration curve is forced through zero. The r value for the calibration curve should be better than 0.995.

Interferences

Divalent cobalt (Co(II)) forms a stable violet complex with ferrozine, which causes a positive interference with the iron determination. In most environmental samples, however, Co is much lower in concentration than Fe. Unpreserved Fe(II) standards and samples are subject to rapid oxidation to Fe(III) by atmospheric oxygen. Samples should be preserved with HCl and kept in completely full glass bottles, cold and dark.

Method performance

Method detection limits are determined as 2.998 times the standard deviation of 8 independent analyses near the detection limit (LOD). The spiking level should be 1-5 times the calculated LOD. The detection limit was determined to be 2 µg l^{-1} (0.036 µmol l^{-1}) for the conditions described.

Data Analysis

The concentration of Fe(II) or total Fe is determined by comparing the absorption A of the sample with the calibration curve, using the following equation, where m is the slope of the linear calibration curve.

[Fe], $\mu g\ l^{-1} = A / m$

Fe Species in Sediment [133]

Reagents

Solution 1: 11.915 g of HEPES and 1 g of Ferrozine are made up to 1000 cm^3 with pure water.

Solution 2: Take 100 cm^3 of solution 1 and add 1 g of hydroxyl ammonium chloride ($NH_4OH*HCl$).

Extraction step

Add 1-2 g wet sediment to 30 ml HCl (1M) and let it shake for 24 hours in the shaker.

(For carbonate-rich sediments more HCl has to be added until the pH of the suspension is smaller than 1.)

Then the samples are centrifuged for 15 min at the highest possible speed of rotation. The liquid phase is filtrated (0.2 µm), filled into bottles and used for the iron-determination.

The sediment remains in the centrifuge tube and is stored for the later determination of the dry mass.

Determination Procedure

Determination of Fe(II): From solution A you take 5 ml and add 100 µl sample, shake well and wait for exactly 20 min. (Final pH-value>5). Measure absorbance at 562 nm.

Determination of Fetotal: Take 5 ml of solution 2 and add 100 µl sample (final 4<pH-value<5). After exactly 20 min. measure the absorbance at 562 nm [153].

ANNEX II TABLES

Table 13. Certified quality values for the CRM's used during the trace metal analyses in seawater, NASS-6 and CASS-5 (National Research Council Canada; information values identified as * refer to elements which could not be certified because of insufficient information for accurate assessment of the associated uncertainties)

	NASS-6	CASS-5
Element	Mass Concentration (µg/l)	
As	1.43±0.12	1.21±0.09
Cd	0.0311±0.0019	0.0215±0.0018
Cr	0.118±0.008	0.106±0.013
Co	0.015*	0.095*
Cu	0.248±0.025	0.380±0.028
Fe	0.495±0.046	1.44±0.11
Pb	0.006±0.002	0.011±0.002
Mn	0.530±0.050	2.62±0.20
Mo	9.89±0.72	9.82±0.72
Ni	0.301±0.025	0.330±0.023
U	3*	3.18±0.11
V	1.46±0.17	1.32±0.14
Zn	0.257±0.020	0.719±0.068

Table 14. Certified quality values for the CRM used during the trace metal analyses in sediments, QTM089MS (Quasimeme Laboratory Performance Studies)

Element	Assigned value	Units
Al	3.79	%
As	17.3	mg/kg
Cd	443	µg/kg
Cr	57.0	mg/kg
Cu	15.3	mg/kg
Fe	2.23	%
Li	33.3	mg/kg
Pb	41.6	mg/kg
Mn	700	mg/kg
Hg	454	µg/kg
Ni	19.9	mg/kg
Sc	6.61	mg/kg
Zn	143	mg/kg

Table 15. LODs and LOQs for FAAS and GFAAS for different trace elements analysed in the LEC

	FAAS		GFAAS	
Trace Element	LOD	LOQ	LOD	LOQ
Al	0.05 ppm	0.17 ppm		
Fe	0.04 ppm	0.12 ppm		
Cd			0.154 ppb	0.462 ppb
Cu	0.02 ppm	0.07 ppm	1.77 ppb	5.31 ppb
Mn	0.05 ppm	0.2 ppm	0.34 ppb	1.02 ppb
Ni			1.32 ppb	4.42 ppb
Zn	0.02 ppm	0.07 ppm		
Pb	0.05 ppm	0.2 ppm	1.60 ppb	3.24 ppb

Table 16. Average Concentrations of Rb, Te, Tl, Ba and Sr in seawater

Average concentration in seawater	Rb (ppb)	Te (ppb)	Tl (ppb)	Ba (ppb)	Sr (ppm)
	125	0,006*	0,012-0,016	13	7.2-7.8
References		Geological Survey of Finland	Flegal, 1985		Angino et al., 1966

*referred for stream waters, such information for seawater has not been reported yet.

Table 17. Carbonate system parameters (EXPERIMENT I; mean values, standard deviations, minimum and maximum values) for seawater, as calculated by 'Seacarb' package for field (absolute values) and experiment microcosms (OA and C) based on the known values of AT, pHT, nutrients and salinity at the temperature of the experiment.

		pH_T	A_T	pCO_2	CO_2	HCO_3^-	CO_3^{2-}	DIC	$\Omega_{ar.}$	Ω_{ca}
	(units)		µmol kg^{-1}	µatm	µmol kg^{-1}	µmol kg^{-1}	µmol kg^{-1}	µmol kg^{-1}		
	field	7.72	2769.3	797	27.82	2413.76	146.25	2587.8	2.19	3.38
OA	mean	6.63	4017.3	31,416	1153.3	3986.6	13.09	5152.9	0.20	0.30
	max	6.97	5341.0	67,398	2458.6	5311.8	20.39	6825.3	0.31	0.47
	min	6.47	2772.7	6765	247.5	2720.0	2.23	2987.9	0.03	0.05
	St. dev.	0.18	1118.7	21,075	768.1	1117.8	6.08	1379.8	0.09	0.14
C	mean	7.85	2749.1	847	31.0	2404.4	140.43	2575.9	2.10	3.26
	max	8.06	2858.5	1,206	44.3	2606.2	202.77	2754.9	3.04	4.71
	min	7.69	2677.4	442	16.1	2181.5	97.99	2400.3	1.47	2.28
	St. dev.	0.15	61.7	321	11.9	153.6	40.85	126.1	0.61	0.95

Table 18. DOC and Nutrient species (EXPERIMENT I; mean values) for seawater (OA and C conditions).

Cond.	Days	DOC (µmol l^{-1})	NO_3^- (µmol l^{-1})	NO_2^-(µmol l^{-1})	NH_4^+ (µmol l^{-1})	TDN (µmol l^{-1})	DON (µmol l^{-1})
OA	1	166,7	2,89	0,30	1,40	45,9	32,93
	4	150,0	2,52	0,40	0,80	41,0	38,02
	7	166,7	12,55	0,50	1,80	43,6	22,22
	10	166,7	7,14	0,40	1,90	24,0	27,76
	14	191,7	4,13	0,20	2,20	24,8	38,39
	18	166,7	3,92	0,10	2,20	20,8	27,58
C	1	158,3	2,70	0,20	1,90	54,9	34,28
	4	141,7	15,15	0,50	1,40	34,1	22,15
	7	158,3	21,53	1,60	0,70	20,7	8,39
	10	166,7	19,72	1,10	0,20	12,3	0,93
	14	166,7	18,86	0,80	0,10	22,0	2,20
	18	150,0	15,33	0,30	0,40	22,0	6,37
Cond.	Days	PO_4^{3-} (µmol l^{-1})	TDP (µmol l^{-1})	DOP (µmol l^{-1})	SiO_4 (µmol l^{-1})	DIN:DIP	
OA	1	0,50	3,0	2,5	18,8	9,2	
	4	0,55	3,9	3,3	35,9	7,4	
	7	0,50	6,3	5,8	26,8	29,7	
	10	0,35	12,4	12,0	28,0	31,5	
	14	0,35	12,9	12,5	35,2	21,8	
	18	0,50	8,2	7,7	37,4	20,7	
C	1	0,55	1,0	0,5	13,6	8,0	
	4	0,45	1,5	1,1	27,9	42,6	
	7	0,35	3,0	2,7	24,9	79,4	
	10	0,40	10,7	10,3	26,0	70,1	
	14	0,45	13,9	13,4	27,6	49,4	
	18	0,60	9,2	8,6	30,1	32,1	

Table 19. Seawater concentrations during Experiment I for OA and C conditions; As, Cd, Pb, Co, Cu, Ni and Cr in nmol l^{-1} and V, Fetotal, Fe(III), Fe(II), Mn and Al in µmol l^{-1} (LODs included for each trace metal).

Cond.	Days	As (nmol l^{-1})	V (µmol l^{-1})	Cd (nmol l^{-1})	Pb (nmol l^{-1})	Co (nmol l^{-1})	Fetotal (µmol l^{-1})	Fe(III) (µmol l^{-1})
	LOD	**0.63**	**0.006**	**1.03**	**3.06**	**0.255**	**0.062**	**0.029**
OA	1	47,24	0,117	3,56	7,71	6,50	0,751	0,661
	7	49,66	0,087	4,13	6,31	5,50	0,264	0,249
	14	37,33	0,074	3,27	2,92	2,90	0,326	0,298
	18	43,85	0,105	3,88	4,18	2,48	0,203	0,198
C	1	59,43	0,150	3,54	7,41	3,66	0,277	0,236
	7	55,65	0,120	4,03	4,19	3,67	0,097	0,083
	14	46,67	0,104	2,79	1,53	3,55	0,125	0,114
	18	67,31	0,152	4,09	2,31	2,94	0,109	0,109
Cond.	Days	Cu (nmol l^{-1})	Ni (nmol l^{-1})	Mn (µmol l^{-1})	Al (µmol l^{-1})	Cr (nmol l^{-1})	Fe(II) (µmol l^{-1})	
	LOD	**8.45**	**8.20**	**0.005**	**0.586**	**55.08**	**0.033**	
OA	1	6,58	38,32	0,060	0,370	36,50	0,091	
	7	17,18	80,48	0,176	0,947	68,25	0,015	
	14	15,80	77,40	0,196	0,237	25,99	0,028	
	18	17,82	98,24	0,203	0,173	33,44	0,006	
C	1	11,24	37,13	0,089	0,394	65,65	0,041	
	7	13,13	49,89	0,042	0,333	96,44	0,014	
	14	18,21	61,50	0,016	0,431	31,25	0,012	
	18	14,05	76,39	0,013	0,417	80,07	0,000	

Table 20. Sediment concentrations during Experiment I for OA and C conditions (mean values and standard deviations); moisture, OC, IC, TN, TP, CaCO3, S, Al, and Fe in %; As, Mn, Cr, Cu, Ni, Pb, Cd, Co and V in mg/kg; Fetotal, Fe(II) and Fe(III) in % refer colorimetric determination as described by Bloom calculated for dry sediment

condition	Moisture	OC	IC	TN	TP	CaCO3	S							
field	60,7	2,35	5,62	0,28	0,07	46,8	0,80							
OA	57,8	1,67	5,97	0,19	0,05	49,7	0,81							
stdev	1,7	0,14	0,36	0,01	0,03	3,0	0,08							
C	47,9	1,84	5,49	0,20	0,04	45,7	0,79							
stdev	9,9	0,25	0,22	0,02	0,02	1,8	0,07							
condition	As	Mn	Cr	Cu	Ni	Pb	Cd	Al	Co	V	Fe	Fetotal	Fe(II)	Fe(III)
field	15,9	330,0	101,8	63.2	130,1	108,4	0,431	3,5	5.26	66,2	2,08	0,71	0,17	0,54
OA	15,3	327,0	130,7	25.4	118,9	80,8	0,342	3,2	6.25	63,5	1,85	0,74	0,17	0,57
stdev	1,2	11,1	6,9	1.5	0,7	2,4	0,063	0,1	0.91	1,5	0.03	0,01	0,01	0,00
C	15,4	325,0	120,5	29.1	114.5	77,6	0,353	3,2	6.34	65,6	1.84	0,73	0,13	0,60
stdev	1,6	32,5	12,2	1.1	2.7	33,4	0,137	0,1	1.20	0,8	0.00	0,00	0,01	0,01

Table 21. Carbonate system parameters (EXPERIMENT II; mean values, standard deviations, minimum and maximum values) for seawater, as calculated by 'Seacarb' package for field (absolute values) and experiment microcosms (OA and C) based on the known values of AT,

		pH_T	A_T	pCO_2	CO_2	HCO_3^-	CO_3^{2-}	DIC	$\Omega_{ar.}$	Ω_{ca}
	(units)		µmol kg^{-1}	µatm	µmol kg^{-1}	µmol kg^{-1}	µmol kg^{-1}	µmol kg^{-1}		
field	2m	8.03	2974.0	522	13.7	2237.3	306.8	2557.8	4.80	7.19
	10m	8.05	2990.9	504	15.1	2334.4	274.1	2623.6	4.18	6.38
	20m	7.76	2978.6	1,089	36.0	2644.4	139.7	2820.1	2.11	3.24
	32 m	7.62	2974.9	1,538	52.3	2726.1	100.5	2879.0	1.51	2.33
OA	mean	6.65	3622.2	18,868	641.1	3586.1	15.1	4242.4	0.22	0.34
	max	6.73	4340.9	22,526	766.3	4292.3	20.3	4956.9	0.31	0.47
	min	6.58	3062.4	14,103	479.8	3039.1	12.4	3667.5	0.15	0.24
	st. dev.	0.06	475.4	2,810	94.9	469.5	2.7	523.8	0.05	0.08
C	mean	7.62	3143.2	1,660	56.49	2893.7	107.06	3057.2	1.61	2.49
	max	7.66	3308.5	1,813	61.67	3201.9	132.53	3394.5	2.00	3.08
	min	7.58	3064.5	1,526	51.91	2759.0	98.25	2914.7	1.48	2.29
	st. dev.	0.03	107.34	117	3.99	162.3	12.67	176.1	0.19	0.29

Table 22. DOC and Nutrient species (EXPERIMENT II; mean values) for seawater (OA and C conditions).

Cond.	Days	DOC (µmol l^{-1})	NO_3^- (µmol l^{-1})	NO_2^- (µmol l^{-1})	NH_4^+ (µmol l^{-1})	TDN (µmol l^{-1})	DON (µmol l^{-1})
field (Depth)	0	175,0	0,322	0,100	0,331	12,247	11,5
	10	275,0	0,355	0,120	0,370	9,554	8,7
	20	133,3	1,338	0,607	1,785	12,361	8,6
	30	125,0	0,177	0,072	9,722	22,387	12,4
OA (Days)	1	250,00	0,73	0,27	15,68	30,00	13,3
	4	325,00	0,66	0,29	14,62	36,41	20,8
	5	225,00	0,57	0,36	16,47	41,45	24,0
	8	175,00	0,55	0,44	16,69	40,36	22,7
	10	208,33	0,82	0,63	16,91	44,28	25,9
	12	216,67	0,39	0,93	14,81	47,29	31,2
	15	200,00	0,49	1,12	14,94	39,27	22,7
	18	158,33	1,23	1,71	10,60	34,63	21,1
	25	120,83	2,45	2,68	7,92	31,63	18,6
	33	187,50	6,31	5,86	3,23	24,84	9,4
C (Days)	1	350,00	0,66	0,17	19,05	32,63	12,8
	4	237,50	0,86	0,42	16,84	40,50	22,4
	5	266,67	0,64	0,72	19,00	40,43	20,1
	8	191,67	0,75	3,15	11,96	43,10	27,2
	10	208,33	0,88	6,19	11,19	42,91	24,6
	12	170,83	1,04	8,41	7,21	44,90	28,2
	15	195,83	1,04	11,07	3,40	34,17	18,7
	18	150,00	3,04	8,17	1,65	24,48	11,6
	25	170,00	1,37	2,32	2,61	25,00	18,7
	33	158,33	1,54	0,29	1,29	16,44	13,3

Cond.	Days	PO_4^{3-} (µmol l^{-1})	TDP (µmol l^{-1})	DOP (µmol l^{-1})	SiO_4 (µmol l^{-1})	DIN:DIP	
field (Depth)	0	0,011	2,938	2,927	0,80	66,4	
	10	0,011	8,623	8,612	0,98	74,5	
	20	0,358	2,163	1,805	18,67	10,4	
	30	3,684	4,001	0,317	56,17	2,7	
OA	1	2,65	2,66	0,15	71,4	6,30	
	4	2,45	2,75	0,43	66,8	6,36	
	5	2,60	3,31	0,71	36,6	6,69	
	8	2,35	3,40	1,26	38,6	7,52	
	10	2,50	2,60	0,60	33,2	7,35	
	12	2,20	2,75	0,71	42,8	7,33	
	15	2,29	3,16	0,79	39,6	7,22	
	18	2,01	3,24	1,25	41,3	6,74	
	25	1,98	3,33	1,31	51,2	6,61	
	33	2,10	4,42	1,33	49,0	7,00	
C	1	2,30	2,62	0,32	79,7	8,64	
	4	1,75	2,14	0,92	34,8	10,35	
	5	2,10	2,81	0,71	34,5	10,12	
	8	2,10	2,86	0,96	43,0	10,20	
	10	1,85	2,45	1,00	40,2	9,87	
	12	1,80	2,59	1,20	42,4	9,26	
	15	2,01	1,78	1,31	41,0	7,73	
	18	1,76	2,16	1,63	44,1	7,31	
	25	1,45	2,06	1,87	51,3	4,35	
	33	1,52	3,26	1,74	49,6	2,05	

Table 23. Seawater concentrations during field sampling and Experiment II for OA and C conditions; As, Cd, Pb, Co, Cu, Ni, V and Cr in nmol l^{-1} and Fetotal, Fe(III), Fe(II), Mn and Al in µmol l^{-1} (LODs included for each trace metal).

Cond.		As (nmol l^{-1})	V (nmol l^{-1})	Cd (nmol l^{-1})	Pb (nmol l^{-1})	Co (nmol l^{-1})	Fetotal (µmol l^{-1})	Fe(III) (µmol l^{-1})
LOD		**0.63**	**6.07**	**1.03**	**3.06**	**0.255**	**0.062**	**0.029**
field (Depth)	2	6,03	5,08	0,676	0,81	0,48	0,04	0,01
	10	6,80	3,33	0,676	4,38	0,33	0,07	0,05
	20						0,09	0,06
	30	21,53	1,78	2,195	0,752	2,616	1,97	1,76
OA (days)	1	42,65	40,58	1,198	0,686	0,883	0,62	0,59
	4	43,54	94,23	1,441	2,036	1,153	1,33	1,27
	5	43,60	85,37	1,102	1,498	1,073	2,02	1,90
	8	44,59	74,46	1,551	1,393	0,960	1,42	1,34
	10	35,03	85,09	1,080	6,014	0,725	2,22	2,14
	12	37,51	62,44	1,028	1,674	0,680	2,10	2,01
	15	36,55	60,44	1,271	3,225	0,570	2,09	1,98
	18	33,70	56,91	1,654	1,201	0,575	1,41	1,36
	25	30,59	47,24	0,912	4,501	1,072	1,41	1,33
	33	31,11	74,50	0,529	1,172	0,419	0,63	0,54
	1	44,86	65,88	1,446	3,181	1,412	0,54	0,51
	4	47,15	69,48	1,754	1,321	1,376	1,19	1,15
	5	46,12	57,10	1,641	1,177	1,047	1,53	1,47
	8	46,21	51,09	1,575	1,019	0,573	1,01	0,96
	10	43,21	42,56	1,354	1,105	0,383	1,16	1,08
	12	39,27	42,97	1,273	0,895	0,367	1,08	1,02
	15	43,24	38,50	1,441	1,008	0,385	1,02	0,95
	18	39,15	46,34	1,796	0,908	0,513	4,95	4,90

	25	40,71	70,01	0,538	1,262	0,968	3,90	3,85
	33	51,43	113,13	0,649	1,242	0,745	1,22	1,20
Cond.	Days	**Cu (nmol l^{-1})**	**Ni (nmol l^{-1})**	**Mn (µmol l^{-1})**	**Al (µmol l^{-1})**	**Cr (nmol l^{-1})**	**Fe(II) (µmol l^{-1})**	
LOD		**8.45**	**8.20**	**0.005**	**0.586**	**55.08**	**0.033**	
field (Depth)	2	12,53	3,53	0,040	0,22	20,69	0,03	
	10	10,68	4,25	0,048	0,46	21,27	0,02	
	20						0,03	
	30	2,28	7,66	4,272	0,770	20,73	0,21	
OA	1	10,05	27,82	0,109	0,431	34,85	0,04	
	4	13,61	31,64	0,300	0,392	33,45	0,06	
	5	15,23	31,23	0,201	0,362	29,80	0,12	
	8	17,07	33,75	0,262	0,548	37,28	0,08	
	10	16,80	28,92	0,269	0,436	25,76	0,08	
	12	18,21	30,72	0,210	0,119	19,12	0,09	
	15	16,71	29,98	0,226	0,413	27,22	0,11	
	18	14,18	29,48	0,169	0,453	39,76	0,09	
	25	7,54	30,65	0,236	0,646	42,82	0,09	
	33	6,26	27,22	0,032	0,185	19,39	0,09	
C	1	10,61	20,41	0,186	0,143	25,27	0,02	
	4	14,55	22,13	0,231	0,204	30,89	0,03	
	5	13,60	21,15	0,147	0,168	28,79	0,06	
	8	14,58	20,39	0,064	0,180	31,38	0,05	
	10	16,18	18,57	0,053	0,074	18,09	0,08	
	12	16,45	17,47	0,038	0,169	22,53	0,06	
	15	17,09	17,01	0,039	0,225	22,44	0,08	
	18	18,95	17,36	0,065	0,303	44,56	0,05	
	25	10,49	19,88	0,094	0,330	20,40	0,05	
	33	11,20	22,64	0,026	0,224	17,04	0,02	

Table 24. Sediment concentrations during Experiment I for OA and C conditions (mean values and standard deviations); moisture, OC, IC, TN, TP, CaCO3, S, Al, and Fe in %; As, Mn, Cr, Cu, Ni, Pb, Cd, Co and V in mg/kg; Fetotal, Fe(II) and Fe(III) in % refer colorimetric determination as described by Bloom calculated for dry sediment

condition	Day	Moisture	OC	IC	TN	TP	CaCO3	S
field		75,7	3,22	4,84	0,39	0,05	40,3	0,97
OA	18th	69,1	2,17	4,67	0,25	0,06	38,9	0,86
stdev		2,5	0,26	0,12	0,03	0,01	1,0	0,00
OA	33rd	64,5	1,89	4,39	0,18	0,06	36,6	0,94
stdev		2,8	0,50	0,30	0,02	0,01	2,5	0,00
C	18th	69,8	2,28	4,82	0,27	0,07	40,2	0,81
stdev		0,1	0,24	0,69	0,02	0,00	5,7	0,00
C	33rd	65,4	1,94	5,35	0,31	0,06	44,6	0,88
stdev		4,5	1,04	0,61	0,04	0,00	5,1	0,00

condition	Day	As	Mn	Cr	Cu	Ni	Pb	Cd	Al	Co	V	Fe	Fetotal	Fe(II)	Fe(III)
field		9,81	283,7	116,8	76,0	126,7	101,6	0,301	3,26	7,12	72,3	1,83	0,71	0,14	0,58
OA	18th	15,87	323,6	107,8	47,3	129,5	106,1	0,489	3,48	8,53	70,8	2,14	0,74	0,16	0,58
stdev		0,14	10,1	1,0	2,3	2,7	7,3	0,013	0,14	0,30	0,4	0,08	0,06	0,02	0,04
OA	33rd	16,62	349,8	128,5	42,0	137,7	110,5	0,448	3,57	5,32	62,6	2,14	0,73	0,13	0,60
stdev		0,01	26,9	14,6	4,2	10,4	16,0	0,033	0,24	1,07	5,1	0,13	0,05	0,03	0,02
C	18th	16,06	319,5	103,3	50,6	136,2	111,0	0,475	3,57	7,04	66,8	2,18	0,71	0,15	0,56
stdev		0,08	11,2	4,8	5,3	6,1	4,8	0,003	0,05	0,73	3,5	0,14	0,05	0,01	0,04
C	33rd	16,37	338,5	122,1	45,4	137,3	107,1	0,463	3,39	4,89	60,0	2,20	0,80	0,16	0,64
stdev		3,78	9,0	3,6	23,5	3,5	38,5	0,204	0,34	1,22	1,6	0,22	0,01	0,01	0,00

Table 25. One way ANOVA results (F, p) for Experiment I for all experiment parameters regarding seawater analyses (p values <0.05 are marked bold, which indicate statistical significance between the two treatments)

Parameter	F	p	Parameter	F	p
DO	0.504	0.494	Pb	0.708	0.432
A_T	7.688	**0.020**	V	3.566	0.108
HCO_3^-	11.797	**0.006**	NO_2^-	3.698	0.083
CO_3^{2-}	54.706	**0.000**	NH_4^+	6.474	**0.029**
CO_2	12.805	**0.005**	DIN	8.970	**0.013**
DIC	20.758	**0.001**	TDN	0.550	0.475
pCO_2	12.620	**0.005**	PO_4^{3-}	0.065	0.804
$\Omega_{ar.}$	56.934	**0.000**	TDP	0.190	0.672
$\Omega_{calc.}$	57.061	**0.000**	SiO_4	1.993	0.188
DOC	2.712	0.131	DIN:DIP	5.620	**0.039**
NO_3^-	9.982	**0.010**	DOP	0.057	0.820
DON	4.696	0.073	Co	0.793	0.407
As	6.358	**0.045**	Fe_{total}	3.191	0.124
Mn	9.925	**0.020**	Fe (III)	3.820	0.098
Cd	0.075	0.793	Fe(II)	0.755	0.418
Cu	0.004	0.952	Al	0.045	0.840
Ni	1.317	0.295	Cr	2.667	0.154

Table 26. One way ANOVA results (F, p) for Experiment II for all experiment parameters regarding seawater analyses (p values <0.05 are marked bold, which indicate statistical significance between the two treatments) – the cells marked as grey were the trace elements found below the detection limit.

Parameter	F	p	Parameter	F	p
DO	0.012	0.913	Co	0.052	0.823
A_T	3.462	0.079	NO_2^-	3.662	0.072
HCO_3^-	10.787	**0.004**	NH_4^+	1.882	0.187
CO_3^{2-}	9.934	**0.006**	DIN	0.616	0.443
CO_2	15.512	**0.001**	TDN	0.520	0.480
DIC	15.725	**0.001**	PO_4^{3-}	18.932	**0.000**
pCO_2	15.512	**0.001**	TDP	9.791	**0.006**
$\Omega_{ar.}$	9.934	**0.006**	SiO_4	0.005	0.943
$\Omega_{calc.}$	9.934	**0.006**	DIN:DIP	1.369	0.257
DOC	0.470	0.502	DOP	0.002	0.967
NO_3^-	0.148	0.705	Fe_{total}	7.391	**0.014**
DON	0.164	0.691	Fe (III)	6.957	**0.017**
As	7.816	**0.012**	Fe(II)	11.458	**0.003**
Mn	10.070	**0.005**	Al	20.401	**0.000**
Cd	0.984	0.334	Pb	3.112	0.095
Cu	0.015	0.904	Cr	1.731	0.205
Ni	141.033	**0.000**			

Table 27. One way ANOVA results (F, p) for Experiment I for all experiment parameters regarding sediments; no p values <0.05 were found which indicates no statistical significance between the two treatments in any parameter

Parameter	F	p	Parameter	F	p
Moisture	1,945	0,298	Ni	0,175	0,717
OC	0,716	0,486	Pb	0,019	0,904
IC	2,654	0,245	Cd	0,011	0,925
TN	0,539	0,539	Al	0,070	0,817
TP	0,168	0,721	Co	0,312	0,633
$CaCO_3$	2,654	0,245	V	3,064	0,222
S	0,048	0,847	Fe	0,059	0,831
As	0,005	0,952	Fetotal	3,723	0,193
Mn	0,011	0,925	Fe(II)	13,761	0,066
Cr	6,723	0,122	Fe(III)	11,163	0,079
Cu	0,603	0,519			

Table 28. One way ANOVA results (F, p) for Experiment II for all experiment parameters regarding sediments; no p values <0.05 were found which indicates no statistical significance between the two treatments in any parameter

Parameter	F	p	Parameter	F	p
Moisture	1,945	0,298	Ni	0,175	0,717
OC	0,716	0,486	Pb	0,019	0,904
IC	2,654	0,245	Cd	0,011	0,925
TN	0,539	0,539	Al	0,070	0,817
TP	0,168	0,721	Co	0,312	0,633
$CaCO_3$	2,654	0,245	V	3,064	0,222
S	0,048	0,847	Fe	3,723	0,193
As	0,005	0,952	Fetotal	0,059	0,831
Mn	0,011	0,925	Fe(II)	13,761	0,066
Cr	6,723	0,122	Fe(III)	11,163	0,079
Cu	0,603	0,519			

Table 29. PCA analysis for the Experiments I and II (C and OA conditions; Pattern Matrix, Components 1 and 2); trace metals found below LOD limit were excluded from the calculations

	EXPERIMENT I					EXPERIMENT II			
	C		OA			C		OA	
	Components		Components			Components		Components	
	1	2	1	2		1	2	1	2
pH	0,98	-0,03	-0,98	-0,18	pH	-0,07	0,55	-0,87	0,23
DO	0,23	-1,00	0,26	0,64	DO	-0,90	-0,25	-0,02	0,92
AT	-0,93	0,51	0,94	-0,19	AT	-0,92	0,07	-0,03	0,96
pCO2	-0,99	0,14	0,94	-0,08	pCO2	0,10	-0,65	0,92	0,33
HCO3	-1,00	0,21	0,95	-0,19	HCO3	-0,23	-0,69	0,15	0,98
CO3	0,98	0,02	-0,85	-0,56	CO3	-0,66	0,53	-0,85	0,22
DIC	-1,00	0,28	0,95	-0,15	DIC	-0,25	-0,73	0,44	0,93
DOC	0,23	-0,75	0,49	-0,58	DOC	0,71	0,48	-0,48	-0,62
NH4	0,89	0,31	0,99	-0,08	NH4	0,79	0,55	0,38	-0,82
NO2	0,06	-0,89	-0,46	0,68	NO2	0,03	-0,94	-0,33	0,84
NO3	-0,60	-0,63	0,066	0,916	NO3	-0,60	-0,29	-0,47	0,70
DIN	-0,52	-0,676	0,130	0,909	DIN	0,951	0,09	0,17	-0,56
PO4	0,26	0,839	-0,85	0,463	PO4	0,932	0,07	-0,20	-0,88
SiO4	-0,96	-0,10	0,98	-0,08	SiO4	-0,27	0,56	-0,85	-0,43
TDN	0,99	-0,01	0,20	-0,52	TDN	0,819	-0,34	0,92	-0,08
TDP	-0,84	-0,09	0,87	-0,30	DON	0,331	-0,50	0,94	0,03
DON	0,85	0,37	0,05	-0,95	TDP	-0,08	0,53	-0,19	0,75
DOP	-0,84	-0,11	0,88	-0,31	DOP	-0,75	0,35	-0,08	0,89
DIN_DIP	-0,23	-0,81	0,63	0,72	DIN_DIP	0,97	-0,16	0,51	0,44
Fetotal	0,77	0,37	-0,90	-0,46	Fetotal	0,68	-0,21	0,92	-0,05
FeIII	0,70	0,45	-0,91	-0,45	FeII	0,30	-0,84	0,68	0,43
Mn	0,97	0,11	0,97	0,26	FeIII	0,67	-0,17	0,92	-0,07
As	-0,13	0,85	-0,62	0,73	Mn	0,47	0,64	0,67	-0,40
Cd	-0,01	0,37	-0,02	0,94	As	0,77	0,297	0,733	-0,21
Ni	-1,00	0,30	0,912	0,37	Cd	0,77	-0,21	0,306	-0,46
Cu	-0,68	-0,40	0,90	0,47	Ni	-0,08	0,84	0,57	-0,28
Co	0,83	-0,71	-0,94	0,25	Cu	-0,43	-0,65	0,900	-0,17
Pb	0,94	0,187	-0,93	0,31	Co	0,15	0,84	-0,00	-0,61
V	0,14	0,92	-0,69	0,55	V	-0,60	0,72	0,27	-0,23

ANNEX III FIGURES

Experiment I

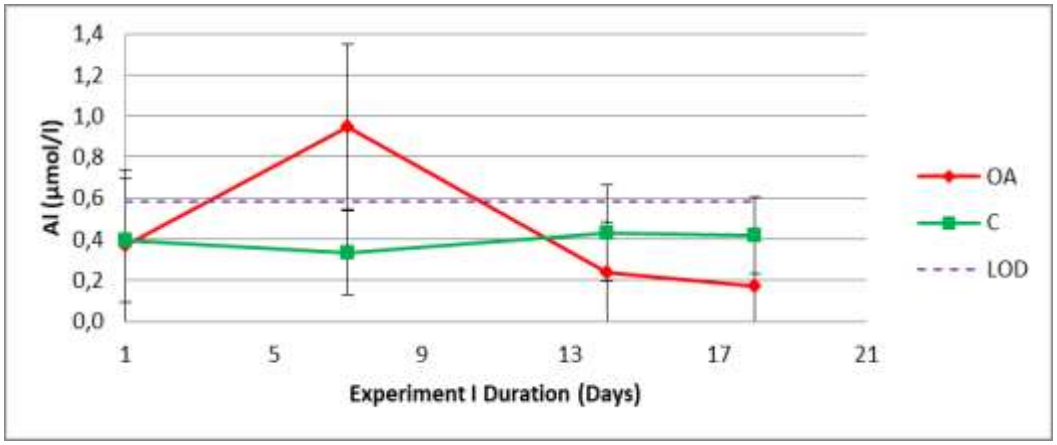

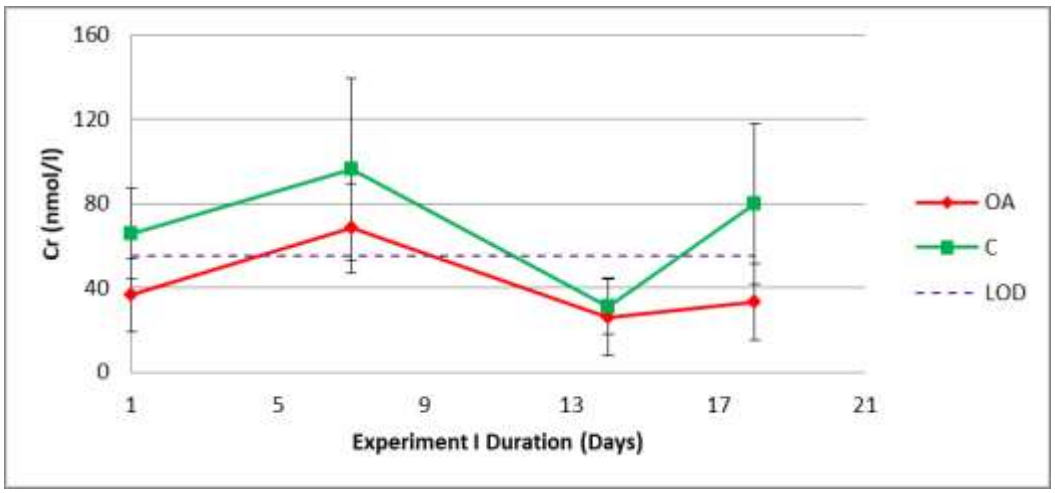

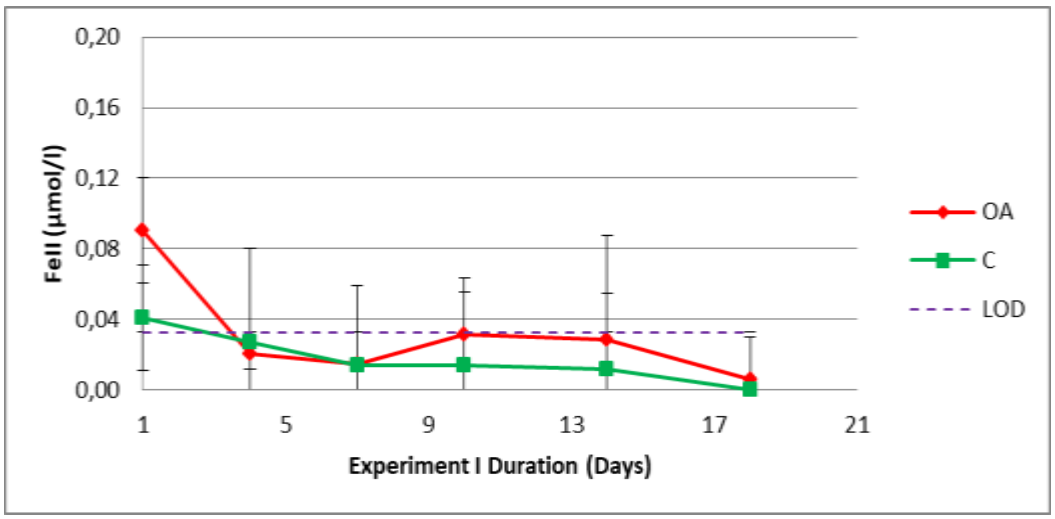

Figure 45. Cr (in nmol l^{-1}), Al and Fe(II) concentrations (in µmol l^{-1}) for the duration of the Experiment I which appear below the LOD; mean values and standard deviations for the two replicates of each treatment).

Experiment II

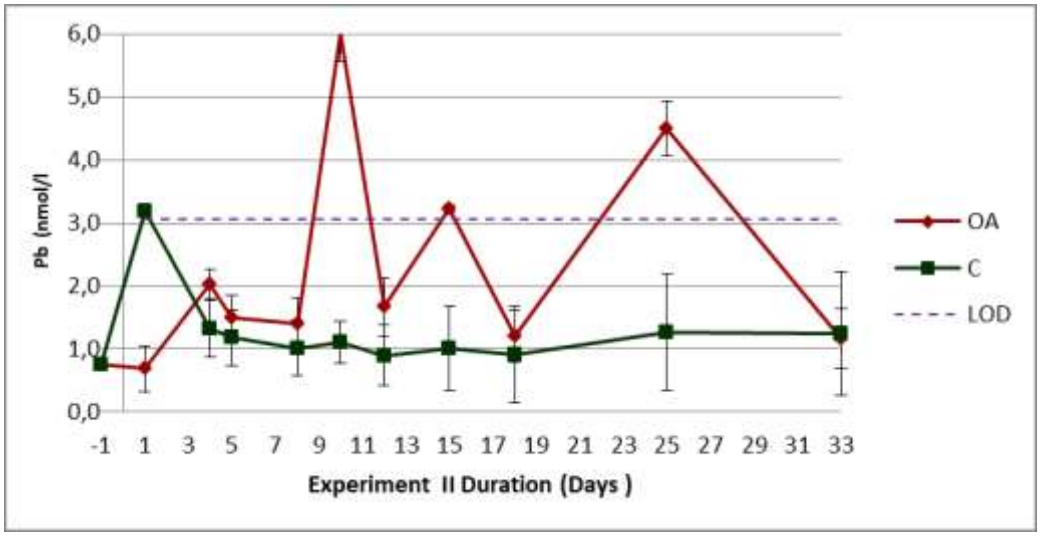

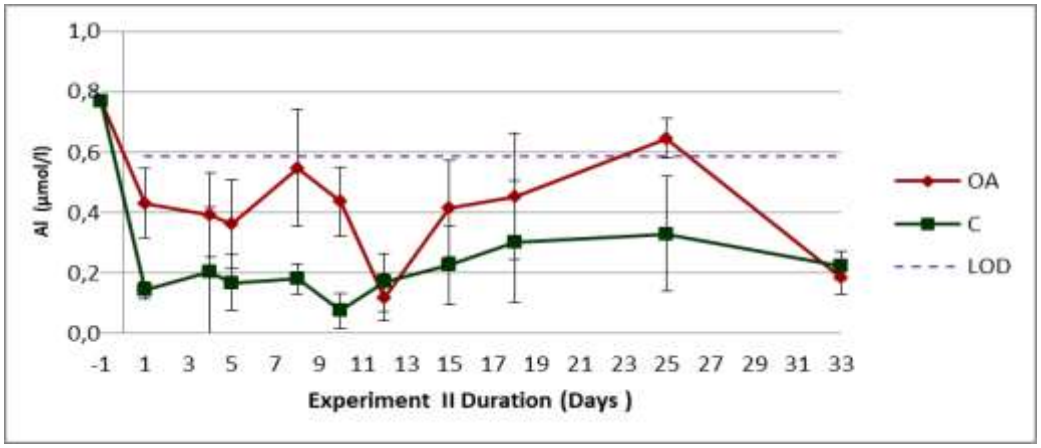

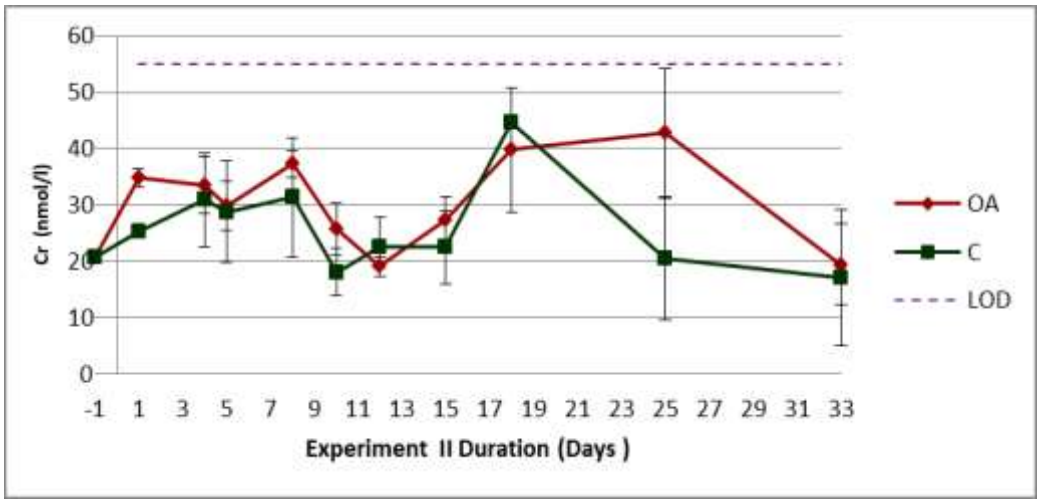

Figure 46. Cr, Pb (in nmol l^{-1}) and Al concentrations (in µmol l^{-1}) for the duration of the Experiment II which appear below the LOD; mean values and standard deviations for the two replicates of each treatment).

REFERENCES

1. Gattuso J.P., Lavigne H., Technical Note: Approaches and software tools to investigate the impact of ocean acidification. Biogeosciences, 2009. 6: p. 2121-2133.
2. Schneider A., Tanhua T., Körtzinger A., Wallace D. W. R. , High anthropogenic carbon content in the eastern Mediterranean. J. Geophys. Res., 2010. 115(C12050).
3. NASA, Global Climate Change-Vital Signs of the Planet. https://climate.nasa.gov/vital-signs/carbon-dioxide/. Retrieved 28/5/2018.
4. Climate Change 2014 Synthesis Report Summary for Policymakers, in 5th Assessment Report, IPCC, Editor.
5. Le Quere C., Moriarty R., Andrew R., Peters G., Ciais P., Friedlingstein P., Jones S., Sitch S., Tans R., Arneth A., Boden T., Bopp L., Bozec Y., Canadell J., Chini L., Chevallier F., Cosca C., Harris I., Hopema M., Houghton R., Kouse J., Jain A., Johannessen T., Kato E., Keeling R., Kitidis V., Klein Goldewijk K., Koven C. et al., Global Carbon Budget 2014. Earth System Science Data, 2015. 7: p. 47-85.
6. Krasakopoulou E., Souvermezoglou E., Goyet C., Anthropogenic CO2 fluxes in the Otranto Strait (E. Mediterranean) in February 1995. Deep-Sea Research, 2011. I(58): p. 1103-1114.
7. Ciais P., Sabine C., G. Bala, L. Bopp, V. Brovkin, J. Canadell, A. Chhabra, R. DeFries, J. Galloway, M. Heimann, C. Jones, C. Le Quéré, R.B. Myneni, S. Piao and P. Thornton, Carbon and Other Biogeochemical Cycles, in Climate Change 2013: The Physical Science Basis. Contribution of Working Group I to the Fifth Assessment Report of the Intergovernmental Panel on Climate Change D.Q. Stocker T.F., G.-K. Plattner, M. Tignor, S.K. Allen, J. Boschung, A. Nauels, Y. Xia, V. Bex and P.M. Midgley, Editor. 2013, Cambridge University Press: Cambridge, United Kingdom and New York, NY, USA.
8. Caldeira K., Wickett M., Ocean Model predictions of chemistry changes from carbon dioxide emissions to the atmosphere and ocean. Journal of Geophysical Research, 2005. 110.

9. Andersson A., Bates N., Mackenzie F., Dissolution of Carbonate Sediments Under Rising pCO2 and Ocean Acidification: Observations from Devil's Hole, Bermuda. Aquat Geochem, 2007. 13: p. 237-264.
10. Turley C, Gattuso J. P. (2012). "Future biological and ecosystem impacts of ocean acidification and their socioeconomic-policy implications." Current Opinion in Environmental Sustainability 4: 278-286.
11. Beman M., Chow C., King A., Feng Y., Fuhrman J., Andersson A., Bates N., Popp B., Hutchins D. Global declines in oceanic nitrification rates as a consequence of ocean acidification. PNAS, 2011. 108, 208-2013.
12. Burdige D.J., Geochemistry of Marine Sediments. 2006, Princeton University: Princeton University Press.
13. Feely R., Alin S., Newton J., Sabine C., Warner M., Devol A., Krembs C., Maloy C., The combined effects of ocean acidification, mixing, and respiration on pH and carbonate saturation in an urbanized estuary. Estuarine, Coastal and Shelf Science, 2010. 88: p. 442-449.
14. Gazeau F., Van Rijswijk P., Pozzato L., Middleburg J. Impacts of Ocean Acidification on Sediment Processes in Shallow Waters of the Arctic Ocean. PLOS ONE, 2014. 9, 1-11.
15. Gruber N., Warming up, turning sour, losing breath: ocean biogeochemistry under global change. Phil. Trans. R. Soc., 2011. 369: p. 1980-1996.
16. Ianson D., Allen S.E., Moore-Maley B. L., Johannessen S. C., Macdonald R. W. , Vulnerability of a semienclosed estuarine sea to ocean acidification in contrast with hypoxia. Geophysical research Letters, 2016. 43.
17. Gobler C., De Pasquale E., Griffith A., Baumann H. Hypoxia and Acidification Have Additive and Synergistic Negative Effects on the Growth, Survival, and metamorphosis of Early Life Stage Bivalves. PLoS ONE, 2014. 9.
18. Diaz R., Overview of Hypoxia around the World. Journal of Environmental Quality, 2001. 30(2): p. 275-281.

19. Hofmann A., Peltzer E., Walz P., Brewer P., Hypoxia by degrees:Establishing definitions for a changing ocean. Deep-Sea Research, 2011. 58: p. 1212-1226.
20. Howarth R., Chan F., Conley D., Garnier J., Doney S., Marino R., Billen G., Coupled biogeochemical cycles: eutrophication and hypoxia in temperate estuaries and coastal marine ecosystems. Front Ecol Environ, 2011. 9(1): p. 18-26.
21. Cai W., Hu X., Huang W., Murrel M., Lehrter J., Lohrenz S., Chou W., Zhai W., Hollibaugh J., Wang Y., Zhao P., Guo X., Gundersen K., Dai M., Gong G. Acidification of subsurface coastal waters enhanced by eutrophication. Nature Geoscience, 2011. 4, 766-770 DOI: 10.1038/ngeo1297.
22. Caldeira, K., Wickett M.E., Oceanography: Anthropogenic carbon and ocean pH. Nature, 2003. 425(6956): p. 365-365.
23. Melzner F, Thomsen J., Koeve W.,Oschlies A., Gutowska M., Bange H., Hansen H., Kortzinger A., Future ocean acidification will be amplified by hypoxia in coastal habitats. Mar Biol, 2013. 160: p. 1875-1888.
24. Ardelan M., Steinnes E., Lierhagen S., Linde S.O., Effects of experimental CO2 leakage on solubility and transport of seven trace metals in seawater and sediment. Science of the Total Environment, 2009. 407: p. 6255-6266.
25. Roberts D., Birchenough S., Lewis C., Sanders M., Bolam T., Sheahan D., Ocean Acidification increases the toxicity of contaminated sediments. Global Change Biology, 2013. 19: p. 340-351.
26. Atkinson C., Jolley D., Simpson S., Effect of overlying water pH, dissolved oxygen, salinity and sediment disturbances on metal release and sequestrtaion from metal contaminated marine sediments. Chemosphere, 2007. 69(9): p. 1428-1437.
27. Paulmier A., Ruiz-Pino D., Garcon V., CO2 maximum in the oxygen minimum zone (OMZ). Biogeosciences, 2011. 8: p. 239-252.
28. Borges A., Do we have enough pieces of the jigsaw to Integrate CO2 Fluxes in the Coastal Ocean? Estuaries, 2005. 28(1): p. 3-27.

29. Borges A., Dellile B., Frankignoulle M., Budgeting sinks and sources of CO2 in the coastal ocean: Diversity of ecosystems counts. Geophysical research Letters, 2005. 32.
30. Borges A., Schiettecatte L., Abril G., Delille B., Gazeau F., Carbon dioxide in European coastal waters. Estuarine, Coastal and Shelf Science, 2006. 70: p. 375-387.
31. Gypens N., Borges A., Lancelot C., Effect of eutrophication on air-sea CO2 fluxes in the coastal Southern North Sea: a model study of the past 50 years. Global Change Biology, 2009. 15: p. 1040-1056.
32. Hagens M., Slomp C., Meysmann F. J. R., Seitaj D., Harlay J., Borges A., Middelburg J. J., Biogeochemical processes and buffering capacity concurrently affect acidification in a seasonally hypoxic coastal marine basin. Biogeosciences, 2015. 12: p. 1561-1583.
33. Wallace R. , Baumann H., Grear J., Aller R., Gobler R., Coastal ocean acidification: The other eutrophication problem. Estuarine, Coastal and Shelf Science, 2014. 148: p. 1-13.
34. Ingrosso G., Giani M., Cibic T.,Karuza A., Krajl M., Del Negro P. , Carbonate chemistry dynamics and biological processes along a river–sea gradient (Gulf of Trieste, northern Adriatic Sea). Journal of Marine Systems, 2016. 155: p. 35-49.
35. Levin L., Liu K., Emeis K., Breitburg D., Cloern J., Deutsch C., Giani M., Goffart A., Hofmann E., Lachkar Z., Limburg K., Liu S., Montes E., Naqvi W., Ragueneau O., Rabouille C., Kumar Sarkar S., Swaney D., Wassman P., Wishner K., Comparative biogeochemistry–ecosystem–human interactions on dynamic continental margins. Journal of Marine Systems, 2015. 141: p. 3-17.
36. Oschlies A., Schultz K., Riebesell U., Schmittner A., Simulated 21st century's increase in oceanic suboxia by CO2-enhanced biotic carbon export. Global Biogeochem. Cy., 2008. 22(GB4008).
37. Hutchins D., Mulholland M., Feixue F., Nutrient Cycles and Marine Microbes in a CO2-Enriched Ocean. Oceanography, 2009. 22(4): p. 128-145.

38. Hassoun, Abed El Rahman, et al., Modeling of the Total Alkalinity and the Total Inorganic Carbon in the Mediterranean Sea. Journal of Water Resources and Ocean Science, 2015: p. 24-32.
39. Alvarez M., San Leon-Bartolome H., Tanhua T., Mintrop L., Luchetta A., Cantoni C., Schroeder K., Civitarese G., The CO2 system in the Mediterranean Sea: a basin wide perspective. Ocean Sci J., 2014. 10: p. 69-92.
40. Howes E., Stemmann L., Assailly C., Irisson J., Dima M., Bijma J., Gattuso J., Pteropod time series from the North Western Mediterranean (1967−2003): impacts of pH and climate variability. Mar Ecol Prog Ser, 2015. 531: p. 193-206.
41. Duarte C., Agusti S., Kennedy H., Vaque D., The Mediterranean climate as a template for Mediterranean marine ecosystems: the example of the northeast Spanish littoral. Progress in Oceanography, 1999. 44: p. 245-270.
42. Hassoun A., Gemayel E., Krasakopoulou E., Goyet C., Abboud-Abi Saab M., Guglielmi V., Touratier F., Falco C., Acidification of the Mediterranean Sea from anthropogenic carbon penetration. Deep-Sea Research, 2015. 1(102): p. 1-15.
43. Borges A., Gypens N., Carbonate chemistry in the coastal zone responds more strongly to eutrophication than to ocean acidification. Limnol. Oceanogr., 2010. 55(1): p. 436-353.
44. Duarte C., Hendriks I., Moore T., Olsen Y., Steckbauer A., Ramajo L., Carstensen J., Trotter J., McCulloch M., Is Ocean Acidification an Open-Ocean Syndrome? Understanding Anthropogenic Impacts on Seawater pH. Estuaries and Coasts, 2013. 36: p. 221-236.
45. Luchetta, A., Cantoni, C., Catalano, G. , New observations of CO2-induced acidification in the northern Adriatic Sea over the last quarter century. Chem. Ecol., 2010. 26: p. 1-17.
46. Touratier F., Goyet C., Decadal evolution of anthropogenic CO2 in the northwestern Mediterranean Sea from the mid-1990s to the mid-2000s. Deep-Sea Research, 2009. 56: p. 1708-1716.

47. Giani M., Djakovac T., Degobbis D., Cozzi S., Solidoro C., Umani S., Recent changes in the marine ecosystems of the northern Adriatic Sea. Estuarine, Coastal and Shelf Science, 2012. 115: p. 1-13.
48. Hilmi N., Allemand D., Cinar M., Cooley S., Hall-Spencer J., Haraldsson G., Hattam C., Jeffree R., Orr J., Rehdanz K., Reynaud S., Safa A., Dupont S., Exposure of Mediterranean Countries to Ocean Acidification. Water 2014. 6: p. 1719-1744.
49. Djakovac T., Supic N., Aubry F. B., Degobbis D., Giani M., Mechanisms of hypoxia frequency changes in the northern Adriatic Sea during the period 1972–2012. journal of Marine Systems, 2015. 141: p. 179-189.
50. Cantoni C., Luchetta A., Celio M., Cozzi S., Raicich F., Carbonate system variability in the Gulf of Trieste (North Adriatic Sea). Estuarine, Coastal and Shelf Science, 2012. 115: p. 51-62.
51. Ingrosso G., Giani M., Comici C., Krajl M., Piacentino S., De Vittor C., Del Negro P., Drivers of the carbonate system seasonal variations in a Mediterranean gulf. Esuarine, Coastal and Shelf Science, 2016. 168: p. 58-70.
52. Takahashi T., Olaffson J., Goddard J., Chipman D.W., Sutherland S.C. (1993). "Seasonal variation of CO2 and nutrients in the high-latitude surface oceans: a comparative study." Global Biogeochem. Cy. 7: 843-878.
53. Riebesell U., Schultz K.G., Bellerby R. G. J., Botros M., Fritsche P., Meyerhofer M., Neill C., Nondal G., Oschlies A., WohlersJ., Zollner E., Enhanced biological carbon consumption in a high CO2 ocean. Nature, 2007. 450: p. 545-549.
54. Kapsenberg L., Alliouanne S., Gazeau F., Mousseau L., Gattuso J. P., Coastal ocean acidification and increasing total alkalinity in the northwestern Mediterranean Sea Ocean Sci, 2017. 13: p. 411-416.
55. Hernandez-Ayon J.M., Zirino A., Dickson A., Camiro-Vargas T., Valenzuela-Espinoza E., Estimating the contribution of organic bases from microalgae to the titration alkalinity in coastal seawaters. Limnol. Oceanogr.: Methods, 2007. 4: p. 225-232.
56. Takahashi T., Sutherland S. C., Sweeney C., Poisson A., Metzl N., Tillbrook B., Bates N., Wanninkhof R., Feely R.A., Sabine C., Olafsson

J., Nojiri Y. (2002). "Global sea–air CO2 flux based on climatological surface ocean pCO2, and seasonal biological and temperature effects." Deep-Sea Research 49: 1601-1622.

57. Louis J., Guieu C., Gazeau F., Nutrient Dynamics under different icean aciidification scenarios in a low nutrient low chlorophyll system: The Nortwestern Mediterranean Sea. Estuarine, Coastal and Shelf Science, 2016: p. 1-15.
58. Dickson A.G., Sabine C.L., Christian J.R. Guide to best practices for ocean CO2 measurements. 2007, North Pacific Marine Science Organization: Sidney, British Columbia.
59. Scoullos M., Chemical Oceanography, An Introduction in the Chemistry of the Marine Environment. 4th ed. 2008, Athens: Symmetria.
60. De Carlo E., Mousseau L., Passafiume O., Drupp P., Gattuso J., Carbonate Chemistry and Air–Sea CO2 Flux in a NW Mediterranean Bay Over a Four-Year Period: 2007–2011. Aquat Geochem, 2013. 19: p. 399-442.
61. Catalano, G., Azzaro M., Bastianini M., Bellucci L. G., Bernardi Aubry F., Bianchi F., Burca M., Cantoni C., Caruso G., Casotti R., Cozzi S., Del Negro P., Fonda Umani S., Giani M., Giuliani S., Kovacevic V., La Ferla R., Langone L., Luchetta A., Monticelli L. S., Piacentino S., Pugnetti A. , Ravaioli M., Socal G., Spagnoli F., Ursella L. , The carbon budget in the northern Adriatic Sea, a winter case study. j. Geophys. Res.: Biogeosciences, 2014. 119: p. 1399-1417.
62. González-Dávila, M., Santana-Casiano M., Petihakis G., Ntoumas M., Suarez de Tangil M., Krasakopoulou E. (2016). "Seasonal pH variability in the Saronikos Gulf: A year-study using a new photometric pH sensor." Journal of Marine Systems 162: 37-46.
63. Petihakis G., Perivoliotis L., Korres G., Ballas D., Frangoulis C., Pagonis P., Ntoumas M., Pettas M., Chalkiopoulos A., Sotiropoulou M., Bekiari M., Kalampokis A., Ravdas M., Bourma E., Christodoulaki S., Zacharioudaki A., Kassis D., Potiris E., Triantafyllou G., Tsiaras K., Krasakopoulou E.. Velanas S., Zisis N. (2018). "An integrated open-coastal biogeochemistry, ecosystem and biodiversity observatory of the

Eastern Mediterranean. The Cretan Sea component of POSEIDON system." Ocean Sci. Discuss. 2018: 1-40.

64. Bennett W., Teasdale P., Panther J., Welsh D., Zhao H., Jolley D., Investigating Arsenic speciation and mobilization in sediments with DGT and DET: a mesocosm evaluation of oxic-anoxic transitions. Environmental Science and Technology (Washington) 2012. 46(7): p. 3981-3989
65. Dimitriou E., Mentzafou A., Zogaris S., Koutsikos N., Colombari E., Markogianni V., Konstantinopoulou A., Stathopoulou E., Dasenakis M., Katsiapi S., Moustaka M., Monitoring of the Ecological Quality of Koumoundourou Lake and designing of management, restoration and developmental actions. 2011, IIW - HCMR.
66. Waters F., J. (2012). Measurement of Seawater pH: A Theoretical and Analytical Investigation. Marine and Atmospheric Chemistry. Coral Gables, Florida, University of Miami. PhD.
67. Dickson A.G., pH scales and proton-transfer reactions in saline media such as sea water. Geochimica et Cosmochimica Acta, 1984. 48: p. 2299-2308.
68. Rerolle V. M.C. , Floquet C.F.A., Mowlem M. C. ,Bellerby R. , Connelly D. P., Achterberg E. P. , Seawater-pH measurements for ocean-acidification observations. Trends in Analytical Chemistry, 2012. 40: p. 146-157.
69. Hansson I. A new set of ppH-scales and standard buffers for sea water. Deep-Sea Research, 1973. 20(479-491).
70. Karageorgis A.P., Katsanevakis S., Kaberi H. (2009). "Use of enrichment factors for the assessment of heavy metal contamination in the sediments of Koumoundourou Lake, Greece." Water Air Soil Pollution 204: 243-258.
71. Riebesell U., Fabry V.J., Hansson L., and Gattuso J-P., Guide to Best Practices for Ocean Acidification Research and Data Reporting 2010: Luxemburg Publication Office of the European Union.
72. Kim H., Review of Inorganic Nitrogen Transformations and Effect of Global Climate Change on Inorganic Nitrogen Cycling in Ocean Ecosystems Ocean Sci J., 2016. 51(2): p. 159-167.

73. Falkowski P., Evolution of the nitrogen cycle and its influence on the biological sequestration of CO2 in the ocean. Nature, 1997. 387: p. 272-275.
74. Ward B.B., (2011). Measurement and Distribution of Nitrification Rates in the Oceans. Methods in Enzymology. K. M.G., Burlington: Academic Press. **486:** 307-323.
75. Huesemann M., Skillman A., Crecelius E., The inhibition of marine nitrification by ocean disposal of carbon dioxide. Marine Pollution Bulletin, 2002. 44: p. 142-148.
76. Widdicombe S., Needham H., Impact of CO2-induced seawater acidification on the burrowing activity of Nereis virens and sediment nutrient flux. Mar Ecol Prog Ser, 2007. 341: p. 111-122.
77. Widdicombe S., Dashfield S., McNeil C., Needham H., Beesly A., McEvoy A., Oxnevad S., Clarke K., Berge J., Effects of CO2 induced seawater acidification on infaunal diversity and sediment nutrient fluxes. Mar Ecol Prog Ser, 2009. 379(59): p. 59-75.
78. Paytan A., Mc Laughlin K., The Oceanic Phosphorus Cycle. Chem. Rev., 2007. 107(2): p. 563-576.
79. Delanney M.L., Phosphorus accumulation in marine sediments and the oceanic phosphorus cycle Global Biogeochem. Cy., 1998. 12(4): p. 563-572.
80. Benitez-Nelson C., The biogeochemical cycling of phosphorus in marine systems. Earth-Science Reviews, 2000. 51: p. 109-135.
81. Struyf E., Smis A., Van Damme S., Meire P., Conley D., The Global Biogeochemical Silicon Cycle. Silicon, 2009. 1: p. 207-213.
82. Treguer P. J., De la Rocha C.L., The World ocean Silica Cycle. Annu. Rev. Mar. Sci. , 2012. 5(5).
83. Treguer P., Nelson D., Van Bennekom A., DeMaster D., Leynaert A., Queguiner B., The Silica Balance in the World Ocean: A Reestimate Science, 1995. 268(5209): p. 375-379.
84. Milligan A., Varela D., Brzezinski M., Morel F., Dynamics of Silicon metabolism and silicon isotopic discrimination in a marine diatom as a function of pCO2. Limnol. Oceanogr., 2004. 49(2): p. 322-329.

85. Hoffmann L., Breitbarth E., Boyd P., Hunter K. , Influence of ocean warming and acidification on trace metal biogeochemistry. Marine Ecology progress Series, 2012. 470: p. 191-205.
86. Mackenzie F., Stoffyn M., Aluminum in Seawater: Control by Biological Activity. Science, 1978. 199: p. 680-682.
87. Chou L., Wollast R., Biogeochemical behavior and mass balance of dissolved aluminum in the western Mediterranean Sea Deep-Sea Research II, 1997. 44(3-4): p. 741-768.
88. Maher W., Butler E., Arsenic in the marine environment, Review. Applied Organometallic Chemistry, 1988. 2: p. 191-214.
89. Mucci A., Richard L., Lucotte M., Guignard C., The Differential Geochemical Behaviour of Arsenic and Phosphorus in the water column and sediments of the Saguenay Fjord Estuary, Canada. Aquatic Geochemistry 2000. 6: p. 293-324.
90. Yeats P., The Distribution of Trace Metlas in Ocean Waters. The Science of Total Environment, 1988. 72: p. 131-149.
91. Simpson W.R., A Critical Review of Cadmium in the Marine Environment Prog. Oceanog., 1981. 10: p. 1-70.
92. Rai D., Eary L., Zachara J., Environmental Chemistry of Chromium. The Science of Total Environment, 1989. 86: p. 15-23.
93. Moffett J., Ho J., Oxidation of cobalt and manganese in seawater via a common microbially catalyzed pathway. Geochimica et Cosmochimica Acta, 1996. 60(18): p. 3415-3424.
94. Saito M., Moffett J., Temporal and spatial variability of cobalt in the Atlantic Ocean. Geochimica et Cosmochimica Acta, 2002. 66(11): p. 1943-1953.
95. Cox P.A., Elements on Earth. 1995.
96. Scoullos M., Chemical Oceanography Part B, Marine Pollution. 1999, Athens: Interdisciplinary Postgraduate Course of Oceanography.
97. Scoullos M., Constantianos V., Assessment of the state of pollution of the Mediterranean sea by Zinc, Copper and their compounds, in MAP Technical Reports Series No. 105. 1996: Athens.
98. Sclater F., Boyle E., Edmond J., On the Marine Geochemistry of Nickel. Earth and Planetary Science Letters, 1976. 31: p. 119-128.

99. Chester R., Stoner J., The Distribution of Zinc, Bickel, Manganese, Cadmium, Copper and Iron in some surface waters from the world ocean. Marine Chemistry, 1974. 2: p. 17-32.
100. Byrne R., Inorganic speciation of dissolved elements in seawater: the influence of pH on concentration ratios. Geochemical Transactions, 2002. 3(2): p. 11-16.
101. Colina M., Gardiner P.H.E., Rivas Z., Troncone F., Determination of vanadium species in sediment, mussel and fish muscle tissue samples by liquid chromatography–inductively coupled plasma-mass spectrometry. Analytica Chimica Acta, 2005. 538: p. 107-115.
102. Jeandel C., Caisso M., Minster J.F., Vanadium Behaviour in the Global Ocean and in the Mediterranean Sea Marine Chemistry, 1987. 21: p. 51-74.
103. Viollier E., Inglett P., Hunter K., Roychoudhury A., Van Cappellen P., , The ferrozine method revisited: Fe(II)/Fe(III) determination in natural waters. Applied Geochemistry, 2000. 15: p. 785-790.
104. Kuma K., Nishioka J., Matsunaga K., Controls on iron(III) hydroxide solubility in seawater: The influence of pH and natural organic chelators Limnol. Oceanogr., 1996. 41(3): p. 396-407.
105. Breitbarth E., Bellerby R., Neill C., Ardelan M., Meyerhofer M., Zollner E., Croot P., Riebesell U., Ocean acidification affects iron speciation during a coastal seawater mesocosm experiment. Biogeosciences, 2010. 7: p. 1065-1073.
106. Tebo B., Clement B., Dick G. , Biotransformations of Manganese, in Manual of Environmental Microbiology, C.R. Hurst C., Garland J., Lipson D., Mills A., Stetzenbach L., Editor. 2007, ASM Press: Washington, DC. p. 1223-1238.
107. Glasby G., Manganese: Predominant Role of Nodule and Crusts, in Marine Geochemistry, Z.M. Schultz H., Editor. 2006. p. 371-427.
108. Ardelan M., Steinnes E., Changes in mobility and solubility of the redox sensitive metals Fe, Mn and Co at the seawater-sediment interface following CO2 seepage. Biogeosciences, 2010. 7: p. 569-583.
109. Sakellari A., Biogeochemical Investigation of Metals: Study of trace element cycles in seawater and sediment and impact investigation on

the food chain, in School of Science, Department of Chemistry. 2006, National and Kapodistrian University of Athens: Athens.

110. Burdige D.J., The biogeochemistry of manganese and iron reduction in marine sediments. Earth-Science Reviews, 1993. 35: p. 249-284.
111. Angelidis M., Exchange of Pollutants (TraceElements) at the Sediment Boundary. Hdb Env Chem 2005. 5: p. 319-341.
112. Millero F., Woosley R., Di TRolio B., Waters J., Effect of Ocean Acidification on the Speciation of Metals in Seawater. Oceanography, 2009. 22(4): p. 72-85.
113. Pascal P., Fleeger J., Galvez F., Carman K., The toxicological interaction between ocean acidity and metals in coastal meiobenthic copepods. Marine Pollution Bulletin, 2010. 60: p. 2201-2208.
114. Richards R., Chaloupka M., Sanò M., Tomlinson R., Modelling the effects of 'coastal' acidification on copper speciation. Ecological Modelling, 2011. 222: p. 3559-3567.
115. De Orte M. R., Sarmiento A.M., Bassalote M. D., Rodríguez-Romero A., Riba I., Del Valls A., Effects on the mobility of metals from acidification caused by possible CO2 leakage from sub-seabed geological formations. Science of the Total Environment, 2014. 470-471: p. 356-363.
116. Rodriguez-Romero A., Bassalote M., De Orte M., DelValls A., Riba I., Blasco J., Simulation of CO2 leakages during injection and storage in sub-seabed geological formations: Metal mobilization and biota effects. Environment International, 2014. 68: p. 105-117.
117. Wang Z., Wang Y., Zhao P., Chen L., Yan C., Yan Y., Chi Q., Metal release from contaminated coastal sediments under changing pH conditions: Implications for metal mobilization in acidified oceans. Marine Pollution Bulletin, 2015.
118. Widdicombe S., Dupont S., Thorndyke M., Laboratory experiments and benthic mesocosm studies, in Guide to best practices for ocean acidification research and data reporting, U. Riebesell, Fabry, V. J., Hansson, L., and Gattuso, J-P., Editor. 2010, Publications Office of the European Union: Luxembourg. p. 113-122.

119. Pavlidou A. , Kontoyiannis H., Anagnostou Ch.,Siokou–Frangou I. , Pagou K. , Krasakopoulou E. , Assimakopoulou G. , Zervoudaki S. , Zeri Ch., Chatzianestis J. ,Psyllidou-Giouranovits R. , Biogeochemical Characteristics in the Elefsis Bay (Aegean Sea, Eastern Mediterranean) in Relation to Anoxia and Climate Changes, in Chemical Structure of Pelagic Redox Interfaces: Observation and Modeling, Y. E.V., Editor. 2013, Springer-Verlag Berlin Heidelberg. p. 161-202.
120. Scoullos M., Rilley J., Water circulation in the Gulf of Elefsis, Greece. Thalassia Jugoslavica, 1978. 14(3/4): p. 357-370.
121. Dimitriou, E., Karaouzas, I., Sarantakos, K., Zacharias, I., Bogdanos, K., Diapoulis, A., Groundwater risk assessment at a heavily industrialised catchment and the associated impacts on a peri-urban wetland. Journal of Environmental Management, 2008. 88: p. 526-538.
122. Pantazidou M., Kapniaris S., Katsiri A., Christidis A., Pollutant trends and hazard ranking in Elefsis Bay, Greece. Desalination, 2007. 210: p. 69-82.
123. Scoullos M., Trace Metals in a landlocked intermittently anoxic basin, in Trace Metals in sea water, B.E. Wong C., Bruland K., Burton J., Goldberg E., Editor. 1983, NATO scientific Affairs Division. p. 351-366.
124. Scoullos M., Dassenakis M., Paraskevopoulou V., Botsou F., Sakellari Aik., Karavoltsos S., Mantzara V., Zeri C., Krasakopoulou E., Zervoudaki T., Trace metals in seawater and sediments of the Gulf of Elefsis: 1977 – 2015, in “Environmental Perspectives of the Gulf of Elefsis A Mediterranean case study where Science meets the Society”. 2015, Mediterranean Information Office for Environment, Culture and Sustainable Development (MIO-ECSDE): Elefsis, Greece. p. 16-19.
125. Priority issues in the Mediterranean environment EEA Report No4/2006. 2006, European Environment Agency: Copenhagen.
126. Scoullos M., Chemical Studies of the Gulf of Elefsis, Greece, in Dept. of Oceanography. 1979, University of Liverpool.
127. Friligos N., Preliminary Observations on Nutrient Cycling and a Stoichiometric Model for Elefsis Bay, Greece Marine Environmental Research, 1983. 8: p. 197-213.

128. Mavrakis A., Theoharatos G., Asimakopoulos D., Christides A., Distribution of trace metals in the sediments of Elefsis Gulf. Mediterranean Marine Science, 2004. 5(1): p. 151-158.
129. Scoullos M., *Lead in Coastal Sediments: The case of Elefsis Gulf, Greece.* The Science of Total Environment, 1986. **49**: p. 199-219.
130. Friligos N., Barbetseas S., Water masses and eutrophication in a Greek anoxic marine bay Toxicological & Environmental Chemistry, 1990. 28: p. 11-23.
131. Friligos N., Some Consequences of the Decomposition of Organic Matter in the Elefsis Bay, an Anoxic Basin Marine Pollution Bulletin, 1982. 13(3): p. 103-106.
132. Bartlett R., Mortimer R.J.G., Morris K. , Anoxic nitrification: Evidence from Humber Estuary sediments (UK). Chemical Geology, 2008. 250: p. 29-39.
133. Hulth S., Aller R., Gilbert F., Coupled anoxic nitrification/manganese reduction in marine sediments. Geochimica et Cosmochimica Acta, 1999. 63(1): p. 49-66.
134. Scoullos, M., 1983. Nitrogen micronutrients in an intermittently anoxic basin. Vies J. Etud. Poll., pp. 139-143, Cannes, France.
135. Voutsinou-Taliadouri F., Metal Pollution in the Saronikos Gulf Marine Pollution Bulletin, 1981. 12(5): p. 163-168.
136. Pavlidou A., Simboura N., Rousselaki E., Tsapakis M.,Pagou K.,Drakopoulou P.,Assimakopoulou G., Kontoyiannis H.,Panayotidis P., Methods of eutrophication assessment in the context of the water framework directive: Examples from the Eastern Mediterranean coastal areas. Continental Shelf Research, 2015. 108: p. 156-168.
137. Pavlidou, A., Pagou, K., Assimakopoulou, G., Rousselaki, E., Evolution over the last 30 years of the trophic conditions in the Gulf of Elefsis, in “Environmental Perspectives of the Gulf of Elefsis A Mediterranean case study where Science meets the Society”. 2015, Mediterranean Information Office for Environment, Culture and Sustainable Development (MIO-ECSDE): Elefsis, Greece. p. 20-22.
138. Scoullos M., Sakellari A., Giannopoulou K., Paraskevopoulou V., Dassenakis M., Dissolved and particulate trace metal levels in the

Saronikos Gulf, Greece, in 2004. The impact of the primary Wastewater Treatment Plant of Psittalia. Desalination, 2007. 210: p. 98-109.

139. Rousselaki E., Pavlidou A., Michalopoulos P., Kaberi H.,. Nutrient fluxes in a hypoxic marine environment of East Mediterranean. in Goldschmidt Conference. 2014. Sacramento, California
140. Rousselaki E., Pavlidou A., Michalopoulos P., Dassenakis M., Scoullos M. . Nutrient benthic fluxes and porewater concentrations in the Gulf of Elefsis. . in Proceedings of the International Conference: Environmental Perspectives of the Gulf of Elefsis, A Mediterranean case study where Science meets the Society. 2015. Elefsis, Greece: Sustainable Mediterranean.
141. Rousselaki E., Pavlidou A., Michalopoulos P., Prifti E., Kaberi H. Benthic fluxes of ex situ incubations and porewater nutrient concentrations near the wastewater treatment plant of Athens, Saronikos Gulf, Greece. in Goldschmidt. 2015. California.
142. Prifti E., Kaberi H., Zeri C., Rousselaki H., Michalopoulos P., Dassenakis M., Calculation of benthic fluxes of metals using the pore water metal concentrations and the results from incubation experiments., in 11th Panhellenic Symposium on Oceanography & Fisheries «Aquatic Horizons: Challenges & Perspectives». 2015, Department of Marine Sciences, University of the Aegean: Mytilene, Lesvos Island, Greece.
143. Griggs G., Grimanis A., Grimani M., Bottom Sediments in a Polluted Marine Environment, Upper Saronikos Gulf, Greece. Environmental Geology, 1978. 2(2): p. 97-106.
144. Barry J., Tyrell T., Hansson L., Plattner G., Gattuso J., Atmospheric CO2 targets for ocean acidifi cation perturbation experiments, in Guide to best practices for ocean acidification research and data reporting, U. Riebesell, Fabry, V. J., Hansson, L., and Gattuso, J-P., Editor. 2010, Publications Office of the European Union: Luxembourg. p. 53-66.
145. Havenhand J., Dupont S., Quinn G., Designing ocean acidification experiments to maximise inference, in Guide to best practices for ocean acidification research and data reporting, U. Riebesell, Fabry, V. J., Hansson, L., and Gattuso, J-P., Editor. 2010, Publications Office of the European Union: Luxembourg. p. 67-80.

146. Paraskevopoulou Vasiliki, Transport and chemical Distribution of Heavy Metals in a Sea Area Affected by Industrial Pollution (NW Saronic Gulf), in School of Science. 2009, National and Kapodistrian University of Athens: Athens.
147. Parinos K., Study of the Chemical behavior and transport of heavy metals and nutrients in estuarine systems affected by human pollutant activities in Department of Chemistry. 2010, National and Kapodistrian University of AThens: Athens. p. 325.
148. Pavlidou A., Investigation of Metal species in microenvironments of Elefsis Gulf using Anodic Stripping Voltametry (AVS), in Department of Chemistry. 1998, National and Kapodistrian University of Athens: Athens. p. 272.
149. Method 1640: Determination Of Trace Elements In Water By Preconcentration And Inductively Coupled Plasma-Mass Spectrometry, O.o.S.a.T. Office of Water, Editor. 1997, U.S. Environmental Protection Agency Washington DC, USA.
150. Method 3050B: Acid Digestion of Sediments, Sludges, and Soils, O.o.S.a.T. Office of Water, Editor. 1996, U.S. Environmental Protection Agency: Washington DC, USA.
151. Bloom N., SG-033 Iron Speciation in Aqueous Samples by Ferrozine Complexation Colorimetric Detection at 562 nm. 2004. p. C 298-302.
152. Stookey L., Ferrozine-A New Spectrophotometric Reagent for Iron. Analytical Chemistry, 1970. 42(7): p. 779-781.
153. Method/Description Fe-extraction from the sediment and Fe(II)/Fe(III)-determination. Available from: http://www.geomar.de/en/research/fb2/fb2-mg/benthic-biogeochemistry/mg-analytik/method-description-fe-extraction-from-the-sediment-and-feiifeiii-determination/.
154. Carpenter J., The Accuracy of the Winkler Method for Dissolved Oxygen Analysis. Limnology and Oceanography, 1965.
155. Pérez F., Fraga F., 1987a. A precise and rapid analytical procedure for alkalinity determination. Marine Chemistry, 21, 169-182.

156. Pérez F., Rios A., Rellan T., Alvarez M., Improvements in a fast Potentiometric Seawater Alkalinity Determination. Ciencias Marinas 2000. 26(003): p. 463-478.
157. Methods of Seawater Analysis, Third Edition, ed. K.K. Grasshof K., Ehrhardt M. 1999.
158. Solorzano L., Determination of Ammonia in Natural Waters by the Phenolhypochlorite method Limnology and Oceanography, 1969. 14(5): p. 799-801.
159. Valderrama J., The Simultaneous Analysis of Total Nitrogen and Total Phosphorus in Natural Waters. Marine Chemistry, 1981. 10: p. 109-122.
160. Gattuso J.P., Epitalon J.M., Lavigne H., Orr J., Gentili B., Hoffmann A., Proye A., Soetaert K., Rae J., Seawater Carbonate Chemistry with R Package 'seacarb'. 2014.
161. Lueker T., Dickson A., Keeling C., Ocean pCO calculated from dissolved inorganic carbon, alkalinity, and equations for K and K : validation based on laboratory measurements of CO in gas and seawater at equilibrium. Marine Chemistry, 2000. 70: p. 105-119.
162. Perez F., Fraga F., Association Constant Of Fluoride And Hydrogen Ions In Seawater. Marine Chemistry, 1987. 21: p. 161-168.
163. Dickson A.G., Standard potential of the reaction: AgCl(s) +1/2H,(g) = Ag(s) + HCl(aq), and and the standard acidity constant of the ion HSO4- in synthetic sea water from 273.15 to 318.15 K. J. Chem. Thermodynamics, 1990. 22: p. 113-127.
164. Lee K., Kim T.-W., Byrne R., Millero F., Feely R., Liu Y.-M., The universal ratio of boron to chlorinity for the North Pacific and North Atlantic oceans. Geochimica et Cosmochimica Acta, 2010. 74: p. 1801-1811.
165. Trends in Atmospheric Carbon Dioxide. Available from: https://www.esrl.noaa.gov/gmd/ccgg/trends/.
166. Laverock B., Kitidis V., Tait K., Gilbert J., Osborn A., Widdicombe S., Bioturbation determines the response of benthic ammonia-oxidizing microorganisms to ocean acidification. Phil. Trans. R. Soc., 2014. 368(B): p. 1-13.

167. Kitidis V., Laverock B., McNeill L., Beesley A., Cummings D., Tait K., Osborn M., Widdicombe S., Impact of ocean acidification on benthic and water column ammonia oxidation. Geophysical research Letters, 2011. 38: p. 1-5.
168. Wood H., Spicer J., Widdicombe S., Ocean Acidification may increase calcification rates, but at a cost. Pr. R. Soc. B, 2008. 275: p. 1767-1773.
169. Wallstedt T., Borg H., Effects of experimental acidification on mobilisation of metals from sediments of limed and non-limed lakes. Environmental Pollution, 2003. 126: p. 381-391.
170. Krumins V., Gehlen M., Arndt S., Van Cappellen P., Regnier P., Dissolved inorganic carbon and alkalinity fluxes from coastal marine sediments: model estimates for different shelf environments and sensitivity to global change. Biogeosciences, 2013. 10: p. 371-398.
171. Apostolaki E., Holmer M., Marba N., Karakassis I., Degrading seagrass (Posidonia oceanica) ecosystems: a source of dissolved matter in the Mediterranean. Hydrobiologia, 2010. 649: p. 13-23.
172. Thomas H., Schiettecatte L., Suykens K., Kone Y., Shadwick E., Prowe A., Bozec Y., de Baar H., A. Borges, Enhanced ocean carbon storage from anaerobic alkalinity generation in coastal sediments. Biogeosciences, 2009. 6: p. 267-274.
173. Barker Jorgensen B, Kasten S., Sulfur cycling and methane oxidation, in Marine Geochemistry, 2nd revised updated and extended edition, Z.M. Schulz H., Editor. 2006, Springer.
174. Hu, X., Cai, W. J, An assessment of ocean margin anaerobic processes on oceanic alkalinity budget. Global Biogeochem. Cy., 2011. GB 3003.
175. Dickson A., An exact definition of total alkalinity and a procedure for the estimation of alkalinity and total inorganic carbon from titration data. Deep-Sea Research, 1981. 28A(6): p. 609-623.
176. Ge C., Chai Y., Wang H., Kan M., Ocean acidification: One potential driver of phosphorus eutrophication. Marine Pollution Bulletin, 2016. 115(1-2): p. 149-153.
177. Tanaka T., Thingstad T., Løvdal T., Grossart H., Larsen A., Allgaier M., Meyerhofer M., Schulz K., Wohlers J., Zollner E., Riebesell U., Availability of phosphate for phytoplankton and bacteria and of glucose

for bacteria at different pCO2 levels in a mesocosm study. Biogeosciences, 2008. 5: p. 669-678.

178. Hee C., Pease T., Alperin M., Martens C., Dissolved organic carbon production and consumption in anoxic marine sediments: A pulsed-tracer experiment. Limnol. Oceanogr., 2001. 46(8): p. 1908-1920.
179. Zark M., Riebesell U., Dittmar T., Effects of ocean acidification on marine dissolved organic matter are not detectable over the succession of phytoplankton blooms. Ocean Chemistry, 2015. 1(9).
180. Aparicio F., Nieto-Cid M., Borryl E., Calvo E., Pelejero C., Sala M., Pinhassi J., Gasol J., Marrase C. , Eutrophication and acidification: Do they induce changes in the dissolved organic matter dynamics in the coastal Mediterranean Sea? Science of the Total Environment, 2016. 563-564: p. 179-189.
181. Celussi M., Malfatti F., Annalisa F., Gazeau F., Giannakourou A., Pitta P., Tsiola A., Del Negro P., Ocean acidification effect on prokaryotic metabolism tested in two diverse trophic regimes in the Mediterranean Sea. Estuarine, Coastal and Shelf Science, 2017. 186(A): p. 125-138.
182. Chin Y.-P., Traina S., Swank C., Abundance and properties of dissolved organic matter in pore waters of a freshwater wetland Limnol. Oceanogr., 1998. 43(6): p. 1287-1296.
183. Kulinski, K., Schneider, B., Hammer, K., Machulik, U., Schulz-Bull, D., The influence of dissolved organic matter on the acid–base system of the Baltic Sea. Journal of Marine Systems, 2014. 132: p. 106-115.
184. Bassalote M., Rodriguez-Romero A., De Orte M., Del Valls A., Riba I., Evaluation of the threat of marine CO2 leakage-associated acidification on the toxicity of sediment metals to juvenile bivalves. Aquatic Toxicology, 2015. 166: p. 63-71.
185. Stockdale A., Tipping E., Lofts S., Mortimer R., Effect of Ocean Acidification on Organic and Inorganic Speciation of Trace Metals. Environmental Science Technology, 2016. 50: p. 1906-1913.
186. Sullivan T., Byrne C., Harman L., Davenport J., McAllen R., Regan F., Determination of spatial and temporal variability of pH and dissolved oxygen concentrations in a seasonally hypoxic semi-enclosed marine basin using continuous monitoring. Analytical Methods, 2014. 6(15).

187. Ying S., Kocar B., Fendorf S., Oxidation and competitive retention of arsenic between iron- and manganese oxides. Geochimica et Cosmochimica Acta, 2012. 96: p. 294-303.
188. Scoullos M., Plavsic M., Karavoltsos S., Speciation studies of copper in the Gulf of Elefsis: the role of the macroalgae Ulva rigida. Marine Chemistry, 2004. 86: p. 51-63.
189. Dortch Q., The interaction between ammonium and nitrate uptake in phytoplankton. Marine Ecology progress Series, 1990. 61: p. 183-201.
190. Ignatiades L., Gotsis-Skretas O., A Review on Toxic and Harmful Algae in Greek Coastal Waters (E. Mediterranean Sea). Toxins, 2010. 2(5): p. 1019-1037.
191. Moncheva S., Gotsis-Skretas O., Pagou K. Krastev A., Phytoplankton Blooms in Black Sea and Mediterranean Coastal Ecosystems Subjected to Anthropogenic Eutrophication: Similarities and Differences. Estuarine, Coastal and Shelf Science, 2001. 53: p. 281-295.
192. Houghton R. A., H. The Contemporary Carbon Cycle. Major Reservoirs and Natural Fluxes of Carbon. Woods Hole Research Center, USA.
193. Ochsenkuhn-Petropulu M., O.K., Milonas I., Parissakis G., Separation and Speciation of Inorganic- and Methylarsenic Compounds in Marine Samples, in 40th Canadian Spectroscopy Conference. 1995: Halifax, Canada.
194. Scoullos M., Botsou F., Zeri C., Linking Environmental Magnetism to Geochemical Studies and Management of Trace Metals. Examples from Fluvial, Estuarine and Marine Systems Minerals, 2014. 4: p. 716-745.
195. Chen-Tung A. C., Shelf-vs. dissolution-generated alkalinity above the chemical lysocline. Deep-Sea Research II, 2002. 49: p. 5365-5375.
196. Chen-Tung A. C., Kon-Kee L., Macdonald R. (2003). Chapter 3: Continental Margin Exchanges. Ocean Biogeochemistry: The Role of the Ocean Carbon Cycle in Global Change. M. J. R. Fasham. Berlin, Heidelberg, Springer Berlin Heidelberg: 53-97.
197. Louis J., Guieu C., Gazeau F., Nutrient Dynamics under different icean aciidification scenarios in a low nutrient low chlorophyll system: The Nortwestern Mediterranean Sea. Estuarine, Coastal and Shelf Science, 2016: p. 1-15.

PUBLICATIONS - CONFERENCES

Mediterranean Marine Science

Vol. 19, 2018

Simulation of Coastal Processes affecting pH with Impacts on Carbon and Nutrient Biogeochemistry

KAPETANAKI NATALIA — Laboratory of Environmental Chemistry, Department of Chemistry, National and Kapodistrian University of Athens

KRASAKOPOULOU EVANGELIA — Department of Marine Sciences, University of the Aegean

STATHOPOULOU ELENI — Laboratory of Environmental Chemistry, Department of Chemistry, University of Athens

PAVLIDOU ALEXANDRA — Institute of Oceanography, Hellenic Centre for Marine Research

ZERVOUDAKI SOULTANA — Institute of Oceanography, Hellenic Centre for Marine Research

DASSENAKIS MANOS — Laboratory of Environmental Chemistry, Department of Chemistry, University of Athens

SCOULLOS MICHAEL — Laboratory of Environmental Chemistry, Department of Chemistry, University of Athens

http://dx.doi.org/10.12681/mms.14439

Mediterranean Marine Science
Indexed in WoS (Web of Science, ISI Thomson) and SCOPUS
The journal is available online at http://www.medit-mar-sc.net
DOI: http://dx.doi.org/10.12681/mms.14439

Research Article

Simulation of Coastal Processes affecting pH with Impacts on Carbon and Nutrient Biogeochemistry

NATALIA KAPETANAKI[1], EVANGELIA KRASAKOPOULOU[2], ELENI STATHOPOULOU[1], ALEXANDRA PAVLIDOU[3], SOULTANA ZERVOUDAKI[3], MANOS DASSENAKIS[1] and MICHAEL SCOULLOS[1]

[1] Laboratory of Environmental Chemistry, Department of Chemistry, University of Athens,
[2] Department of Marine Sciences, University of the Aegean,
[3] Institute of Oceanography, Hellenic Centre for Marine Research,

Corresponding author: nataliak@hcmr.gr
Handling Editor: Ioanna Siokou

Received: 15 September 2017; Accepted: 13 February 2018; Published on line: 28 June 2018

Abstract

Naturally occurring microbial decomposition of organic matter (OM) in coastal marine environments cause increased acidity in deeper layers similar or even exceeding the future predictions for global ocean acidification (OA). Experimental studies in coastal areas characterized by increased inputs of OM and nutrients, coping with intermittent hypoxic/anoxic conditions, provide better understanding of the mechanisms affecting nutrients and carbon biogeochemistry under the emerging effects of coastal pH decrease. Laboratory CO_2-manipulated microcosm experiments were conducted using seawater and surface sediment collected from the deepest part of Elefsis Bay (Saronikos Gulf, Eastern Mediterranean) focusing to study the co-evolution of processes affected by the decline of dissolved oxygen and pH induced by (a) OM remineralization and (b) the future anthropogenic increase of atmospheric CO_2. Under more acidified conditions, a significant increase of total alkalinity was observed partially attributed to the sedimentary carbonate dissolution and the reactive nitrogen species shift towards ammonium. Nitrate and nitrite decline, in parallel with ammonium increase, demonstrated a deceleration of ammonium oxidation processes along with decrease in nitrate production. The decreased DIN:DIP ratio, the prevalence of organic nutrient species against the inorganic ones, the observations of constrained DON degradation and nitrate production decline and the higher DOC concentrations revealed the possible inhibition of OM decomposition under lower pH values. Finally, our results highlight the need for detailed studies of the carbonate system in coastal areas dominated by hypoxic/anoxic conditions, accompanied by other biogeochemical parameters and properly designed experiments to elucidate the processes sequence or alterations due to pH reduction.

Keywords: carbonate chemistry; carbon; nitrogen; phosphorus; microcosm experiment; Ocean acidification; coastal ocean; sediment.

Introduction

World Oceans currently absorb about one fourth of the anthropogenic carbon dioxide (CO_2) emissions into the atmosphere (Le Quéré *et al*., 2015). The uptake of anthropogenic CO_2 from the oceans leads to pH decline and reduction of the carbonate ion concentration, a process usually referred as ocean acidification (e.g. Caldeira & Wickett, 2005). Since the beginning of the Industrial Revolution the average pH of ocean surface waters has fallen by about 0.1 units and is expected to decrease by 0.2 to 0.4 units by the end of the century (Ciais *et al*., 2013).

In the Mediterranean Sea, recent studies report that anthropogenic carbon has penetrated throughout the water column, with higher concentrations than the global average (Schneider *et al*., 2010; Hassoun *et al*., 2015). A net flux of anthropogenic carbon from the Atlantic towards the Mediterranean basin has been identified being responsible for 25% of the basin-wide CO_2 uptake over the last 200 years (Flecha *et al*., 2015 and references therein). From the pre-industrial period until 2013 the pH in Mediterranean Sea has decreased by 0.055 - 0.156 pH units (Hassoun *et al*., 2015) with an annual decreasing trend of 0.0044 ± 0.00006 (Flecha *et al*., 2015). Model simulations predict a further decrease in the pH of Mediterranean surface waters of 0.3-0.4 units by the year 2100 (Howes *et al*., 2015). In shallow nearshore Mediterranean areas, although seawater pH is influenced by various natural and anthropogenic processes other than CO_2 uptake (Borges & Gypens, 2010; Duarte *et al*., 2013; Hagens *et al*., 2015), long term data-based estimations at coastal

monitoring sites also indicate a shift towards more acidic conditions (e.g. Luchetta *et al*., 2010; Howes *et al*., 2015; Kapsenberg *et al*., 2017).

The changes associated with the uptake of the excess CO_2 by the ocean cause an additional abiotic stressor for marine ecosystems (Andersson *et al*., 2007). The oceans' response to acidification will not be uniform; different regions and different depths already exhibit different trends, and the activities of organisms may accelerate or modulate these trends (Beman *et al*., 2011). In an acidifying ocean, microbial community responses to reduced seawater pH and elevated seawater partial pressure of CO_2 (pCO_2) may act as positive or negative feedbacks to carbon and nitrogen critical biogeochemical processes. In coastal areas, even in the presence of oxygen, the flow of the organic load is high and the aerobic degradation of organic matter leads to a higher CO_2 production, causing dissolution of existing sedimentary carbonates (Andersson *et al*., 2007 and references therein). Furthermore, ocean acidification can interact with other natural and anthropogenic environmental processes in coastal areas, to accelerate local declines in pH and carbonate mineral saturation states (Feely *et al*., 2010).

While acidification in the open ocean is mainly driven by the atmospheric CO_2, in coastal zones this process may be minor and the signal of CO_2-induced acidification may not be actually distinct, particularly at eutrophic marine areas where excessive nutrient loading and organic matter production have been associated with hypoxic events (Wallace *et al*., 2014, Hagens *et al*., 2015; Ingrosso *et al*., 2016a).

In subsurface waters the same respiratory processes that lower dissolved oxygen concentrations, add CO_2 to solution, reduce pH, and, over longer time scales, can exacerbate the ocean acidification process (Cai *et al*., 2011). There are some good examples available worldwide indicating the inverse relationship between pH and dissolved oxygen in stratified hypoxic coastal regions (Hagens *et al*., 2015 and references therein). Elefsis Bay is a small (68 km^2) and shallow (with a mean and maximum depth of 20 m and 35 m, respectively), almost enclosed embayment with limited water exchange through narrow and shallow connections with the adjacent Saronikos Gulf (Aegean Sea, Eastern Mediterranean Sea; Fig. 1). During the period from May to late October, the development and establishment of a strong temperature-driven pycnocline results in the isolation of the deeper part of the water column, leading to insufficient oxygen supply. In parallel the organic matter degradation reduces oxygen levels promoting the development of hypoxic/anoxic conditions and the accumulation of high amounts of silicate, phosphate and ammonium at the near-bottom layers (Scoullos & Rilley, 1978; Pavlidou *et al*., 2013). Studies conducted in Elefsis Bay in late '70s during the stratification period, have reported surface pH values of 8.4 - 8.5 while for the bottom water the respective values were much lower 7.9-7.8 (Scoullos, 1979; Friligos, 1982) unequivocally linked to the CO_2 release during the microbial remineralization of organic matter in the subthermocline layer. It is thus evident that during summer stratified conditions the close to the bottom waters of Elefsis Bay would be an ideal system to study the co-evolution of various biogeochemical

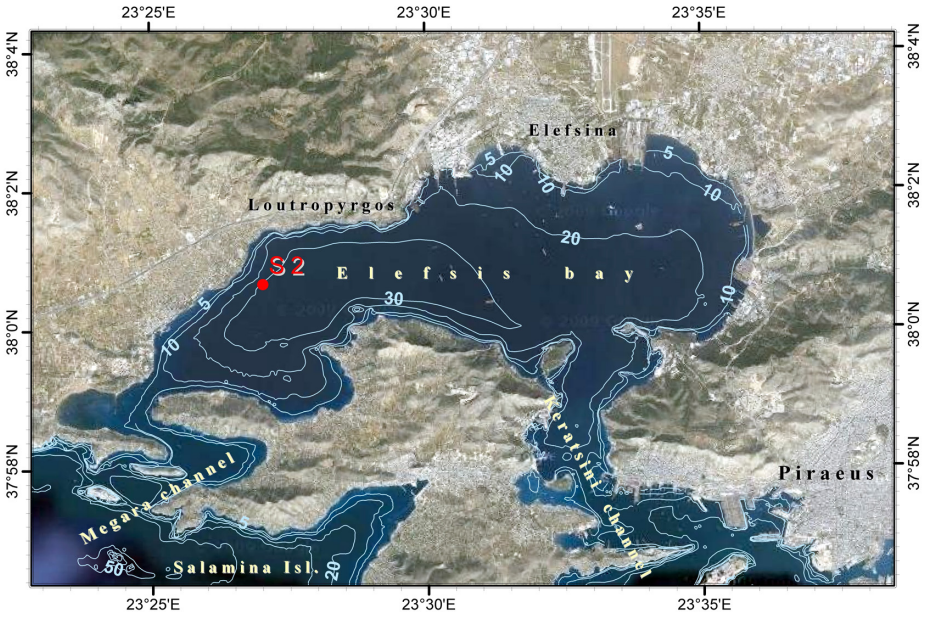

Fig. 1: Bathymetric map of Elefsis Bay (Saronikos Gulf, Eastern Mediterranean Sea). The location of the sampling site is also shown.

processes affected by the decline of both pH and dissolved oxygen.

The aim of this research is to investigate, in parallel, the response of carbon and nutrient biogeochemistry to the effect of pH decrease induced by (a) the organic matter remineralization and (b) the future anthropogenic increase of atmospheric CO_2. For this purpose, seawater and sediment from the deepest part of Elefsis Bay, an intermittently anoxic coastal system, were tested in a 20-days microcosm-scale lab experiment performed under controlled pH and temperature conditions. This experimental attempt intends to enhance our understanding of how pH changes could impact the basic but complex biogeochemical processes which are taking place in coastal areas coping with hypoxic/anoxic conditions.

Materials and Methods

Experimental Setup and Analyses

Field sampling was performed at the deepest western part of Elefsis Bay (Longitude: 23° 25' 48''E; Latitude: 38° 03' N; Depth: 33m; Fig. 1) in June 2014 with the *R/V Aegaeo* of the Hellenic Centre for Marine Research. Hydrographic parameters (salinity, temperature, depth) were recorded with a Sea Bird Electronics CTD instrument (SBE-9) associated with a General Oceanic rosette sampler, equipped with twelve 10 L Niskin bottles. Subsamples of seawater from the deepest part of the water column (33 m) were collected and measured immediately for pH and redox potential with laboratory pHmeter and redox potential probe (Jenway 3310). In addition, seawater (unfiltered) was collected in polycarbonate bottles. Surface sediment sample (0-10 cm, untreated) was also collected using a $0.1m^2$ box corer.

Seawater and sediment were carefully transferred to the laboratory into four 25 L polycarbonate bottles, at a proportion 80% and 20% v/v respectively, and kept in the dark in a temperature-controlled room that was set at the *in situ* temperature (15.6 °C). The seawater-sediment systems were left to settle, untreated, for a week with CO_2-free air supply through a pump; the CO_2-free air was introduced over the seawater surface in each tank in order to maintain the *in situ* oxygen saturation for the duration of the experiment. For the 20 days experimental period controlled CO_2 aeration was applied with a continuous flow system (IKS Aquastar, IKS Computer Systeme GmbH) which automatically adjusted CO_2 gas addition directly to the microcosms, in order to regulate and maintain stable pH value close to the target pH levels (Fig. 2). Each tank was monitored constantly (every 5 minutes) throughout the experiment by the IKS System using probes recording temperature (accuracy ±0.3°C), pH (accuracy ±0.05), and DO (accuracy ±12 μmol kg^{-1}). The pH probes were calibrated daily, using certified buffers to avoid drifting. The measured pH values by the IKS system were corrected with the parallel use of a Jenway 3310 laboratory pH meter calibrated in NBS scale (accuracy ±0.02); the pH

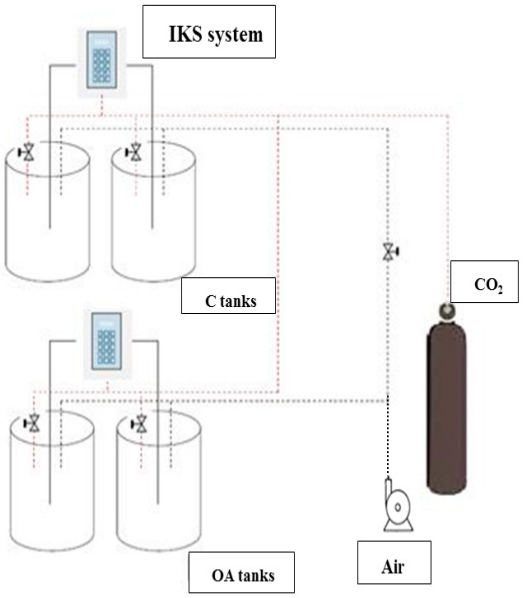

Fig. 2: Design of the experimental set-up demonstrating the two tanks for each pH treatment (OA and C), the IKS system monitoring the CO_2 gas supply and the air pump providing air to the systems.

values were then converted to the total scale (pH_T) (Dickson *et al.*, 2007).

The nominal pH values selected for the two treatments (experiment conditions) were: (i) for the control tanks (C) the pH value measured during sampling (7.85, NBS) and (ii) for the ocean acidification tanks (OA) the pH value predicted for the year 2300 (6.80 NBS), which corresponds to the highest total cumulative future CO_2 emission scenario, for latitudes corresponding to the Mediterranean Sea (Caldeira & Wickett, 2005). Each one of the two treatments was applied in two replicate tanks (Fig. 2). Thus all results regarding seawater samples for OA and C conditions refer to the mean value of two replicates (standard deviation is included in diagrams of each individual parameter). The temperature of the thermostated room and the pH selected for the C condition tanks were the recorded *in situ* values during sampling, in order to simulate as close as possible the natural system. Any change observed in the C condition tanks is considered to be a change naturally occurring, in order to investigate and fully comprehend the effects of acidification on the selected parameters.

Seawater samples were taken from the microcosms every 3 days and analyzed immediately for the determination of DO according to Winkler method, modified by Carpenter (1965) and the potentiometric determination of total alkalinity (A_T) according to Perez & Fraga (1987a) and Perez *et al.* (2000). The precision of A_T analysis was

determined by titrating bottled seawater samples having the same temperature and salinity and was 8.1 μmol kg^{-1}, calculated as 3 times the standard deviation of 10 measurements. The accuracy was assessed by titration of sodium carbonate standard with known alkalinity fortified to the ionic strength of seawater and was 8.4 μmol kg^{-1}, calculated as 3 times the standard deviation of 12 measurements. Samples for dissolved organic carbon (DOC) and nutrients were collected and filtered immediately through 0.45 μm polycarbonated membranes and stored in -18°C until their analysis. The DOC analysis was performed with the High Temperature Catalytic Oxidation method, using a Shimadzu 5000 total organic carbon analyzer, according to instrument's instructions; the Limit of Quantification (LOQ) for DOC was 39.5±4.9 μmol kg^{-1}. Nutrients were determined spectrophotometrically with a Varian Cary 1E UV-visible spectrophotometer, using a 1 cm cell for nitrate, ammonium and silicate while for nitrite and phosphate a 5 cm cell was used. The analytical procedures followed were the ones described by Grasshoff *et al*., 1999; for ammonium (4500-NH_3 –F a modification of the Solorzano method (1969); LOQ: 0.8±0.2 μmol kg^{-1}), nitrite (4500-NO_2– B; LOQ: 0.14±0.02 μmol kg^{-1}), nitrate (4500-NO_3 –E; LOQ: 0.21±0.07 μmol kg^{-1}), phosphate (4500-P –E; LOQ: 0.11±0.03 μmol kg^{-1}), silicate (4500-SiO_2 –E; LOQ: 0.6±0.2 μmol kg^{-1}). Total dissolved nitrogen (TDN; LOQ: 0.13±0.04 μmol kg^{-1}) and total dissolved phosphorus (TDP; LOQ: 0.21±0.07 μmol kg^{-1}) were determined as described by Valderrama (1981). Dissolved organic nitrogen (DON) and phosphorus (DOP) were calculated by subtraction of dissolved inorganic nitrogen forms (DIN) from TDN and of phosphate from TDP. Based on pH_T and A_T values, the rest of the carbonate system parameters, specifically pCO_2, CO_2 concentration, dissolved inorganic carbon (DIC), bicarbonate (HCO_3^-) and carbonate (CO_3^{2-}) ions, aragonite's and calcite's saturation states ($\Omega_{ar.}$ and $\Omega_{calc.}$ respectively) were calculated through the 'Seacarb' software package (Gattuso *et al*., 2014) including also the respective phosphate and silicate concentrations. The 'Seacarb' calculations were performed using the apparent dissociation constants of carbonic acid (K_1 and K_2) of Lueker *et al*. (2000), the equilibrium constant of hydrogen fluoride of Perez and Fraga (1987b), the stability constant of hydrogen sulfate ion of Dickson (1990) and the boron to chlorinity ratio of Lee *et al.* (2010).

Top 0-2 cm of surface sediments were sampled from each tank at the end of the experiment on the 20th day for supplementary analyses. In any case, the system volume, both water and sediment, was not reduced to more than 15% of the initial one (Riebesell *et al*., 2010), in order to be considered undisturbed. The organic carbon (OC) and the total carbon (TC) and nitrogen (TN) of the sediment were determined with a Thermo Scientific FLASH 2000 CHNS elemental analyzer according to the analytical procedure described by Karageorgis *et al*. (2009). Inorganic carbon was calculated by subtracting organic carbon from the total carbon, and subsequently carbonate content was calculated. Total phosphorus and sulfur content was determined through X-ray fluorescence (XRF) analysis. Furthermore, X-ray powder diffraction (XRD) analyses were conducted to evaluate the main minerals prevailing in the sediment phases.

Data Analysis

A one-way analysis of variance (ANOVA) was performed to test the statistical significance of variation ($p<0.05$) between the two experimental conditions for both water and sediment samples (Riebesell *et al*., 2010; results are shown in Table 2). Data were first checked to ensure they conformed to the assumptions of ANOVA (normality: Kolmogorov-Smirnov test and homogeneity of variance test). Principal component analysis (PCA) was performed to evaluate the effects of the selected experimental treatments (pH) on nutrient species and carbon-carbonate parameters of the water-sediment laboratory systems. A Promax with Kaiser Normalization was used for rotation method, converged in 3 iterations (results are shown in Fig. 7). For PCA analysis, Ω-values were not used for data reduction since they are linearly correlated with CO_3^{2-}; also, only pCO_2 values were used

Table 2. One-way ANOVA results (F, p) for all experiment parameters regarding seawater analyses (p values <0.05 are marked bold, which indicate statistically significant difference between the two treatments).

Parameter	F	p	Parameter	F	p
DO	0.504	0.494	NO_3^-	9.982	0.010
A_T	7.688	0.020	NO_2^-	3.698	0.083
HCO_3^-	11.797	0.006	NH_4^+	6.474	0.029
CO_3^{2-}	54.706	0.000	DON	9.982	0.010
DIC	20.758	0.001	PO_4^{3-}	0.065	0.804
$\Omega_{ar.}$	56.934	0.000	DOP	0.191	0.672
$\Omega_{calc.}$	57.061	0.000	SiO_4	1.993	0.188
DOC	2.712	0.131	DIN:DIP	5.620	0.039

while CO_2 concentrations were excluded as they are also inextricably related. Both ANOVA and PCA analyses were performed using the SPSS software package.

Results

During sampling, the difference in temperature between surface and bottom was 10°C; dissolved oxygen was found 225.77 μmol kg^{-1} in the surface, whereas the respective bottom value was relatively low (99.45 μmol kg^{-1}). pH and Redox potential in Elefsis bottom seawater were 7.85 and 194.3 mV, respectively while A_T attained rather high concentration (2769 μmol kg^{-1}). Relatively elevated nitrate concentrations (4.35 μmol kg^{-1}) were measured, followed by nitrite (1.30 μmol kg^{-1}) and phosphate (0.08 μmol kg^{-1}) along with high silicate (13.83 μmol kg^{-1}) values. The pCO_2 calculated in the bottom seawater of Elefsis Bay was 797 μatm, almost double the current atmospheric pCO_2 value (https://www.esrl.noaa.gov/gmd/ccgg/trends/); however, both Ω_{ar} and Ω_{calc} indicated well saturated conditions.

During the experiment, temperature was kept quite stable at 15.1±0.3°C inside the incubator room. pH_T fluctuated slightly in both treatments (6.63±0.18 pH units for OA and 7.82±0.15 pH units for C treatment, Table 1). DO varied between 130±6 μmol kg^{-1} and 138±12 μmol kg^{-1} for OA and C conditions respectively (Fig. 6D) showing no statistical difference (F=0.504, p=0.494). Salinity was constant throughout the experiment at 38.7.

Carbonate System Parameters

Total alkalinity (A_T, Fig. 3A) in OA condition increased dramatically, with the significant increase occurring between the 4th and the 10th day of the experiment, while in C condition little variations were observed. Total dissolved inorganic carbon (DIC, Fig. 3B) also increased in both conditions, with elevated values for OA especially during the last days of the experiment (F=7.688, p=0.020). During the course of the experiment, bicarbonate ions (Fig. 3C) were found to increase in both C and OA conditions reaching considerably higher levels in OA (Table 1; F=11.797, p=0.006). Carbonate ions (Fig. 3D) decreased substantially in OA (F=54.706, p=0.000) in favor of HCO_3^- and DIC, probably reflecting the shift of carbonate system equilibria to compensate the CO_2 increase; CO_3^{2-} for C followed the pH slight variations. In C condition, saturation states for the two carbonate minerals ($\Omega_{ar.}$, $\Omega_{calc.}$, Table 1) were above 1, whereas in OA condition, both Ω_{ar} and Ω_{calc} were lower than 1.

Nutrient Species and Carbon

During the experiment, nitrate in C condition presented a sharp increase (from 2.7 μmol kg^{-1} to 21.2 μmol kg^{-1}) until the 7th day, followed by a declining trend to 15.1 μmol kg^{-1} (Fig. 4A). In OA condition, nitrate showed similar pattern until the 7th day (from 2.5 to 12.5 μmol kg^{-1}), with final values remarkably lower than the ones determined in C condition (F=9.982, p=0.010). Nitrite (Fig. 4B) in C condition showed a similar increase (from 0.2 μmol kg^{-1} to 1.6 μmol kg^{-1}), followed by a decreasing trend to values corresponding to the initial ones (0.3 μmol kg^{-1}). In OA condition, nitrite slightly increased from 0.2 to 0.5 μmol kg^{-1}, followed by a declining trend to values below the LOQ of the method (F=3.698, p=0.083). Ammonium (Fig. 4C) in C condition showed a decreasing trend from 1.9 to values below LOQ. On the contrary, in OA condition after the decrease observed until the 4th day (from 1.4 μmol kg^{-1} to 0.8 μmol kg^{-1}), an increase was found until the end of the experiment (2.2 μmol kg^{-1}; F=6.474, p=0.029).

Phosphate (Fig.5A) showed a decreasing trend in C condition until the 10th day (from 0.6 μmol l^{-1} to 0.3 μmol kg^{-1}) followed by a slight increase (0.6 μmol kg^{-1}) until the end of the experiment; in OA condition, phosphate appeared constant until the 10th day (0.5 μmol kg^{-1}) and then followed the same trend with C condition to final values of 0.5 μmol kg^{-1} (F=0.065, p=0.804). Silicate concentrations presented negligible variations between the two conditions (F=1.193, p=0.188).

Dissolved organic carbon (DOC; Fig.6B) concentrations showed the same trend in both conditions until the 10th day, while increased values were recorded for OA condition towards the end of the experiment (F=2.712, p=0.131).

Dissolved organic nitrogen (DON) followed the same decreasing pattern with ammonium in C condition till the end of the experiment (Fig. 4D); in OA condition DON varied between 21.9 μmol kg^{-1} and 37.6 μmol kg^{-1} reaching a final value of 27.3 μmol kg^{-1} (F=9.982, p=0.010). Dissolved organic phosphorus (DOP) (Fig. 5B) showed similar increasing trend for both conditions until the 14th day of the experiment, and a decrease at the end of the experiment (F=0.191, p=0.672).

Dissolved inorganic nitrogen (DIN; stands for nitrate+nitrite+ammonium) to phosphate ratio (DIN:DIP from now on; Fig. 6C) in C condition increased from 8.0 to 79.4 until the 7th day followed by a decrease to 32.1. In OA condition, this increase was less significant (from 8.0 to 31.5 on the 10th day) and then the ratio remained constant at 21 (F=5.620, p=0.039).

Sediment composition

Sediment granulometry showed that Elefsis Bay is characterized by fine surface sediments of <63μm in a percentage between 95-100%. The main sediment minerals were calcite ($CaCO_3$) and quartz (SiO_2), followed by aragonite ($CaCO_3$) and cinochlore $(Mg_5Al)(AlSi_3)O_{10}(OH)_8$. This indicates sediment phases rich in carbonates and silica along with aluminium and magnesium. The carbonate content of the Elefsis Bay sediment was 46.8±0.95%; the respective values for OA and C were 47.6±2.6% and 47.0±1.3 respectively (Table 3). The OC analyses in sediment revealed high organic content

Table 1. Seawater carbonate system parameters (mean values, standard deviations, minimum and maximum values) for field and experiment microcosms (OA: Ocean Acidification condition, C: Control condition).

		pH_T	A_T	pCO_2	CO_2	HCO_3^-	CO_3^{2-}	DIC	$\Omega_{ar.}$	Ω_{cal}
			µmol kg^{-1}	*µatm*	µmol kg^{-1}	µmol kg^{-1}	µmol kg^{-1}	µmol kg^{-1}		
OA	**field**	7.72	2769.3	797	27.82	2413.8	146.25	2587.8	2.19	3.38
	mean	6.63	4017.3	2340	1153.3	3986.6	13.09	5152.9	0.20	0.30
	max	6.97	5341.0	2833	2458.6	5311.8	20.39	6825.3	0.31	0.47
	min	6.47	2772.7	1909	247.5	2720.0	2.23	2987.9	0.03	0.05
	st.dev.	0.18	569.8	822	768.1	1117.8	6.08	1379.8	0.09	0.14
C	mean	7.85	2749.1	974	31.0	2404.4	140.43	2575.9	2.10	3.26
	max	8.06	2858.5	1184	44.3	2606.2	202.77	2754.9	3.04	4.71
	min	7.69	2677.4	805	16.1	2181.5	97.99	2400.3	1.47	2.28
	st.dev.	0.15	329.6	364	11.9	153.6	40.85	126.1	0.61	0.95

The partial pressure of CO_2 (pCO_2), the concentration of CO_2, HCO_3^-, CO_3^{2-}, dissolved inorganic carbon (DIC), and the saturation state of aragonite ($\Omega_{ar.}$) and calcite ($\Omega_{cal.}$) were calculated with 'Seacarb' package from pH_T, total alkalinity, salinity, temperature, phosphate and silicate data.

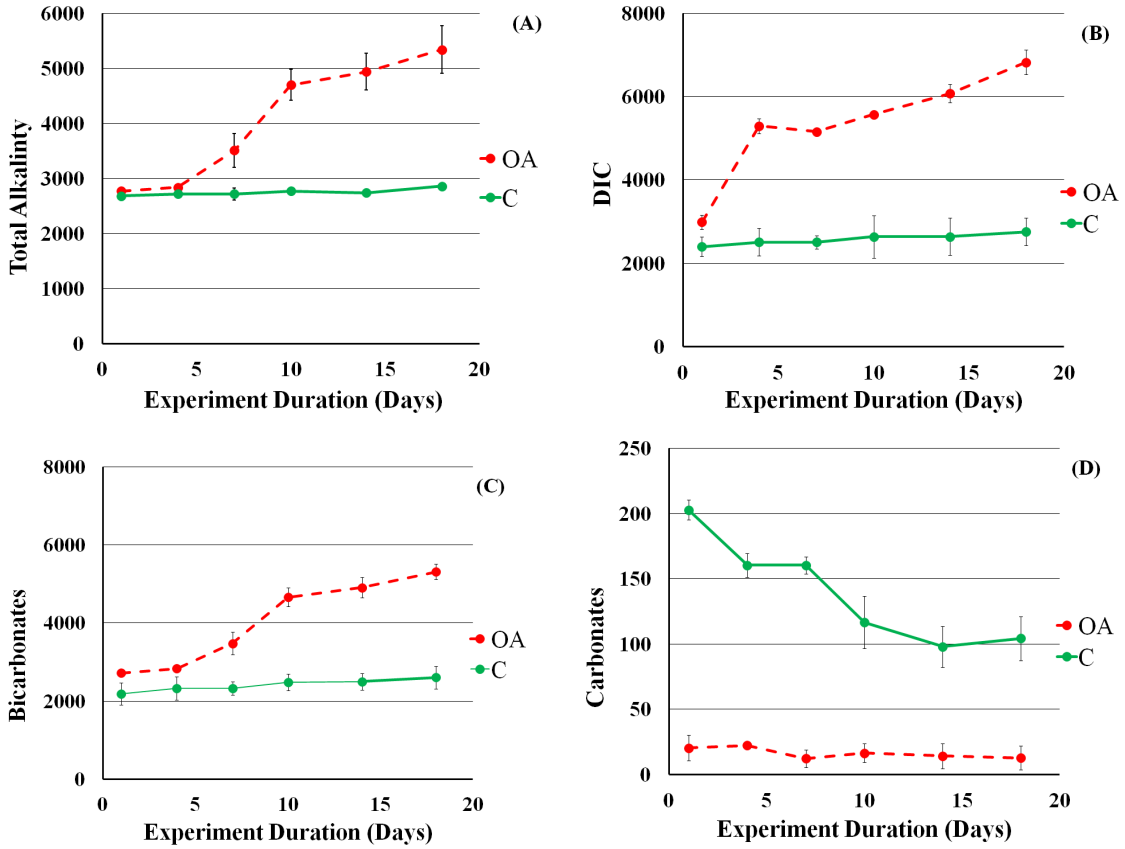

Fig. 3: Alkalinity, DIC, Bicarbonates (HCO_3^-) and Carbonates (CO_3^{2-}) concentrations (in µmol kg^{-1}) for the duration of the experiment; mean values and standard deviations for the two replicates of each treatment (OA: Ocean Acidification condition, C: Control condition).

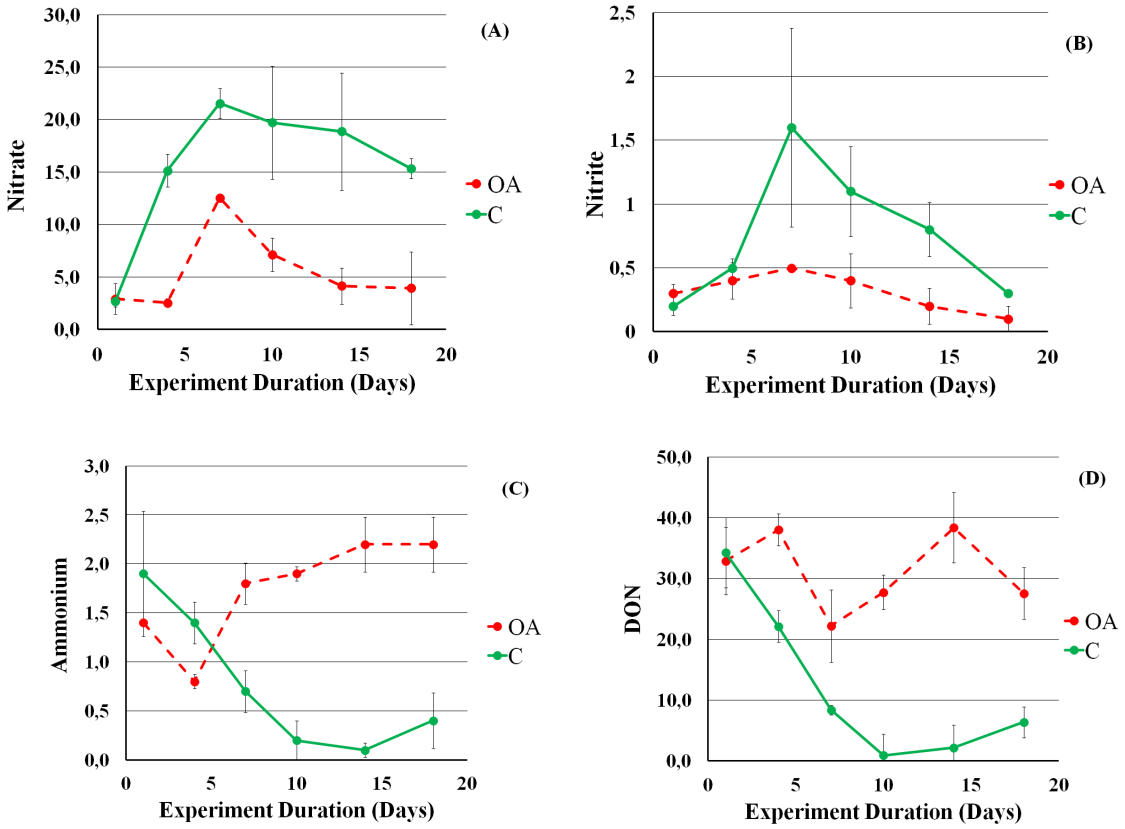

Fig. 4: Nitrate, Nitrite, Ammonium and DON concentrations (in µmol kg^{-1}) for the duration of the experiment; mean values and standard deviations for the two replicates of each treatment (OA: Ocean Acidification condition, C: Control condition).

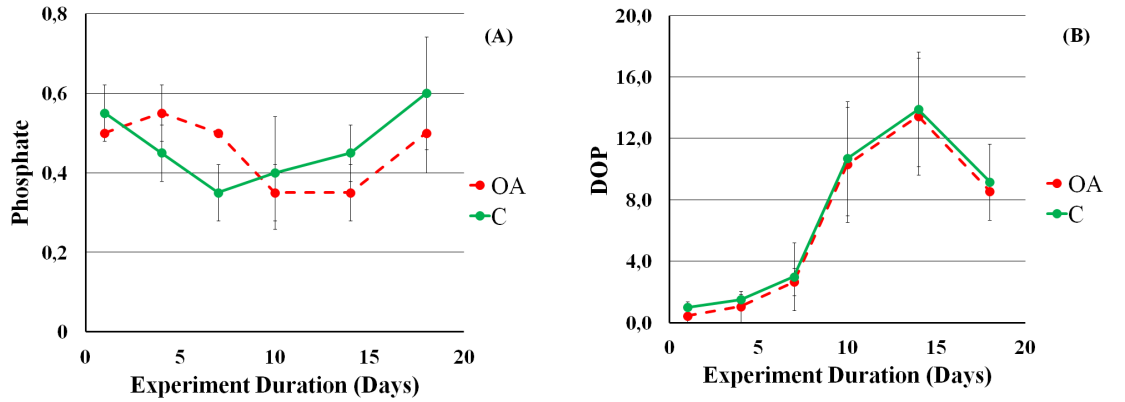

Fig. 5: Phosphate and DOP concentrations (in µmol kg^{-1}) for the duration of the experiment; mean values and standard deviations for the two replicates of each treatment (OA: Ocean Acidification condition, C: Control condition).

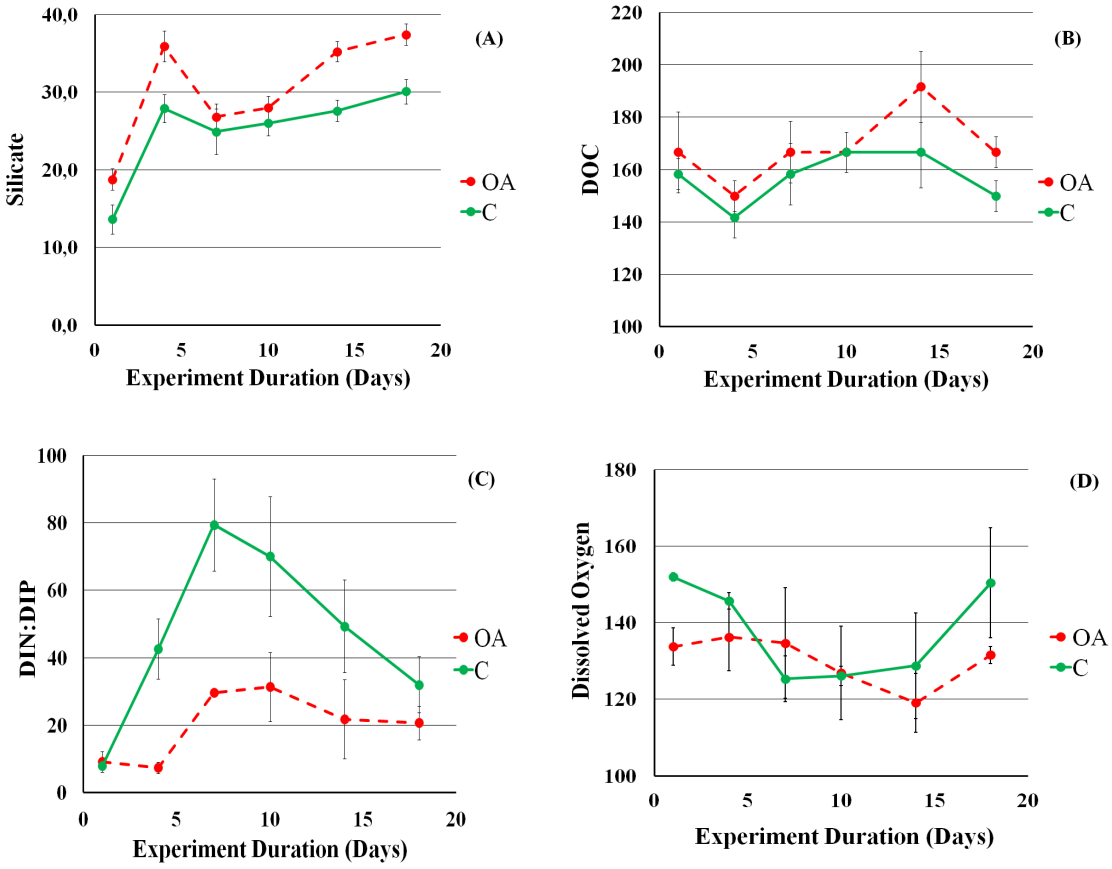

Fig. 6: Silicate, DOC and DO concentrations (in µmol kg^{-1}), and DIN:DIP molar ratio for the duration of the experiment ; mean values and standard deviations for the two replicates of each treatment (OA: Ocean Acidification condition, C: Control condition).

(2.35%) and showed a decrease throughout the experiment for both conditions (1.77±0.14%, 1.67±0.25 for OA and C respectively). The sulfur content was found 0.80±0.01 % with no variations during the experiment. The sediment nitrogen content (TN) for field samples was found 0.27±0.02%; for OA treatment TN varied between 0.20±0.01% and for C treatment 0.19±0.02 %. The phosphorus sediment content (TP) for field samples was found 0.07±0.02% with negligible variations for both treatments (Table 3). The one-way ANOVA results, showed no statistically significant difference of the sediment characteristics (OC, $CaCO_3$, TN, TP and S) between the two treatments.

Principal Components Analysis (PCA)

PCA for the C treatment explained 86.9% of variation in the first two principal components (Fig.7A). The first axis (PC1) explained 61.6% of total variance and was positively related to A_T (0.94), DOP (0.89), pCO_2 (1.00), HCO_3^- (1.00) and DIC (1.00) and was negatively related to pH (-0.98), NH_4^+ (-0.81) and CO_3^{2-} (-0.96). The second principal component (PC2) explained 25.3% of total variation and was positively correlated with NO_2^- (0.92), DIN:DIP (0.98), DIN (0.87), DO (0.86), and NO_3^- (0.81) and was negatively correlated with PO_4^{3-} (-0.98).

PCA for OA treatment explained 70.1% of variation in the first two principal components (Fig.7B). The first component (PC1) explained 40.9% of total variance and was positively related with A_T (0.99), HCO_3^- (0.99), DOP (0.88), NH_4^+ (0.86), DIC (0.85), and was negatively related to PO_4^{3-} (-0.96). The second component (PC2) explained 29.3% of total variance and was only negatively correlated with pCO_2 (-0.90).

Discussion

This study, which was based on a microcosm lab simulation, was a first overall assessment of basic biogeochemical interactions/alterations of nutrients and carbon that are taking place in a restricted marine system under the emerging effects of coastal pH decrease. Previous

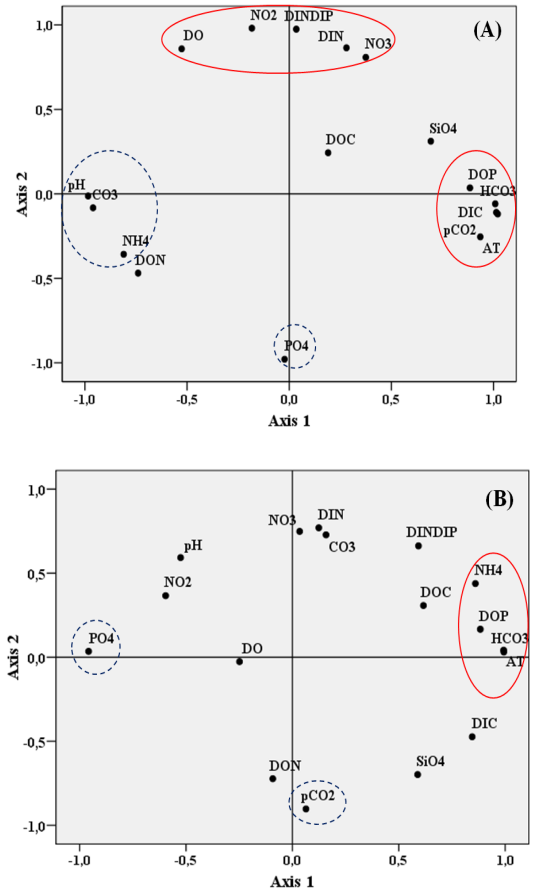

Fig. 7: Principal Component Analyses (PCA) graphs for (A) Control (C) and (B) Ocean Acidification (OA) treatments. Red circles indicate positive significant correlations while blue circles indicate negative significant correlations.

Table 3. Sediment analyses (OC, $CaCO_3$, TN, TP and S in % on dry weight) for OA (Ocean Acidification) and C (Control) experimental conditions; mean values and standard deviations for the two replicates of each treatment.

		OC %	TN %	TP %	$CaCO_3$ %	S %
field		2.35	0.28	0.07	46.8	0.80
OA	mean	1.67	0.19	0.05	49.7	0.81
	stdev	0.14	0.01	0.03	3.00	0.08
C	mean	1.84	0.20	0.04	45.8	0.79
	stdev	0.25	0.02	0.02	1.8	0.07

studies were focused either in predicting the effects of future pH reduction or investigating the biogeochemical outcomes of coastal pH decline on certain organisms' response/survival or merely on the processes ultimately determining CO_2 fate and impact in aquatic systems (e.g. Andersson *et al.*, 2007; Kitidis *et al.*, 2011; Widdicombe *et al*., 2009; Laverock *et al*., 2014). Marine systems however, constitute of specific features, more complex than simple chemical or thermodynamic equilibria which are necessary, nonetheless, for any calculation or prediction model. So this experimental study tries to fill this gap by examining the co-evolution of basic geochemical processes.

Carbonate system processes - Evidence of alkalinity generation

Following the *in situ* DO measurements (99.45 μmol kg^{-1}), the experiment for both C and OA treatments was conducted under low DO conditions, characterized as mild hypoxic based on the threshold of 107 $\mu molO_2\ kg^{-1}$ cited by Hofmann *et al*. (2011).

In C condition, carbonate ions decrease throughout the experiment with a 50% decline in final values; carbonate mineral saturation states also present the same trend. Total alkalinity, DIC and bicarbonate ions slightly increase in this case. Although CO_2 was periodically injected in C condition tanks in order to maintain a stable pH value, CO_2 concentration and pCO_2 exhibit considerable increase from the beginning till the end of the experiment. The naturally occurring respiration and organic matter degradation as well as the modification of the equilibria between the different forms of dissolved inorganic carbon with an increase of the proportion of both CO_2 and bicarbonate ions at the expense of carbonate ions are the most likely processes to explain the observed trends. The carbonate precipitation would also be suggested as possible explanation of the carbonate ions decrease however, is not depicted on the sediment carbonate content, neither is supported by the declining trend of carbonate mineral saturation states.

In OA condition, an immediate decrease in carbonate ions in relation to C condition is found at the beginning with stable concentrations till the end of the experiment. These variations lead to Ω_{ar} and Ω_{cal} values below 1, while in sediments no differentiations were observed. The system response to CO_2 addition was immediate for DIC which was augmented probably as the combined result of decaying phytoplankton cells and zooplankton carcasses present in the experimental tanks in addition to system response to CO_2 addition. Total alkalinity and bicarbonate ions amplification followed as expected.

A significant increase of 90% was observed for A_T with a corresponding DIC increase of 120%, making clear that other mechanisms besides the carbonate system equilibria affect alkalinity. The enhanced A_T in more acidified conditions is generally attributed to carbonate minerals dissolution from sediment (Andersson *et al*., 2007; Kru-

mins *et al*., 2013). However, no noticeable decrease of sedimentary carbonates was found here. This is not surprising if the high $CaCO_3$ content of the sediment, as well as the relatively short duration of the experiment, are considered. Assuming that the observed A_T increase (ΔA_T = ~2500 μmol kg^{-1}) in the overlying water was generated by the dissolution of sedimentary $CaCO_3$, then the corresponding change in inorganic carbon percentage of the sediment would be about 0.002% w/w that is much lower than the methodological error of the particulate inorganic carbon determination and thus cannot be safely detected. However it seems very likely that the pH decline in the overlying water has lead to an analogous shift of pH in sediment porewater that induced the development of under-saturated conditions for calcium carbonate minerals in pore waters leading to dissolution of $CaCO_3$ and DIC and A_T generation. Unfortunately, as no pH, A_T and/or DIC data were aquired for the sediment porewater during this study, it is impossible to assess the response of the sediment to pH changes in porewater and evaluate the contribution of this process to the observed ΔA_T. A previous study in Saronikos Gulf has shown that under dark conditions DIC efflux from the sediment towards the water column takes place that is negatively related with DO suggesting mineralization processes (Apostolaki *et al*., 2010).

It has to be noted that variations in the overlying water A_T are not only due to carbonate dissolution; several other biogeochemical processes could contribute to the A_T increase that was recorded in the current study. Important alkalinity generation (benthic alkalinity) in shallow sediments due to anaerobic degradation of disposed organic matter has been well reported (Thomas *et al*., 2009; Krumins *et al*., 2013; Ingrosso *et al*., 2016a). Remineralization of particulate organic matter and subsequent nutrient release directly affect A_T, depending on the reactive nitrogen species produced (e.g. 1 mole of ammonium or nitrate release leads to an increase or decrease, respectively, of A_T by 1 mole; Hernández-Ayón *et al*., 2007). During more acidified conditions, in this study, the steady increase of ammonium over time along with the respective decrease in nitrate and nitrite concentrations could contribute positively to A_T levels. Moreover, recent estimates of alkalinity fluxes from coastal marine sediments underline the significant contribution of net sulfate reduction to alkalinity generation (up to 70-82%; Krumins *et al*., 2013), especially in sediments in highly productive and/or oxygen-depleted coastal waters (e.g. in the Black Sea; Barker Jorgensen & Kasten, 2006). It is definite that organic matter degradation and nutrient related processes (e.g. denitrification) could not be solely responsible for the significant A_T increase reported here. During organic matter oxidation, when the available oxygen diminishes, respiration processes retreat while sulfate and Fe reduction take over; sulfate reduction producing hydrogen sulfide followed by Mn and Fe reduction result in bicarbonate generation which in turn increase total alkalinity (Krumins *et al*., 2013; Hu & Cai, 2011; Hulth *et al*., 1999).

PCA performed on the C treatment results revealed the effect of pH change on carbonate system parameters primarily, along with ammonium and DOP (PC1), as well as nitrogen and phosphorus species transformations through organic matter degradation and denitrification, as a result of oxygen availability (PC2). The same analysis performed on OA treatment results showed the strong impact of OM degradation, ammonium, organic phosphorus and bicarbonates on A_T, whereas pCO_2 even in excess was a factor that had minor effect on the system. The fact that under more acidified and low oxygen conditions, only OM degradation and bicarbonate ions are correlated in the first component could also be an indication of sulfate reduction processes releasing considerable amounts of bicarbonates. Through net denitrification and net sulfate reduction, nitrate and sulfate transfer their negative charge to HCO_3^- by oxidizing organic carbon producing the anion which contributes to DIC and alkalinity (Hulth *et al*., 1999; Hu & Cai, 2011; Krumins *et al*., 2013). High values of hydrogen sulfide measured *in situ* at the near bottom water layer support the sulfate reduction scenario (Pavlidou & Hatzianestis unpublished data). Bicarbonate, sulfide, ammonium and phosphate concentrations utterly contribute to the final A_T concentration (Dickson *et al.*, 2007). As it appears here, these chemical species affect A_T to a larger extent under lower pH values; from the PCA analysis for OA treatment, ammonium, DOP, HCO_3^-, and DIC were found to contribute strongly to A_T, while phosphate seem to have a negative feedback on it. Normally, phosphate contribute positively to A_T by definition, which indicates that in more acidified conditions with lower available oxygen, a strong complex of phosphate is formed with other substances (e.g. metals or carbonates) which in turn seem to be a reducing factor in the final A_T budget (Ge *et al*., 2016). Furthermore, it has been shown that in areas with restricted mixing, and/or characterized by appreciable autotrophic DOM production and/or significant inputs of DOM from land, organic bases contribute significantly to A_T (Hernández-Ayón *et al*., 2007; Kulinski *et al*., 2014). Accumulation of DOM in the near-bottom layer of Elefsis Bay, which is enriched in phosphorus relatively to carbon and nitrogen, has been reported during conditions of stratification (Pavlidou *et al*., 2013) which could be a further contribution to the system alkalinity.

Processes affecting organic carbon and nutrients

Considering that the basic biogeochemical processes were investigated, the normal mechanisms of the specific study area could be summarized as those pointed out for C condition. In C condition the DON appeared to convert to ammonium which in turn was consumed and rapidly oxidized to NO_2^-/NO_3^-; this process reached a plateau in the middle of the experiment after which NO_2^-/NO_3^- were no longer produced (Fig. 4). Nitrite and nitrate, were favoured against ammonium in this case throughout the experiment, indicating nitrification to be the main prevailing

process. In addition, sedimentary TN decreased indicating dissolution into soluble forms; ammonium and nitrite efflux from the sediment to the water column have been reported for the specific area (Rousselaki et al., 2014).

In OA condition, after the 5th day of the experiment, DON degradation was constrained, in relation to C condition (Fig. 4D). In parallel, the originally existing ammonium was no longer oxidized and as the experiment proceeded, ammonium accumulated while nitrate production declined, implying reduced nitrification processes. It has been reported that in Elefsis Bay sediment acts as a source of ammonium to the overlying water, under specific conditions (e.g. hypoxia; Rousselaki *et al*., 2014). Additionally, OA was previously found to cause ammonium efflux from fine-grained sediment towards water (Widdicombe *et al*., 2009); OA can also reduce nitrification rates, reducing oxidized nitrogen supply in the upper water layers (Beman *et al*., 2011). The increased N-content, under lower pH with higher dissolved organic N forms pointed out here, indicates inhibited organic N mineralization processes and a possible N-buildup. The suppression in ammonium oxidation mechanism followed by decrease of nitrate production and subsequently ammonium accumulation, is in consistency with already published studies showing a deceleration of the ammonium oxidation mechanism as pH decreases (Beman *et al*., 2011 and references therein). Efflux of nitrate and nitrite has been previously reported under lower pH values (Widdicombe *et al.*, 2009) depending on sediment granulometry. The signal of TN release from the sediment is not depicted in the concentrations of nitrite and nitrate, possibly indicating a denitrification mechanism, producing N_2 gas (and small amounts of N_2O) which likely escaped from the system. Phosphate presents similar trend with C condition (Fig. 5A), with negligible variation up to the 10th day. No significant acidification impact was observed in phosphate and silicate, as has been reported in previous studies (Widdicombe *et al*., 2009; Tanaka *et al.*, 2008).

The concentration of the sedimentary organic carbon drops by 20% in C condition and by 30% in OA condition at the end of the experiment, as a result of the first step of its degradation, fueling the DOC pool of the overlying water that exhibits a 20% increase in DOC concentration in both cases. DOC was found relatively high throughout the experiment in both treatments (Fig. 6B). The final higher DOC concentrations observed for OA condition, although not statistically different from those in C condition, could implicate inhibition of dissolved organic matter decomposition under lower pH values. The limitation of DOC decay could be attributable to the reactivity of the compounds produced in the first step of organic matter degradation during which particulate organic carbon is converted to dissolved forms. The produced compounds may be resistant to further degradation, due to their inherent stability or as a result of abiotic reactions that protect the molecule from enzymatic attack (Hee *et al*., 2001). Despite any indications revealed here, no similar published results were found; earlier experiments, conducted under CO_2-perturbed conditions that also included the sediment phase, have not examined the features and fate of DOC released by the sedimentary organic carbon degradation. However, recent results from mesocosm experiments in the Mediterranean that examined the effect of increased pCO_2 and/or nutrient concentrations on dissolved organic matter dynamics indicated that eutrophication modified the structure of the organic matter into more complex material, while a weak aromatization of the DOM was observed under higher pCO_2 conditions (Aparicio *et al*., 2016) influencing the organic matter lability. Furthermore, experimental observations demonstrated that at lower pH, dissolved organic molecules are becoming more condensed being thus less susceptible or even refractory to biodegradation (Chin *et al*., 1998).

The DIN:DIP ratio was found decreased in more acidified conditions (Fig. 6C); since no prominent variation was observed in phosphate concentrations, the DIN reduction is considered to be the main factor affecting the DIN:DIP ratio. The decreased DIN:DIP ratio, the prevalence of organic nutrient species against the inorganic ones, the observations of constrained DON degradation and nitrate production decline and the higher DOC concentrations under lower pH values can also support inhibition of organic matter decomposition.

Implications for enclosed embayment in future CO_2 conditions

The results of this study showed that the near bottom waters of Elefsis Bay during June were characterized by mild hypoxic conditions (Hofmann *et al*., 2011) and presented increased acidity (7.85 in NBS scale) in relation to typical surface values (pH=~8.1). In some of the oldest studies regarding Elefsis Bay (June 1975; May-June, 1977), surface pH values of 8.4-8.5 have been reported along with seasonal near bottom pH decrease reaching values of 7.9-7.8 (all in NBS scale; Scoullos, 1979; Friligos, 1982); this pH difference between surface and near bottom waters has been solely pointed out through individual studies and unfortunately systematic high-frequency pH measurements were never performed. The bottom pH nowadays (7.85, June 2014) was found to be at the same level with values reported about 40 years ago for corresponding time periods, implying that the area has been well affected by the seasonal pH decline manifoldly and in quite unpredicted pathways. Elefsis Bay is a restricted coastal system with intensive urban and industrial activities, receiving increased N and C inputs, which enhance biological primary productivity and promote subsequent organic matter decomposition. The dramatic DO decrease during stratification along with enhanced CO_2 production and more elevated pCO_2 values caused by OM degradation, induce non-equilibrium between bottom and surface layers.

Total alkalinity in Elefsis bottom water (2769 μmol kg^{-1}) was found markedly higher to the values reported recently for open Eastern Mediterranean Sea waters

(2600 μmol kg^{-1}; Hassoun *et al*., 2015). This value is similar to those reported for the deep layer of the Gulf of Trieste in the northern Adriatic Sea that is a coastal system with shallow depths and seasonal stratification (e.g. Cantoni *et al*., 2012; Ingrosso *et al*., 2016a). This enhanced alkalinity first of all reflects the alkalinity input in Mediterranean coastal areas by the weathering of the land limestones; additionally, this study revealed the significant contribution of nutrient species and possibly of sulfate reduction in total alkalinity (Section 4.2). The penetration of anthropogenic CO_2 into the Mediterranean has led to lower saturation degree of calcium carbonate in relation to the preindustrial era (Hassoun *et al*., 2015). During the period 1967−2003, the estimated Ω_{ar} in a coastal site in the western Mediterranean displayed a decreasing trend and fluctuated between the highest value of 4.3 observed in 1968 and a minimum of 3.1 in 2003 (Howes *et al*., 2015); the calculated $\Omega_{ar.}$, in the bottom waters of Elefsis Bay was found 2.19. Similar low Ω_{ar} values have been recorded in the deep layer of the Gulf of Trieste, under the occurrence of strong remineralization processes during summer (Cantoni *et al*., 2012). Considering that the anoxic layer in Elefsis Bay is an intermittent feature that is developed annually from depths >15 m (Scoullos & Rilley, 1978; Scoullos, 1983; Pavlidou *et al*., 2013) and that the same processes promoting hypoxia also acidify the water column (Wallace et al. 2014) during stratification periods, it would be expected to detect more increased DIC and CO_2 concentrations, higher pCO_2 (probably above 1000 μatm) and eventually even lower pH values. Concomitantly, the water column would be more corrosive in respect to aragonite and calcite, an effect relevant to what is expected in the future due to OA, but with undefined impacts on the ecosystem. Relevant findings were reported for the Gulf of Trieste (Cantoni *et al*., 2012) where the intense remineralization of organic carbon in its deeper waters releases CO_2, leading to pCO_2 values up to 1043 μatm during hypoxic periods. Water column mixing, drives the penetration of these increased amounts of CO_2 to the surface waters, resulting in their supersaturation, and eventually emitting carbon dioxide to the atmosphere (Ingrosso *et al*., 2016b).

When hypoxic conditions characterize the marine ecosystem, both nitrification and denitrification processes can occur (Cai *et al*., 2011) and since nitrite and nitrate both serve as substrates for denitrifying bacteria, it is possible that an inhibition of nitrification could result in a decrease of denitrification process as well (Huesemann *et al*., 2002). Denitrification and nitrate reduction to nitrite are typical processes taking place during June in Elefsis bottom waters that are becoming evident from the decrease and disappearance of nitrate and the low values of oxygen (Friligos & Barbetseas, 1990; Pavlidou *et al*. 2013). Moreover, the ocean acidification would decrease ammonium conversion to nitrate through nitrification processes and eventually would deplete nitrate supply in surface waters. In this way, smaller phytoplankton organisms, such as dinoflagellates will be favored, against diatoms which show a preference for growth on nitrate (Dortch, 1990), possibly triggering the development of HABs (Harmful Algal Blooms; Huesemann *et al*., 2002; Beman *et al*., 2011). In Elefsis Bay, the occurrence of HABs is sporadic in time and recurrence of the causative species (Ignatiades & Gotsis-Skretas, 2010). Eventually, more acidified conditions could impact the processes determining the final N-species available for biological consumption, a shift which is controlled by a series of biological and physical interactions including global climatic changes (Moncheva *et al*., 2001).

Conclusions

This experimental study was a quite integrated simulation that examined the response, alterations and interactions of nutrients and carbon biogeochemistry under the emerging effects of coastal pH decrease. More acidified conditions have been previously reported in coastal areas characterized by temperature-induced stratification and increased inputs of OM and nutrients through anthropogenic activities and which have similar features with the Elefsis Bay. It is a fact that the 'hot, sour, and breathless' conditions predicted for the future open ocean (Gruber *et al*., 2011) can already be found in today's coastal zones during summer, and especially within the close-to-the-bottom layer where pH and DO levels are generally lower than the upper water column (Wallace *et al*., 2014). Normally anthropogenic CO_2 is the major driver of OA in open ocean; in shallow coastal areas, this driver may have a minor role as multiple human activities operating at various spatial scales affect the carbonate system equilibria. The increase of anthropogenic nutrient and organic matter inputs by rivers, groundwaters, and atmosphere (eutrophication) is considered a significant driver of enhanced coastal acidification, especially in hypoxic bottom waters (Borges & Gypens, 2010; Strong *et al*., 2014). The main differentiation between the evolvement of acidification in coastal zone and in open ocean is that in the former human actions influence the coastal ocean carbonate system through an indirect mechanism which in addition has a strong bottom to surface orientation. Despite this significant discordance, both mechanisms are expected to present similar final outcomes in coastal systems' biogeochemistry.

It has been demonstrated that under more acidified conditions, significant alkalinity release occurred, whereas the water became undersaturated in both carbonate minerals, namely aragonite and calcite. This alkalinity increase was partially associated with sedimentary carbonate dissolution and the reactive nitrogen species shift towards ammonium. In addition there is evidence that organic compounds containing basic functional groups originating from the DOM pool and sulfate reduction processes would contribute to the alkalinity production during the experiment.

The ammonium production by the organic matter degradation and the subsequent ammonium oxidation normally occurring under hypoxic conditions, are intercepted in more acidified conditions. The decline of nitrate and nitrite in parallel with ammonium increase, indicate a deceleration of the ammonium oxidation processes along with decrease in nitrate production. These could lead in a decline of nitrification mechanisms that could eventually affect the phytoplanktonic community composition and the relative species abundances. Phosphate and silicate were not affected by the further pH decline. Organic forms of N and P along with DIN:DIP ratio during more acidified conditions imply possible N-limitation and inhibition of organic matter decomposition.

Although Elefsis Bay is one of the most studied areas in Greece, there is a sparseness of recent pH measurements. The pH decline reported in this study, however, has been documented since the 1970's; the weak water mass renewal, in combination with organic load and high biological production, result in the entrapment and recycling of a large amount of organic matter (Pavlidou *et al*., 2013). The microbial decomposition of this organic matter has caused a local bottom increase in CO_2 concentrations causing carbonate system alterations similar to the future predictions for global ocean acidification. This CO_2 release by respiratory processes, along with the development of hypoxia and anoxia has altered decidedly the biogeochemical cycling of carbon and nutrients in the subpycnocline waters of Elefsis Bay; upward spreading of these waters would have potentially important consequences in the biogeochemistry of the upper pycnocline layer.

Currently, OA is not the main factor affecting the Elefsis Bay but long-term trends in pH, resulting from increased prevalence of bottom-water hypoxia is known to be substantial compared to the pH trend resulting from anthropogenic CO_2 acidification, in coastal waters (Hagens *et al*., 2015). It has also been suggested that the eutrophication-induced hypoxia could amplify the susceptibility of coastal waters to ocean acidification (Cai *et al*., 2011), thus making the coastal realm most vulnerable to ecological and biogeochemical perturbations.

The key findings of this study may contribute to future research efforts regarding the carbon and nutrient cycling in relation with increasing atmospheric CO_2 in intermittently hypoxic/anoxic coastal systems of the Mediterranean Sea. However, in such highly variable coastal environments high-frequency monitoring of the marine carbonate system is essential in order to document and interpret the long-term trends in inorganic carbon dynamics and regional ocean acidification. In parallel, detailed studies of other biogeochemical parameters accompanied by properly designed experiments are needed to improve our understanding of the factors that regulate the carbonate system and elucidate the possible impact of the increasing CO_2 on the complex biogeochemical processes taking place in coastal areas.

Acknowledgements

Part of this research was funded by the EU Research Project "ARISTEIA- EXCELLENCE 640" (2012-2015) entitled *"Integrated Study of Trace Metals Biogeochemistry in the Coastal Marine Environment* (ISMETCO-MAREN)*"*. Part of this project is implemented under the Operational Programme "Education and Lifelong Learning" and funded by European Social Fund and national resources. The authors wish to thank the GIS Lab of HCMR for preparing the manuscript map. Authors thank also the Athens Water Supply and Sewerage Company for supporting the field sampling. The support and assistance of the officers and crew of the R/V Aegaeo during sampling is highly appreciated. The authors would also like to thank two anonymous reviewers for their constructive comments that helped to significantly improve the quality of the manuscript during the revision process

References

Andersson, A., Bates N., Mackenzie, F., 2007. Dissolution of Carbonate Sediments under Rising pCO_2 and Ocean Acidification: Observations from Devil's Hole, Bermuda. *Aquatic Geochemistry,* 13, 237-264.

Aparicio, F.L., Nieto-Cid, M., Borrull, E., Calvo, E., Pelejero, C., *et al*., 2016. Eutrophication and acidification: Do they induce changes in the dissolved organic matter dynamics in the coastal Mediterranean Sea?. *Science of the Total Environment*, 563-564, 179-189.

Apostolaki, E., Holmer, M., Marbá, N., Karakassis, I., 2010. Degrading seagrass (Posidonia oceanica) ecosystems: a source of dissolved matter in the Mediterranean. *Hydrobiologia*, 639, 13-23.

Barker Jorgensen, B., Kasten, S., 2006. Sulfur cycling and methane oxidation. p. 271-310. In: *Marine Geochemistry*, Springer, Berlin Heidelberg, 574 p.p.

Beman ,M., Chow, C., King, A., Feng, Y., Fuhrman, J. *et al*., 2011. Global declines in oceanic nitrification rates as a consequence of ocean acidification. *Proceedings of the National Academy of Science*, 108, 208-213.

Borges, A., Gypens, N., 2010. Carbonate chemistry in the coastal zone responds more strongly to eutrophication than to ocean acidification. *Limnology and Oceanography*, 55 (1), 346-353.

Cai, W., Hu, X., Huang, W., Murrel, M., Lehrter, J. *et al*., 2011. Acidification of subsurface coastal waters enhanced by eutrophication. *Nature Geoscience,* 4, 766-770, DOI: 10.1038/ngeo1297.

Caldeira, K., Wickett, M., 2005. Ocean Model predictions of chemistry changes from carbon dioxide emissions to the atmosphere and ocean. *Journal of Geophysical Research,* 110, 1-12, DOI: 10.1029/2004JC002671.

Cantoni, C., Luchetta, A., Celio, M., Cozzi, S., Raicich, F., 2012. Carbonate system variability in the Gulf of Trieste (North Adriatic Sea). *Estuarine, Coastal and Shelf Science,* 115, 51-62, http://dx.doi.org/10.1016/j.ecss.2012.07.006.

Carpenter, J., (1965). "The Accuracy of the Winkler Method for Dissolved Oxygen Analysis." Limnology and Oceanography.

Chin, W.C., Orellana, M.V., Verdugo, P., 1998. Spontaneous assembly of marine dissolved organic matter into polymer gels. *Nature,* 391, 568-572. http://dx.doi.org/10.1038/35345.

Ciais, P., Sabine, C., Bala, G., Bopp, L., Brovkin, V. *et al*., 2013. Carbon and Other Biogeochemical Cycles. In: *Climate Change 2013: The Physical Science Basis*. Contribution of Working Group I to the Fifth Assessment Report of the Intergovernmental Panel on Climate Change, Cambridge, United Kingdom and New York, NY, USA.

Dickson, A.G., 1990. Standard potential of the reaction: AgCI(s) + $1/2H_2(g)$ = Ag(s) + HCI(aq), and the standard acidity constant of the ion HSO_4 in synthetic sea water from 273.15 to 318.15 K. *Journal of Chemical Thermodynamics,* 22, 113-127.

Dickson, A.G., Sabine, C.L., Christian, J.R (Eds.), 2007. *Guide to best practices for ocean CO_2 measurements*. North Pacific Marine Science Organization, Special Publication 3, Sidney, British Columbia, 191 pp.

Dortch, Q., 1990. The interaction between ammonium and nitrate uptake in phytoplankton. *Marine Ecology Progress Series,* 61, 183-201.

Duarte, C., Hendriks, I., Moore, T., Olsen, Y., Steckbauer A, *et al.,* 2013. Is Ocean Acidification an Open-Ocean Syndrome? Understanding Anthropogenic Impacts on Seawater pH. *Estuaries and Coasts,* 36, 221-236.

Feely, R., Aline, S., Newton, J., Sabine, C., Warner, M. *et al*. 2010. The combined effects of ocean acidification, mixing, and respiration on pH and carbonate saturation in an urbanized estuary. *Estuarine, Coastal and Shelf Science*, 88, 442-449.

Flecha, S., Pérez, F.F., García-Lafuente, J., Sammartino, S., Ríos, A., Huertas, I.E., 2015. Trends of pH decrease in the Mediterranean Sea through high frequency observational data: indication of ocean acidification in the basin. *Scientific Reports,* 5, 16770. http://dx.doi.org/10.1038/srep16770

Friligos, N., 1982. Some Consequences of the Decomposition of Organic Matter in the Elefsis Bay, an Anoxic Basin. *Marine Pollution Bulletin,* 13 (3), 103-106.

Friligos, N., Barbetseas, S., 1990. Water masses and eutrophication in a Greek anoxic marine bay. *Toxicological & Environmental Chemistry,* 28 (1), 11-23.

Gattuso, J.P., Lavigne, H., Epitalon, J.M., 2014. Seawater Carbonate Chemistry with R Package 'seacarb'. https://cran.r-project.org/web/packages/seacarb/index.html (Accessed 11 April 2017)

Ge, C., Chai, Y., Wang, H., Kan, M., 2016. Ocean acidification: One potential driver of phosphorus eutrophication. *Marine Pollution Bulletin,* 115 (1-2), 149-153.

Grasshoff, K. Kremling, K. Ehrhardt, M., 1999. *Methods of Seawater Analysis*, Wiley VCH, 577 pp.

Gruber, N., 2011. Warming up, turning sour, losing breath: ocean biogeochemistry under global change. *Philosophical Transactions of the Royal Society of London,* 369, 1980-1996.

Hagens, M., Slomp, C., Meysmann, F.J.R., Seitaj, D., Harlay, J. *et al*., 2015. Biogeochemical processes and buffering capacity concurrently affect acidification in a seasonally hypoxic coastal marine basin. *Biogeosciences*, 12, 1561-1583.

Hassoun, A., Gemayel, E., Krasakopoulou, E., Goyet, C., Abboud-Abi Saab, M. *et al*., 2015. Acidification of the Mediterranean Sea from anthropogenic carbon penetration. *Deep-Sea Research,* 1 (102), 1-15.

Hee, C.A., Pease, T.K., Alperin, M.J., Martens, C.S., 2001. Dissolved organic carbon production and consumption in anoxic marine sediments: a pulsed-tracer experiment. *Limnology and Oceanography*, 46, 1908–1920.

Hernández-Ayón, J.M., Zirino, A., Dickson, A., Camiro-Vargas, T., Valenzuela-Espinoza, E., 2007. Estimating the contribution of organic bases from microalgae to the titration alkalinity in coastal seawaters. *Limnology and Oceanography*, Methods 5, 225-232.

Hofmann, A., Peltzer, E., Walz, P., Brewer, P., 2011. Hypoxia by degrees: Establishing definitions for a changing ocean. *Deep-Sea Research,* 58, 1212-1226.

Howes, E., Stemmann, L., Assailly, C., Irisson, J., Dima, M. *et al*., 2015. Pteropod time series from the North Western Mediterranean (1967-2003): impacts of pH and climate variability. *Marine Ecology Progress Series*, 531, 193-206.

Hu, X., Cai, W.J., 2011. An assessment of ocean margin anaerobic processes on oceanic alkalinity budget. *Global Biogeochemical Cycles*, GB 3003, 1-11.

Huesemann, M., Skillman, A., Crecelius, E., 2002. The inhibition of marine nitrification by ocean disposal of carbon dioxide. *Marine Pollution Bulletin,* 44, 142-148.

Hulth, S., Aller, R., Gilbert, F., 1999. Coupled anoxic nitrification/manganese reduction in marine sediments. *Geochimica et Cosmochimica Acta,* 63 (1), 49-66.

Ignatiades, L., Gkotsis.-Skretas, O. 2010. A Review on Toxic and Harmful Algae in Greek Coastal Waters (E. Mediterranean Sea). *Toxins*, 2 (5), 1019-1037.

Ingrosso, G., Giani, M., Cibic, T., Karuza, A., Kralj, M. *et al*., 2016a. Carbonate chemistry dynamics and biological processes along a river–sea gradient (Gulf of Trieste, northern Adriatic Sea). *Journal of Marine Systems,* 155, 35-49.

Ingrosso, G., Giani, M., Comici, C., Kralj, M., Piacentino, S. *et al*., 2016b. Drivers of the carbonate system seasonal variations in a Mediterranean gulf. *Estuarine, Coastal and Shelf Science,* 168, 58-70.

Kapsenberg, L., Alliouane, S., Gazeau, F., Mousseau, L., Gattuso, J.P., 2017. Coastal ocean acidification and increasing total alkalinity in the northwestern Mediterranean Sea. *Ocean Science*, 13, 411-416.

Karageorgis, A.P., Katsanevakis, S., Kaberi, H., 2009. Use of enrichment factors for the assessment of heavy metal contamination in the sediments of Koumoundourou Lake, Greece. *Water Air Soil Pollution*, 204, 243-258.

Kitidis, V., Laverock, B., McNeill, L., Beesley, A., Cummings, D. *et al*., 2011. Impact of ocean acidification on benthic and water column ammonia oxidation. *Geophysical research Letters,* 38, 1-5.

Krumins, V., Gehlen, M., Arndt, S., Van Cappellen, P., Regnier, P., 2013. Dissolved inorganic carbon and alkalinity fluxes from coastal marine sediments: model estimates for different shelf environments and sensitivity to global change. *Biogeosciences,* 10, 371-398.

Kulinski, K., Schneider, B., Hammer, K., Machulik, U., Schulz-Bull, D. 2014. The influence of dissolved organic matter on the acid–base system of the Baltic Sea. *Journal of Marine Systems,* 132, 106-115.

Laverock, B., Kitidis, V., Tait, K., Gilbert, J., Osborn, A. *et al*., 2014. Bioturbation determines the response of benthic ammonia-oxidizing microorganisms to ocean acidification. *Philosophical Transactions of the Royal Society of London*, 368 (B), 1-13.

Lee K., Tae-Wook K., Byrne R.H., Millero F.J., Feely R.A., Liu Y-M, 2010. The universal ratio of the boron to chlorinity for the North Pacific and North Atlantoc oceans. *Geochimica et Cosmochimica Acta* 74, 1801-1811.

Le Quéré, C., Moriarty, R., Andrew, R.M., Canadell, J.G., Sitch S. *et al*., 2015. Global Carbon Budget, *Earth System Science Data*, 7, 349-396, DOI:10.5194/essd-7-349-2015.

Luchetta, A., Cantoni, C., Catalano, G. 2010. New observations of CO_2-induced acidification in the northern Adriatic Sea over the last quarter century. *Journal of Chemical Ecology*, 26, 1-17.

Lueker, T.J., Dickson, A.G., Keeling, C.D., 2000. Ocean pCO_2 calculated from dissolved inorganic carbon, alkalinity, and equations for K1 and K2: validation based on laboratory measurements of CO_2 in gas and seawater at equilibrium. *Marine Chemistry,* 70, 105-119.

Moncheva, S., Gotsis-Skreta,s O., Pagou, K., Krastev, A., 2001. Phytoplankton Blooms in Black Sea and Mediterranean Coastal Ecosystems Subjected to Anthropogenic Eutrophication: Similarities and Differences. *Estuarine, Coastal and Shelf Science*, 53, 281-295.

Pavlidou, A., Kontoyiannis, H., Anagnostou, Ch., Siokou–Frangou, I., Pagou, K. *et al*., 2013. Biogeochemical Characteristics in the Elefsis Bay (Aegean Sea, Eastern Mediterranean) in Relation to Anoxia and Climate Changes, p. 161-202, *Chemical Structure of Pelagic Redox Interfaces: Observation and Modeling,* Yakushev. E., Springer-Verlag Berlin Heidelberg**.**

Pérez, F., Fraga, F., 1987a. A precise and rapid analytical procedure for alkalinity determination. *Marine Chemistry,* 21, 169-182.

Pérez F. F., Fraga F., 1987b. Association constant of fluoride and hydrogen ions in seawater. *Marine Chemistry,* 21, 161-168.

Pérez, F., Rios, A., Rellan, T., Alvarez, M., 2000. Improvements in a fast Potentiometric Seawater Alkalinity Determination. *Ciencias Marinas,* 26 (003), 463-478.

Riebesell, U., Fabry, V.J., Hansson, L., Gattuso, J-P., 2010. *Guide to best practices for ocean acidification research and data reporting*. Luxembourg, Publications Office of the European Union, 259 pp.

Rousselaki, E., Pavlidou, A., Michalopoulos, P., Kaberi, H., 2014. Nutrient fluxes in a hypoxic marine environment of East Mediterranean. p.2123. *In: Proceedings of the Goldschmidt Conference 2014, California, 8-13 June 2014*, Sacramento, California.

Schneider, A., Tanhua, T., Körtzinger, A., Wallace, D.W.R., 2010. High anthropogenic carbon content in the eastern Mediterranean. *Journal of Geophysical Research*, 115 (C12), 1-11, DOI: 10.1029/2010JC006171.

Scoullos, M., 1979. *Chemical Studies of the Gulf of Elefsis*, Greece. PhD thesis, University of Liverpool, Dept. Oceanography, 328 p.p.

Scoullos, M.,1983. Nitrogen micronutrients in an intermittently anoxic basin. p. 139-143.In: *Proceedings of VIes Journées d'études sur les pollutions marines en Méditerranée, Cannes, France 2-4 décembre 1982*, Secrétariat général de la C.I.E.S.M., 1983.

Scoullos, M., Rilley, J., 1978. Water circulation in the Gulf of Elefsis, Greece. *Thalassia Jugoslavica*, 14 (3/4), 357-370.

Solorzano, L., 1969. Determination of Ammonia in Natural Waters by the Phenolhypochlorite method, *Limnology and Oceanography*, 14 (5), 799-801.

Strong, A., Kroeker, K., Teneva, L., Mease, L.A., Kelly, P., 2014. "Ocean Acidification 2.0: Managing our Changing Coastal Ocean Chemistry." *Bioscience,* 64 (7), 581-592.

Thomas, H., Schiettecatte, L., Suykens, K., Kone, Y., Shadwick, E. *et al*., 2009. Enhanced ocean carbon storage from anaerobic alkalinity generation in coastal sediments. *Biogeosciences*, 6, 267-274.

Valderrama, J., 1981. The Simultaneous Analysis of Total Nitrogen and Total Phosphorus in Natural Waters. *Marine Chemistry*, 10, 109-122.

Wallace, R., Baumann, H., Grear, J., Aller, R., Gobler, R., 2014. Coastal ocean acidification: The other eutrophication problem. *Estuarine, Coastal and Shelf Science*, 148, 1-13.

Widdicombe, S., Dashfield, S., McNeil, C., Needham, H., Beesly, A. *et al*., 2009. Effects of CO_2 induced seawater acidification on infaunal diversity and sediment nutrient fluxes. *Marine Ecological Progress Series*, 379 (59), 59-75.

11ο Πανελλήνιο Συμπόσιο Θαλασσογραφίας + Αλιείας

ΠΡΑΚΤΙΚΑ

ΥΔΑΤΙΝΟΙ ΟΡΙΖΟΝΤΕΣ
ΠΡΟΚΛΗΣΕΙΣ & ΠΡΟΟΠΤΙΚΕΣ

Πανεπιστήμιο Αιγαίου, Μυτιλήνη, Λέσβος **13-17 ΜΑΪΟΥ 2015**

Φωτογραφία: Γιάννης Υφαντής / www.yfantis.com | Αφίσα: Μ. Κουμάτσος / Τμήμα Εκδόσεων, ΕΛΚΕΘΕ

11ο Πανελλήνιο Συμπόσιο Ωκεανογραφίας & Αλιείας

«Υδάτινοι Ορίζοντες: Προκλήσεις & Προοπτικές»

Μυτιλήνη, 13-17 Μαΐου 2015

Τμήμα Επιστημών της Θάλασσας, Πανεπιστήμιο Αιγαίου

Πρακτικά

Διοργάνωση:

Πανελλήνιος Σύλλογος Εργαζομένων στο ΕΛΚΕΘΕ

Σύλλογος Ερευνητών ΕΛΚΕΘΕ

Σε συνεργασία με το

Τμήμα Επιστημών της Θάλασσας, Πανεπιστημιακή Μονάδα Λέσβου, Πανεπιστήμιο Αιγαίου

Υπό την αιγίδα του Ελληνικού Κέντρου Θαλάσσιων Ερευνών

Με τη στήριξη της Γενικής Γραμματείας Αιγαίου & Νησιωτικής Πολιτικής

Implications of Hypoxia on Ocean Acidification effects in a Coastal Marine Environment: preliminary results of a Perturbation Experiment on C, N and P Biogeochemistry

Kapetanaki N.[1], Stathopoulou E.[1], Krasakopoulou E.[2], Zervoudaki S.[3], Dassenakis E.[1], Scoullos M.[1]
[1] *Laboratory of Environmental Chemistry, Department of Chemistry, University of Athens, nataliekapetanaki@gmail.com, estath@chem.uoa.gr, edasenak@chem.uoa.gr, scoullos@chem.uoa.gr*
[2] *Department of Marine Sciences, University of the Aegean, ekras@marine.aegean.gr*
[3] *Institute of Oceanography, Hellenic Centre for Marine Research, tanya@ath.hcmr.gr*

Abstract

Hypoxic coastal areas are considered of high-priority for Ocean Acidification (OA) research, because the co-occurrence and interaction of low oxygen with other environmental stressors i.e. elevated pCO_2, warming, and eutrophication may pose them at greater risk. In this work, a hypoxic coastal phenomenon exhibiting relatively reduced pH at the near bottom water layer was studied combining in situ and microcosm experiment measurements. It became clear that CO_2 content is not regulated by equilibrium with the atmosphere but by CO_2 produced by organic matter decomposition at the bottom layers, and that acidification could spread towards shallower depths and neighboring less affected areas. The combination of hypoxia and OA was found to affect the nitrification/denitrification processes, inhibiting the consumption of N species, probably leading to nitrogen accumulation and eutrophication.

Keywords: anoxia, synergistic effect, CO_2 addition, nutrients, microcosm experiment

1. Introduction

Ocean uptake of anthropogenic CO_2 alters ocean chemistry, leading to more acidic conditions and lower chemical saturation states (Ω) for calcium carbonate ($CaCO_3$) minerals, a process commonly termed “ocean acidification” (OA) (e.g. Caldeira & Wickett, 2005).

In coastal regions, the organic load input is high and the aerobic degradation of organic matter leads to a higher CO_2 production (Andersson et al., 2007). Hypoxic or anoxic systems are more acidic than normal marine environments, as the biochemical oxygen consumption is inextricably linked to the production of soluble inorganic carbon, including CO_2. In hypoxic coastal systems, the gas exchange balance with the atmosphere is not achieved, meeting extremely high pCO_2 levels (>1,000 μatm) (Feely et al., 2010), indicating that OA in such environments is already taking place and possibly spreading to adjacent systems.

Wallace et al. (2014) confirmed the hypothesis that the same processes promoting hypoxia also acidify the water column in coastal ecosystems. OA especially when combined with hypoxic phenomena has direct impacts on carbon biogeochemistry, causing dissolution of existing sedimentary carbonates (Andersson et al., 2007) and alkalinity release in the supernatant water column, plus alterations on nutrient cycles, with decline in nitrification rates (Beman et al., 2011). Therefore, experiments combining acidification and low oxygen conditions are essential to fully understand and correlate the various observations in coastal environments.

2. Materials and methods

The main scope of this experimental research was to investigate the nutrient and carbon cycle of an anoxic environment under acidification conditions. The aim of the experiment was to simulate the biogeochemistry and physicochemical conditions of the natural system including consideration of all vital parameters. The study area is the Elefsis Bay (Attica, Greece), a relatively shallow, semi-closed industrialised coastal system, which, due to the increased organic matter input and its hydromorphological characteristics, result in intermittently anoxic conditions during summer (Scoullos, 1983a). The field sampling took place in September 2014 with the R/V AEGAEO (HCMR). Hydrographical data were recorded through CTD measurements. Seawater and surface sediment from the deepest-anoxic-station (33m) were collected untreated and placed in four 25L Nalgene

Polycarbonate containers (at a proportion 80% to 20% respectively) in a thermostatic chamber (17,5°C). The seawater-sediment systems were left to equilibrate for a week in an atmosphere of Ar gas in order to maintain the anoxic field conditions. This was followed by the four weeks period of the experiment where CO_2 was also added to the microcosms; the stability of pH was maintained using a continuous flow system (IKS Aquastar, IKS ComputerSysteme GmbH) which automatically adjusted CO_2 gas addition to the microcosms. The measured pH values by the IKS system were corrected with the parallel use of a laboratory pHmeter (Jenway 3310) calibrated in NBS scale; the pH values were converted in total H^+ scale (pH_T) (Dickson, 2007). The pH values selected for the experiment conditions were (a) for the control conditions (C) the pH value measured during sampling, and (b) for the ocean acidification conditions (OA) the pH value predicted for the year 2300 (6,80 NBS), for latitudes corresponding to Mediterranean (Caldeira & Wickett, 2005). Each one of the two conditions was applied in two replicate tanks. Field (during the cruise) and microcosms (every 2 days) were sampled for the determination of the following parameters: dissolved oxygen (DO; Winkler Method), dissolved organic carbon (DOC; High Temperature Catalytic Oxidation on a Shimadzu 5000 total organic carbon analyser), total alkalinity (A_T) (SMWW 2320), ammonia, nitrite, nitrate and phosphate (spectrophotometrically with a Varian Cary 1E UV-visible spectrophotometer; Grasshoff et al., 1999). Based on pH_T and A_T values the rest of carbonate system parameters were calculated through the R package *seacarb* (Lavigne & Gattuso, 2011).

3. Results/Discussion

In Elefsis Bay, the near bottom physicochemical parameters (Table 1) indicate a quite acidic and reducing environment. The value of 7,75 pH units corresponds approximately to the predicted pH levels for 2100, while the negative redox potential along with the minimal DO concentrations, reflect the anoxic conditions prevailing in the deeper parts of the area during summer.

Table 1. pH (in NBS scale), Redox Potential (mV) and Dissolved Oxygen (DO; in mL/L), PO_4^{3-} (μmol P/L), NH_4^+, NO_3^- and NO_2^- (μmol N/L) concentrations and DIN:DIP ratio for seawater field samples (absolute values).

	pH	Redox	DO	PO_4^{3-}	NH_4^+	NO_3^-	NO_2^-	DIN:DIP
Elefsis - surface	8,16	112,9	5,25	0,20	2,24	0,14	0,14	12,9
Elefsis -bottom	7,75	-50,7	0,84	2,20	23,91	0,91	0,08	11,3
Ranges from Time series (1987-2008) in Elefsis bottom waters in September (Pavlidou *et al.* 2013)	-	-	0,00-2,00	1,00-7,00	8,00-18,00	0,00-2,50	0,50-0,60	0,17-6,44

NO_3^- and NO_2^- show moderate variations from surface to bottom, within the range of the time series values (Table 1; Pavlidou *et al.*, 2013). On the contrary, NH_4^+, was found ten times higher than surface, as has been previously reported (Scoullos, 1983b), along with increased concentration and accumulation of PO_4^{3-}, due to organic matter degradation and redox processes at the sea bottom. During the experiment (not shown), in C conditions, NO_3^- and NO_2^- show similar trend with almost exponential rise till the 15th day (to 15 μmol N/L and 12 μmol N/L, respectively) followed by significant decline to values similar to the ones determined in the field after day 25. Contrariwise, in OA conditions, NO_3^- and NO_2^- appear to rise evenly throughout the duration of the experiment (to 5 μmol N/L and 3 μmol N/L, respectively). NH_4^+ concentration, in C conditions, drops significantly to ~1μmol/L, while in OA conditions it declines less dramatically until it reaches a medium value of 8 μmol N/L. PO_4^{3-} show similar gradually declining trends in both OA and C conditions, from 3 to 2 μmol P/L and 2 to 1 μmol P/L respectively. Widdicombe et al. (2009) reported that, in acidification experiments, in the presence of sandy sediments, pH decrease caused inhibition of NO_3^- and NO_2^- release from sediment to the water column, with parallel increase in NH_4^+ release and no impact in

PO_4^{3-} flux. In C conditions, sediments have been previously found to act as sources of NO_3^- and NO_2^-, having different pattern regarding nitrification-denitrification processes in relation to OA conditions.

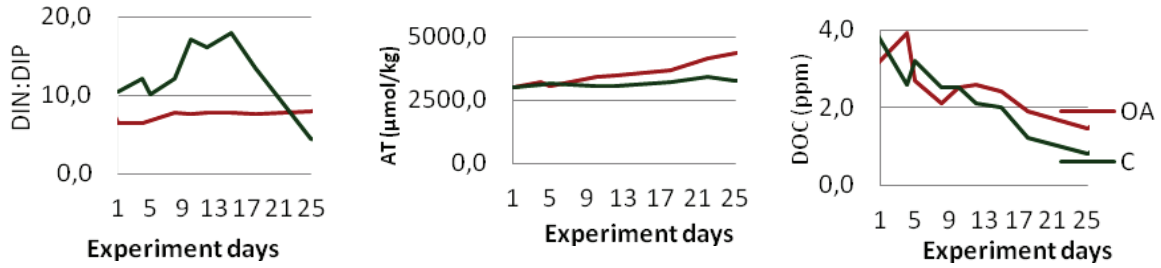

Fig. 1. DIN:DIP ratio, Total Alkalinity (A_T) and DOC variations during the experiment for the OA (ocean acidification) and C (control) conditions.

It is noteworthy that the DIN:DIP ratio in Elefsis Bay (surface) varies between 20,0 in winter and 13,7 during summer, whereas it decreases in anoxic bottom to 4,2 (Pavlidou et al., 2013). In this experiment (Fig. 1), during C conditions, the DIN:DIP ratio varies between 10,0 and 18,0 until the 15th day, and after it decreases sharply to below 5,0. Such low ratios may indicate N_2 or N_2O gas release. In minimum oxygen conditions denitrification and anammox take place having an additional indirect implication on the carbon reservoir. The resulting decrease in N reserve causes reduction of primary production limiting thus the CO_2 ocean sequestration (Paulmier et al., 2011). On the contrary, during OA conditions, there were little DIN:DIP variations until the ratio remained constant at 8,0. CO_2 increase is known to cause inhibition of denitrification (Paulmier et al., 2011) and perhaps also in anammox rates that could result in build up of N which when dispersed after re-oxygenation could induce eutrophication phenomena with potential detrimental impacts on aquatic systems.

Table 2. Carbonate system parameters as calculated by *seacarb* package for field (absolute values) and OA and C microcosms (mean values, standard deviations) (A_T, CO_2, HCO_3^-, CO_3^{2-}, DIC all in μmol/kg, pCO_2 in μatm; $\Omega_{ar.}$: aragonite saturation state, $\Omega_{calc.}$: calcite saturation state).

		pH_T	A_T	pCO_2	CO_2	HCO_3^-	CO_3^{2-}	DIC	$\Omega_{ar.}$	$\Omega_{calc.}$
Elefsis - surface		8,03	2974,0	523	13,7	2237,5	306,8	2558,0	4,79	7,19
Elefsis - bottom		7,62	2974,9	1539	52,4	2728,3	100.6	2881,2	1,51	2,33
OA	mean	6,90	3595,1	14024	476	3500,6	40.5	4002,2	0,61	0,94
	st.dev	0,42	569,8	8227	279	543,1	50.7	670,3	0,76	1,18
C	mean	7,24	3356,2	7902	269	3174,3	76,9	3519,9	1,16	1,79
	st.dev	0,30	329,6	4639	158	286,5	48,2	375,8	0,73	1,12

The bottom dissolved CO_2 concentration and the pCO_2 in Elefsis Bay (Table 2) follow the same pattern, appearing to triple in relation to surface values, indicating that the CO_2 content in the sea bottom is not regulated by an equilibrium with the atmosphere but by the decomposition of organic carbon in the sediment and the lower parts of the stratified water column.

During the experiment, DO exhibited only slight variations as the anoxic conditions were maintained by supplying inert gas (Ar) to the system. A_T in OA conditions increases (Fig. 1), as a result of enhanced alkalinity release from carbonate dissolution of the sediment, while both OA and C conditions are subject to A_T additions due to anaerobic sulphate reduction. DOC concentrations in both conditions are higher than the field values (1,5 ppm). This could be attributed to increased excretions as a result of intense biological stress imposed to condition alterations; in C conditions (Fig. 1), showed a steady decline during the experiment while in OA conditions, DOC content initially increased and then followed a declining pattern, similar to that of the C conditions though, with

higher final concentration. The saturation state of both carbonate minerals (Ω_{ar}, $\Omega_{calc.}$) in OA conditions (Table 2), are calculated as <1, which is also evident from the decreased experimental CO_3^{2-} ions values compared to the ones of the field, indicating undersaturation of the system in aragonite and calcite. Extrapolating the experimental results to the field, the observed decrease in Ω_{ar} and $\Omega_{calc.}$ would have deleterious impact on the growth and survival of calcifying organisms.

4. Conclusions

The results of this research showed that anoxic phenomena in coastal systems may result in increased pCO_2 and thus decreased pH values in their deeper layers, which could lead to acidification spreading towards shallower depths and adjacent areas. The combination of anoxia and OA results in alkalinity increase, because of carbonate dissolution from sediment and anaerobic sulphate reduction, while overlying water becomes corrosive for both carbonate minerals. Lastly, OA and anoxia in synergy affect nitrification and denitrification processes, preventing the consumption of N species, thus leading to nitrogen accumulation promoting thus eutrophication development after re-oxygenation and water mixing.

5. Acknowledgments

Part of this research was funded by the EU Research Project "ARISTEIA- EXCELLENCE 640" (2012-2015) entitled "*Integrated Study of Trace Metals Biogeochemistry in the Coastal Marine Environment* (ISMET-COMAREN)". Part of this project is implemented under the Operational Programme "Education and Lifelong Learning" and funded by European Social Fund and national resources. Authors thank the Athens Water Supply and Sewerage Company for supporting the field sampling.

6. References

Andersson, A., Bates, N. and Mackenzie, F. 2007. Dissolution of Carbonate Sediments Under Rising pCO_2 and Ocean Acidification: Observations from Devil's Hole, Bermuda. *Aquatic Geochemistry,* 13, 237-264.

Beman, M., Chow, C., King, A., Feng, Y., Fuhrman, J. *et al*. 2011. Global declines in oceanic nitrification rates as a consequence of ocean acidification. *PNAS*, 108, 208-213

Caldeira, K. and Wickett, M. 2005. Ocean Model predictions of chemistry changes from carbon dioxide emissions to the atmosphere and ocean. *Journal of Geophysical Research*, 110, 1-12.

Clesceri, L., Greenber, A., Eaton, A. (eds.) 1999. *Standard Methods for the Examination of Water and Wastewater*, 20th edition, American Public health Association.

Dickson A., Sabine, C. and Christian, J. 2007. *Guide to best practices for ocean CO2 measurements.* Sidney, British Columbia, North Pacific Marine Science Organization, 176pp. (PICES Special Publication, 3).

Feely, R.A., Aline, S.R., Newton, J., Sabine, C.L., Warner, M. *et al*. 2010 The combined effects of ocean acidification, mixing, and respiration on pH and carbonate saturation in an urbanized estuary. *Estuarine, Coastal, and Shelf Science*, 88, 442–449.

Gattuso, J.P., Epitalon, J.M., Lavigne, H., Orr, J., Gentili, B. *et al*. 2011. Seawater Carbonate Chemistry with R Package 'seacarb'. http://CRAN.R-project.org/package=seacarb

Grasshoff, K., Kremling, K., Ehrhardt, M. 1999. *Methods of Seawater Analysis*, Wiley VCH, 1999, pp. 159–226.

Pavlidou, A., Kontoyiannis, H., Anagnostou, Ch., Siokou–Frangou, I., Pagou, K., *et al*. 2013. Biogeochemical Characteristics in the Elefsis Bay (Aegean Sea, Eastern Mediterranean) in Relation to Anoxia and Climate Changes. p. 161-202. In: *Chemical Structure of Pelagic Redox Interfaces: Observation and Modeling,* Yakushev. E., Springer-Verlag, Berlin Heidelberg.

Paulmier, A., Ruiz-Pino, D. and Garcon, V. 2011. CO_2 maximum in the oxygen minimum zone (OMZ). *Biogeosciences*, 8, 239-252.

Scoullos, M. 1983a. Trace Metals in a Landlocked Intermittently Anoxic Basin, p. 351–365. In: *Trace Metals in Sea Water.* Wong, C.S., Bouyle, E., Bruland, K.W., Burton, J.D., Goldberg, E.D. (eds). Plenum Press, NY, USA.

Scoullos, M. 1983b. Nitrogen micronutrients in an intermittently anoxic basin. Vies J. Etud. Poll., 139-143, Cannes, France.

Wallace R., Baumann H., Grear J., Aller R. and Gobler R. 2014. Coastal ocean acidification: The other eutrophication problem. *Estuarine, Coastal and Shelf Science*, 148, 1-13.

Widdicombe S., Dashfield S.L., McNeil C.L., Needham H.R., Beesly A. *et al*. 2009. Effects of CO_2 induced seawater acidification on infaunal diversity and sediment nutrient fluxes. *Marine Ecology Progress Series,* 379 (59), 59-75.

Sustainable Mediterranean

MEDITERRANEE DURABLE • ΒΙΩΣΙΜΗ ΜΕΣΟΓΕΙΟΣ • MEDITERRANEO SOSTENIBLE • المتوسطية المستدامة

Issue No 71, Dec 2015

Proceedings of the International Conference

"Environmental Perspectives of the Gulf of Elefsis
A Mediterranean case study where Science meets the Society"

Elefsis, Greece, 11-12 September 2015

This issue of Sustainable Mediterranean is co-produced by the City of Elefsis, UNEP/MAP, the Ministry of Environment and Energy, the University of Athens and MIO-ECSDE.

UNEP MAP

40 Years TOGETHER FOR A SUSTAINABLE MEDITERRANEAN

Environmental Chemistry Laboratory

United Nations Educational, Scientific and Cultural Organization

UNESCO Chair on Sustainable Development Management and Education in the Mediterranean HELLENIC REPUBLIC National and Kapodistrian University of Athens

MINISTRY OF RECONSTRUCTION OF PRODUCTION, ENVIRONMENT & ENERGY

MIO-ECSDE

Nutrient cycle alterations in Elefsis Gulf under simulated ocean acidification conditions

Kapetanaki, N.[1], Stathopoulou, E.[1], Pavlidou, A.[2], Zachioti, P.[2], Zervoudaki, S.[2], Krasakopoulou, E.[3], Dassenakis, E.[1], Scoullos, M.[1]

[1]Laboratory of Environmental Chemistry, Department of Chemistry, University of Athens, nataliekapetanaki@gmail.com, estath@chem.uoa.gr, edasenak@chem.uoa.gr, scoullos@chem.uoa.gr
[2]Institute of Oceanography, Hellenic Centre for Marine Research, aleka@hcmr.gr, yioulaz@hcmr.gr, tanya@ath.hcmr.gr
[3]Department of Marine Sciences, University of the Aegean, ekras@marine.aegean.gr

Abstract

Hypoxic coastal areas are considered as high-priority for Ocean Acidification (OA) research, because the co-occurrence and interaction of low oxygen with other environmental stressors, such as elevated pCO_2, warming and eutrophication, may put them at greater risk. In this work, a hypoxic coastal phenomenon exhibiting relatively reduced pH at the near bottom water layer was studied, combining in situ and microcosm experiment measurements. The results revealed that CO_2 content is not regulated by equilibrium with the atmosphere, but by CO_2 produced by organic matter decomposition at the bottom layers, and that acidification could spread towards shallower depths and neighboring less affected areas. The combination of hypoxia and OA was found to affect the nitrification/denitrification processes, inhibiting the consumption of N species, probably leading to nitrogen accumulation and eutrophication.

Keywords: experiment, microcosm, anoxia, nitrogen, phosphorus.

Introduction

Ocean uptake of anthropogenic CO_2 alters ocean chemistry, leading to more acidic conditions and lower chemical saturation states (Ω) for calcium carbonate ($CaCO_3$) minerals, a process commonly termed "ocean acidification" (OA) (e.g. Caldeira and Wickett, 2005). In coastal regions, the organic load input is usually high and the aerobic degradation of organic matter leads to a higher CO_2 production (Andersson *et al*., 2007). Hypoxic or anoxic systems are more acidic than normal marine environments, as the biochemical oxygen consumption is inextricably linked to the production of soluble inorganic carbon, including CO_2. In hypoxic coastal systems, the gas exchange balance with the atmosphere is not achieved, meeting extremely high pCO_2 levels (>1,000 μatm) (Feely *et al*., 2010), indicating that OA in such environments is already taking place and possibly spreading to adjacent systems.

Wallace *et al*. (2014) confirmed the hypothesis that the same processes promoting hypoxia also acidify the water column in coastal ecosystems. OA has direct impacts on carbon biogeochemistry, causing dissolution of existing sedimentary carbonates (Andersson *et al*., 2007) and alkalinity release in the supernatant water column, plus alterations on nutrient cycles, with decline in nitrification rates (Beman *et al*., 2011). Therefore, experiments combining acidification and low oxygen conditions are essential to fully understand and correlate the various observations in coastal environments.

The main scope of this experimental research was to investigate the nutrient cycle of an anoxic environment under acidification conditions. The aim of the experiment was to simulate the biogeochemistry and physicochemical conditions of the natural system including consideration of all vital parameters.

Methodologies

This research was conducted in Elefsis Gulf (Attica, Greece), a relatively shallow, semi-closed industrialised coastal system, which, due to the increased organic matter input and its hydromorphological characteristics, has intermittently anoxic conditions during summer (Scoullos, 1983). Field sampling took place in September 2014 with the R/V AEGAEO (HCMR). Hydrographical data

were recorded through CTD measurements. Seawater and surface sediment from the deepest-anoxic-station (33m) was collected untreated and placed in four 25L Nalgene Polycarbonate containers (at a proportion 80% to 20%, respectively) in a thermostatic chamber (17.5°C). The seawater-sediment systems were left to equilibrate for a week in Ar atmosphere in order to maintain the anoxic field conditions. This was followed by the four week period of the experiment where CO_2 was also added to the microcosms.The stability of pH was maintained using a continuous flow system (IKS Aquastar, IKS Computer Systeme GmbH) which automatically adjusted CO_2 gas addition to the microcosms. The measured pH values by the IKS system were corrected with the parallel use of a laboratory pH meter (Jenway 3310) calibrated in NBS scale. The pH values selected for the experiment conditions were: (a) for the Control conditions (C), the pH value measured during sampling, and (b) for the Ocean Acidification conditions (OA), the pH value predicted for the year 2300 (6,80 NBS), for latitudes corresponding to the Mediterranean (Caldeira & Wickett, 2005). Each one of the two conditions was applied in two replicate tanks. Seawater from field (during the cruise) and microcosms (every 2 days) was sampled and filtered through 0.45μm pore size membranes, for the determination of ammonia, nitrite, nitrate phosphate, silicate, total dissolved nitrogen (TDN) and total dissolved phosphorus (TDP) (spectrophotometrically with a Varian Cary 1E UV-visible spectrophotometer; Grasshoff *et al*., 1999). Supplementary analyses included dissolved oxygen (DO; Winkler Method), dissolved organic carbon (DOC; High Temperature Catalytic Oxidation on a Shimadzu 5000 total organic carbon analyser), total alkalinity (A_T) (SMWW 2320), calculation of the rest of the carbonate system parameters based on pH_T and A_T values (in combination with PO_4^{3-} and SiO_4 determinations) through the R package seacarb, preconcentration method for the determination of trace metals with ICP-MS.

Results and Discussion

The near bottom physicochemical parameters shown in Table 1, indicate a reducing coastal environment of quite increased acidity. The value of 7,75 pH units corresponds approximately to the predicted pH levels for 2100 (Caldeira & Wickett, 2005), while the negative redox potential along with the minimum DO concentrations, reflect the anoxic conditions prevailing in the deeper parts of the area during summer. This enhanced CO_2 near-bottom content is not regulated by equilibrium with the atmosphere but by the decomposition of organic matter in the sediment and the lower parts of the stratified water column.

Nitrate and nitrite concentrations show moderate variations from surface to bottom, within the range of the time series values (Table 1). On the contrary, ammonium concentrations in the bottom were found significantly higher than at the surface, along with increased concentration and accumulation of phosphates and silicates. The main process affecting nitrogen species under low oxygen conditions in Elefsis is denitrification; in the absence of oxygen, nitrates become the most abundant respiratory oxidant in seawater, converting them to nitrogen gases released from the system. The ammonia, phosphates and silicates accumulation, resulting from organic matter oxidation are followed by nitrates, at first, and sulfates and MnO_2 reduction, then, leading to H_2S and dissolved Mn accumulation in the bottom water. For phosphorus, it seems that there is an increase in sediment-released phosphates from Fe-oxyhydroxides, to the pore water and subsequently to the water column via diffusion, resuspension or bio-irrigation mechanisms. This study, corroborates with previous findings (Scoullos, 1983, Pavlidou *et al*., 2013) regarding elevated $NH_4^{+,}$ PO_4^{3-} and SiO_4 near-bottom concentrations.

During the experiment, DO exhibited insignificant variations, as the anoxic conditions were maintained by supplying inert gas (Ar) to the system. Nitrates and nitrites show a similar trend in C conditions, during the experiment (not shown), with almost exponential rise till the 15th day (to 15 μmol/L and 12 μmol/L, respectively) followed by significant decline to values similar to the ones determined in the field after day 25. Contrariwise, in OA conditions, NO_3^- and NO_2^- appear to rise evenly throughout the duration of the experiment to final values of 5.1 μmol/L and 2.7 μmol/L, respectively. NH_4^+ concentrations, in C conditions, drop significantly to ~1μmol/L, while in OA conditions they decline less dramatically until they reach a medium value of 8 μmol/L. It seems that under enhanced OA conditions, even while anoxia prevails, nitrification is the dominant process taking place, consuming ammonia with subsequent production of nitrites followed by nitrites oxidation, to nitrates. Nitrite and nitrate concentrations, throughout the experiment, show that these are the main stable inorganic N species. PO_4^{3-} show similar gradually declining trends in both OA and C conditions, from 3 to 2 μmol/L and 2 to 1 μmol/L, respectively, which also indicates an elevated P reserve in the system under more acidified conditions. SiO_4 concentrations present minimum variations throughout the experiment for both conditions. Widdicombe *et al*. (2009) has reported that, in acidification experiments, in the presence of sandy sediments, pH decrease caused inhibition of NO_3^- and NO_2^- release from sediment to the water column, with parallel increase in NH_4^+ release and no impact in PO_4^{3-} and SiO_4 flux. In C conditions, sediments have been previously found to act as sources of NO_3^- and NO_2^-, having different pattern regarding nitrification-denitrification processes in relation to OA conditions. TDN appears to have the same gradually increasing trend for both OA and C conditions until the 12th day, followed by decreasing values with higher final values for OA conditions. TDP also presents the same behavior for both conditions until the 12th day, with higher final values for OA conditions.

It is noteworthy that the DIN:DIP ratio in Elefsis Bay (surface) varies between 20 in winter and 13.7 during summer, whereas it decreases in an anoxic bottom to 4.2 (Pavlidou *et al*., 2013). DIN in the water column appears to increase during summer, whereas in winter it decreases followed by elevated DON concentrations, indicating oxidation mechanisms of organic nitrogen to inorganic species during the warm period. (Pavlidou, 2013) In this

	pH	Redox	DO	PO4 3-	SiO4	NH4+	NO3-	NO2-	TDN	TDP	DIN:DIP
Elefsis - surface	8,16	112,9	4,62	0,011	0,797	0,331	0,322	0,100	12,247	2,938	66,40
Elefsis -bottom	7,75	-50,7	0,00	3,684	56,17	9,722	0,177	0,072	22,387	4,001	2,71
Ranges from Time series (1987-2008) in Elefsis bottom waters in September (Pavlidou et al. 2013)	-	-	0,00-2,00	1,00-7,00	14,5-43,5	8,00-18,00	0,00-2,50	0,50-0,60			0,17-6,44

Table 1: pH (in NBS scale), Redox Potential (mV) and Dissolved Oxygen (DO; in mL/L), PO_4^{3-} and TDP (μmol/L), NH_4^+, NO_3^- NO_2^- and TDN (μmol /L), SiO_4 (μmol /l) concentrations and DIN:DIP ratio for seawater field samples (absolute values).

experiment (Fig. 1), during C conditions, the DIN:DIP ratio varied between 10 and 18 until the 15th day, and after it decreased sharply to below 5. In OA conditions, the ratio is stabilized between 7.7-8.0 indicating a preserved elevated content of inorganic nitrogen species and phosphates in the water column in relation to C conditions. In parallel with phosphates release from the sediment, these two processes become the controlling factor of DIN:P ratios in the near-bottom waters. However, it becomes clear that under OA conditions, nitrites and nitrates are favored against ammonia

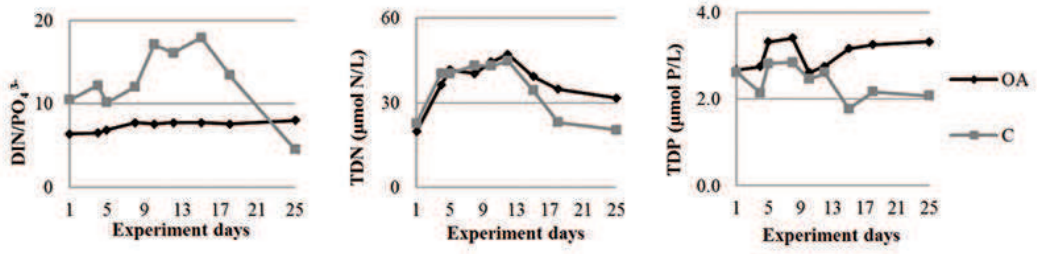

Fig.1: DIN:DIP ratio, TDN and TDP variations during the experiment for the OA and C conditions.

throughout the experiment, indicating decreased denitrification mechanisms and probably enhanced nitrification processes, in the presence of more acidic environments. This dissolved N content preservation is also obvious through TDN and TDP determinations in OA conditions with elevated final values related to C conditions. From previous studies, in minimum oxygen conditions denitrification and anaerobic ammonia oxidation (anammox) take place having an additional indirect implication on the carbon reservoir, resulting in decreased N reserve and causing reduction of primary production along with limited CO_2 ocean sequestration (Paulmier *et al*., 2011). CO_2 increase, though, is known to cause inhibition of denitrification (Paulmier *et al*., 2011) and perhaps also in anammox rates that could result in build-up of N.

Conclusions

The results of this research showed that anoxic phenomena in coastal systems result in significantly decreased pH values in their deeper layers. This enhanced CO_2 near-bottom content is not regulated by an equilibrium with the atmosphere but by the decomposition of organic matter in the sediment and the lower parts of the stratified water column, a process that could lead to acidification spreading towards shallower depths and adjacent areas. While phosphates and silicates appear to be slightly affected or invariable, the combination of anoxia and OA conditions seem to increase nitrification processes against denitrification, preventing the consumption of inorganic N species, thus leading to nitrogen accumulation, possibly triggering and promoting eutrophication development after re-oxygenation and water mixing.

Acknowledgments

Part of this research was co-financed by the European Union (European Social Fund) and National Funds (Hellenic General Secretariat for Research and Technology) in the framework of the project *ARISTEIA I*, 640 "*Integrated Study of Trace Metals Biogeochemistry in the Coastal Marine Environment*", within the "Lifelong Learning Programme". Part of this project is implemented under the Operational Programme "Education and Lifelong Learning" and funded by the European Union (European Social Fund) and national resources. The authors thank the Athens Water Supply and Sewerage Company (EYDAP SA) for supporting the field sampling of their study.

References

Andersson, A., Bates, N., Mackenzie, F., 2007. Dissolution of Carbonate Sediments Under Rising pCO_2 and Ocean Acidification: Observations from Devil's Hole, Bermuda, *Aquatic Geochemistry*, 13, 237-264.

Beman, M., Chow, C., King, A., Feng, Y., Fuhrman, J., Andersson, A., Bates, N., Popp, B., Hutchins, D., 2011. Global declines in oceanic nitrification rates as a consequence of ocean acidification. PNAS 108, 208-213.

Caldeira, K. and Wickett, M., 2005. Ocean Model predictions of chemistry changes from carbon dioxide emissions to the atmosphere and ocean. *Journal of Geophysical Research*, 110, 1-12.

Feely, R.A., Alin, S.R., Newton, J., Sabine, C.L., Warner, M., Devol, A., Krembs, C., Maly, C., 2010 The combined effects of ocean acidification, mixing, and respiration on pH and carbonate saturation in an urbanized estuary. *Estuarine, Coastal, and Shelf Science*, 88, 442–449.

Grasshoff, K., Kremling, K., Ehrhardt, M., 1999. Methods of

Seawater Analysis, Wiley VCH, pp. 159–226.
Pavlidou, A., Kontoyiannis, H., Anagnostou, Ch., Siokou–Frangou, I., Pagou, K., *et al*., 2013, Biogeochemical Characteristics in the Elefsis Bay (Aegean Sea, Eastern Mediterranean) in Relation to Anoxia and Climate Changes, Chemical Structure of Pelagic Redox Interfaces: Observation and Modeling, Yakushev. E., Springer-Verlag Berlin Heidelberg, 161-202
Paulmier, A., Ruiz-Pino, D., Garcon, V., 2011. CO_2 maximum in the oxygen minimum zone (OMZ). *Biogeosciences*, 8, 239-252.
Scoullos, M., 1983. Nitrogen micronutrients in an intermittently anoxic basin. *Vies J. Etud. Poll.*, pp. 139-143, Cannes, France.
Wallace, R., Baumann, H., Grear, J., Aller, R., Gobler, R., 2014. Coastal ocean acidification: The other eutrophication problem. *Estuarine, Coastal and Shelf Science*, 148, 1-13.
Widdicombe, S., Dashfield, S.L., McNeil, C.L., Needham, H.R., Beesly, A., *et al*. 2009. Effects of CO_2 induced seawater acidification on infaunal diversity and sediment nutrient fluxes. *Marine Ecology Progress Series* 379(59): 59-75.

Sampling in the Gulf of Elefsis in the 80s.

Sea bottom sediments of Elefsis Gulf: A potential secondary source of metals under simulated ocean acidification conditions

Tziava, A., Stathopoulou, E.[1], Kapetanaki, N., Dassenakis, E., Scoullos, M.

Laboratory of Environmental Chemistry, Department of Chemistry, University of Athens, aspatziava@gmail.com, estath@chem.uoa.gr, nataliekapetanaki@gmail.com, edasenak@chem.uoa.gr, scoullos@chem.uoa.gr

Abstract

Hypoxic coastal areas are considered as high-priority systems for Ocean Acidification (OA) research, because the co-occurrence and interaction of low oxygen with other environmental stressors, such as elevated pCO_2, warming and eutrophication, may put them at greater risk. In this work, an anoxic coastal phenomenon exhibiting relatively reduced pH at the near bottom water layer was studied. *In-situ* and microcosm experiment measurements, simulating OA conditions, were conducted in order to assess the fate of dissolved trace metals that could either sink towards the sediment or be released towards the water column. OA conditions seem to induce the release of Al, Ni, Cd, Fe, Mn and As from the sediment while, in combination with anoxia, a restriction in this dissolution mechanism was found. Cr, Zn and Pb seem to follow a sink type mechanism under more acidified conditions while, in addition to anoxia, a source type mechanism is revealed. Hg seems to follow a source type mechanism under OA in any case. Regarding Fe species, it becomes evident that Fe (II) is the dominant species, indicating an increased stability as a result of acidified conditions.

Keywords: experiment, arsenic, iron, manganese, mercury, copper.

Introduction

Ocean uptake of anthropogenic CO_2 alters ocean chemistry, leading to more acidic conditions and lower chemical saturation states (Ω) for calcium carbonate ($CaCO_3$) minerals, a process commonly termed "ocean acidification" (OA). OA, especially when combined with hypoxic phenomena (Melzner, 2013), affects carbon and nutrient biogeochemistry, dissolved trace metal species and complexes' stability and sediment mineral phases, causing changes in benthic fluxes in the sediment-water interface (Ardelan *et al*., 2009, Atkinson *et al*. 2007, Scoullos, 1983) . Therefore, experiments combining acidification and low oxygen conditions are essential to fully understand and correlate the aforementioned observations in coastal environments (Melzner, 2013).

The aim of this project was to study the impacts of ocean acidification on a coastal industrialised system (Elefsis Gulf), affected by intermittent anoxic conditions, in order to distinguish if sediments act like a source or a sink for trace metals. Furthermore, it was evaluated, whether these sediment processes are imposed to alterations, as a result of acidification combined with intermittent anoxia.

Materials and methods

Elefsis Gulf is a small sized coastal system characterized by shallow depths (68 km^2, maximum depth 33 m) and limited communication with the wider Saronic (Scoullos, 1983). Due to the increased organic load and physiographic region, the inflow and the water exchange is restricted, resulting in the development of hypoxic/anoxic conditions during summer (intermittently anoxic) (Scoullos, 1983). Two laboratory experiments (I concerning only ocean acidification impact and II combining anoxia with ocean acidification) were conducted using experiment microcosms (25L), containing water and sediment from the greater depth (33 m) of the Gulf (at a proportion 80% to 20%, respectively). In both experiments, the stability of pH was maintained using a continuous flow system (IKS Aquastar, IKS Computer Systeme GmbH), which automatically adjusted CO_2 gas addition to the systems; in experiment II, the anoxic field conditions were also maintained by Ar supply. During exp. II, on the 25th day of the experiment, the Ar supply was ceased and the systems were left to re-oxygenate until day 33 in order to fully simulate the intermittent anoxic conditions of the study area. The pH values selected for the experiment conditions were (a) for the control conditions (C) the pH value measured during sampling

(7.85 for exp. I – 7.75 for exp. II), and (b) for the ocean acidification conditions (OA) the pH value predicted for the year 2300 (6.80) for latitudes corresponding to the Mediterranean (Caldeira and Wickett, 2005). Each one of the two conditions was applied in two replicate tanks. Water samples were collected daily during the four week period of the experiment; sediments were collected and treated according to EPA 3050 for final measurement with ICP-MS for As, Cr, Cu, Ni and Pb using the Collision Cell Technology (CCT) mode of the instrument, FAAS for Al, Fe, Mn and Zn, GFAAS for Cd and CVAAS for Hg. A colorimetric determination of Fe species was also applied for wet sediment samples (combined method of Bloom, 2004 and GEOMAR). All determinations were checked with Certified Reference Material treatment and analysis. Supplementary analyses included organic and inorganic carbon determinations (TOC and $CaCO_3$), nutrients' determinations (TP, TN) and mineral composition with XRF,XRD analyses.

Results

In exp. I, sedimentary Cr appears to decrease under OA conditions, whereas in exp. II, this process seemed to be restricted in OA along with anoxic conditions. This decrease in Cr particulate form, could be attributed to an increase in Cr solubility as a result of enhanced CO_2; in C conditions no such variation was observed indicating perhaps a restrictive mechanism in Cr solubilization.

Sedimentary Al appeared to slightly decrease in exp. I, under OA conditions, indicating perhaps release from the sediment but in the second experiment, a sharp increase was observed in both conditions. For Cr and Al, from previous experiments (Ardelan, 2009), it was found that under enhanced CO_2 concentrations, they are both effectively removed in dissolved forms as a result of increased solubility.

Ni also presented a similar trend to Cr, with a decrease in sedimentary concentrations in exp. I, under OA conditions; in exp. II, in OA conditions combined with anoxia, particulate Ni seemed to sink on sediment surface. From previous experiments, Ni has been found to dissociate more rapidly from the sediment into more labile phases towards the pore water and the supernatant seawater, which was confirmed in this study. Thus, the minimum oxygen conditions seem to restrain this solubilisation mechanism and preserve particulate Ni phases within the sediment. (Roberts *et al*., 2013)
In exp. I, Cu, Zn, Pb decrease to a lesser extent in OA conditions, in relation to C conditions; in exp. II, Cu decreased dramatically in both OA and C conditions. In anoxia, a direct extraction from the sediment with concomitant Cu dissolution from the suspended material became more effective within the first days of exp. II for both conditions, indicating that sediment acts as a source of Cu. From this study, sedimentary Zn and Cu, under OA conditions and OA combined with anoxia, seemed to act as a source for solubilised metals toward the water column, in contrast to previous results in the area (Prifti *et al*., 2015) that show that unaffected sediments act as a sink for these two metals under oxic conditions. A potential cause of this alteration could be the different redox conditions during our experiment, as acidified conditions were implemented along with minimum oxygen conditions, in contrast with oxic conditions implemented in the Prifti *et al*. (2015) study.

Cd appeared to decrease in exp. I, in both conditions, while in exp. II, an increase of Cd concentration was observed for both conditions. For Pb and Cd during OA conditions along with anoxia, a sink type mechanism of particulate phases precipitating on sediment surface was found; this is in agreement with the mechanism reported under oxic conditions for Pb and Cd (Prifti *et al*., 2015) while, a source type mechanism from the sediment toward the water column was observed for these two metals, when only acidified conditions prevail.

Hg presented a decrease in sediment concentration in both experiments; in exp. I, under OA conditions the decrease seems to be restricted in relation to C conditions. In exp. II, the Hg decrease was not affected by OA conditions, a distribution which seems to be affected only by the anoxia prevailing. Hg distribution, usually presents decreased surface values either because of its increased volatility or its precipitation in particulate phases. In stratified environments, an elevated content is found in the thermocline zone while it decreases below the thermocline. Hg is known to accumulate in deeper anoxic areas, removing dissolved Hg from the surface water. In reducing aquatic environments, Hg(0) is known to be the most stable Hg species, which is released as a gas towards the atmosphere. In this case, the sediment acts as a source but it is not clear to what extent Hg remains in the water column or it it eludes into the atmosphere (Colombo *et al*., 2013).

Fe seemed to slightly decrease during exp. I in OA conditions, while no changes were observed during C conditions; in exp. II a slight increase was observed for both conditions. Sedimentary Mn appeared to remain invariable in exp. I, during OA conditions, while in C conditions, a decrease was observed. In exp. II, both in OA and C conditions, an increase was observed. Under oxic conditions, it was previously found that sedimentary Fe acts as a source while Mn acts as a sink toward the sediment (Prifti *et al*., 2015). It has been shown (Ardelan *et al*., 2009) that CO_2 seepage is able to transform sedimentary Fe and Mn, leading to an enhanced release of these metals from the sediment to the overlying water, both as dissolved and suspended particulate forms.

As presented different trends during the two experiments. In exp. I, a decrease in both OA and C conditions was observed, leading to the assumption that sediment acts as a source of As towards the water column. In exp. II, an increase in As concentration was found, being more significant under acidified conditions; in this case, it appears that sediment act as a sink for As. From previous experiments, it was found that under anoxic conditions, As (III) being the major arsenic species, is mobilized from the upper sediment surface to the overlying water (Bennet, 2012). The mobility of As in sediments is known to be closely linked to Fe biochemistry. Fe(III) (hydr)

oxide minerals strongly adsorb dissolved inorganic As via complexation. Reductive dissolution of these arsenic-bearing Fe(III) (hydr)oxides, under anoxic conditions, can release dissolved As into the porewater and result fluxes of As to the overlying water column. In this study, under OA conditions, a sharp decrease of sedimentary As was observed, while for Fe only slight alterations were detected. Moreover, in OA along with anoxia, although Fe remains invariable, Mn tends to precipitate to a larger extent leading to As accumulation (Bennet, 2012), a phenomenon that was verified in the present study as a significant increase of As concentration in the sediment was observed. It has been previously demonstrated, that metal release from metal-contaminated sediments is influenced by Fe and Mn redox chemistry (Atkinson *et al*., 2007). From previous experiments, the rate of oxidative precipitation of released Fe and Mn increases, as pH decreases, and appear to greatly influence the sequestration rate of released Pb and Zn. Released metals were sequestered less rapidly in waters with lower dissolved oxygen concentrations (Atkinson *et al*., 2007).

From the Fe ratio results (Fig. 1), it becomes obvious that, in both experiments Fe (II) is the dominant Fe species, even without anoxia prevailing. Under acidified conditions, Fe (II) is likely to show increased stability (Breitbarth *et al*., 2010), which is evident during the experiment, as Fe (II) remains high, even in ordinary oxic conditions. In exp. I, the Fe (II) ratio seems to decrease in OA conditions, while the Fe (III) ratio seems to increase. During exp. II, Fe (II) ratio seems to increase slightly for OA conditions, whereas a significant decrease was observed for C conditions after the re-oxygenation phase. The Fe (III) ratio presented the opposite trend, with a decrease in the OA conditions and an increase in C conditions. At the current pH of surface seawater, Fe (III) is at its minimum solubility and as pH decreases, solubility increases. A decrease in pH from 8.1 to 7.4 would increase the solubility of Fe (III) by approx. 40%, which could have a large impact on the biogeochemical cycles, because Fe is an important micronutrient (Millero *et al*., 2009). During this study, the increasing Fe (III) ratio in OA conditions in exp. I indicates an increase in the Fe oxidation rate that may also increase Fe(III) solubility towards the water column. In exp. II, the Fe (III) ratio decreased, as a result of the anoxic conditions, which indicates a reduction mechanism of Fe (III) to Fe (II), with possible restrictive Fe (III) solubilization mechanisms.

Conclusions

The results of this study revealed that under OA conditions, metals such as Al, Ni, Cd, Fe, Mn and As seem to follow a source type mechanism from sediments towards the water column. In contrast, in anoxic conditions, a diverse sink type mechanism for these metals was observed. Cr, Zn and Pb, followed a sink-type mechanism under enhanced CO_2, while in OA along with anoxic conditions, a source type mechanism from the sediment towards the water column was found. Hg seemed to act as a source type mechanism under acidification, regardless of the oxygen conditions but it remains unknown whether it is maintained in the dissolved form or it is released in the atmosphere. Regarding the Fe ratio, it became evident that in both experiments Fe (II) was the dominant Fe species, even without anoxic conditions prevailing, indicating the increased stability of Fe (II) as a result of increased CO_2.

Exp.	cond.	Exp. day	As	Fe	Mn	Cr	Cu	Ni	Pb	Zn	Cd	Al	Hg
	field	-1	12,6	2,04	330	117	63,2	130	108	414	0,37	3,50	0,29
	OA	25	10,9	1,93	335	101	26,4	118	79,1	301	0,30	3,05	0,20
I	C	25	9,79	2,05	302	124	8,3	156	54,0	206	0,26	3,30	0,16
	filed	-1	9,12	1,88	284	122	107	127	102	506	0,26	3,26	0,42
		18	12,6	1,95	324	112	33,0	130	106	411	0,42	3,48	0,22
	OA	33	12,1	2,12	350	112	33,4	138	111	408	0,39	3,57	0,21
		18	11,4	2,03	327	120	38,9	141	108	386	0,41	3,60	0,21
II	C		10,9	2,09	345	108	15,1	140	79,9	350	0,27	3,63	0,19

Table 2: Trace metal concentrations for field and experimental samples under the different conditions (cond.) and during the experiment days (Exp. day) [As, Mn, Cr, Cu, Ni, Pb, Zn, Cd and Hg in mg/kg, Fe and Al in %]

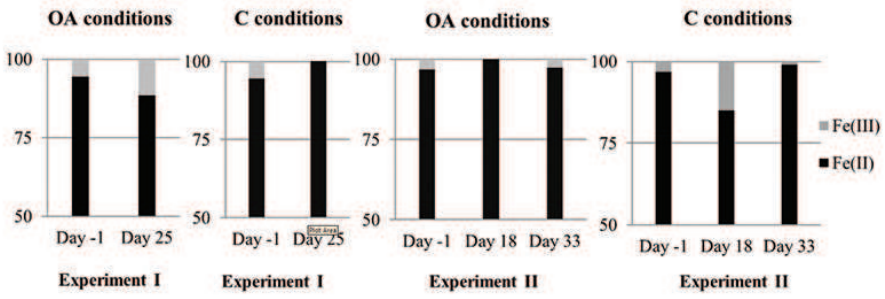

Fig.2: Fe species ratios in % (Fe(II)/Fe total and Fe(III)/Fe total) variation during the two experiments

Acknowledgements

Part of this research was co-financed by the European Union (European Social Fund) and National Funds (Hellenic General Secretariat for Research and Technology) in the framework of the project *ARISTEIA I*, 640 "*Integrated Study of Trace Metals Biogeochemistry in the Coastal Marine Environment*", within the "Lifelong Learning Programme". Part of this project is implemented under the Operational Programme "Education and Lifelong Learning" and funded by European Social Fund and national resources. Authors thank the Athens Water Supply and Sewerage Company for supporting the field sampling.

References

Ardelan, M., Steinne, S., Lierhagen, S., Linde, S.O., 2009. Effects of experimental CO_2 leakage on solubility and transport of seven trace metals in seawater and sediment. *Science of the Total Environment* 407: 6255-6266.

Atkinson, C.J.D. and Simpson, S., 2007. Effect of overlying water pH, dissolved oxygen, salinity and sediment disturbances on metal release and sequestrtaion from metal contaminated marine sediments. *Chemosphere* 69(9): 1428-1437.

Bennett, W., Teasdale, P., Panther, J., Welsh, D., Zhao, H., Jolley, D.F., 2012. Investigating arsenic speciation and mobilization in sediments with DGT and DET: a mesocosm evaluation of oxic-anoxic transitions. *Environmental science & technology* 46 (7), 3981-3989.

Caldeiram, K. and Wickett, M., 2005. Ocean Model predictions of chemistry changes from carbon dioxide emissions to the atmosphere and ocean. *Journal of Geophysical Research* 110

Colombo, M.J., Ha, J., Reinfelder, J.R., Barkay, T., Yee, N., 2013. Anaerobic oxidation of Hg(0) and methylmercury formation by Desulfovibrio desulfuricans ND132, *Geochim, Cosmochimica Acta*, 166-177

Melzner, F., Thomsen, J., Koeve, W., Oschlies, A., Gutowska, M., Bange, H., Hansen, H., Kortzinger, A., 2013. Future ocean acidification will be amplified by hypoxia in coastal habitats. *Mar Biol* 160: 1875-1888.

Millero, J., Woosly, R., Ditrolio, B., Waters, J., 2009. Effect of Ocean Acidification on the Speciation of Metals in Seawater. *Oceanography* 22(4): 72-85.

Prifti, E., Kaberi, H., Zeri, C., Rousselaki, E., Michalopoulos, P., Dassenakis, M., 2015. Calculation of benthic fluxes of metals using the pore water metal concentrations and the results from incubation experiments, *11th Panhellenic Symposium on Oceanography and Fisheries*, Mytilene, Lesvos Island, Greece

Roberts, D., Lewis C., Sanders, M., Bolam, T., Sheahan, D., 2013. Ocean Acidification increases the toxicity of contaminated sediments. *Global Change Biology* 19: 340-351.

Rodriguez-Romero, A., Bassalote, M.D., Orte, M.R.D., DelValls, A., Riba, I., Blasco, J., 2014. Simulation of CO2 leakages during injection and storage in sub-seabed geological formations: Metal mobilization and biota effects. *Environment International* 68: 105-117.

Scoullos, M., 1983. Trace Metals in a Landlocked Intermittently Anoxic Basin, p. 351–365. In: Trace Metals in Sea Water. Wong, C.S., Bouyle, E., Bruland, K.W., Burton, J.D., Goldberg, E.D. (eds.). Plenum Press, NY, USA

Biogeochemical processes under anoxic conditions affecting Arsenic (As) distribution in Elefsis Gulf: possible alterations due to simulated ocean acidification conditions - a preliminary assessment

Kapetanaki, N.[1], Stathopoulou, E.[1], Karavoltsos, S.[1], Katsouras, G.[1], Krasakopoulou, E.[2], Dassenakis, E.[1], Scoullos, M.[1]

[1]*Laboratory of Environmental Chemistry, Department of Chemistry, University of Athens, nataliekapetanaki@gmail.com, estath@chem.uoa.gr, gkatsouras@chem.uoa.gr, skarav@chem.uoa.gr, edasenak@chem.uoa.gr, scoullos@chem.uoa.gr*
[2]*Department of Marine Sciences, University of the Aegean, ekras@marine.aegean.gr*

Abstract

Arsenic (As) is a trace element well acknowledged for its toxicity. However, only few studies regarding its fate in marine environments have been conducted in Greece. The As cycle in the marine environment is closely linked to iron (Fe) and manganese (Mn) biogeochemistry, with direct adsorption on Fe-rich particulates and Mn particulate phases.

Hypoxic coastal areas are considered as high-priority for Ocean Acidification (OA) research, because the co-occurrence and interaction of low oxygen with other environmental stressors, such as elevated pCO_2, warming and eutrophication, may put them at greater risk. In this work, As distribution influenced by an intermittent anoxic coastal phenomenon, exhibiting already reduced pH at the near bottom water layer, was studied. In addition, a simulation of OA conditions was conducted in order to fully comprehend possible alterations of As. The results showed a nutrient-type As distribution, with depleted surface values and near-bottom accumulation, in full agreement with Fe and Mn near-bottom reductive dissolution from sediment surface, as a result of the prevailing anoxia. Regarding the OA experiment, As presented a decreased availability in dissolved forms, in contrast to both Fe and Mn, which could indicate a restrictive dissolution mechanism when anoxia and OA are both induced.

Keywords: iron, iron speciation, manganese, experiment, microcosm.

Introduction

Total dissolved As concentration in seawater is normally between 1.0-2.0 μg/l, while particulate As is negligible (Maher *et al*., 1988). Elevated As levels in sediments can be attributed to Fe-rich particulates settling and to direct adsorption on to the sediment surface. Although Fe may be crucial in the binding of As to sediments, there is a strong correlation between solid-phase As and Mn possibly because the two elements have similar geochemical mobilities. The prime mechanism for the release of As into porewaters is the dissolution of hydrous oxide phases to which the metalloid is adsorbed. Dissolution occurs by the reduction of Fe (III) and Mn (IV) to their soluble lower oxidation states, Fe (II) and Mn (II) (Bennet *et al*., 2012). Fe (III) (hydr)oxide minerals formed under oxic conditions, strongly adsorb dissolved inorganic arsenic via complexation and their dissolution can release dissolved As into the porewater and result in fluxes towards the overlying water column. Release of As from the decomposition of organic matter in sediments has not been demonstrated, even in anoxic sediments where ammonia and phosphate concentrations increased markedly with depth (Maher, 1988).

Ocean uptake of anthropogenic CO_2 alters ocean chemistry, leading to more acidic conditions and lower chemical saturation states (Ω) for calcium carbonate ($CaCO_3$) minerals, a process commonly termed "ocean acidification" (OA) (e.g. Caldeira & Wickett, 2005). In coastal regions, the organic load input is high and the aerobic degradation of organic matter leads to a higher CO_2 production. Anoxic systems are more acidic than normal marine environments, as the gas exchange balance with the atmosphere is not achieved, indicating that OA in such environments is already taking place and possibly spreading to adjacent systems. OA, especially when combined with hypoxic phenomena, affects carbon and

nutrient biogeochemistry, dissolved trace metal species and complexes' stability and sediment mineral phases, causing changes in benthic fluxes in the sediment-water interface. OA is known to reduce both hydroxide (OH^-) and carbonate (CO_3^{2-}) concentrations in most natural waters (by 82% and 77% respectively). These anions form strong complexes in ocean water with divalent and trivalent metals, and such a decrease would influence trace metal speciation. Therefore, these metals would have a higher fraction in their free forms. In addition, the lower pH values will also affect trace metal adsorption on organic materials, with less available sites for adsorption. Finally, most metals are more soluble in waters of increased acidity, so their concentrations are expected to change as well (Millero, 2009). Therefore, experiments combining acidification and low oxygen conditions are essential to fully understand and correlate the various observations in coastal environments.

The main scope of this experimental research was to investigate As distribution in an intermittent anoxic environment and its possible alterations under simulated acidification conditions. The aim of the experiment was to simulate the biogeochemistry and physicochemical conditions of the natural system including consideration of all vital parameters.

Materials and Methods

This work was carried out in Elefsis Gulf (Attica, Greece), a relatively shallow, semi-closed industrialised coastal system, which, due to the increased organic matter input and its hydromorphological characteristics, result in intermittently anoxic conditions during summer (Scoullos, 1983). Field sampling took place in September 2014 with the R/V AEGAEO (HCMR). Hydrographical data were recorded through CTD measurements. Seawater and surface sediment from the deepest-anoxic-station (33m) were collected untreated and placed in four 25L Nalgene Polycarbonate containers (at a proportion 80% to 20% respectively) in a thermostatic chamber (17.5°C). The seawater-sediment systems were left to equilibrate for a week in Ar atmosphere in order to maintain the anoxic field conditions. This was followed by the four week period of the experiment where CO_2 was added to the microcosms; the stability of pH was maintained using a continuous flow system (IKS Aquastar, IKS Computer Systeme GmbH) which automatically adjusted CO_2 gas addition to the microcosms. The measured pH values by the IKS system were corrected with the parallel use of a laboratory pHmeter (Jenway 3310) calibrated in NBS scale. On the 25th day of the experiment, the Ar supply was ceased and the systems were left to re-oxygenate until day 33 in order to fully simulate the intermittent anoxic conditions of the study area. The pH values selected for the experiment conditions were (a) for the control conditions (C) the pH value measured during sampling, and (b) for the ocean acidification conditions (OA) the pH value predicted for the year 2300 (6,80 NBS), for latitudes corresponding to the Mediterranean (e.g. Caldeira & Wickett, 2005). Each one of the two conditions was applied in two replicate tanks. Seawater from the field (during the cruise, referred as day -1 in the experiment) and from the microcosms (every 2 days) was sampled for the determination of trace elements. For As, and Mn determination, the EPA methods 1640, 6020 were followed for preconcentration and final measurement with ICP-MS using the Collision Cell Technology (CCT) mode of the instrument; in order to evaluate the method performance Certified Reference Materials (CASS-5 and NASS-6, National Research Council Canada) were also treated and analysed the same as the samples. For total Fe and Fe(II), the colorimetric determination as described by Bloom (Bloom, 2004) was implemented while Fe(III) was calculated by substraction. It should be noted that all determinations refer to the total dissolvable metal content. Sediments were collected twice during the experiment and treated according to EPA 3050 for final measurement of As and Mn with ICP-MS and FAAS for Fe.

Results and Discussion

Results of the near bottom physicochemical parameters (pH=7.75) indicate a reducing coastal environment of quite increased acidity. This value corresponds approximately to the predicted pH levels for 2100, while the negative redox potential (-50.7 mV) along with the minimal DO concentrations (0.84 ml/L), reflect the anoxic conditions prevailing in the deeper parts of the area during summer.

The only available published data on dissolved As in Elefsis bay, are for near-coast areas with surface values between 2.9-3.6 μg/l (Ochsenkuhn-Petropulu *et al*., 1995); the results of the present study indicate that nowadays, the inner Elefsis bay, presents lower As concentrations despite the significant industrial activities dominating the surrounding area.

In this study, Fe low surface values were observed (2.24 μg/l) along with quite increased bottom values (110,0 μg/l) while Mn presents depleted surface values (2.74 μg/l) and significantly increased bottom values (234,7 μg/l).

The results show a vertical As distribution (Fig. 1) with low surface concentrations and an accumulation of As near the water-sediment interface, suggesting that it is taken up similarly to the nutrient elements by biological activity in the surface mixed layer and is partially regenerated at depth, especially near the anoxic interface (Maher, 1988).

Fe and Mn distribution (Fig. 1) consorts with previous findings, with higher dissolved forms in the bottom of Elefsis, as a result of their dissolution from sediment surface. Dissolution of sinking Fe particles and soluble Fe species formation could also be attributed to the specific profiles. Mn (IV) (present mainly as MnO_2 in the sediment) is reduced to dissolved Mn(II) eluding from the sediment to the overlying water; thus, this solubilised Mn is shortly re-precipitated at the oxic-anoxic layer which is found close to the bottom (Scoullos, 1983).

The increased bottom value of Fe and Mn is typical in anoxic environments (Scoullos, 1983), which explains the also elevated As bottom values. Particulate metals,

Fig.3: Total dissolvable As, Mn and Fe (ppb) for the water column of Elefsis Gulf

coprecipitated with Fe and Mn in oxic surface waters, sink downwards due to gravity, are deposited in the sediments and reduced in the suboxic or anoxic zone. Reductive dissolution of hydrated oxides of Fe (III) and Mn (III, IV) controls the supply of dissolved reduced forms of these metals in the anoxic zone. In Elefsis Gulf, the prevailing anoxia in summer, leads to reductive conditions with more soluble Fe and Mn forms and concomitant dissolution and accumulation of As near the water-sediment interface.

During the experiment, As showed the same trend both in OA and C conditions (Fig. 2), with elevated initial values in relation to field values (3.20-3.36 ppb and 1.61 ppb respectively), followed by small variations until the end of the experiment; in OA conditions the concentrations appear relatively lower than in C conditions, with no effect of the re-oxygenation phase. On the contrary, in C conditions the re-oxygenation phase resulted in As sediment release with concomitant elevated As values in the supernatant water (3.05 to 3.85 ppb, respectively). The total dissolved As concentration decreased with acidification has been previously reported in experiments conducted with CO_2. These results, which are in agreement with the results of this study, indicate that the total As in seawater would be less available to the marine biota under acidic conditions (Bassalote *et al*., 2015).

Mn concentrations (Fig. 2), also showed the same trend both in OA and C conditions, with significantly decreased values in relation to field values (5.98-10.20ppb and 234.7 ppb, respectively); in contrast to As, in OA conditions the total dissolvable Mn concentrations appeared higher than C conditions with lower final concentrations after the re-oxygenation (1.76 ppb and 1.46 ppb respectively).

For As, it appears that sediment oxygenation and irrigation leads to sediment release towards the water column with elevated initial values for the experiment in relation to field values; for Mn an opposite mechanism of water to sediment flux is found, which was also recently observed in benthic fluxes incubations for the specific area (Prifti *et al*., 2015). Apart from the decreased initial values, in OA conditions, Mn appears to prevail in more soluble forms and only after re-oxygenation, its particulate phase is favored leading to precipitation.

At the beginning of the experiment, total Fe showed decreased values (Fig. 3) for both OA and C conditions in relation to the field values (34.65 -30 ppb and 109.98, respectively), having the same trend until the 25th day. From day 5th, in OA conditions, total dissolvable Fe appear increased in relation to C conditions until the 25th day when re-oxygenation took place leading to approximate concentrations of 35,15 ppb and 45,78 ppb respectively. Fe (III) showed an increasing trend until the 5th day in both conditions; for C conditions Fe (III) decreased gradually until the re-oxygenation phase when it increased. In OA, Fe(III) increased more on the 11th day and decreases gradually till the end of the experiment. Fe (II) appeared to decrease from field values in relation to experiment initial values for both OA and C conditions (78,39 ppb and 1.96-1,82 ppb, respectively) which could be attributed to oxygenation of seawater during the transfer to the laboratory and experiment set-up. The re-oxygenation phase, in C conditions, appears to release Fe from the sediment to the overlying water in the Fe(III) form; in OA conditions this release is also evident but in both Fe(II) and Fe(III) forms. At the current surface pH of seawater, Fe (III) is at its minimum solubility; as pH decreases, solubility increases. A decrease in pH from 8.1 to 7.4 would increase the solubility of Fe (III) by about 40%, which could have a large impact on biogeochemical

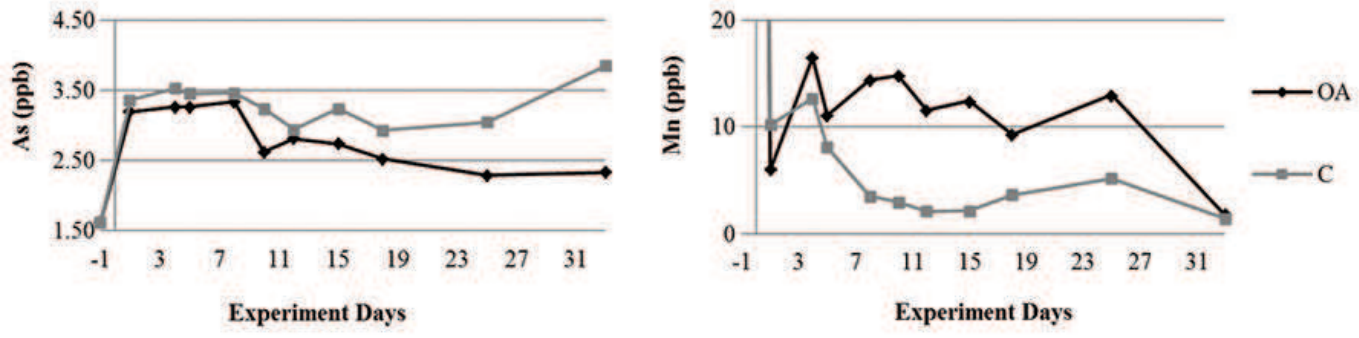

Fig.4: Total dissolvable As and Mn variation throughout the duration of the experiment

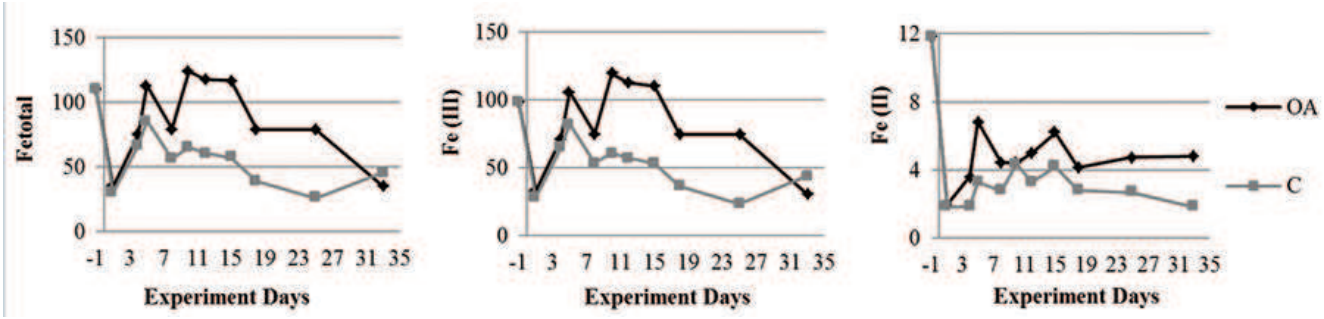

Fig.5: Total dissolvable Fe, Fe(II) and Fe(III) (in **µ**g/l) variation throughout the duration of the experiment

cycles (Millero *et al*., 2009). Under acidified conditions, Fe (II) is likely to show increased stability that is evident during the experiment, from the 18th day until the end (OA conditions), with no oxidation to Fe (III) observed, despite re-oxygenation taking place (Breitbarth *et al*., 2010).

The low solubility plus the rapid oxidation rate of Fe could be responsible for its precipitation during the experimental time, and thus removing other metals by adsorption. Additionally, a disturbance in the Fe–Mn shuttle in the sediment could lead to increased concentrations of toxic metals. From previous experiments, Fe and Mn precipitation as hydroxides on the sediment surface can be disturbed by more acidic conditions leading to inhibited removal of dissolved Fe, Mn forms into the sediment which could result in increased concentrations in the seawater; this increase is evident during the first days of the experiment while, as the CO_2 supply continues, this increase is limited. This contrast could be attributed to the extraction of the easily leachable metal fractions from the sediment and suspended particles during the early phase of the experiment. The elevated dissolved values for these two trace metals during the OA conditions indicate an inhibited precipitation mechanism from the water to the sediment, preserving an elevated content in the water column. As on the contrary, during more acidic conditions appears slightly decreased in relation to C conditions with steady concentrations from day 18th till the end of the experiment, with no effect of the re-oxygenation phase. It appears that OA, in addition to anoxic conditions, acts as a restrictive factor for As dissolution in the water, maintaining slightly lower values in relation to C conditions. It could be presumed that for As, in acidic conditions, the sediment acts like a sink.

Conclusions

This study showed an As distribution with depleted surface values and near-bottom accumulation during summer; this trend indicates that the main process affecting As concentrations is coprecipitation with Fe and Mn (oxy)hydroxides in the oxic surface followed by their reductive dissolution in the anoxic zone, leading to solubilised forms of Fe and Mn along with extended release of dissolved As. Regarding the OA experiment, Fe and Mn precipitation as hydroxides seem to be disturbed by more acidic conditions leading to inhibited removal into sediment and elevated dissolved values for these two metals. On the contrary, OA, in addition to anoxic conditions, acts as a restrictive factor for As availability in dissolved forms, maintaining slightly lower As content in the water column in relation to less acidified conditions, probably leading to the assumption that, in such conditions, the sediment acts like a sink for As.

Acknowledgements

Part of this research was co-financed by the European Union (European Social Fund) and National Funds (Hellenic General Secretariat for Research and Technology) in the framework of the project *ARISTEIA I*, 640 "*Integrated Study of Trace Metals Biogeochemistry in the Coastal Marine Environment*", within the "Lifelong Learning Programme". Part of this project is implemented under the Operational Programme "Education and Lifelong Learning" and funded by European Social Fund and national resources. Authors thank the Athens Water Supply and Sewerage Company for supporting the field sampling.

References

Bassalote, M.D., Orte, M.R.D., DelValls, A., Riba, I., 2015. Evaluation of the threat of marine CO2 leakage-associated acidification on the toxicity of sediment metals to juvenile bivalves. *Aquatic Toxicology* 166: 63-71.

Bennett, W., Teasdale, P., Panther, J., Welsh, D., Zhao, H., Jolley, D., 2012. Investigating Arsenic speciation and mobilization in sediments with DGT and DET: a mesocosm evaluation of oxic-anoxic transitions. *Environmental Science and Technology,* Washington 46(7): 3981-3989.

Bloom, N., 2004. Iron Speciation in Aqueous Samples by Ferrozine Complexation Colorimetric Detection at 562 nm. C SG-033, 298-302.

Breitbarth, E., Achterberg, E.P., Ardelan, M.V., Baker, A.R., Buccarelli, E., Chever, *et al.*, 2010. Iron biogeochemistry across marine systems–progress from the past decade. *Biogeosciences*, 7, 1075–1097.

Caldeira, K. and Wickett, M., 2005. Ocean Model predictions of chemistry changes from carbon dioxide emissions to the atmosphere and ocean. *Journal of Geophysical Research*, 110, 1-12.

Maher, W. and Butler, E., 1988. Arsenic in the marine environment, Review." *Applied Organometallic Chemistry* 2: 191-214.

Millero, J., Woosly, R., Ditrolio, B., Waters, J., 2009. Effect of Ocean Acidification on the Speciation of Metals in Seawater. *Oceanography* Vol.22, No4: 72-85.

Ochsenkuhn-Petropulu, M.O.K., Milonas, I., Parissakis, G., 1995. Separation and Speciation of Inorganic- and Methylarsenic Compounds in Marine Samples. *40th Canadian Spectroscopy Conference.* Halifax, Canada. 40.

Prifti, E., Kaberi, H., Zeri, C., Rousselaki, E., Michalopoulos, P.,

Dassenakis, M., 2015. Calculation of benthic fluxes of metals using the pore water metal concentrations and the results from incubation experiments. *11th Panhellenic Symposium on Oceanography & Fisheries,* Mytilene, Greece.
Scoullos, M., 1983. Trace Metals in a Landlocked Intermittently Anoxic Basin, p. 351–365. In: Trace Metals in Sea Water. Wong, C.S., Bouyle, E., Bruland, K.W., Burton, J.D., Goldberg, E.D. (eds.). Plenum Press, NY, USA.

Hendrik Hondius, "Attica, Megarica, Corinthiaca, Boeutia, Phocis Locri", Atlas Novus…, Amsterdam 1639.